UNIVERSITY OF BIRMINGHAM

Constraining *in situ* denitrification and its role as nitrous oxide sink in conventional and regenerative agriculture

By

Gianni Micucci

A Thesis Submitted to the University of Birmingham for the degree of

DOCTOR OF PHILOSOPHY

School of Geography, Earth and Environmental Sciences

College of Life and Environmental Sciences

University of Birmingham

October 2023

Abstract

The current food production system is responsible for 19 to 29% of the overall global emissions of greenhouse gases. In particular, it contributes about 75% of the global anthropogenic nitrous oxide (N_2O) emissions, a greenhouse gas with 298 times greater radiative forcing than carbon dioxide (CO_2). These emissions mostly result from the large quantities of synthetic nitrogen (N) fertilizer applied in arable agriculture. In the UK, intensive cultivation practices are the main contributors to the ~£1.2 billion annual costs of soil degradation, which represents 30% of the UK farm gate income. To ensure future food security whilst addressing these environmental and economic challenges, a transition to less intensive food production systems and a better understanding of the mechanisms and controls of N_2O emissions are needed. However, this better understanding can only be complete by constraining the denitrification process.

Denitrification is the anaerobic microbial respiration process which transforms soil nitrate (NO_3^-) into gaseous dinitrogen (N_2). When incomplete, it can be a predominant source of N_2O in soil, while its full sequence of reaction is the only natural terrestrial sink for N_2O emissions. The high sensitivity needed to distinguish small soil-N_2 fluxes from the high N_2 atmospheric background (~78%) unfortunately restricts its measurement to peak events. A new methodology is therefore needed to resolve the enigma of denitrification quantification in soil.

In contrast with conventional farming management, regenerative agriculture aims to restore degraded lands and maintain soil fertility using crop rotations, including 3– 4 year “ley” mixture comprising of grasses and nitrogen-fixing legumes such as clovers. These leys have the double benefit of increasing soil organic carbon and naturally fertilizing soil with nitrogen,

reducing reliance on synthetic fertilizer. However, little is known about the impact of these leys on the soil nitrogen cycle and their potential contribution to greenhouse gas emission reduction.

The present work aims to investigate the importance of denitrification in conventional agriculture and long term ley rotations; in particular in response to N fertilizer application. To address the challenges of denitrification quantification, a new methodology combining ^{15}N tracer and N_2-depleted artificial atmosphere has been developed and subsequently used for a one-year field campaign. This successful campaign was the first UK attempt to characterize *in situ* denitrification rates under artificial atmosphere.

The newly developed method enabled the detection of soil-N_2 fluxes 90% of the time, with an 8 fold greater sensitivity than conventional methods and allowing the simultaneous incubation of 24 soil cores; capturing spatial variability at farm scale. The field campaign spanned from March 2022 to May 2023 and was characterized by a large denitrification activity in the arable control following fertilizer application. Indeed, 15 kgN ha^{-1} were lost in this field (~8% of the 200 kgN ha^{-1} applied) through denitrification between April and October 2022. Our measurements indicated that 9 % of this flux occurred as N_2O rather than N_2. The application of fertilizer in leys also resulted in 3 times higher N_2O emissions and an N_2O sink efficiency dropping from 93% to 85%.

The present work improves the characterization and understanding of the denitrification process and highlights the high existing correlation between nitrous oxide sink efficiency and soil nitrate availability; calling for new strategies of fertilizer application in agricultural fields.

Acknowledgements

PhD is a long adventure, but not necessarily a lonely one. Therefore, I would first like to thank the University of Birmingham, NERC, CENTA and UKRI for placing their trust in me for this project and providing me with financial support. This present thesis would not have existed without them. I also want to express a very warm “thank you” to FarmED, without whose support my thesis would probably not have existed either. In addition to all the friendly and welcoming staff there, I particularly want to thank Ian Wilkinson and Danielle Semple for their precious help and allowing me to sleep on site, saving my poor PhD student’s RTSG hundreds of pounds! I would also like to thank all of the actors of the SARIC project led by Jonathan Leake, for allowing me to benefit from the experimental field trials. A special shout out to my supervisors, Stefan Krause, Iseult Lynch, Felicity Roos and Niall McNamara for the guidance, correction of manuscripts and friendly chats. And of course to Fotis Sgouridis, who, although not originally on board for this project, has been a constant and crucial help. Thank you for all the meetings, all the corrections, all the freely analysed samples, for welcoming me to Bristol, for the hundreds of long spreadsheets and for the manuscripts! I don’t forget the Soil group with Yafei, Johanna, Novalia and so many others! Finally to James Gore, who, although working on a completely different project, has always been a life-saviour during my most desperate lab moments, in addition to being a good friend and a music fellow.

I was lucky to go through this adventure with the best PhD fellows, who endured this difficult journey with me, my “brothers in arms”. To all our nights, our Bratby drinks, our birthday parties, our Mojito Mondays, our climbing sessions, our lunch breaks, our trips…. To all the moments we spent together. To Adrià (aka the “focking mate”), Andrea (my housemate), Lisa (the group’s mom), Nine (our comedy girl), Klaske (our D&D ranger), Aaron (my own personal

Roger Waters), Jess (our real-life hobbit), Grace and Grace (respectively best Disney and Eminem impersonators), Manon (my constant emotional support, or the other way around?), Alex (the P-Diddy Style Shrimping Vessel Captain and gym bro) and Dom (the best friend known too late), thank you all and good luck for those of you who have not yet completed their PhD journey.

To my family, who have always been here for me, no matter my choices. Without them, I would probably have quit the PhD after my 3 months of long COVID. To my mum and dad, whose support and affection are my strength to always carry on, even when I feel defeated. To my brothers Vincent and Alexis, that I miss every day and wish I could see more often.

To my best friend ever, Pierre, with whom “distance” seems to be nothing but a word.

To my Bordeaux crew, Paul, Alex, Bachir, Kilian, Vaïana, Thomas.

To the best supervisor ever, who also gave me his trust in this project and has always been a caring and dedicated supervisor, dare I say, “a dad”?! For all the times I knocked at your door and disrupted your busy brain, for all the cigarettes, for our Valentine’s night in Cambridge where we got rejected from a restaurant with disdain, for all the food you brought to me when I was sick… For all of your guidance in the path of science, thank you Sami Ullah.

Finally to my Bibu, now and always.

Into this house we are born. Into this world we are thrown.

Content

List of figures

List of Tables

List of abbreviations:

^{15}NGF: ^{15}N Gas Flux method

% v/v: volumetric percentage

°C: Celsius degree

AIT: Acetylene Inhibition Technique

ANOVA: Analysis of Variance

at %: atom percent

Atm: atmosphere (pressure unit)

a_a: the ^{15}N enrichment of the atmosphere

a_p: the ^{15}N enrichment of the soil denitrifying pool

BNF: Biological Nitrogen Fixation

C: Carbon

CH_4: Methane

CO_2: Carbon Dioxide

d: the proportion of N_2 that derives from denitrification

DOC: Dissolved Organic Carbon

eqCO_2: Equivalent CO_2

DNRA: Dissimilatory Nitrate Reduction to Ammonium

g: grams

GC: Gas Chromatography

GWP: Greenhouse Warming Potential

ha: Hectare

He/O_2 GFSC: Helium Oxygen Gas Flow Soil Core method

ID: Inner Diameter

IRMS: Isotope Mass Ratio Spectrometry

LC: Liner Chamber approach

m^2: squared meter

mol: mole

SPC: Source Partitioning Coefficient

NA: Natural Abundance

N: Nitrogen

N_2: Dinitrogen

N_2O: Nitrous oxide

NH_4^+: ammonium

NO: Nitric oxide

NO_2^-: Nitrite

NO_3^-: Nitrate

NOSE: Nitrous Oxide Sink Efficiency

O: Oxygen

OD: Outer Diameter

OM: Organic matter

ppb: Part Per Billion

ppm: Part Per Million

PCC: Pearson Correlation Coefficient

PR: Product Ratio.

SO_3^{2-}: Sulphite

SOC: Soil Organic Carbon

SE: Standard Error

t: tonne

TDN: Total Dissolved Nitrogen

Chapter 1: Introduction

1.1) The origins of agriculture

Emerging more than 10 000 years ago (Stephens et al., 2019), during the Neolithic revolution, agriculture has enabled the rise and sustainability of the human species (Sanderman et al., 2017). It appeared simultaneously in different parts of the world such as China, India, the Middle East, Mesoamerica or Sub-Saharan Africa (**Figure 1**); where humans started to domesticate plants and animals by controlling their reproduction and evolution (Nayak et al., 2022). From these niches, agriculture expanded to the whole world and cereals like wheat and barley started to be produced in Europe around 6 000 BC (Jovanović et al., 2021). The food security provided by agriculture enabled a wide-scale transition from hunter/gatherer societies to sedentary populations (Bocquet-Appel & Bar-Yosef, 2008) and later to the rise of the first great civilizations. During antiquity, several innovations enabled to increase yields and ensure the stability of these civilizations, such as irrigation (Yannopoulos et al., 2020), application of manure (Araus et al., 2014), crop rotation (White, 1970), animal traction (Pigière & Smyth, 2023) or the stocking of cereals (Ben-Noun, 2017). These innovations continued in the Middle Ages with the development of new tools (windmill, metal scythes…) or new crop rotation plans, such as the three-field system. In this system, a crop is planted the first year, a different one the second year and finally the field is left to fallow during the third year. Fallowing is an agricultural technique in which arable land is intentionally left unsown for one or more growing seasons. This practice allows the land to replenish its fertility. Crop rotation, as a part of this system, also helped control pest life cycles and the development of pathogens that often occur with monoculture. This system continued for

centuries. However, the exponential rise of the human population in the last three centuries has necessitated drastic changes in agricultural practices and land uses (Ramankutty & Foley, 1999).

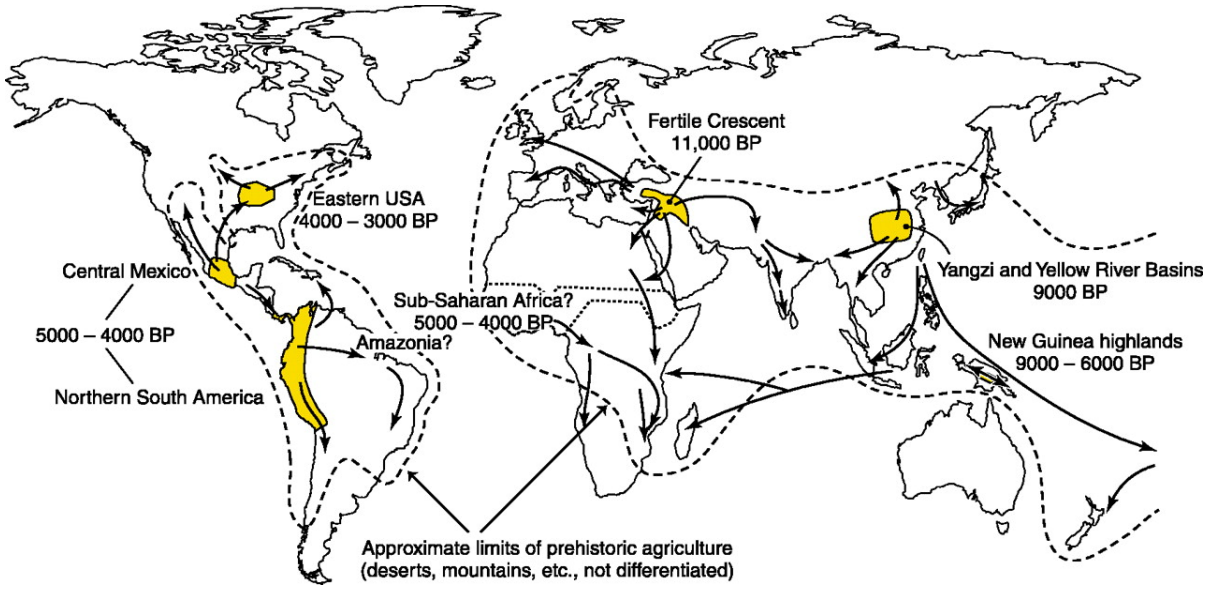

***Figure 1**: The birth of agriculture and its expansion into the world.*

This map from Diamond & Bellwood (2003) represent the inferred places and dates (based on radiocarbon data) of the different agricultural homelands.

The second agricultural revolution occurred during the 18th century in Britain and was mainly carried out by Jethro Tull and Charles Townshend. This revolution saw a huge increase in yields per land and labour. For example, wheat yields increased by about 25 % between 1700 and 1800 (Overton, 1996). The limiting factor of cereal yields before 1830 was nitrogen and the newly developed methods during this revolution enabled to fix this issue. The major development was the Norfolk four-course system, imported from the Waasland region (actual Belgium), which replaced the medieval three-field system. It involved a sequence of four crops: wheat, turnips, barley, and clovers and thus reduced the need for fallow periods. The

introduction of turnips and clover into the crop rotation had great benefits for the agricultural system and became known as "ley-farming" in England (Overton, 1996). Clovers, originating from the legume family, have the unique ability to fix atmospheric nitrogen into the soil through Biological Nitrogen Fixation (BNF), effectively addressing the nitrogen limitation that fields faced in the 18th century.

Turnips and clovers both served as fodder and grazing crops, allowing livestock to be raised year-round. Additionally, turnips can be cultivated during the winter and have deep roots that can access minerals inaccessible to shallow-rooted crops. The other major innovations of this second agricultural revolution were newly improved ploughing techniques, selective breeding of livestock and the introduction of new crops. This new system of farming significantly and sustainably increased food production, without endangering soil health, local environment and fauna, soil and air pollution or contributing to global warming. As mentioned by Overton (2011), during the third agricultural revolution, “an essentially organic agriculture was gradually replaced by a farming system that depended on energy-intensive inputs dependent on the exploitation of fossil fuels”.

1.2) Conventional and regenerative agriculture

Modern conventional agriculture was born with the third agricultural revolution (so called “Green revolution”), which started in the early 20th century and combined the use of synthetic nitrogen fertilizer, chemical pesticides, the selection of high-yield species, controlled irrigation, and mechanization of agriculture. In 1918, the German Fritz Haber received the Nobel Prize for the synthesis of ammonia from atmospheric dinitrogen. Under high temperature (450°C) and high pressure (200 atm), this process revolutionized agriculture and science by allowing the industrial fixation of dinitrogen (**Figure 2**). This process enabled to

reach much greater nitrogen contents in soil compared to the natural fertilization performed by clovers in the Norfolk four course-system. The ammonia produced with the Haber process still enables today the production of 174 million tonnes of nitrogen fertilizer per year, 85% of which is used in fertilizers (Pfromm, 2017).

Figure 2*: Laboratory reactor used by Fritz Haber to synthetize ammonia ca. 1909.*
Public domain picture.

However, farmers quickly realized that application of fertilizer to the traditional wheat varieties would not result in increased grain yield because straws grew too tall and lodged (Silverstone & Sun, 2000). Therefore, smaller varieties of wheat had to be found or bred so higher application of nitrogen fertilizer would result in higher yields. The semi-dwarf wheat variety “Norin 10” was developed in Japan and brought back to the United States after World

War II. The *Rht1* and *Rht2* genes present in Norin 10 reduced its height to 60–110 cm, compared to >150 cm for regular wheat (Lumpkin, 2015). Norman Borlaug used this variety of wheat to create new semi-dwarf and disease-resistant varieties, for which he won the Nobel Peace Prize in 1970. Currently, almost all commercial wheat employs one of the *Rht* mutant alleles (Silverstone & Sun, 2000). Other than wheat, hybrid high-yielding varieties of corn and rice were also developed. However, high-yielding varieties did not always result in high yields after plantation. Typically, in a well-irrigated area and with the use of fertilizer, these varieties offered a 40% higher yield. In dry areas however, the gains were often inferior to 10 % (Pingali, 2012). Therefore, massive investments in irrigation infrastructure were made (Cassman & Pingali, 1995). The synthesis of chemical pesticides also greatly helped this green revolution. The use of pesticides has grown steadily since the late 1940s (Pimentel, 1996) and has reached about 2.5 million tonnes per year today (FAO, 2022**a**).

Today, conventional agriculture produces 9.5 billion tonnes of food (FAO 2022**b**), however, it has a large impact on the environment. It is responsible for 10 to 12% of overall global emissions of greenhouse gases (Kristensen et al., 2011). As a fuel-dependent industry (cultivation, application of manure, transport of animals, processing and transport of feed) it is an important source of carbon dioxide (CO_2). However, most of the warming potential of agriculture comes through methane (CH_4) and nitrous oxide (N_2O) emissions. Methane is a greenhouse gas with 25 times greater radiative forcing than CO_2 (IPCC, 2013) and its emissions mainly result from ruminant livestock. On the other hand, nitrous oxide has 298 times greater radiative forcing than CO_2 (IPCC, 2013) and is also involved in the depletion of the ozone layer (Ravishankara et al., 2009). Agriculture is responsible for 75% of N_2O emissions globally (Velthof & Rietra, 2018), these emissions mostly result from the application of N fertilizer in arable fields. Around 120 million tonnes of N fertilizer are used yearly (FAO, 2017) ; however,

it is estimated that half of this fertilizer is lost to the environment (Lassaletta et al., 2014), in particular as N_2O. It can also be emitted as nitric oxide (NO) or as ammonia (NH_3). Nitric oxide is also involved in the depletion of the ozone layer and can cause acid rain (Pilegaard, 2013). Volatilisation of ammonia is another big consequence of fertilizer application and may result in acidification of water and soil (Haas et al., 2001). The excesses of N fertilizer can also leach in the form of nitrate (NO_3^-) and contaminate waterways, causing eutrophication (Guerci et al., 2013). Eutrophication of water results from an excess of nutrients, causing increased plant and microbial growth (especially algae). This growth is at the expense of the already present species and results in lower amounts of dissolved oxygen. Conversion of native soil to agricultural uses generally comes with a loss of soil organic carbon (SOC), with median losses of 26% in the top 30 cm (Sanderman et al., 2017). The main driver of the loss of SOC in agricultural lands is the use of tillage (Juřicová et al., 2022). These losses lead to poor soil structure which facilitates soil erosion by wind and water which in turn, further accelerates the loss of SOC. In the context of rising atmospheric CO_2 levels, soil carbon sequestration could be part of the solution to fight global warming, while the loss of SOC from agricultural practices only increases atmospheric CO_2 concentrations (Houghton, 2007). The destruction of ecosystems for cultivation and application of pesticides also result in the endangering of local species, affecting the biological cycles of soil. Finally, intensive conventional agriculture causes economic issues. For example, in the UK, it is the main contributor to the ~£1.2 billion annual costs of soil degradation, which represents 30% of the UK farm gate income (Graves et al., 2015). Continuous cropping, ploughing, short rotations and intensive use of agro-chemicals have contributed to declines in soil quality, constraining yields and profits (Townsend et al., 2016).

To mitigate these impacts, regenerative agriculture aims to restore degraded lands and prevent the loss of arable soils while addressing the climate change issues associated with agriculture. It revolves around five key principles: minimum mechanical soil disturbance (i.e., no tillage), permanent soil organic cover, species diversification, keeping living roots in the soil and integrating animals (Miller-Klugesherz & Sanderson, 2023). Ley-farming, as introduced during the second agricultural revolution (see **chapter 1.1**), is a perfect example of regenerative agriculture. During one year (or up to four years in the case of soil restoration), the field is under permanent organic cover and is being regenerated for the next culture. In particular, the presence of legumes associated with nitrogen-fixing bacteria enables the ley to naturally fertilize soil. It has been estimated that BNF has the ability to fix roughly 200 million tonnes of nitrogen annually (Biswas & Gresshoff, 2014), which is more nitrogen than is currently produced using the Haber process. Bringing animals into the mix not only enables the leys to be grazed and thus prepared for the next culture, but also participates in soil quality improvement and higher economic returns (Cooledge et al., 2022). Leys participate to soil species diversification which, as mentioned previously, is an efficient way to control pest life cycles and development of pathogens compared to monoculture. Regenerative agriculture often results in an increase of soil organic carbon and thus in water retention capacity (Guest et al., 2022), reducing the risk of flooding under high precipitation conditions. Currently, it is estimated that only 1.4% of total agricultural land is dedicated to organic farming (which includes regenerative agriculture), with 181 countries practicing organic activities (FiBL & IFOAM, 2019).

1.3) The nitrogen cycle in soil

Nitrogen is a key nutrient for any life form on earth and exists in many forms that are exchanged and transformed in complex biogeochemical cycles (Butterback-Bahl, 2011).

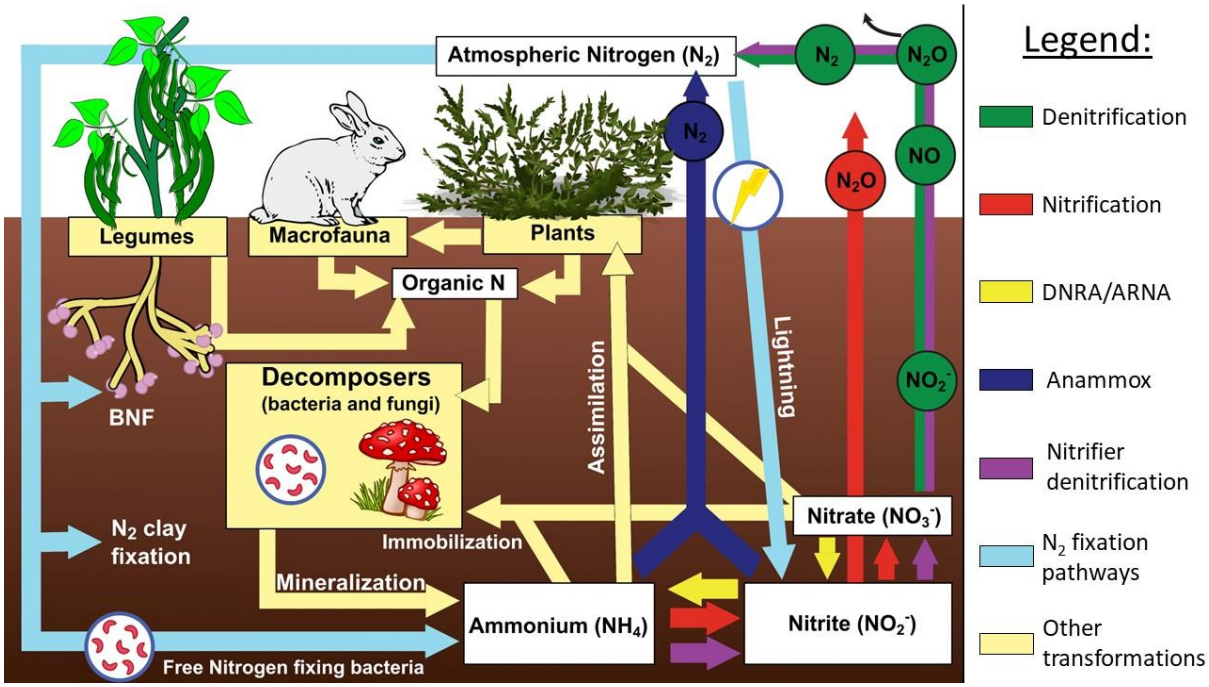

***Figure 3**: The nitrogen cycle in soil*

Nitrogen is transformed via many complex processes and is exchanged between atmosphere, soil and biological individuals (microbes and animals). Abiotic processes are not represented in this figure for clarity.

Living organisms use nitrogen for the synthesis of complex organic molecules (such as amino acids, nucleic acids, chitin and proteins). These organic compounds are released in the soil via root exudates, biological excretions or the necromass (dead plants, microbes or animals in soil). Once in the soil, these molecules are decomposed by soil microbes via mineralization of soil organic matter (**Figure 3**). This mineralization consists in successive depolymerisations of the complex organic molecules down to simple plant-available minerals (ammonium in the

case of nitrogen). On the other hand, soil microorganisms can also assimilate these nitrogen minerals for their own metabolism, reducing the amount of available nitrogen. This is referred as nitrogen immobilization. Ammonium in the soil can be transformed into nitrates through nitrification (Davidson et al., 1991), an aerobic metabolic process. Nitrate is also a nutrient available for plants and microbes but can be transformed into inert gaseous dinitrogen (N_2) via denitrification (see **chapters 1.4** and **1.5**), which is a microbial respiration process under suboxic conditions. Incomplete denitrification leads to emissions of N_2O. Dissimilatory reduction of nitrate to ammonium (DNRA) is another anaerobic microbial respiration process, which transforms nitrate in ammonium. If this ammonium is assimilated to the microbe's metabolism at the end of the process, it is referred as assimilatory reduction of nitrate to ammonium (ANRA; Sparacino-Watkins et al., 2014). In-between nitrification and denitrification, nitrifier-denitrification is a process in which soil ammonia is oxidized into nitrite; and this nitrite is then reduced according to the sequential steps of the denitrification process (i.e. into NO, N_2O and N_2). This process differs from coupled nitrification/denitrification by the fact that the whole sequence is carried out by a single organism. Nitrifier-denitrification is carried out by autotrophic nitrifiers (Wrage et al., 2001). Anaerobic ammonium oxidation (Annamox) is a metabolic microbial process in which ammonium and nitrite are converted into dinitrogen. Although predominant in aquatic ecosystems, anammox bacteria have been found in agricultural soils (Humbert et al., 2010). Other abiotic processes can further transform nitrogen in soil (such as chemo-denitrification or decomposition of hydroxylamine) but these are considered negligible compared to the biological processes (Zhu-Barker et al., 2015). The inputs of nitrogen in soil can come from different ways. In the absence of anthropogenic disturbance or animal inputs, nitrogen enters soil via BNF, N_2 adsorption onto clay or lightning interaction with air (**Figure 3**). In either case,

nitrogen comes from the atmosphere, which is the biggest pool of nitrogen on earth (constituted of 78% N_2). However, the robust triple covalent bond in the N_2 molecules renders them largely unusable by the majority of living organisms. The tremendous amount of energy released by lightning can break this bond and ionize N_2 and H_2O in the atmosphere to produce nitrite (NO_2^-); which can then penetrate soil through raindrops. However, this pathway contributes at most to about 10 % of the total annual yield of natural soil nitrogen inputs (Jeffery Leigh, 2002). On the other hand, N_2 adsorption onto clay is usually negligible. BNF was for a long time the main source of nitrogen in soil (Ladha et al., 2022). This process can occur symbiotically with certain families of bacteria, such as *rhizobium* (**Figure 4**). These bacteria infect plant cells to form root nodules in which they exchange organic nitrogenous molecules with the host plant against carbon rich photosynthesis compounds. The *rhizobium* bacteria primarily associate with legumes (clover, beans, lentils, soybeans, chick peas, etc.).

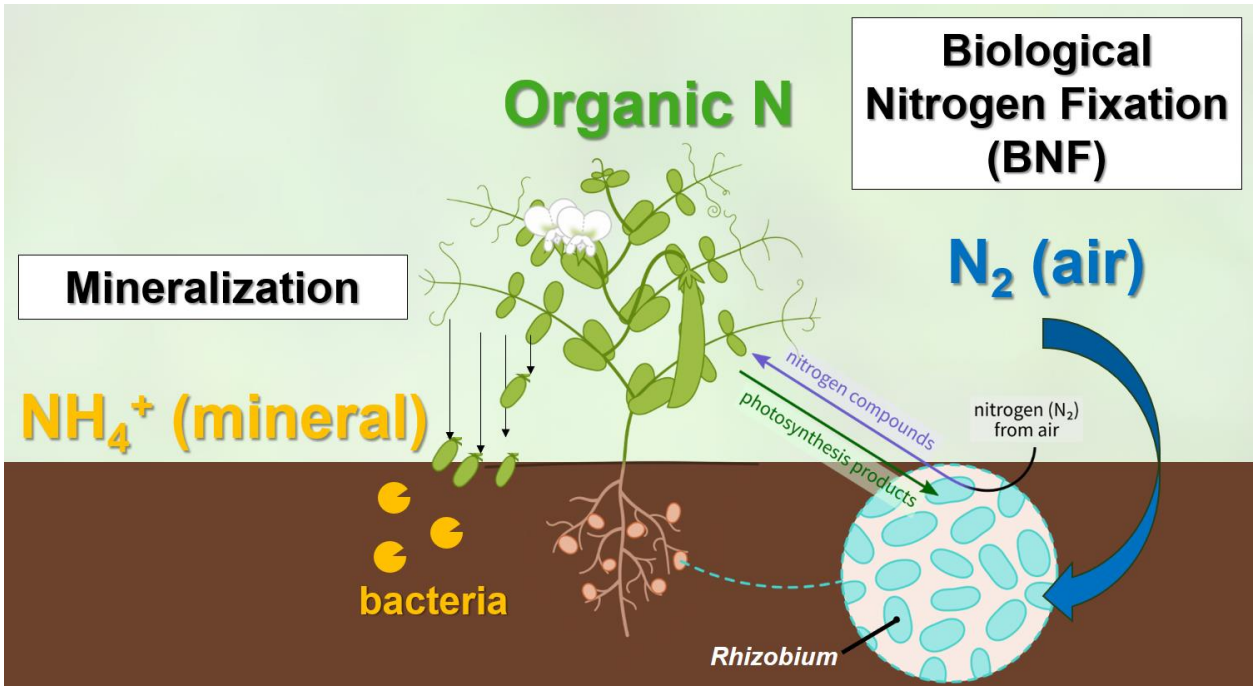

***Figure 4**: Biological nitrogen fixation performed by legumes*

Modified version from Wikimedia commons “Nitrogen fixation Fabaceae (CC BY-SA 4.0)”. This figure illustrates how legumes (here beans) fix nitrogen from the atmosphere. This process is actually carried by bacteria (from the Rhizobium family) living symbiotically in nodules located at the root of the plant.

There also exist free living N fixing bacteria in soil, which contribute more to N inputs in the soil that was previously thought (Ladha et al., 2016). For a long time, the only anthropic N input was organic amendment, such as compost or manure; which’s nitrogen content is variable and generally low (NFU, 2022). Today however, synthetic N fertilizer is the main source of nitrogen input in soil, with yearly applications as high as 450 or even 750 kgN ha^{-1} (Jarvis et al., 1991). These excesses have driven the consequences mentioned in **section 1.2** but they also have altered the biological cycle of microorganisms (Sivojiene et al., 2021). For example, under amendment of fertilizer, large N_2O emissions from soil microorganisms are typically observed (Loick et al., 2017).

1.4) Sources of N_2O in soil

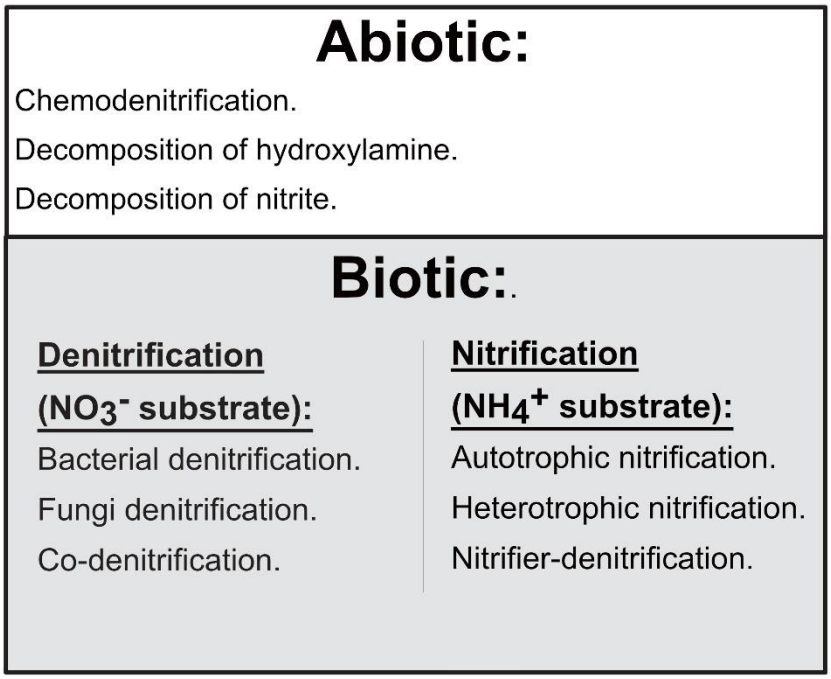

***Figure 5**: The different sources of N_2O in soil.*

Both microbial and abiotic processes are at the origin of N_2O emissions.

The emissions of N_2O from soil can originate from several sources (**Figure 5**). The three main sources are denitrification (the biological pathway in which nitrate is transformed into N_2O), nitrification (the biological pathway in which ammonium is transformed into N_2O) and soil abiotic processes. As mentioned previously, denitrification is a microbial respiration process under suboxic conditions and is primarily performed by microbes living in soil anaerobic microsites. Since oxygen does not diffuse much in soil, nitrate is used as an alternative electron acceptor. Nitrate is indeed the soil inorganic substance which's reduction yields the highest energy (ΔG ~ -28.4 kcal mol^{-1} e^{-1} compared to -29.9 kcal mol^{-1} e^{-1} for O_2; Megonigal et al., 2004). The denitrification process occurs in step as:

$NO_3^- + 2\ H^+ + 2\ e^- \rightarrow H_2O + NO_2^-$ [1]

$NO_2^- + 2\ H^+ + e^- \rightarrow H_2O + NO$ [2]

$2\ NO + 2\ H^+ + 2\ e^- \rightarrow H_2O + N_2O$ [3]

$N_2O + 2\ H^+ + 2\ e^- \rightarrow H_2O + N_2$ [4]

It is a sequence of reductions from nitrate, to nitrite (NO_2^-), to nitric oxide, nitrous oxide and finally to dinitrogen (N_2). Each reaction necessitates a specific reductase enzyme. A wide range of bacterial groups are capable of performing denitrification: *Bacillus*, *Enterobacter*, *Micrococcus*, *Pseudomonas*, *Spirillum*, *Proteus*, *Aerobacter* and *Flavobacterium* (Meng et al., 2014). Fungi also possess the capability for denitrification although in general, they lack the reductase enzyme necessary to reduce N_2O into N_2 (Matsuoka et al., 2017). For this reason, it is assumed that fungi contribute mostly to N_2O emissions (Laughlin et al., 2002). Co-denitrification is an alternative denitrification reactional pathway in which one N atom is derived from the nitrate pool while the second one derives from the organic pool (Spott et al., 2011). For this reason, it is considered a hybrid process.

As previously mentioned, nitrification is a metabolic process nitrifying bacteria use for their own metabolism and growth. It occurs under aerobic conditions in two distinct steps:

$NH_3 + O_2 \rightarrow NO_2^- + 3\ H^+ + 2\ e^-$ [5]

$NO_2^- + H_2O \rightarrow NO_3^- + 2\ H^+ + 2\ e^-$ [6]

N_2O can be formed during either of these steps. In the case of autotrophic nitrification, two distinct microbial communities carry out a sole reactional step in syntrophy. Ammonia oxidizer bacteria (and archaea) carry out the first reactional step, the product of which is used by nitrite oxidizer bacteria (and archaea) to carry out the second reactional step.

Heterotrophic nitrification on the other hand is carried out by a wide range of fungi and bacteria who can transform organic and inorganic N into nitrate. The cellular rate of heterotrophic nitrification are lower than this of autotrophic nitrifiers and it is unclear what are the benefits of nitrification for heterotrophs, although it can be significant in acid soils or soils with high C:N ratios and biomass (Prosser, 2004). One possible explanation is that heterotrophic nitrification participates to the provision of nitrate under aerobic conditions which would then be available for denitrifying organisms once the conditions become anaerobic (Castignetti & Hollocher, 1984).

As mentioned previously, nitrifier-denitrification can be a source of N_2O in soil since it follows the sequence of both nitrification and denitrification, which can both emit nitrous oxide.

Finally, N_2O can be formed abiotically via chemo-denitrification, where soil nitrate and nitrite are chemically reduced by ferrous iron (Fe(II)) in the same stepwise process as classic denitrification (Buessecker et al., 2019). Other abiotic sources of N_2O include nitrite decomposition, hydroxylamine decomposition or reaction of nitrite with hydroxylamine, but all these abiotic processes are considered negligible (Bremner, 1997).

1.5) The importance of the denitrification process

Denitrification is a key process of nitrogen removal in soil. In agricultural lands, it is one of the main ways of fertilizer loss (along with nitrate leaching and ammonia volatilization; Lassaletta et al., 2014). As mentioned in the previous paragraph, denitrification is a source of N_2O, however, due to its full sequence of reaction, it is also the only natural sink for respiratory reduction of N_2O into N_2. Denitrification measurements are unfortunately rare. Firstly, because it is a highly variable process (both temporally and spatially; Philip Robertson, 1997),

and secondly because the high atmospheric N_2 background renders the detection of soil emitted N_2 molecules particularly difficult (Groffman et al., 2006). Currently, the ^{15}N Gas flux method (^{15}NGF) is the best suited technique to measure *in situ* denitrification dynamics. Briefly, it uses a ^{15}N-labelled nitrate tracer applied to incubated soil to derive the fluxes of denitrified N_2O and N_2 via their isotopic signature in the headspace of the incubation vessel. As for all the methods of denitrification measurement, it is currently limited by its sensitivity; which makes *in situ* N_2 flux detection difficult outside of peak events. A further characterization of denitrification is the partitioning of N_2O sources, notably the contributions of bacteria and fungi to denitrified N_2O emissions. Whilst this is not currently doable using a ^{15}N tracer, newly developed methods using naturally abundant (NA) isotopes enable to constrain the different processes mentioned in **chapter 1.4**.

Although environmentally benign, characterization of N_2 emissions is of primary importance to determine the denitrification product ratio (PR), defined as the proportion of denitrified N_2O relative to the total denitrification emissions (N_2O + N_2). This PR enables to fully characterize the last process step, the reduction of N_2O into N_2 and thus the efficiency of denitrification as sink of nitrous oxide (e.g. a product ratio of 5% means that the nitrous oxide sink efficiency was 95%). Increased temperature and moisture tend to decrease the PR but increase the magnitude of flux, which might lead to higher N_2O fluxes (Granli & Bockman, 1994; Clayton et al., 1997). It has also been shown that pH reduction (through the application of lime) leads to the decrease of the PR and magnitude of N_2O emissions (Zhang et al., 2023). On the other hand, increased PR has been correlated with higher levels of nitrate concentration (Blackmer & Bremner, 1978; Warner et al., 2019). The main expected difference between conventional and regenerative agriculture is probably the nitrate levels,

which are highly increased under amendment of fertilizer. Therefore, we expect a higher denitrification PR and N_2O emissions in conventional agriculture.

1.6) Research questions and thesis layout

This present work aims to first elucidate the enigma of denitrification quantification, before investigating its importance in conventional and regenerative agriculture; in particular in response to N fertilizer application.

Our research questions were:

- How much can we increase the limit of detection of the ^{15}NGF by combining it with an artificial atmosphere?
- Is the denitrification process stimulated by the addition of a ^{15}N-NO3 tracer? And by the addition of large quantities of nitrogen fertilizer?
- How much fertilizer is lost to the environment via denitrification after application?
- How do leys compare to conventional agriculture in terms of denitrification during and outside of the cultivation period? Is there a significant difference between unfertilized and fertilized ley?
- Is denitrification constant over time or does it follow temporal patterns?
- How much global warming potential can be saved with regenerative agriculture?
- Can we combine the ^{15}NGF and naturally abundant isotopes to completely partition the sources of N_2O?

We hypothesized that denitrification would be a less efficient sink for nitrous oxide emissions in conventional agriculture than in regenerative agriculture and that the application of fertilizer would result in large quantities of nitrogen lost via denitrification. Furthermore, we

hypothesized that denitrification would exhibit large temporal variations that have not been properly characterized so far due to the technical difficulties involved. Finally, we hypothesized that denitrified N_2O emissions in conventional agriculture would be dominated by bacteria rather than fungi.

In **Chapter 2** of this thesis, we will study the strengths and weaknesses of ^{15}N Gas Flux method for the measurement of *in situ* denitrification and the associated technical challenges to overcome in order to increase its sensitivity. **Chapter 3** describes the one-year method development in which we combined the ^{15}NGF to an artificial atmosphere for field measurement of denitrification, using either modified static chambers or plastic liners. **Chapter 4** is dedicated to a one-year field campaign where we further validated the new denitrification measurement method as well as measured *in situ* denitrification, greenhouse gas emissions and key soil parameters (nitrate and ammonium contents, moisture, dissolved organic and nitrogen contents or laboratory potential of mineralization). These measurements took place in two types of long-term ley rotations (regenerative agriculture) and an arable control (conventional agriculture). In **Chapter 5**, we are combining the ^{15}NGF to naturally abundant ^{15}N isotopes to completely partition the sources of N_2O of the arable soil studied during the one-year campaign. Finally, **Chapter 6** will synthetize all the results of the present thesis and offer a future outlook perspective on potential research for the measurement of denitrification and its importance in agriculture.

1.7) Experimental design

This PhD benefited from the Sustainable Agriculture Research and Innovation Club (SARIC) project "Restoring soil quality through re-integration of leys and sheep into arable rotations". As described by the project's name, the aim was to evaluate the impact of long ley rotations

(5 years) coupled with sheep grazing on restoration of damaged agricultural lands. Two types of leys were studied in this project, **grass/clover ley** and **herbal ley**. The traditional grass/clover mix is the most predominant form for ley and rotational grazing in the UK (Kingston-Smith et al., 2013) and its high proportion of white and red clovers (*trifolium repens* and *trifolium pratense* respectively) usually enables higher levels of nitrogen in the soil. Herbal leys have been promoted for over a century in temperate regions (Jordon et al., 2022) and consist in more complex mixes of legumes, perennial forbs and grasses which bring a wide range of ecological benefits in addition to nitrogen fertilization; amongst which: enhanced soil health and reduced soil erosion thanks to deep and dense rooted systems, improved biodiversity or enhanced pest and disease resistance.

The SARIC project benefited from four split-field experiments where a single agricultural field was split into three parts, one for an herbal ley, one for a grass clover ley and one for conventional agriculture.

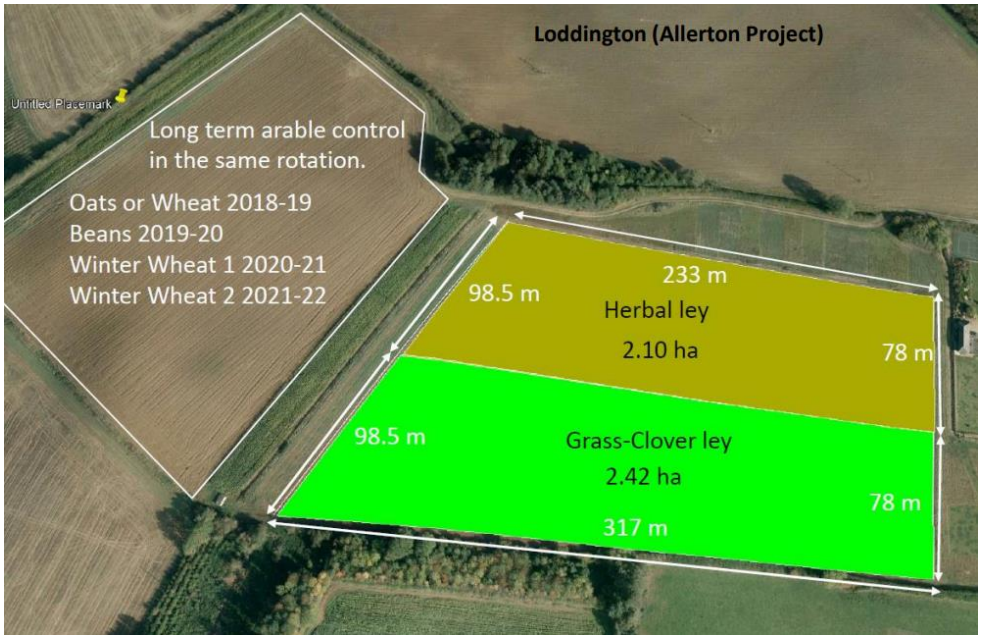

***Figure 6**: The experimental layout at the Allerton Project site.*

The methodological development of **Chapter 3** was performed at The Allerton Project Game & Wildlife Conservation Trust (Loddington, UK), part of the SARIC project (**Figure 6**). However, with this project coming to an end at the end of 2021, another site had to be selected for the one-year field campaign of **Chapter 4**. The FarmED site near Shipton-under-Wychwood in the Cotswolds (UK) offered an ideal setup for the one-year field campaign, with strips of herbal leys of different age and a conventional agriculture control plot. Since this site did not have a conventional grass/clover ley however, we had to find a nearby field under such management (**Figure 7**).

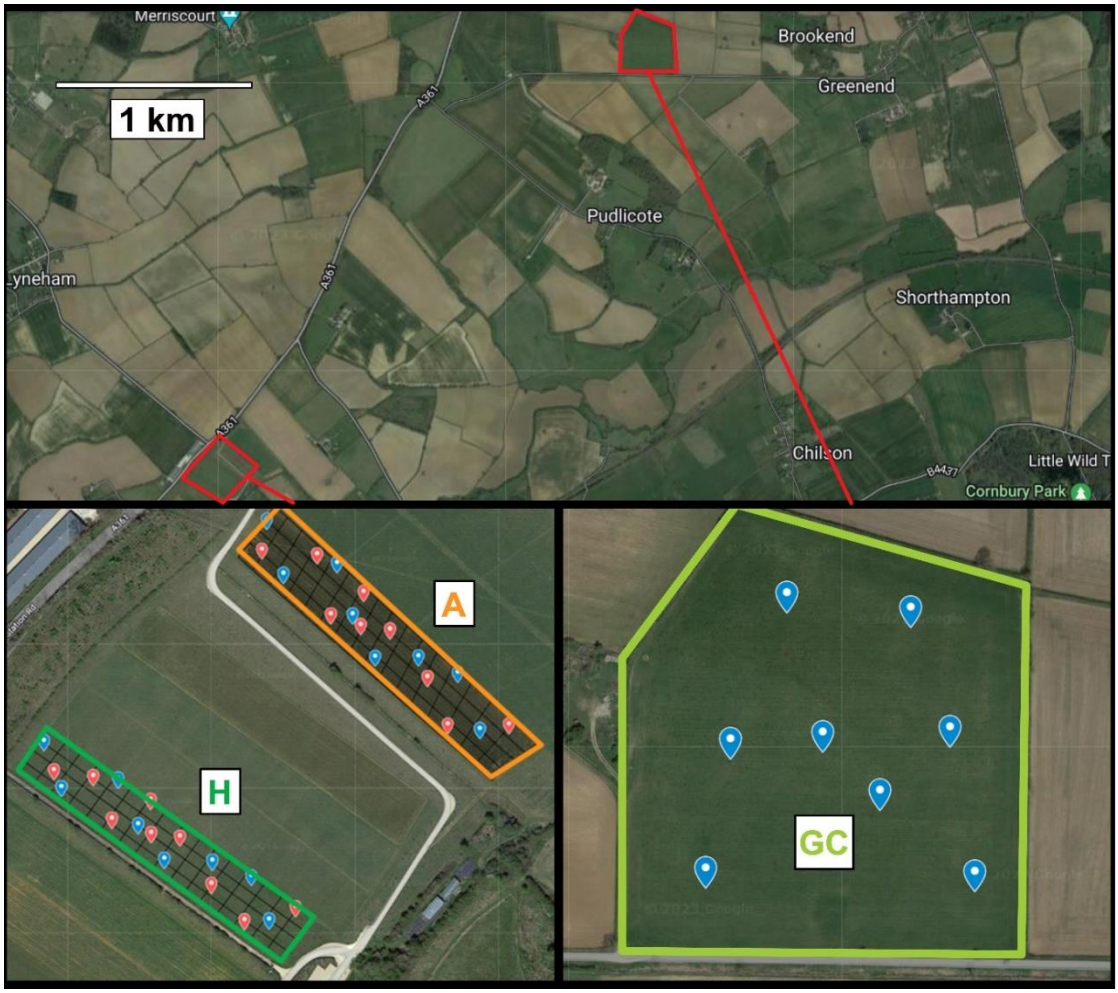

***Figure 7**: Experimental layout for the one-year field study of Chapter 4.*

FarmED site (left) and nearby grass/clover ley (right) studied during our one-year field campaign. The red pins represent static greenhouse gas chamber locations while the blue pins represent the sampling locations for denitrification measurements (see **chapter 4**).

1.8) References

Araus, J. L., Ferrio, J. P., Voltas, J., Aguilera, M., & Buxó, R. (2014). Agronomic conditions and crop evolution in ancient near east agriculture. *Nature Communications*, *5*(May). https://doi.org/10.1038/ncomms4953

Ben-Noun, L. (2017). *Food preservation from antiquity to the present*.

Biswas, B., & Gresshoff, P. (2014). The Role of Symbiotic Nitrogen Fixation in Sustainable Production of Biofuels. *International Journal of Molecular Sciences*, *15*(5), 7380–7397. https://doi.org/10.3390/ijms15057380

Blackmer, A. M., & Bremner, J. M. (1978). Inhibitory effect of nitrate on reduction of N2O to N2 by soil microorganisms. *Soil Biology and Biochemistry*, *10*(3), 187–191. https://doi.org/10.1016/0038-0717(78)90095-0

Bocquet-Appel, J.-P., & Bar-Yosef, O. (Eds.). (2008). *The Neolithic Demographic Transition and its Consequences*. Springer Netherlands. https://doi.org/10.1007/978-1-4020-8539-0

Bremner, J. M. (1997). Sources of nitrous oxide in soils. In *Nutrient Cycling in Agroecosystems* (Vol. 49). Kluwer Academic Publishers.

Buessecker, S., Tylor, K., Nye, J., Holbert, K. E., Muñoz, J. D. U., Glass, J. B., Hartnett, H. E., & Cadillo-Quiroz, H. (2019). Effects of sterilization techniques on chemodenitrification and N2O production in tropical peat soil microcosms. *Biogeosciences*, *16*(23), 4601–4612. https://doi.org/10.5194/bg-16-4601-2019

Butterback-Bahl, K. (2011). Nitrogen processes in terrestrial ecosystems BT - The European Nitrogen Assessment. *The European Nitrogen Assessment*, *6*, 1–27. papers2://publication/uuid/024161DF-0449-45F9-8D10-B697C11032FC

Cassman, K. G., & Pingali, P. L. (1995). Intensification of irrigated rice systems: Learning from the past to meet future challenges. *GeoJournal*, *35*(3), 299–305. https://doi.org/10.1007/BF00989137

Castignetti, D., & Hollocher, T. C. (1984). Heterotrophic nitrification among denitrifiers. *Applied and Environmental Microbiology*, *47*(4), 620–623. https://doi.org/10.1128/aem.47.4.620-623.1984

Clayton, H., McTaggart, I. P., Parker, J., Swan, L., & Smith, K. A. (1997). Nitrous oxide emissions from fertilised grassland: A 2-year study of the effects of N fertiliser form and environmental conditions. *Biology and Fertility of Soils*, *25*(3), 252–260. https://doi.org/10.1007/s003740050311

Cooledge, E. C., Chadwick, D. R., Smith, L. M. J., Leake, J. R., & Jones, D. L. (2022). Agronomic and environmental benefits of reintroducing herb and legume-rich multispecies leys into arable rotations: a review. *Frontiers of Agricultural Science and Engineering*, *9*(2), 245–271. https://doi.org/10.15302/J-FASE-2021439

Davidson, E. A., Hart, S. C., Shanks, C. A., & Firestone, M. K. (1991). Measuring gross nitrogen mineralization, and nitrification by 15 N isotopic pool dilution in intact soil cores. *Journal of Soil Science*, *42*(3), 335–349. https://doi.org/10.1111/j.1365-2389.1991.tb00413.x

Diamond, J., & Bellwood, P. (2003). Farmers and Their Languages: The First Expansions. *Science*, *300*(5619), 597–603. https://doi.org/10.1126/science.1078208

FAO - Food and Agriculture Organization of the United Nations (2017). *World fertilizer trends and outlook to 2020*. Retrieved from https://www.fao.org/3/i6895e/i6895e.pdf (consulted 27/07/2023).

FAO - Food and Agriculture Organization of the United Nations (2022a). *Pesticides use, pesticides trade and pesticides indicators*. Retrieved from https://www.fao.org/3/cc0918en/cc0918en.pdf (consulted 27/07/2023).

FAO - Food and Agriculture Organization of the United Nations (2022b). *Agricultural production statistics 2000–2021*. Retrieved from https://www.fao.org/3/cc3751en/cc3751en.pdf (consulted 27/07/2023).

FiBL, & IFOAM. (2019). *The World of Organic Agriculture Statistics and Emerging Trends 2019 Edited by Helga Willer and Julia Lernoud For PDF* (H. Willer & J. Lernoud (Eds.)). https://orgprints.org/id/eprint/37018/1/willer-lernoud-2019-world-of-organic-low.pdf

Granli, T. and Bockman, O.C. (1994) Nitrogen Oxide from Agriculture. Norwegian Journal of Agriculture Science, 12, 7-127.

Graves, A. R., Morris, J., Deeks, L. K., Rickson, R. J., Kibblewhite, M. G., Harris, J. A., Farewell, T. S., & Truckle, I. (2015). The total costs of soil degradation in England and Wales. *Ecological Economics*, *119*, 399–413. https://doi.org/10.1016/j.ecolecon.2015.07.026

Groffman, P. M., Altabet, M. A., Böhlke, J. K., Butterbach-Bahl, K., David, M. B., Firestone, M. K., Giblin, A. E., Kana, T. M., Nielsen, L. P., & Voytek, M. A. (2006). Methods for measuring denitrification: Diverse approaches to a difficult problem. In *Ecological Applications* (Vol. 16, Issue 6, pp. 2091–2122). https://doi.org/10.1890/1051-0761(2006)016[2091:MFMDDA]2.0.CO;2

Guerci, M., Bava, L., Zucali, M., Sandrucci, A., Penati, C., & Tamburini, A. (2013). Effect of farming strategies on environmental impact of intensive dairy farms in Italy. *Journal of Dairy Research*, *80*(3), 300–308. https://doi.org/10.1017/S0022029913000277

Guest, E. J., Palfreeman, L. J., Holden, J., Chapman, P. J., Firbank, L. G., Lappage, M. G., Helgason, T., & Leake, J. R. (2022). Soil macroaggregation drives sequestration of organic carbon and nitrogen with three-year grass-clover leys in arable rotations. *Science of The Total Environment*, *852*, 158358. https://doi.org/10.1016/j.scitotenv.2022.158358

Haas, G., Wetterich, F., & Köpke, U. (2001). Comparing intensive, extensified and organic

grassland farming in southern Germany by process life cycle assessment. *Agriculture, Ecosystems and Environment*, *83*(1–2), 43–53. https://doi.org/10.1016/S0167-8809(00)00160-2

Houghton, R. A. (2007). Balancing the Global Carbon Budget. *Annual Review of Earth and Planetary Sciences*, *35*(1), 313–347. https://doi.org/10.1146/annurev.earth.35.031306.140057

Humbert, S., Tarnawski, S., Fromin, N., Mallet, M. P., Aragno, M., & Zopfi, J. (2010). Molecular detection of anammox bacteria in terrestrial ecosystems: Distribution and diversity. ISME Journal, 4(3), 450–454. https://doi.org/10.1038/ismej.2009.125

IPCC. (2013). Climate change 2013: The physical science basis. Contribution of Working Group I to the Fifth Assessment Report of the Intergovernmental Panel on Climate Change (Rep., 1535 pp.). Cambridge, UK and New York.

Jarvis, S. C., Barraclough, D., Williams, J., & Rook, A. J. (1991). Patterns of denitrification loss from grazed grassland: Effects of N fertilizer inputs at different sites. *Plant and Soil*, *131*(1), 77–88. https://doi.org/10.1007/BF00010422

Jeffery Leigh, G. (2002). *Nitrogen Fixation at the Millennium*. Elsevier. https://doi.org/10.1016/B978-0-444-50965-9.X5000-9

Jordon, M. W., Willis, K. J., Bürkner, P.-C., & Petrokofsky, G. (2022). Rotational grazing and multispecies herbal leys increase productivity in temperate pastoral systems – A meta-analysis. *Agriculture, Ecosystems & Environment*, *337*, 108075. https://doi.org/10.1016/j.agee.2022.108075

Jovanović, J., Power, R. C., de Becdelièvre, C., Goude, G., & Stefanović, S. (2021). Microbotanical evidence for the spread of cereal use during the Mesolithic-Neolithic transition in the Southeastern Europe (Danube Gorges): Data from dental calculus analysis. *Journal of Archaeological Science*, *125*(November 2020). https://doi.org/10.1016/j.jas.2020.105288

Juřicová, A., Chuman, T., & Žížala, D. (2022). Soil organic carbon content and stock change after half a century of intensive cultivation in a chernozem area. *Catena*, *211*(December 2021). https://doi.org/10.1016/j.catena.2021.105950

Kingston-Smith, A. H., Marshall, A. H., & Moorby, J. M. (2013). Breeding for genetic improvement of forage plants in relation to increasing animal production with reduced environmental footprint. *Animal*, *7*(SUPPL.1), 79–88. https://doi.org/10.1017/S1751731112000961

Kristensen, T., Mogensen, L., Knudsen, M. T., & Hermansen, J. E. (2011). Effect of production system and farming strategy on greenhouse gas emissions from commercial dairy farms in a life cycle approach. *Livestock Science*, *140*(1–3), 136–148. https://doi.org/10.1016/j.livsci.2011.03.002

Ladha, J. K., Peoples, M. B., Reddy, P. M., Biswas, J. C., Bennett, A., Jat, M. L., & Krupnik, T. J. (2022). Biological nitrogen fixation and prospects for ecological intensification in cereal-based cropping systems. *Field Crops Research*, *283*, 108541. https://doi.org/10.1016/j.fcr.2022.108541

Ladha, J. K., Tirol-Padre, A., Reddy, C. K., Cassman, K. G., Verma, S., Powlson, D. S., Van Kessel, C., De Richter, D. B., Chakraborty, D., & Pathak, H. (2016). Global nitrogen budgets in cereals: A 50-year assessment for maize, rice, and wheat production systems. *Scientific Reports*, *6*(October 2015), 1–9. https://doi.org/10.1038/srep19355

Lassaletta, L., Billen, G., Grizzetti, B., Anglade, J., & Garnier, J. (2014). 50 year trends in nitrogen use efficiency of world cropping systems: The relationship between yield and nitrogen input to cropland. *Environmental Research Letters*, *9*(10). https://doi.org/10.1088/1748-9326/9/10/105011

Laughlin, R. J., Stevens, R. J., Laughlin, R. J., & Stevens, R. J. (2002). *Evidence for Fungal Dominance of Denitrification and Codenitrification in a Grassland Soil Optimal soil moisture content, glucose con-centration, and inhibitor concentrations were determined in*.

Loick, N., Dixon, E., Abalos, D., Vallejo, A., Matthews, P., McGeough, K., Watson, C., Baggs, E. M., & Cardenas, L. M. (2017). "Hot spots" of N and C impact nitric oxide, nitrous oxide and nitrogen gas emissions from a UK grassland soil. *Geoderma*, *305*, 336–345. https://doi.org/10.1016/j.geoderma.2017.06.007

Lumpkin, T. A. (2015). How a Gene from Japan Revolutionized the World of Wheat: CIMMYT's Quest for Combining Genes to Mitigate Threats to Global Food Security. In *Advances in Wheat Genetics: From Genome to Field* (pp. 13–20). Springer Japan. https://doi.org/10.1007/978-4-431-55675-6_2

Matsuoka, M., Kumar, A., Muddassar, M., Matsuyama, A., Yoshida, M., & Zhang, K. Y. J. (2017). Discovery of Fungal Denitrification Inhibitors by Targeting Copper Nitrite Reductase from Fusarium oxysporum. *Journal of Chemical Information and Modeling*, *57*(2), 203–213. https://doi.org/10.1021/acs.jcim.6b00649

Megonigal, J. P., Hines, M., & Visscher, P. T. (2004). Anaerobic metabolism: linkages to trace gases and aerobic processes. In W. H. Schlesinger (Ed.), *Biogeochemistry*.

Meng, P., Pei, H., Hu, W., Shao, Y., & Li, Z. (2014). How to increase microbial degradation in constructed wetlands: Influencing factors and improvement measures. *Bioresource Technology*, *157*, 316–326. https://doi.org/10.1016/j.biortech.2014.01.095

Miller-Klugesherz, J. A., & Sanderson, M. R. (2023). Good for the soil, but good for the farmer? Addiction and recovery in transitions to regenerative agriculture. *Journal of Rural Studies*, *103*, 103123. https://doi.org/10.1016/j.jrurstud.2023.103123

National Farmer Union – NFU (2022). Manure versus fertiliser – get the facts. Retrieved from: https://www.nfuonline.com/updates-and-information/manure-versus-fertiliser-get-the-facts/#:~:text=For%20example%2C%20cattle%20farmyard%20manure,that%20one%20tonne%20of%20fertiliser (consulted 18/10/2023).

Nayak, A., Basa, K. K., Boivin, N. L., Fuller, D. Q., Mohanty, R. K., Kingwell-Banham, E., Murphy, C., Roberts, P. J., Lee-Thorp, J., & Bogaard, A. (2022). A stable isotope perspective on archaeological agricultural variability and Neolithic experimentation in India. *Journal of Archaeological Science*, *141*(April), 105591. https://doi.org/10.1016/j.jas.2022.105591

Overton, M. (1996). Re-establishing the english agricultural revolution. *Agricultural History Review*, *44*(1), 1–20.

Overton, M. (2011, February 17). Agricultural Revolution in England 1500 – 1850. Retrieved from: https://www.bbc.co.uk/history/british/empire_seapower/agricultural_revolution_01.shtml (consulted 26/07/2023)

Pfromm, P. H. (2017). Towards sustainable agriculture: Fossil-free ammonia. *Journal of Renewable and Sustainable Energy*, *9*(3), 034702. https://doi.org/10.1063/1.4985090

Philip Robertson, G. (1997). Nitrogen Use Efficiency in Row-Crop Agriculture: Crop Nitrogen Use and Soil Nitrogen Loss. In *Ecology in Agriculture* (pp. 347–365). Elsevier. https://doi.org/10.1016/B978-012378260-1/50011-7

Pigière, F., & Smyth, J. (2023). First evidence for cattle traction in Middle Neolithic Ireland: A pivotal element for resource exploitation. *PLOS ONE*, *18*(1), e0279556. https://doi.org/10.1371/journal.pone.0279556

Pilegaard, K. (2013). Processes regulating nitric oxide emissions from soils. *Philosophical Transactions of the Royal Society B: Biological Sciences*, *368*(1621). https://doi.org/10.1098/rstb.2013.0126

Pimentel, D. (1996). the Science of the Total Environment An llIt~Clll~J Jo~l~l 1o¢ ,St'k~tlllc 11 f~nll¢~l Imo t h r~ml*Am~t mn la It ttMl~ Green revolution agriculture and chemical hazards. *The Science of the Total Environment*, *188*, 86–98.

Pingali, P. L. (2012). Green revolution: Impacts, limits, andthe path ahead. *Proceedings of the National Academy of Sciences of the United States of America*, *109*(31), 12302–12308. https://doi.org/10.1073/pnas.0912953109

Prosser, J. I. (2004). Nitrogen in Soils - Nitrification. *Encyclopedia of Soils in the Environment*, *4*, 31–39. https://doi.org/10.1016/B0-12-348530-4/00512-9

Ramankutty, N., & Foley, J. A. (1999). Estimating historical changes in global land cover: Croplands from 1700 to 1992. *Global Biogeochemical Cycles*, *13*(4), 997–1027. https://doi.org/10.1029/1999GB900046

Ravishankara, A. R., Daniel, J. S., & Portmann, R. W. (2009). Nitrous oxide (N2O): The dominant ozone-depleting substance emitted in the 21st century. *Science*, *326*(5949), 123–125. https://doi.org/10.1126/science.1176985

Sanderman, J., Hengl, T., & Fiske, G. J. (2017). Soil carbon debt of 12,000 years of human land use. *Proceedings of the National Academy of Sciences of the United States of America*, *114*(36), 9575–9580. https://doi.org/10.1073/pnas.1706103114

Silverstone, A. L., & Sun, T. ping. (2000). Gibberellins and the green revolution. *Trends in Plant Science*, *5*(1), 1–2. https://doi.org/10.1016/S1360-1385(99)01516-2

Sivojiene, D., Kacergius, A., Baksiene, E., Maseviciene, A., & Zickiene, L. (2021). The Influence of Organic Fertilizers on the Abundance of Soil Microorganism Communities, Agrochemical Indicators, and Yield in East Lithuanian Light Soils. *Plants*, *10*(12), 2648. https://doi.org/10.3390/plants10122648

Sparacino-Watkins, C., Stolz, J. F., & Basu, P. (2014). Nitrate and periplasmic nitrate reductases. Chem. Soc. Rev., 43(2), 676–706. https://doi.org/10.1039/C3CS60249D

Spott, O., Russow, R., & Stange, C. F. (2011). Formation of hybrid N2O and hybrid N2 due to codenitrification: First review of a barely considered process of microbially mediated N-nitrosation. In *Soil Biology and Biochemistry* (Vol. 43, Issue 10, pp. 1995–2011). https://doi.org/10.1016/j.soilbio.2011.06.014

Stephens, L., Fuller, D., Boivin, N., Rick, T., Gauthier, N., Kay, A., Marwick, B., Armstrong, C. G., Barton, C. M., Denham, T., Douglass, K., Driver, J., Janz, L., Roberts, P., Rogers, J. D., Thakar, H., Altaweel, M., Johnson, A. L., Sampietro Vattuone, M. M., … Ellis, E. (2019). Archaeological assessment reveals Earth's early transformation through land use. *Science*, *365*(6456), 897–902. https://doi.org/10.1126/science.aax1192

Townsend, T. J., Ramsden, S. J., & Wilson, P. (2016). How do we cultivate in England? Tillage practices in crop production systems. *Soil Use and Management*, *32*(1), 106–117. https://doi.org/10.1111/sum.12241

Velthof, G. L., & Rietra, R. P. J. J. (2018). *Nitrous oxide emission from agricultural soils*. https://doi.org/10.18174/466362

Warner, D. I., Scheer, C., Friedl, J., Rowlings, D. W., Brunk, C., & Grace, P. R. (2019). Mobile continuous-flow isotope-ratio mass spectrometer system for automated measurements of N2 and N2O fluxes in fertilized cropping systems. *Scientific Reports*, *9*(1), 11097. https://doi.org/10.1038/s41598-019-47451-7

White, K. D. (1970). Fallowing, Crop Rotation, and Crop Yields in Roman Times. *Agricultural History*, *44*(3), 281–290. http://www.jstor.org/stable/3741455

Wrage, N., Velthof, G. L., Van Beusichem, M. L., & Oenema, O. (2001). Role of nitrifier denitrification in the production of nitrous oxide. In *Soil Biology and Biochemistry* (Vol. 33, Issues 12–13). https://doi.org/10.1016/S0038-0717(01)00096-7

Yannopoulos, S. I., Grismer, M. E., Bali, K. M., & Angelakis, A. N. (2020). Evolution of the Materials and Methods Used for Subsurface Drainage of Agricultural Lands from Antiquity to the Present. *Water*, *12*(6), 1767. https://doi.org/10.3390/w12061767

Zhang, B., Zhou, M., Zhu, B., Kemmann, B., Pfülb, L., Burkart, S., Liu, H., Butterbach-Bahl, K., & Well, R. (2023). Threshold-like effect of soil NO3− concentrations on denitrification product N2O/(N2O+N2) ratio is mediated by soil pH. *Soil Biology and Biochemistry*, 109213. https://doi.org/10.1016/j.soilbio.2023.109213

Zhu-Barker, X., Cavazos, A. R., Ostrom, N. E., Horwath, W. R., & Glass, J. B. (2015). The importance of abiotic reactions for nitrous oxide production. Biogeochemistry, 126(3), 251–267. https://doi.org/10.1007/s10533-015-0166-4

Chapter 2: The ^{15}N Gas Flux Method for measuring denitrification

The following chapter aims to study and characterize the ^{15}N Gas flux method for the measurement of denitrification; which will be the main technique used in this thesis and which will be enhanced in **Chapter 3** to derive a new methodology. This chapter explores the biogeochemical principles of the ^{15}NGF, its refinement through time and how the 4 key assumptions we identified can cause errors. It then identifies various actions and solutions for mitigating the impact of these errors on the measurement of denitrification, using literature compilation and relevant denitrification simulation. Finally, it explores the main weakness of the ^{15}NGF (its poor sensitivity towards N_2 detection) and suggests several recommendations to enhance it, which will be used in **Chapter 3**.

This chapter is published as a peer-reviewed paper in the Soil Biology and Biochemistry Journal as:

Micucci, G., Sgouridis, F., Mcnamara, N. P., Krause, S., Lynch, I., Roos, F., Well, R., & Ullah, S. (2023). *The 15 N-Gas flux method for quantifying denitrification in soil : Current progress and future directions*. Soil Biology and Biochemistry, 184(June), 109108.

https://doi.org/10.1016/j.soilbio.2023.109108

The literature compilation, simulations, research, and organization of this paper were carried out by Gianni Micucci under the supervision of Sami Ullah and Fotis Sgouridis. All the cited co-authors reviewed and corrected the manuscript (especially world denitrification expert Reinhard Well from Germany).

The ^{15}N-Gas Flux Method for quantifying denitrification in soil: current progress and future directions

Gianni Micucci[1,*], Fotis Sgouridis[2], Niall P. McNamara[3], Stefan Krause[1], Iseult Lynch[1], Felicity Roos[4], Reinhard Well[5] and Sami Ullah[1,6]

- 1. School of Geography, Earth and Environmental Sciences, University of Birmingham, Edgbaston, B15 2TT Birmingham, United Kingdom.
- 2. School of Geographical Sciences, University of Bristol, BS8 1SS Bristol, United Kingdom.
- 3. UK Centre for Ecology & Hydrology, Lancaster Environment Centre, LA1 4AP Lancaster, United Kingdom.
- 4. UK National Trust, SN2 2NA Swindon, United Kingdom.
- 5. Thünen Institute of Climate-Smart Agriculture, Bundesallee 65, 38116, Braunschweig, Germany.
- 6. Birmingham Institute of Forest Research, University of Birmingham, Birmingham, UK.

Keywords: Denitrification, ^{15}N Gas Flux Method, Nitrogen Cycling, Nitrous Oxide Emission, Stable Isotope Tracing.

2.1) Abstract

Denitrification in soil is a challenging process to quantify under *in situ* conditions, which seriously hampers the ability to accurately close or balance the nitrogen budget of terrestrial ecosystems. The ^{15}N Gas Flux method is one of the best-suited techniques for *in situ* measurement of denitrification. Using a stable $^{15}N\text{-}NO_3^-$ tracer injected or applied on the surface of soil under a closed static chamber, this method enables the measurement of both N_2O and N_2 denitrification fluxes. Its main limitation is certainly the poor sensitivity towards N_2 emissions, which is a common weakness of all denitrification measurement methods. We have also identified 4 assumptions on which this technique relies to be accurate: 1) the tracer is distributed homogenously in the confined soil volume, leading to the formation of a single isotopic pool in equilibrium, 2) absence of hybrid molecule forming processes, 3) quantitative recovery of produced denitrification products in the flux chamber headspace (no diffusive losses) and 4) no stimulatory impacts of nitrate tracer addition on the dynamics of the denitrification process. In this review, we revisit the principles of the ^{15}N Gas Flux method, explore its evolution through time as well as the different models of calculation that have been developed; before assessing the impact of the 4 above-mentioned assumptions through literature compilation and simulation. Finally, we elaborate and discuss key technical aspects of this method to help the reader in understanding and optimally applying the ^{15}N Gas Flux method for the measurement of denitrification.

The outcome of this review shows that in order to address the main limitation of the ^{15}N Gas Flux method (poor N_2 sensitivity), a hybrid approach using an artificial N_2-depleted atmosphere in addition to ^{15}N isotopic tracer seems to be a promising lead, although only a few studies have used it so far (even less so in the field). In particular, we demonstrate here

the existence of a threshold of 10% atmospheric N_2 concentration background, below which the sensitivity increases drastically. We also show here that the 4 assumptions mentioned above are unlikely to be fully fulfilled in the field. The non-homogenous distribution of the ^{15}N tracer in soil has been shown by various authors to cause a 25% underestimation of the rate of denitrification at maximum. Through simulation, we show here that the presence of hybrid molecules should have a moderate impact on total fluxes (N_2 or N_2O similarly) as long as they contribute for no more than 50% of the total emissions (at which point they cause a 12.5% overestimation). The underestimation of denitrification due to subsoil diffusion, which has been reported to be as high as 37%, remains a challenge to quantify. Finally, the impact of substrate isotopic tracer and water additions on a hypothetical stimulation of the denitrification process needs further validation. A decision tree has been implemented at the end of this study to help users applying the ^{15}N Gas Flux method optimally. Overall, our findings show that this method still holds a substantial promise for a more accurate quantification of *in situ* denitrification whilst considering the recommended mitigation of the methodological weaknesses in future research.

2.2) Introduction:

Denitrification is defined as the sequential reduction of soil nitrate (NO_3^-) through microbial respiration under anoxic or suboxic conditions. This nitrate is firstly transformed into nitrite (NO_2^-), then into gaseous nitric oxide (NO), gaseous nitrous oxide (N_2O) and finally into dinitrogen gas (N_2) through microbial redox reactions. In soil, denitrification is considered one of the major pathways of reactive nitrogen (N) removal, which is of particular importance for agricultural lands receiving large inputs of N fertilizer (Lassaletta. et al., 2015). The last intermediate of this sequential reaction is N_2O, which is a greenhouse gas 298 times more

potent in inducing global warming than CO_2 over a 100-year period (IPCC, 2013); and which is also involved in the depletion of the ozone layer (Ravishankara et al., 2009). Denitrification has the ambiguous role of being both the only natural sink for respiratory reduction of N_2O into N_2 and a source of N_2O itself through incomplete denitrification. It is thus of primary importance to fully characterize this process and in particular the last step of the sequence, the reduction of N_2O into N_2. However, several difficulties have prevented scientists from accurately measuring denitrification for more than a century now (Almaraz et al., 2020). First, the large temporal and spatial variabilities of this process render it difficult to measure, and then model, global soil denitrification rates (Groffman et al., 1989; Seitzinger et al., 2006). Secondly, *in situ* measurements are hampered by technical complications; the biggest of which being undoubtedly the quantification of small N_2 denitrification fluxes against the high atmospheric N_2 background. Scientists have been working on developing methods to overcome this challenge and today, three techniques are mainly used to measure denitrification rates from soil (Well et al., 2019**a**); the ^{15}N Gas Flux method (^{15}NGF), the He/O_2 Gas Flow Soil Core method (He/O_2 GFSC) and the Acetylene Inhibition Technique (AIT). The ^{15}NGF uses a stable isotopic tracer ($^{15}NO_3^-$) to quantify denitrification by monitoring the ^{15}N signature of the soil-evolved N_2 (and N_2O) using Isotope Ratio Mass Spectrometry (IRMS). The He/O_2 GFSC uses a gas-tight incubation system under laboratory conditions to remove atmospheric N_2 so that the soil-evolved N_2 can be measured via gas chromatography (GC). Finally, the AIT is an indirect method of measurement which uses gaseous acetylene (C_2H_2) to block the N_2O reductase enzyme of denitrifier microbes, preventing them from reducing N_2O into N_2. Total denitrification is then determined by measuring N_2O emissions. This last technique has been widely used because of its simplicity and low cost, however, it has now become unpopular due to several limitations (Saggar et al., 2013). In particular, it has been

shown that acetylene catalyses the oxidation of NO, causing a “scavenging” of NO and thus inhibiting the sequence of denitrification (Bollmann & Conrad, 1997; Nadeem et al., 2013). Furthermore, acetylene has an inhibitory effect on nitrification (which converts NH_4^+ into NO_3^-), leading to a decrease of the denitrification substrate in soil (Seitzinger et al., 1993). Finally, it has been shown that acetylene only partially inhibits the reduction of N_2O to N_2 (Simarmata et al.,1993; Yu et al., 2010). Overall, the use of the AIT leads to an unpredictable underestimation of denitrification. Laboratory studies (Yu et al., 2010) as well as field studies (Sgouridis et al., 2016) compared the AIT to ^{15}N tracer techniques and found significantly lower denitrification rates when using the AIT. The He/O_2 GFSC offers accurate measurements (Butterbach-Bahl et al., 2002; Cárdenas et al., 2003; Wang et al., 2013; Loick et al., 2016), but its need for a sophisticated gas-tight incubation system limits its use to laboratory studies only. The sensitivity of this method is also generally low and depends on the ability to reduce the atmospheric N_2 concentration (Friedl et al., 2020). Denitrification being complexly linked to its microenvironment, it is highly desirable to measure it *in situ*. The ^{15}NGF is considered today, the most viable method for *in situ* measurement of denitrification. Nonetheless, it also has key limitations and relies on certain assumptions that cannot always be met, tested or validated; inevitably causing biases in the estimation of denitrification. In particular, we identified the poor sensitivity towards N_2 emissions due to the very high atmospheric N_2 background as being the main limitation of this technique. Similarly, we identified 4 main assumptions upon which this method relies: 1) homogenous distribution of the label in soil leading to the formation of a single isotopic pool in equilibrium, 2) absence of hybrid molecule forming processes, 3) quantitative recovery of produced denitrification products in the flux chamber (no diffusive losses) and 4) no stimulatory impacts of tracer addition on the dynamics of the denitrification process. These assumptions are explained and detailed in this

review and are in good accordance with those identified in the recent study of Friedl et al. (2020). The other limitations identified by Friedl et al. (2020) are included in the technical challenges of this study (**Chapter 2.6**). The ^{15}NGF is not the only existing ^{15}N tracer technique for the measurement of denitrification, Myrold (1990) made a review about all the existing ones (which are summed up in **Table 1** along with analytical improvements and developments in recent years). However, the ^{15}NGF is currently the most widely used one for application in soil. It is thus important to revisit its history and explain its fundamental concepts, key hypotheses, further refinements over time and its accuracy in light of assumptions and recent advances in measurements under field conditions, which is the purpose of this study. Furthermore, this study suggests further directions via which to address the main limitations of the ^{15}NGF and fine-tune it for more accurate and robust measurements. Such an approach is imperative to resolve the enigma of accurate quantification of denitrification in soil.

***Table 1**: Table of the different existing 15N techniques for measuring denitrification as reviewed by Myrold (1990) with further refinements and references.*

Technique	Principle	Pro	Cons	Further reference
Variations in natural ^{15}N abundance	Studying the isotopic composition of soil N products. The different reactions of the N cycle will slightly discriminate between ^{14}N and ^{15}N atoms.	Does not require expensive ^{15}N tracer Can discriminate origins of N_2O.	Sensitive to temperature changes and C additions. Different pathways of N transformations have their own isotopic signature, making interpretation difficult.	Zaman et al. (2021 see chapter 7), Lewicka-Szczebak et al. (2020**b**)
^{15}N-labeled fertilizers in mass balance studies	Classic mass balance approach but the use of ^{15}N isotopes allows for a better sensitivity.	Integrates biological activity over space and time. Can easily be adapted to large plots in the field.	Difficulties to budget accurately the different ^{15}N pools, to design proper boundaries when in field. The use of microplots is not so accurate in fields. Accumulation of additive errors.	Meyer et al. (1989).
$^{15}NO_3$ Isotope Dilution and N cycle process models	Application of ^{15}N-NO_3 tracer and following the NO_3 concentration and its ^{15}N abundance.	Integrative in time and space and in estimating rates of other N cycle processes.	Assumes that the rate of nitrification and denitrification are constant. If the previous hypothesis is not true, this method requires a more difficult algebraic model. Only consider denitrification as NO_3 transformation and thus does not take in account immobilization, leaching, plant uptake and DNRA.	Müller et al. (2014).
Direct measurements of $^{15}N_2$ and $^{15}N_2O$ evolution	^{15}NGF method and alternative versions.	See this study.	See this study.	See this study.
^{15}N isotopic dilution	Creating a ^{15}N enriched atmosphere and monitor its dilution as denitrification occurs.	Less disruptive to the soil and easily moved from location to location in the field.	Assumes that rate of denitrification is constant and that no N_2 is fixed. Not a good sensitivity.	Yang et al. (2011) and Well & Butterbach-Bahl (2013) "Comments on Yang et al. study of (2011)".

2.3) Evolution of the ^{15}NGF

The use of a ^{15}N stable isotopic tracer for studying N transformations in soil started in the middle of the 1950's (Wijler & Delwich, 1954; Hauck & Melsted, 1956). In particular, Hauck & Melsted (1956) added a ^{15}N-enirched nitrate solution to soil incubated under laboratory

conditions. As this enriched nitrate was denitrified, gaseous ^{15}N-labelled N_2 was emitted and mixed with atmospheric N_2 (present at natural ^{15}N abundance ~0.37%). Hauck et al. (1958) used these data to show that the isotopic rate of exchange between ^{15}N and ^{14}N atoms was too slow to generate an isotopic equilibrium between the atmospheric and denitrifying pools. In other words, emitted and atmospheric N_2 molecules don't exchange ^{15}N isotopes at an appreciable rate, preventing the formation of a single isotopic pool in equilibrium (see **Chapter 2.4**). Using this property, it was possible to quantify the fluxes of denitrification and thus, the ^{15}NGF method was created (Hauck et al., 1958; Hauck & Bouldin, 1961). However, this technique was not popular at that time for several reasons. Firstly, compared to other ^{15}N tracer techniques (see **Table 1**), it requires large amounts of expensive and highly labelled tracer as well as complex gas handling and mass spectrometric techniques (Arah et al., 1993). Inversely, the AIT approach being cheaper and easier to use was preferred and saw an explosion of its use in the 1970's (Myrold, 1990). The unpopularity of the ^{15}NGF at that time can also be explained by the fact that triple collector IRMS, which can measure two ratios at the same time (contrarily to a double-collector IRMS), were only commercially available in the 1980's (Mulvaney, 1984). Triple collector IRMS are particularly convenient to study denitrification since N_2 and N_2O both require two measured ratios (see **Chapter 2.4**). Finally, further studies were necessary to fully develop this method.

In the 1980's and 1990's, the ^{15}NGF saw a renewed interest thanks to numerous experimental and theoretical publications. It began with the work of Siegel et al. (1982) who reported a detection limit of 5 g N_2-N ha^{-1} day^{-1} using highly enriched ^{15}N label and newer mass spectrometers, where previous studies reported a detection limit from 100 to 1 000 g N_2-N ha^{-1} day^{-1} (Myrold, 1990; citing Focht & Stolzy, 1978; Rolston et al., 1978; Rolston et al., 1982). At the same time, Mulvaney & Kurtz (1982) presented a new method that enabled the

measurement of N_2O production with the ^{15}NGF. It was then possible to estimate simultaneously fluxes of N_2 and N_2O using a single method, which was of great convenience. At this point, the theory of the ^{15}NGF was also investigated more deeply. New equations were derived by Mulvaney (1984) and further refined by Mulvaney & Boast (1986) to quantify denitrification. In 1988, a four-part series of articles critically evaluated the theory and assumptions of the ^{15}NGF method, especially the hypothesis that soil forms a sole isotopic pool after tracer injection (Boast et al., 1988; Vanden Heuvel et al., 1988; Mulvaney, 1988 and Mulvaney & Vanden Heuvel, 1988; see **Chapter 2.4.1** of this study for further details). It was followed by the work of Arah (1992) who derived new equations to measure denitrification rates and then proposed a model for apportioning the sources of N_2O using the ^{15}NGF method (Arah, 1997; see **Chapter 2.4.3**). This model was later used and refined by Bergsma (2001). Finally, it is worth mentioning that Laughlin & Stevens (2003) proved that ^{15}N labelled N_2 and N_2O could be stored in 12 mL Extainer® vials without any change of the ^{15}N enrichment. They even developed a model to account for diffusive losses, enabling a safe storage for 50 weeks. All this progress explains why the ^{15}NGF has increasingly become more popular at the start of the 2000's up to now (Stevens et al., 1997; Clough et al., 2001; Stevens & Laughlin 2002; Laughlin & Stevens 2002; Ruser et al., 2006; Cuhel et al., 2010; Baily et al., 2012; McGeough et al., 2012; Sgouridis et al., 2015; Buchen et al., 2016; Krause et al., 2017; Deppe et al., 2017; Liu et al., 2022 amongst others).

The latest and most promising progress for the ^{15}NGF, is surely the use of a hybrid method. Indeed, as will be shown later in this study (**Chapter 2.6.2**), the use of isotopes alone does not always guarantee a detection of denitrification fluxes. Thus, some studies have tried combining the ^{15}NGF method with the He/O_2 GFSC. The aim is to use ^{15}N isotopes under a N_2-depleted atmosphere, which highly increases the limit of detection. Early work of Spott et al.

(2006) reported a detection limit of 4 µg N_2-N m^{-2} h^{-1} or (0.96 g N_2-N ha^{-1} day^{-1}). Although more expensive and more difficult to use, a small number of studies have used this hybrid method in the laboratory (Meyer et al., 2010; Scheer et al., 2016; Lewicka-Szczebak et al., 2017; Lewicka-Szczebak & Well 2020; Kemmann et al., 2021).

Recently, Well et al. (2019**a**) and Buchen-Tschiskale et al. (2023) brought this hybrid technique to the field and successfully measured denitrification with a sensitivity as low as 0.5 g N-(N_2+N_2O) ha^{-1} day^{-1}.

Other recent progresses on the ^{15}NGF include a simulation designed to account for diffusive losses (Well et al., 2019**b**; see **Chapter 2.5.2** of this study) and an evaluation of different tracer addition approaches (Lewicka-Szczebak & Well, 2020**a**) for both *in situ* and laboratory measurements.

Denitrification is still challenging to measure currently but after almost 70 years of development, the ^{15}NGF remains the most robust technique for its evaluation *in situ*.

2.4) Theory of the ^{15}NGF

The principle of the ^{15}NGF consists of applying a $^{15}NO_3^-$ tracer into soil incubated under a gas tight vessel and measuring the abundance of ^{15}N atoms in both denitrified N_2 and N_2O inside the headspace of the vessel. For *in situ* measurements, a chamber is usually fitted over a collar of confined ^{15}N-labelled soil volume. Laboratory incubations typically take place in sealed jars. Because of the already present N_2 and N_2O molecules in the atmosphere (with their natural ^{15}N abundance), equations had to be derived to discriminate the emitted fluxes of nitrogen (either N_2 or N_2O).

2.4.1) Isotopic equilibrium of the pools

We will only study the case of N_2 to illustrate the concept of pool at isotopic equilibrium here (but similar relations exist for N_2O). In the studied system, there are two pools contributing to the mix of N_2 molecules, the atmosphere where the molecules have a natural ^{15}N abundance ($\boldsymbol{a_a}$ ≈0.37%) and the emitted molecules from the soil denitrifying pool. The denitrifying pool emits N_2 molecules with a ^{15}N abundance ($\boldsymbol{a_p}$) that depends on the enrichment level and quantity of tracer injected. When a pool is at isotopic equilibrium, the distribution of an isotope ^{Y}X within the molecules of this pool will follow a binomial law according to the abundance $\boldsymbol{a_p}$ of this isotope in the considered pool. This means that the probability to find $\boldsymbol{k}$ ^{Y}X isotopes in the $\boldsymbol{n}$ atoms of X inside a molecule equals:

$$p([^{Y}X] = k) = \binom{n}{k} {a_p}^{k} (1 - a_p)^{n-k} \qquad [7a]$$

$$a_p = \frac{number\ of\ isotopes\ ^{Y}X\ \ present\ in\ the\ pool}{total\ number\ of\ atoms\ X\ in\ the\ pool} \qquad [7b]$$

where $\boldsymbol{[^{Y}X]}$ is the number of ^{Y}X isotopes inside a molecule containing $\boldsymbol{n}$ atoms of X.

In particular, for N_2 containing two N atoms, a pool with a ^{15}N abundance $\boldsymbol{a_p}$ will have the following distribution of isotopologues (molecules with same atomic identity but different isotope composition):

$$\%^{28}N_2 = (1-a_p)^2 \qquad [8a]$$

$$\%^{29}N_2 = 2 \times a_p \times (1- a_p) \qquad [8b]$$

$$\%^{30}N_2 = (a_p)^2 \qquad [8c]$$

For example, considering that after tracer addition the incubated soil is at isotopic equilibrium and has an abundance $\boldsymbol{a_p}$ = 20% of ^{15}N atoms, the distribution will be 64%, 32% and 4% of

$^{28}N_2$, $^{29}N_2$ and $^{30}N_2$ respectively. This ideal distribution assumes that no isotopic discrimination occurs during production of N_2O and its reduction to N_2. In theory, this hypothesis is not true due to equilibrium and kinetic isotope effects. Indeed, lightest atoms tend to react faster and thus, ^{14}N atoms will react preferentially, inducing a discrimination (also called isotopic fractionation) in favour of the lightest isotopologue ($^{28}N_2$). However, the ideal distribution is experimentally a good approximation (Cho & Sakdinan, 1978) especially when using highly enriched ^{15}N nitrate.

2.4.2) Equations for N_2 flux determination:

Since Hauck et al. (1958) demonstrated that no isotopic exchange occurs at an appreciable rate between atmospheric N_2 and emitted N_2, the mix is therefore in a non-equilibrium state with two pools of different isotopologue distributions. Knowing these distributions, two main sets of equations were derived as shown below:

2.4.2.1) The Mulvaney & Boast model:

This model was clearly established for both double and triple collector IRMS by Mulvaney (1984) with some mathematical approximations. It was later refined by Mulvaney & Boast (1986) without any approximations. Although it was shown that the simplified equations only induce a significant error when the tracer enrichment in the soil is lower than 20%, only the model without simplification will be considered here. These equations are based on the work of Hauck & Bouldin (1961) and use the differences of the R29 and R30 ratios of N_2 before and after soil incubation following ^{15}N tracer addition. For an IRMS with a triple collector, R29 is the ratio of $^{29}N_2$ to $^{28}N_2$ and R30 is the ratio of $^{30}N_2$ to $^{28}N_2$. Hence:

$$R29_0 = \frac{^{29}\mathrm{N}_2\ atmosphere}{^{28}\mathrm{N}_2\ atmosphere}\ (before\ incubation) \qquad [9a]$$

$$R29_t = \frac{^{29}N_2\ atmosphere + {}^{29}N_2\ denitrified}{^{28}N_2\ atmosphere + {}^{28}N_2\ denitrified}\ (after\ incubation) \qquad [9b]$$

$$\Delta R29 = R29_t - R29_0 \qquad [9c]$$

Dividing the top and bottom parts of the $R29_t$ ratio by the total amount of N_2 and using the above-mentioned distribution of isotopologues (equations [8a] to [8c]) enable to rewrite $R29_t$ as:

$$R29_t = \frac{(1-d)(\%^{29}N_2\ atmosphere) + d(\%^{29}N_2\ denitrified)}{(1-d)(\%^{28}N_2\ atmosphere) + d(\%^{28}N_2\ denitrified)} \qquad [9d]$$

$$R29_t = \frac{(1-d)[2a_a(1-a_a)] + d[2a_p(1-a_p)]}{(1-d)(1-a_a)^2 + d(1-a_p)^2} \qquad [9e]$$

where ***d*** is the proportion of N_2 that derives from denitrification,

$$d = \frac{N_2\ denitrified}{N_2\ denitrified + N_2\ atmosphere} \qquad [9f]$$

Similar equations exist for R30.

Note that $\boldsymbol{a_p}$ and $\boldsymbol{a_a}$ have been used here for the ^{15}N abundance of the soil denitrifying pool and of the atmosphere respectively, rather than $\boldsymbol{^{15}X_N}$ and $\boldsymbol{\gamma}$ as in Mulvaney & Boast (1986) to keep a consistent nomenclature.

The authors then isolate $\boldsymbol{a_p}$ from these equations to determine ***d*** with the following equations:

$$a_p = \frac{-B + \sqrt{B^2 - 4AC}}{2A} \qquad [9g]$$

where,

$$A = 1 - 2a_a + 2(1 - a_a)\frac{\Delta R30}{\Delta R29} \qquad [9h]$$

$$B = 2{a_a}^2 - 2(1 - {a_a}^2)\frac{\Delta R30}{\Delta R29} \qquad [9i]$$

$$C = 2a_a(1 - a_a)\frac{\Delta R30}{\Delta R29} - {a_a}^2 \qquad [9j]$$

And finally,

$$d = \frac{\Delta R29(1-a_a)^2}{\frac{2(1-a_p)(a_p-a_a)}{(1-a_a)} + \Delta R29(1-a_a)^2 - \Delta R29\left(1-a_p\right)^2} \qquad [9k]$$

Technically, the ratio ***d*** is defined for a number of molecules (in mol), but under the headspace of an incubation vessel of constant volume, it is possible to express the concentration of soil-evolved N_2 by:

$$[N_2]_{denitrified} = \frac{d}{1-d}[N_2]_{atm} \qquad [9l]$$

where, $[N_2]_{denitrified}$ is the concentration of denitrified N_2 (ppm), $[N_2]_{atm}$ is the concentration of atmospheric N_2 (ppm).

This concentration is also given by:

$$[N_2]_{denitrified} = d[N_2]_{total} \qquad [9m]$$

where, $[N_2]_{total}$ is the total concentration of N_2 after incubation (denitrified + atmosphere, in ppm).

Since the total N_2 concentration does not vary significantly after denitrification (typically $10^{-8} < d < 10^{-4}$), some authors have also calculated the quantity of evolved N_2 as:

$$[N_2]_{denitrified} = d[N_2]_{atm} \qquad [9n]$$

which is a good approximation to the result given with equation [9l] since $(1 - d) \approx 1$.

2.4.2.2) The Arah model:

A second set of equations has been derived by Arah (1992). These equations are based on a mixing model of the ^{15}N pools (denitrified and atmospheric) rather than a difference before

and after incubation. These equations have been rewritten by Russow et al. (1996) and later by Spott et al. (2006). The latter version is the most commonly used and is the one presented here.

Again, soil is incubated in an isolation vessel which encloses the native atmosphere inside it. Initially, the ^{15}N abundance in the headspace of the vessel is the natural ^{15}N abundance $\boldsymbol{\alpha_a}$. After the duration of the incubation, it will change due to the denitrification of the soil ^{15}N-NO_3^- to a new abundance $\boldsymbol{\alpha_m}$, given by:

$$a_m = (1 - d) \times a_a + d \times a_p \qquad [10a]$$

where we denote again $\boldsymbol{\alpha_p}$ to be the enrichment of the soil denitrifying pool while ***d*** is still the proportion of N_2 that derives from denitrification (see equation [9f]). $\boldsymbol{\alpha_m}$ and $\boldsymbol{\alpha_a}$ can be calculated as:

$$a_m = \frac{R_{29}+2R_{30}}{2(1+R_{29}+R_{30})}\ (after\ incubation) \qquad [10b]$$

$$a_a = \frac{R_{29}+2R_{30}}{2(1+R_{29}+R_{30})}\ (before\ incubation) \qquad [10c]$$

The same mixing equation can be used for the proportion of $^{30}N_2$. Let us call $\boldsymbol{\alpha_i}$ the proportion of $^{30}N_2$ in the pool ***i***:

$$\alpha_m = (1 - d) \times \alpha_a + d \times \alpha_p \qquad [10d]$$

Where ***i*** has been replaced with:

- *m* for the mix (atmospheric N_2 + denitrified N_2).
- *a* for the atmospheric pool.
- *p* for the denitrifying pool.

One can calculate $\boldsymbol{\alpha_m}$ as:

$$\alpha_m = \frac{R_{30}}{1+R_{29}+R_{30}} \ (after\ incubation) \qquad [10e]$$

Using the binomial distribution, the authors isolate quantities $\boldsymbol{a_p}$ and $\boldsymbol{d}$ by:

$$a_p = \frac{\alpha_m - a_a a_m}{a_m - a_a} \qquad [10f]$$

$$d = \frac{a_m - a_a}{a_p - a_a} \qquad [10g]$$

The concentration of evolved N_2 inside the incubation vessel is then calculated similarly to the model of Mulvaney & Boast (equations [9l] to [9n]).

2.4.2.3) Discussion and further refinements:

Theoretically, both systems of equations are valid. They indeed give the same and correct results when simulating a mix of two pools at isotopic equilibrium. This can be seen in **Table 2** which simulates a mix of atmospheric N_2 and denitrified N_2 in a 4 L chamber, considering atmospheric pressure and assuming ideal gas law.

***Table 2**: Simulation of a mix between atmospheric and denitrified N_2*

Simulation of a 4L chamber, considering isotopic equilibrium of atmospheric and soil denitrifying pools, as well as atmospheric pressure inside the chamber and the ideal gas law. A coefficient d equal to 5.10− 5 has been set for this simulation. The “Atmosphere” and “Denitrification” lines at the top contain the data used for the simulation. Mulvaney and Boast (1986) and Arah (1992) models both yielded the correct results. This simulation also enables to better apprehend the difference in order of magnitude between the quantities of denitrified and atmospheric N2. See **Chapters 2.4.2.1 and 2.4.2.2** for explanations of the calculated coefficients

Atmosphere						
Number of molecules	a_a	$^{28}N_2$	$^{29}N_2$	$^{30}N_2$		
8.39E+22	0.37%	8.33E+22	6.13E+20	1.13E+18		
Denitrification						
Number of molecules	a_p	$^{28}N_2$	$^{29}N_2$	$^{30}N_2$		
4.20E+18	50%	1.05E+18	2.10E+18	1.05E+18		
Mix						
$^{28}N_2$	$^{29}N_2$	$^{30}N_2$	$R29_{(0)}$	$R29_t$	$R30_{(0)}$	$R30_t$
8.33E+22	6.15E+20	2.18E+18	7.35E-03	7.38E-03	1.35E-05	2.61E-05
Mulvaney & Boast						
ΔR29	ΔR30	A	B	C	$^{15}X_N$ (a_p)	d
2.51E-05	1.26E-05	1.99	-1.00	3.65E-03	50%	5.00E-05
Arah						
a_m	α_m	a_p	d			
3.69E-03	2.59E-05	50%	5.00E-05			

However, different results will be obtained depending on which model is used on real experimental data. It is difficult to predict *a priori* which system will be the most accurate. During one of our laboratory incubations (unpublished data), we compared both models of calculation on N_2O emissions (which can also be calculated via the two models but for which sensitivity is higher, see **Chapter 2.4.3** of this study). The experiment consisted of adding different amounts of $^{15}NO_3^-$ tracer to the same soil mix to target a 20, 30, 40 or 50% ^{15}N enrichment of the soil denitrifying pool. **Figure 8** shows boxplots of the observed enrichments for each treatment (6 replica, 6 hours of incubation) calculated using the two sets of equations.

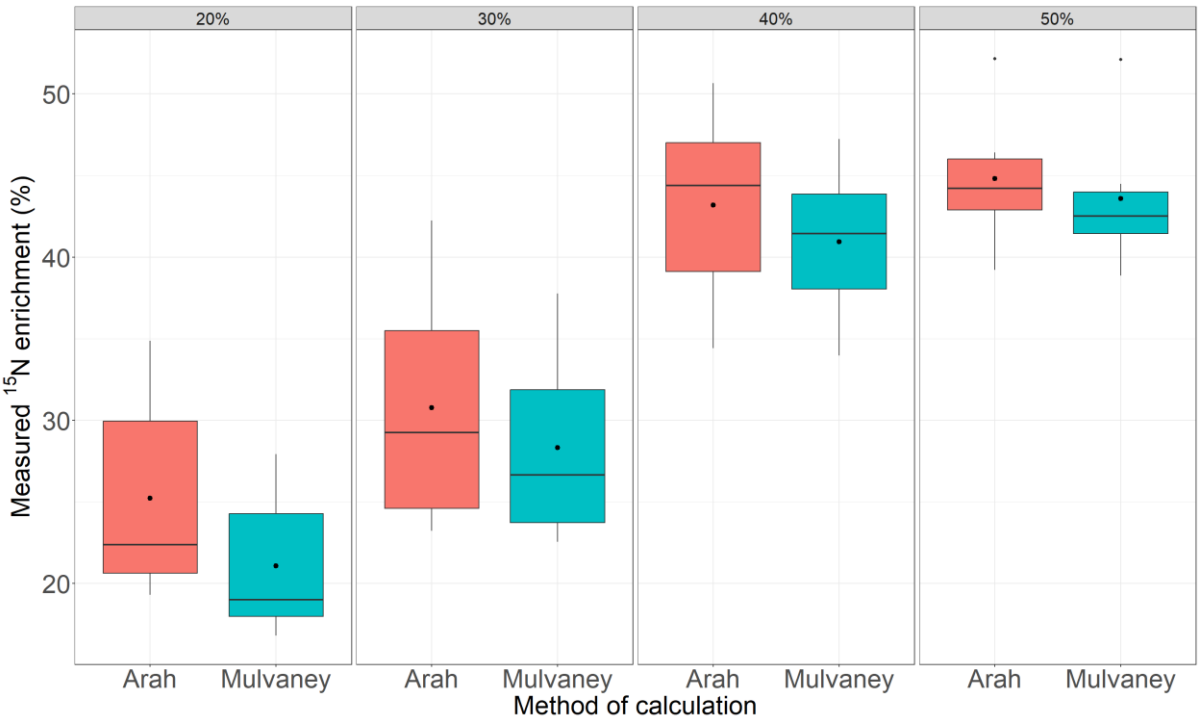

***Figure 8**: Measured ^{15}N enrichment of the soil denitrifying pool for different ^{15}N enrichment targets (20, 30, 40 or 50%)*

Enrichments calculated using either the Arah (red) or Mulvaney (blue) equations during a laboratory experiment. The mean of each series is represented by a large point in the middle of the associated box.

It can be seen from **Figure 8** that using the same raw data, the two systems of calculation yielded different results. Paired student-t tests for each enrichment showed that these systems were statistically different. It is also interesting to note that in exactly each case, the calculated ^{15}N enrichment with the Arah model was strictly superior to the one calculated with the Mulvaney model. After 24 hours, the two models were very comparable, with the Arah model being on average only 2.22% higher. But overall, the Mulvaney model seems to be closer to the targeted enrichment and to have a smaller variability (full study to be published). Ideally, further data would be needed to confirm this trend.

It can also be noted that R30 data are often below the limit of detection of the instrument and difficult to read (see **Chapters 2.6.2** and **2.6.3** of this study), which makes both systems of calculation difficult to use. To solve this issue, Spott et al. (2006) derived an equation from the Arah model that solely uses R29 (after incubation) data. Thus, ***d*** can be calculated as:

$$d = \frac{1}{1-\frac{R29(1-a_p)^2-2a_p(1-a_p)}{R29(1-a_a)^2-2a_a(1-a_a)}} \qquad [11a]$$

This equation is a rewritten version of equation [9k] from the Mulvaney & Boast (1986) model. However, it requires the user to know the degree of enrichment of the soil denitrifying pool $\boldsymbol{a_p}$ which cannot be determined with R29 data alone. A useful tip is to use the enrichment calculated from the N_2O data (see **Chapter 2.4.3** of this study) and hypothesize that N_2O and N_2 have the same degree of ^{15}N enrichment. This is a reasonable assumption since they both originate from the same denitrifying pool, but it could be biased due to heterogeneity of ^{15}N label application and denitrification dynamics (Zaman et al., 2021, chapter 7.2.6.2). However, the isotopic data for N_2O are usually easier to read since the atmospheric background of N_2O is much lower (~0.330 ppm_v, part per million volumetric). In some cases, if the N_2O data cannot be used either (e.g. low N_2O emissions), it is possible to measure the ^{15}N enrichment of the soil denitrifying pool $\boldsymbol{a_p}$ by measuring the ^{15}N enrichment of the soil nitrate $\boldsymbol{a_{NO3}}$ (as in Kulkarni et al., 2014). In theory, $\boldsymbol{a_p}$ and $\boldsymbol{a_{NO3}}$ should be similar, but this is generally not the case due to the dynamics of denitrification in soil, heterogeneity of the label application and dilution of the label by nitrification (Buchen et al., 2016; Deppe et al., 2017; Lewicka-Szczebak & Well 2020**a**; Friedl et al., 2020; Zaman et al., 2021, chapter 7.2.6.2). This is why $\boldsymbol{a_p}$ is more generally referred as the "^{15}N enrichment of the NO_3^- pool undergoing denitrification" and why it needs to be recalculated before the coefficient ***d***.

Although the atmospheric R29 and R30 ratios are supposedly constant, it is recommended to make measurements at t=0 for improved accuracy. Thus, for the model of Mulvaney & Boast (1986), it is probably best to recalculate the ^{15}N abundance of atmosphere $\boldsymbol{a_a}$ just as in the model of Arah (equation [10c]) rather than using the average natural ^{15}N abundance:

$$a_a = \frac{R_{29}+2R_{30}}{2(1+R_{29}+R_{30})}\ (t=0) \qquad [11b]$$

In the case of the Spott et al. (2006) equation using only R29 (equation [11a]), one can recalculate the atmospheric ^{15}N abundance $\boldsymbol{a_a}$ as:

$$a_a = \frac{R_{29}}{2+R_{29}}\ (t=0) \qquad [11c]$$

Finally, the two-pool model can be biased if other sources of N_2 production are present. If a third source comes from an unlabelled soil pool and is at isotopic equilibrium, then this dinitrogen is produced at natural ^{15}N abundance with the same isotopologue distribution as the atmospheric N_2. Hence, a two-pool model is still applicable considering that one of the two pools is the sum of (atmosphere + third source).

The production of hybrid N_2 could however bias the calculations as shown in section **Chapter 2.5.2**.

2.4.3) Methods for determination of N_2O

The total concentration of N_2O can be monitored with GC measurements however, the complementary use of the ^{15}NGF enables measurement of the purely denitrified N_2O contribution, allowing for source partitioning. If hybrid processes are omitted (see **Chapter 2.5.2**), the composition of total measured N_2O after incubation can be represented as shown in **Figure 9** (Bremner, 1997; Wrage et al., 2001; Zou et al., 2014).

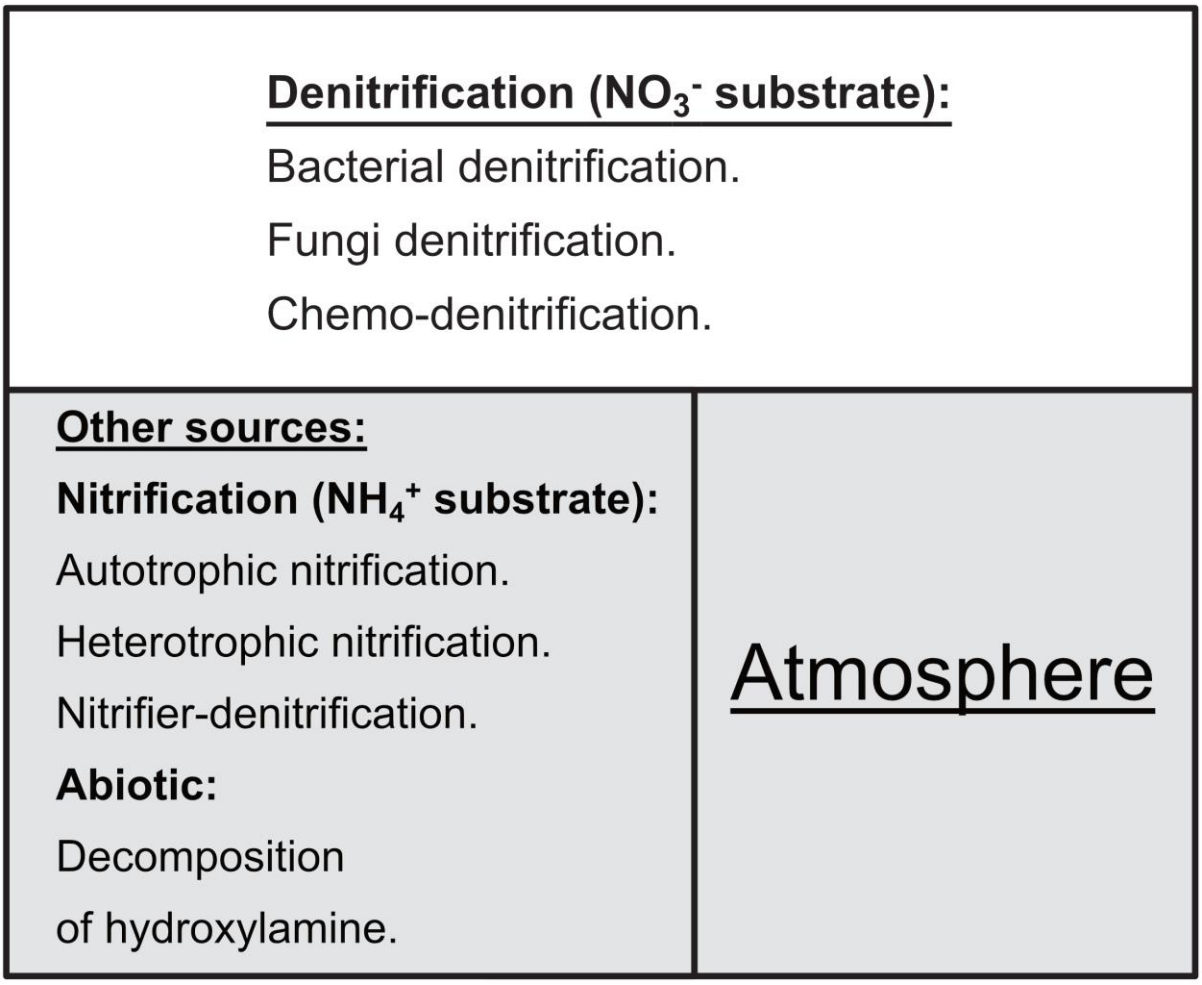

***Figure 9**: Composition of total N_2O after incubation.*

The labelling of the nitrate pool enables the contribution of the denitrification source to be determined against the other sources of N_2O.

The concentration of atmospheric N_2O is assumed to stay constant during the incubation and is given by a GC measurement at t=0 (although it can theoretically be reduced to N_2 via denitrification).

The source partitioning with the use of the ^{15}NGF enables discrimination between nitrate-derived N_2O and the other sources (see **Figure 9**). Nitrification is most likely the biggest of these additional sources of N_2O, thus we will distinguish “denitrification” and “nitrification”

as sources of N_2O from soil for the labelled and unlabelled pools respectively (after subtraction of atmospheric N_2O). It can be added that theoretically, some of the ^{15}N tracer applied as nitrate can be transformed into ammonium through dissimilatory nitrate reduction to ammonium (DNRA) and then be emitted as N_2O through nitrification, thus biasing the source partitioning. This is however unlikely to cause a significant error during the course of an incubation experiment.

The measurement of denitrified N_2O enables quantification of two important parameters of denitrification, which are:

The proportion of emitted N_2O that originates from denitrification (source partitioning coefficient "SPC"),

$$SPC = \frac{N_2O_{denitrified}}{N_2O_{emitted}} \qquad [12a]$$

and the proportion of denitrification products emitted as N_2O, referred as product ratio (PR),

$$PR = \frac{N_2O_{denitrified}}{N_{2\ denitrified} + N_2O_{denitrified}} = 1 - NOSE \qquad [12b]$$

Where NOSE is the nitrous oxide sink efficiency, thus a product ratio of 5% means that 95% of the denitrified N_2O emissions were successfully converted into N_2.

These quantities are probably better characterized by using fluxes calculated from different time step measurements, rather than just the concentration after one time step. However, using multiple time steps for the ^{15}NGF can be rather expensive.

Using the ^{15}NGF method to measure denitrified N_2O allows the accurate determination of the product ratio (equation [12b]), since both N_2O and N_2 have been measured with the same technique. For example, if the denitrifying pool is not uniformly labelled, N_2 emissions will be

underestimated (see **Chapter 2.5.1**). Assuming that N_2O derives from the same soil mineral pool as N_2, the amount of emitted N_2O from denitrification will be underestimated in the same way and thus the denitrification product ratio will be determined more accurately (Bergsma, 2001). Furthermore, if the N_2O emitted by denitrification does derive from the same mineral pool as N_2, then it will have the same ^{15}N abundance (Arah, 1997). Using the ^{15}NGF for N_2O measurement then offers an independent determination of the soil ^{15}N abundance $\boldsymbol{\alpha_p}$ (Bergsma, 2001) and is useful to determine N_2 flux without R30 data (see **Chapter 2.4.2.3**). Partitioning the sources of N_2O is also possible by studying the position of naturally abundant ^{15}N isotopes in the N_2O molecules (Yoshida & Toyoda, 2000; Yu et al., 2020), however, more potential exists in the use of ^{15}N tracer (Stevens et al., 1997).

The first analyses of N_2O using ^{15}N isotopes were performed between the 1970's and the 1980's (Guiraud & Berlier, 1970; Cho & Sakdinan, 1978; Focht et al., 1979 and 1980). The ^{15}N isotope was used to discriminate CO_2 from N_2O since they both have an atomic mass of 44. Thus, the determination of emitted N_2O was made from the measurements at m/z 45 and 46 (Cho & Sakdinan, 1978). However, mass spectrometers at that time were not really designed for measurements at those values and the presence of natural oxygen isotopes complicated the measurements both for CO_2 and N_2O (Mulvaney & Kurtz, 1982). Mulvaney & Kurtz (1982) developed another method involving the dilution of denitrified N_2O with a known amount of N_2 at natural ^{15}N abundance. They then reduced the N_2O gas into N_2, leading to a two-pool system easily resolved with the equations previously derived for N_2. Work from Stevens et al. (1993) represents the first attempt to directly quantify the amount of evolved N_2O through the ratios m/z=44,45,46. Using an N_2O reference of known amount and isotopic composition, the authors were able to directly quantify the fluxes of denitrified N_2O. Later, both Stevens et al. (1997) and Arah (1997) developed models to measure the relative contributions of

nitrification and denitrification to N_2O emissions. Stevens et al. (1997) labelled either the NO_3^- or NH_4^+ pool and then linked the ^{15}N abundance of these pools to the contributions of denitrification and nitrification, respectively. On the other hand, Arah (1997) used the measured ^{15}N abundance from emitted N_2 and hypothesized that the denitrified N_2O evolves from the same mineral pool, having thus the same ^{15}N abundance. However, Arah (1997) states that emitted N_2O evolves in an atmosphere where its initial concentration is negligible. This is not totally true, as the concentration of atmospheric N_2O is approximately 0.330 ppm_v. Bergsma et al. (2001) succeeded to have sensitivity at both this low atmospheric level and at higher concentration and enrichment levels (after incubation following application of ^{15}N tracer) by modifying the head amplifier of their IRMS. By doing so, they developed a new model where N_2O emissions from denitrification can be measured similarly to the way N_2 emissions are measured. Concretely, the same equations as the ones presented in the **Chapters 2.4.2.1** and **2.4.2.2** can be applied if the ratios R29' and R30' (where a prime has been used to distinguish N_2O ratios) are modified to take oxygen isotopes into account:

$$R29' = R45 - R17 \qquad [12c]$$

$$R30' = R46 - (R29)(R17) - R18 \qquad [12d]$$

where R45 and R46 are the ratios for $^{45}N_2O$ and $^{46}N_2O$ respectively, R17 is the $^{17}O/^{16}O$ ratio and R18 is the $^{18}O/^{16}O$ ratio. R17 and R18 are constant at natural abundance, Bergsma et al. (2001) used the values of 0.000373 and 0.0020052 respectively, based on the work of Hayes (1993).

The model of Bergsma et al. (2001) hypothesises that N_2O derived from nitrification has the same ^{15}N natural abundance as atmospheric N_2O. This transforms a three-pool model into a two-pool model, one of these two pools being the sum of (atmosphere + nitrification), as

shown in **Figure 9**. The equations presented in **Chapters 2.4.2.1** or **2.4.2.2** enable the calculation of ***d'***, the fraction of N_2O emitted from denitrification similarly to how ***d*** is calculated for N_2 emissions. This coefficient then needs to be multiplied by the total amount (or concentration) of N_2O measured by GC.

$$[N_2O]_{denitrified} = d'[N_2O]_{total} \qquad [12e]$$

where, $[N_2O]_{denitrified}$ is the concentration of denitrified N_2O (ppm) and $[N_2O]_{total}$ is the concentration of total N_2O (ppm) measured by GC.

The quantity (1-***d***) is the sum of the contributions of atmosphere and nitrification. Nitrification can be determined as:

$$[N_2O]_{nitrification} = [N_2O]_{total} - [N_2O]_{denitrified} - [N_2O]_{atmosphere} \qquad [12f]$$

where, $[N_2O]_{nitrification}$ is the concentration of nitrified N_2O (ppm) and $[N_2O]_{atmosphere}$ is the concentration of atmospheric N_2O (ppm), measured by GC at time 0.

The method of Bergsma et al. (2001) is probably to date, the best method for the evaluation of denitrified N_2O. Furthermore, modern IRMS have a higher range of sensitivity for N_2O analysis and modifying the amplification of the instrument is no longer necessary unless the sample is very concentrated (approx. 5ppm of N_2O, as a general guidance). Similarly to the case of N_2, calculations can be biased if hybrid N_2O is produced, see **Chapter 2.5.2**.

2.5) Assumptions of the ^{15}NGF method

We identified 4 assumptions upon which the ^{15}NGF relies to be accurate. These assumptions are:

1) The tracer is distributed homogenously in the confined soil leading to the formation of a single isotopic pool in equilibrium.
2) No hybrid molecules are formed during the incubation.
3) The denitrification products are recovered quantitatively in the flux chamber (no diffusive losses).
4) No stimulatory impacts of tracer addition on the dynamics of the denitrification process.

In the following section, we discuss how these different assumptions might cause under or over-estimation of the measured denitrifying flux and how we can mitigate their impact.

2.5.1) Homogenous distribution of the tracer in the soil

2.5.1.1) Spatial variations

The calculations of the ^{15}NGF are based on the hypothesis that the soil denitrifying pool of the incubated soil is at isotopic equilibrium. This is very unlikely since soil is highly heterogeneous and because it is virtually impossible to achieve a perfectly homogeneous application of tracer into the soil. For example, in their study of tracer distribution using Bromide (Br-), Berendt et al. (2020) found a theoretical $^{15}NO_3^-$ enrichment of 57-59 at% in the upper 2.5 cm and 26-57 at% in 5-10 cm when targeting a 60% enrichment using different application methods. Furthermore, denitrification presents great spatial variability, occurring typically in anaerobic microsites of soil (Buchen et al., 2016).

Bergsma et al. (1999) used a ternary diagram to represent the distribution of N_2 isotopologues as can be seen in **Figure 10**.

Each side of the triangle represents one of the isotopologues $^{28}N_2$, $^{29}N_2$ and $^{30}N_2$ and any point in the diagram is defined by its unique relative proportions of the three isotopologues. The red line represents isotopic equilibrium. Thus, any pool in such equilibrium is represented by

a point on this curve that solely depends on its ^{15}N abundance. As Bergsma et al. (1999) explained, the two initial pools (A for atmosphere and P for soil) fall on the red curve. The mix (M) is a point that falls on the segment between A and P depending on the relative proportions of atmospheric and emitted N_2. The point M is necessarily below the equilibrium curve, as are all mixes of different pools at isotopic equilibrium (given that those pools have different ^{15}N abundances). In the same idea, the non-ideal soil denitrifying pool could be thought of as the result of different smaller sub-pools at isotopic equilibrium with various ^{15}N abundances, due to the heterogeneity of soil and injected tracer distribution. Then the actual distribution of isotopologues of the denitrified molecules would be represented by a point P_{actual} somewhere beneath the equilibrium curve and necessarily on the line (AM).

Now, when measurements are made, only the composition of atmosphere (A) and the mix (M) are determined. The hypothesis of isotopic equilibrium of the soil denitrifying pool infers that the point P belongs to the red curve ($P_{calculated}$), thus overestimating the real point P_{actual}, as shown in **Figure 10**. The real proportion ***d*** of denitrified N_2 is determined by the ratio AM/AP_{actual} but the one actually calculated is given by $AM/AP_{calculated}$, causing a systematic underestimation.

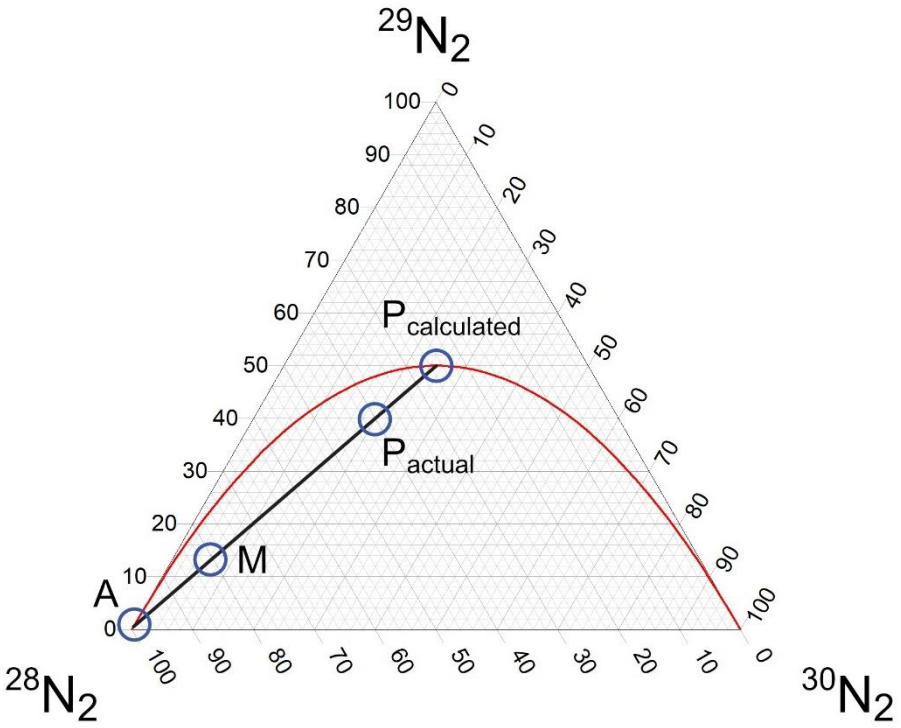

Figure 10 : *Ternary diagram representation of the relative proportions of N_2 isotopologues in a mix between denitrification and atmosphere*

Point A represents the atmospheric N_2. Point M is the mixture of atmospheric and denitrified N_2. Point $P_{calculated}$ represents the estimated isotopologue composition of the denitrifying pool following the isotopic equilibrium hypothesis. Point P_{actual} represents a more realistic isotopologue composition if we consider the soil denitrifying pool as the result of smaller sub-pools at isotopic equilibrium, due to the heterogeneity of soil and injected tracer distribution. Please note this is a schematic view for easier reading, in reality point M will be much closer to point A because of the large proportion of atmospheric N_2.

Boast et al. (1988) and later Arah (1992) both modelled this system in a series of equations to prove that the ^{15}N abundance is always overestimated while the proportion ***d*** is always underestimated when multiple sub-pools exist. Through simulation, Vanden Heuvel et al.

(1988) showed that larger errors arise when the range of enrichments of the sub-pools increases and when the number of pools decreases. This reflects the need to have a homogenous distribution of the tracer in the soil.

Through a series of simulations, Arah (1992) realised that overall, the fraction ***d*** seems to be underestimated by 24% independently of the magnitude of the flux when multiple sub-pools exist. This result has been confirmed independently by Bergsma et al. (1999) using a different model, where the range of the ^{15}N abundances of the sub-pools is distributed uniformly between all of these sub-pools. When using a range from natural abundance to any greater value, they found a systematic underestimation of 25%, which is very close to the result of Arah (1992).

The validity of these conclusions was tested in laboratory studies by Mulvaney (1988) who measured fluxes of N_2O emissions via either GC or the ^{15}NGF (after chemical reduction of total N_2O into N_2 for the ^{15}NGF, see Mulvaney & Kurtz, 1982). Firstly, a good correlation was observed between the two techniques when forming N_2O via chemical oxidation of ^{15}N-labelled NH_2OH/HCl. This means that the emitted N_2O existed as a sole isotopic pool. The same experiment but with two pools of different ^{15}N abundances confirmed that the quantity ***d*** is underestimated with the ^{15}NGF when multiple pools are present, but only significantly when there is a considerable difference in enrichment between the two pools. An underestimation of 10% was reported in this study using a pool enriched at 32% in ^{15}N atoms and one at 53%. Laboratory experiments on soil and soil slurries (to ensure a thorough mixing of the label) offered mixed results. Although the ^{15}NGF often underestimated the rate measured by GC, it also overestimated it in some cases. Mulvaney & Vanden Heuvel (1988) did the same experiment in the field and found similar results, i.e.; the ^{15}NGF often

underestimated the N_2O concentration (by up to 33%) and overestimated it only sometimes (by up to 11%). According to the authors, the underestimations by more than 25% and the overestimations were explained by analytical errors and it was concluded that correct measurements can still be obtained even without perfect distribution of the ^{15}N label in the soil. It can be noted that Figure 2 from Mulvaney & Vanden Heuvel (1988) offers a good visual representation of the spatial heterogeneity of the ^{15}N abundance in soil after tracer injection.

Stevens et al. (1997) also studied the impact of the non-homogenous ^{15}N label distribution on the isotopic equilibrium of the soil denitrifying pool by measuring N_2O emissions but used acetylene (C_2H_2) to block nitrification this time. The ^{15}N abundance of N_2O was then calculated via either R45 or R46 using a one-pool model and values were compared to see if they agreed. Good correlation was observed (Table 2 of the cited reference) which indicates again that the assumption of isotopic equilibrium of the soil denitrifying pool is experimentally a good approximation, even without perfect label distribution.

2.5.1.2) Temporal variations:

As mentioned by Russow et al. (1996), mineralization and nitrification tend to modify the ^{15}N abundance of the soil denitrifying pool after injection of the tracer. Similarly to spatial heterogeneity, if the ^{15}N abundance of nitrate varies over time, the soil denitrifying pool cannot be considered at isotopic equilibrium. The temporal variations are however a bit different as they change the overall ^{15}N abundance of soil nitrate (total number of ^{15}N-labelled nitrate molecules in the studied soil). This is especially relevant for long incubations (>10 hours in the cases of Cuhel et al., 2010; Morse & Bernhardt 2013; Sgouridis & Ullah, 2015 or Xi et al., 2022). It is thus desirable to know the kinetic of dilution of the label in the soil.

It would be very difficult to assess generalities, as the magnitude of transformation of nitrates will vary greatly from one soil to another. Experimental data show that the disappearance of the label can be quite slow. Stevens et al. (1997) observed a decrease from 10% to 5% over ten days and under three different moisture contents (Figure 3 d,e,f, of cited reference). Ruser et al. (2006) observed very little variations over 70 days, usually less than 10% drop (Figure 4 of cited reference). Bergsma et al. (1999) observed a drop from 82% to 72% after three days and half. Rummel et al. (2021) observed different patterns of dilution of the ^{15}N label for different fertilization/plant treatments over a 10-day period (Figure 3 of the cited reference). Although quite variable, we can observe that only a small decrease occurs in the first days.

If a significant drop in the ^{15}N abundance is observed however, it is possible to use the heuristic model of Bergsma et al. (1999) to have an estimation of the induced error and correct for the dilution effect.

2.5.2) Formation of hybrid N_2 and N_2O

The full extent of microbial metabolic transformations in soil is still not totally understood today, yet several reactions could affect the calculations of the ^{15}NGF through formation of hybrid N_2 and N_2O molecules. The term "hybrid" here refers to the fact that within the same molecule, one nitrogen atom comes from the labelled nitrate pool while the other one comes from another source (considered at natural ^{15}N abundance if not labelled). Reactions leading to the formation of hybrid N_2 and N_2O include co-denitrification, anammox and other abiotic processes (Phillips et al., 2016). Co-denitrification was formally identified in the laboratory by Shoun et al. (1992) when amending a fungal strain ("*Fusarium oxysporum*") with NO_3^- enriched at 99% in ^{15}N atoms and observing a significant signal at m/z=29 through a mass spectrometer. This meant that a large number of $^{29}N_2$ molecules were denitrified, which was

not possible given that the nitrate pool was almost exclusively labelled with ^{15}N atoms, which should have led to the production of $^{30}N_2$ molecules only. Tanimoto et al. (1992) demonstrated that one of the two nitrogen atoms was derived from the organic pool of the soil (azide compounds and salicylhydroxamic acid in the case of their study). As explained by Spott et al. (2011**b**), co-denitrification is microbially mediated around neutral pH and most co-denitrifying species are already known as regular denitrifiers (*Pseudomonas sp.*, *Fusarium sp.*, etc.). Furthermore, co-denitrification has already been reported to occur within the three domains Archaea, Bacteria, and Eukarya. Little is known about this process, including its potential magnitude during *in situ* measurements and unfortunately, relatively few studies have focused on its measurement (Laughlin & Stevens, 2002; Spott & Stange, 2011**a**; Long et al., 2013; Selbie et al., 2015; Lewicka-Szczebak et al., 2017; Clough et al., 2017; Rohe et al., 2021). In particular, Laughlin & Stevens (2002) found that 92% of the emitted N_2 was due to co-denitrification rather than denitrification in their study, while Selbie et al. (2015) found a similar percentage of 97%. Lewicka-Szczebak et al. (2017) detected lower contribution from co-denitrification (18% and 5% respectively in two different experiments).

Anammox is the biological process that converts NO_2^- and NH_4^+ into N_2 (see **chapter 1.3**). It is of primary importance in coastal, aquatic and oceanic ecosystems (Thamdrup and Dalsgaard, 2002). However, anammox bacteria have been found in different terrestrial ecosystems such as marshes, lakeshores, permafrost soils or agricultural soils (Humbert et al., 2010).

Abiotic processes leading to the formation of hybrid N_2 and N_2O molecules include chemo-denitrification and decomposition of hydroxylamine (see Phillips et al., 2016 and Zhu-Barker et al., 2015 for further explanations of these processes).

Phillips et al. (2016) described precisely the different ways hybrid N_2 or N_2O molecules can be formed but overall, biotic co-denitrification is probably the predominant process in terrestrial systems.

2.5.2.1) Simulation: How could the presence of hybrid N_2 and N_2O molecules affect the calculations of the ^{15}NGF?

It could be hypothesised that subsequent to the previously mentioned work of Boast et al. (1988), the ^{15}N abundance of the soil denitrifying pool $\boldsymbol{a_p}$ should be overestimated and the proportion of N_2 molecules deriving from denitrification ***d*** underestimated since there is a second pool of nitrogen in the soil. The case is very different here because of the hybrid molecules. The labelled nitrate pool is still considered at isotopic equilibrium, but the hybrid molecules have a different isotopologue distribution. For the emitted N_2 molecules, this distribution can be expressed as:

$$\%^{28}N_2 = (1 - \mathrm{H})(1 - a_p)^2 + H\big(1 - a_p\big)(1 - a_a) \qquad [13a]$$

$$\%^{29}N_2 = (1 - H)2a_p\big(1 - a_p\big) + H\left(a_a\big(1 - a_p\big) + a_p(1 - a_a)\right) \qquad [13b]$$

$$\%^{30}N_2 = (1 - H)a_p^2 + H(a_p a_a) \qquad [13c]$$

Note the appearance of a new term ***H***. It refers to the fraction of emitted hybrid N_2 (hence 0 < ***H*** < 1) and includes all sources of hybrid molecules. We consider the pool of co-substrate (from which the second N atom derives in the hybrid N_2 and N_2O molecules) at natural ^{15}N abundance $\boldsymbol{a_a}$ and we note again $\boldsymbol{a_p}$ the ^{15}N abundance of the soil denitrifying pool. Note that the distribution of isotopologues is analogous to that of Spott & Stange (2011**a**, equations 1, 2 and 3), although here there is no contribution of purely non-hybrid denitrification from the co-substrate. In their case, the co-substrate (hydroxylamine) could be denitrified on its own

abiotically but we will take the more general case where the pool of co-substrate cannot perform denitrification on its own.

Let us compare the ratios R29 and R30 after incubation in the case of pure denitrification and in the case where some hybrid molecules are emitted (***H*** ≠ 0) for the same amount of total denitrified molecules (same coefficient ***d***):

$$R29_D = \frac{(1-d)[2a_a(1-a_a)]+d[2a_p(1-a_p)]}{(1-d)(1-a_a)^2+\mathrm{d}(1-a_p)^2} \qquad [13d]$$

$$R29_H = \frac{(1-d)[2a_a(1-a_a)]+d\left[(1-H)2a_p(1-a_p)+H\left(a_a(1-a_p)+a_p(1-a_a)\right)\right]}{(1-d)(1-a_a)^2+\mathrm{d}\left[(1-\mathrm{H})(1-a_p)^2+H(1-a_p)(1-a_a)\right]} \qquad [13e]$$

$$R30_D = \frac{(1-d)a_a^2+d(a_p)^2}{(1-d)(1-a_a)^2+\mathrm{d}(1-a_p)^2} \qquad [13f]$$

$$R30_H = \frac{(1-d)a_a^2+d\left[(1-H)a_p^2+Ha_pa_a\right]}{(1-d)(1-a_a)^2+\mathrm{d}\left[(1-\mathrm{H})(1-a_p)^2+H(1-a_p)(1-a_a)\right]} \qquad [13g]$$

The subscript “D” refers to the case of classic denitrification and “H” to the case where hybrid sources are present.

With the presence of hybrid molecules, the coefficient ***d*** is renamed “$\boldsymbol{d_{total}}$” and can be more explicitly defined as:

$$d_{total} = d_{denitrification} + d_{hybrid} \qquad [13h]$$

where,

$$d_{denitrification} = (1-H)\, d_{total} \qquad [13i]$$

$$d_{hybrid} = H \times d_{total} \qquad [13j]$$

Similarly, we define:

$$a_{p\ total} = H(\frac{a_a + a_p}{2}) + (1 - H)a_p \qquad [13k]$$

Which is the ^{15}N enrichment of the emitted molecules and could be considered as the apparent ^{15}N enrichment of the soil denitrifying pool, which includes the non-labelled pools contributing to the formation of hybrid molecules.

Given the complexity of the calculations, we made a simulation using Excel (Microsoft, Redmond, WA). For six realistic values of $\boldsymbol{a_p}$ (5%, 10%, 20%, 30%, 40% and 50%), eleven realistic values of $\boldsymbol{d}$ (ranging from 1.10^{-8} to 1.10^{-3}) were used with nine values of H (from 0.01% to 100%) as shown in **Table 6** from the **Supporting Information** (**Chapter 2.8.1**), to create 594 different cases. Using a perfect distribution of isotopologues (as per equations [13d] to [13g]), the ideal gas law and assuming atmospheric pressure in a chamber of 4 L, ideal values of R29 and R30 have been calculated. Then, using the calculations of both Arah (1992) and Mulvaney & Boast (1986), the ^{15}N abundance of the soil denitrifying pool $\boldsymbol{a_{p\ calculated}}$ and the coefficient $\boldsymbol{d_{calculated}}$ have been back-calculated as they would be if ignoring the contribution of co-denitrification. These values have been compared to their real counterpart values used for the simulations and error has been determined as a percentage as:

$$\%err\ d_{total} = 100\left(\frac{d_{calculated} - d_{total}}{d_{total}}\right) \qquad [14a]$$

$$\%err\ d_{denitrification} = 100\left(\frac{d_{calculated} - d_{denitrification}}{d_{denitrification}}\right) \qquad [14b]$$

The first equation refers to the error made in the quantification of all emitted molecules ($\boldsymbol{d_{total}}$) where the second equation refers to the error made regarding only the purely non-hybrid molecules emitted through classic denitrification ($\boldsymbol{d_{denitrification}}$).

Similarly, we define:

$$\%err\ a_{p\ total} = 100\left(\frac{a_{p\ calculated} - a_{p\ total}}{a_{p\ total}}\right) \qquad [14c]$$

$$\%err\ a_{p\ denitrification} = 100\left(\frac{a_{p\ calculated} - a_{p\ denitrification}}{a_{p\ denitrification}}\right) \qquad [14d]$$

which refer to the errors made in the calculation of the ^{15}N-enrichment of the soil denitrifying pool considering respectively, the total apparent enrichment ($\boldsymbol{a_{p\ total}}$) or the enrichment of the labelled pool only ($\boldsymbol{a_{p\ denitrification}}$).

2.5.2.2) Results of the simulation

Firstly, it should be noted that the values obtained in the cases where ***H***=100% will not be taken in account as the coefficients $\boldsymbol{d_{calculated}}$ are superior to 1. It seems that the ^{15}NGF does not work when ***H*** becomes very close to 100%. It still gives a coefficient ***d*** inferior to 1 for ***H***=99.90% (at which point the error on $\boldsymbol{d_{total}}$ > 1 000% however) but not if ***H***=99.99%. Similarly, we will not study the cases where ***H***=0.01% and ***H***=0.1% because the repartition of errors at these levels is somewhat more chaotic than in the other cases. However, the magnitude of error on $\boldsymbol{d_{total}}$, $\boldsymbol{d_{dentrification}}$, $\boldsymbol{a_{p\ total}}$ and $\boldsymbol{a_{p\ denitrification}}$ for ***H***=0.01% and ***H***=0.1% is more than negligible as can be seen in **Table 7** from the **Supporting Information** (**Chapter 2.8.1**). Also, the estimations of $\boldsymbol{d_{total}}$, $\boldsymbol{d_{dentrification}}$, $\boldsymbol{a_{p\ total}}$ and $\boldsymbol{a_{p\ denitrification}}$ based on either the method of Arah (1992) or Mulvaney & Boast (1986) did not differ significantly. Although the calculations of Mulvaney & Boast (1986) were more accurate in 263 cases out of 396 (we did not consider the cases where ***H*** = 100, 0.1 or 0.01%), the difference between the two methods was always less than 0.2%.

The first objective was to determine the correlations between the three parameters (***H***, ***d*** and α_p) and the errors made on d_{total}, $d_{dentrification}$, $\alpha_{p\ total}$ and $\alpha_{p\ denitrification}$.

Thus, we ran correlation tests with SPSS (IBM Corp. Released 2019. IBM SPSS Statistics for Windows, Version 26.0. Armonk, NY: IBM Corp) using either Kendall's tau-b or Spearman coefficients. We did not use the Pearson coefficient as upon visual inspection and Shapiro-Wilk tests, the errors were never distributed normally. The correlation tests were run on sub-datasets where two parameters were constant while the studied one varied. The results in **Table 8** from the **Supporting Information** (**Chapter 2.8.1**) show that the errors made on d_{total}, $d_{dentrification}$, $\alpha_{p\ total}$ and $\alpha_{p\ denitrification}$ are all independent of ***d*** and dependent of ***H***. On the other hand, the errors on $\alpha_{p\ total}$ and $\alpha_{p\ denitrification}$ were dependent on α_p where the ones on d_{total} and $d_{dentrification}$ were not.

Obviously, the ^{15}N abundance of the soil denitrifying pool ($\alpha_{p\ denitrification}$) will be underestimated due to the presence of unlabelled pools contributing to the formation of hybrid molecules. The results of this simulation indicate that the apparent ^{15}N abundance of the denitrifying pool ($\alpha_{p\ total}$) will also be underestimated when hybrid molecules are formed. This can be seen in **Figures 16** and **17** from the **Supporting Information** (**Chapter 2.8.1**) which show the evolution of the errors made on $\alpha_{p\ total}$ and $\alpha_{p\ denitrification}$ with either ***H*** or α_p for different scenarios. All of these errors are negative, thus causing a systematic underestimation. This is contrary to the conclusions of Boast et al. (1988) who showed that the ^{15}N abundance of the soil denitrifying pool should be overestimated when multiple pools are present. However, the case here is different again because the presence of hybrid molecules changes the distribution of isotopologues. Similarly, the presence of hybrid sources systematically causes an overestimation of the fraction ***d*** (either d_{total} or $d_{denitrification}$), inversely to the case of multiple pools in isotopic equilibrium as described by Boast et al.

(1988). We can see this result in **Table 9** from the **Supporting Information** (**Chapter 2.8.1**) which shows the average errors made on d_{total} and $d_{dentrification}$ for different values of H. These averages were calculated using all combinations of a_p and d for the same values of H (n=66), since it was shown that d_{total} and $d_{dentrification}$ were not correlated with a_p and d. Using this property, we can extrapolate the results of a specific case (fixed a_p and d) to represent the evolution of the errors made on d_{total} and $d_{dentrification}$ with H for all cases. **Figure 11** represents this evolution for the case a_p = 40% and d = 1.10^{-4} that we will consider a general trend here. This means that no matter how enriched the soil denitrifying pool is or the amount of soil-emitted molecules, the error caused by the presence of hybrid molecules can be read on **Figure 11**.

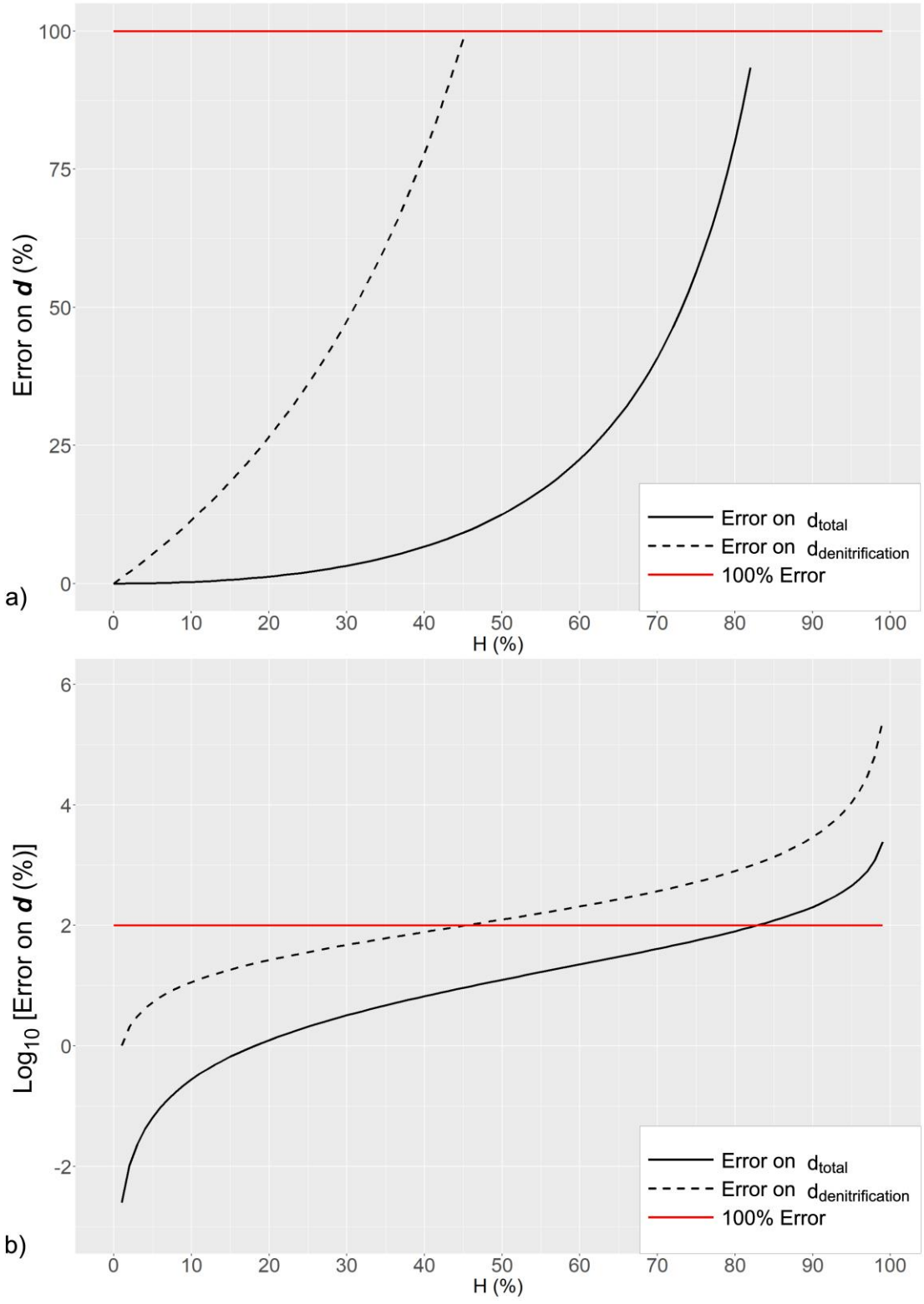

***Figure 11**: (a) Evolution of the error made on the calculation of d_{total} (blue) and $d_{dentrification}$ (pink) with **H** when ignoring the hybrid sources of denitrification, based on 396 simulated cases; (b) same evolution but represented in a logarithmic scale (log 10).*

The horizontal red line represents an error of 100%. The presence of hybrid molecules systematically causes an overestimation of all emitted molecules (d_{total}) and of molecules emitted through classic denitrification ($d_{dentrification}$). The magnitude of these overestimations does not depend on a_p nor d.

We can see that, no matter the quantity of tracer used or the number of emitted molecules, the overestimation of the total number of molecules is insignificant (<1%) until the contribution of hybrid molecules reaches approximately 20%. At 50% of hybrid contribution, the overestimation is 12.5% which can still be acceptable given the general accuracy of the ^{15}NGF. Higher hybrid source contributions however cause great overestimation (80% for H=80%) until H becomes very close to 100%, at which point the error tends to infinity. If studying the quantity of molecules solely emitted through classic denitrification, then the overestimation increases dramatically. It reaches 1% when H=1% already, 26% when H=20% and predicts more than twice the real amount when H=50%.

We verified that all these results and trends were still valid even at a very high enrichment of the soil denitrifying pool and found similar results even at the extreme limit a_p = 100%.

Since the errors made on d_{total}, $d_{dentrification}$, $a_{p\ total}$ and $a_{p\ denitrification}$ are not correlated with the parameter d, the same conclusions should be drawn for N_2O. The study is similar with the exception of the atmospheric background being much smaller (around 0.330 ppm_v) and thus higher d values are typically found. We tested this hypothesis by duplicating the N_2 tables and by only changing the atmospheric background and the range of d values used in the simulations (see **Table 6** from the **Supporting Information** (**Chapter 2.8.1**)). Thus, for sub-datasets of constant H and a_p values, we compared the means of the errors made on d_{total}, $d_{dentrification}$, $a_{p\ total}$ and $a_{p\ denitrification}$ for N_2 and N_2O and expressed a relative difference as:

$$\%err\ W(N_2 - N_2O) = 100 \left| \frac{W_{N_2O} - W_{N_2}}{W_{N_2}} \right| \qquad [14e]$$

where ***W*** is the mean of the errors made on either d_{total}, $d_{dentrification}$, $\alpha_{p\ total}$ or $\alpha_{p\ denitrification}$ for sub-datasets of constant ***H*** and α_p values (n=11). **Table 10** from the **Supporting Information** (**Chapter 2.8.1**) shows that on average, the model for N_2O did not vary significantly from the model for N_2. The highest relative mean of error difference between the two models was for d_{total} and was 1.5×10^{-3} %, the highest coefficient of variation (CV) of a sub-dataset of constant ***H*** and α_p values was 1.18×10^{-8} %; thus, we will consider that similar conclusions can be drawn for N_2 and N_2O.

In conclusion, the formation of hybrid molecules affects N_2 and N_2O emissions similarly (given that the same organism reduces NO and N_2O to N_2O and N_2, respectively). In contrast to the heterogeneous application of the tracer (assumption 1, **Chapter 2.5.1**), it causes an overestimation of the measured quantity of molecules (both the total amount of evolved molecules and the purely denitrified ones) and an underestimation of the enrichment of the soil denitrifying pool (both the total apparent pool which includes the co-substrates and the labelled nitrate pool). The overestimation of the flux does not depend on the quantity of tracer injected (^{15}N enrichment of the soil denitrifying pool α_p) nor the total quantity of emitted molecules (***d***) but only on the proportion of hybrid molecules (parameter ***H***). This might not be true at very low contribution of hybrid molecules (H<1%) but the magnitude of error at this level is so small that it is rendered insignificant. We can add that the underestimation of the ^{15}N enrichment depends on the quantity of tracer injected and the proportion of hybrid molecules, but not on the number of emitted molecules. The total apparent enrichment ($\alpha_{p\ total}$) is not a crucial parameter since the hybrid pool is not at isotopic equilibrium and thus the isotopologue distribution from this source cannot be determined

with it. But it could be an important tool, especially if one wants to prove that hybrid sources contribute to denitrification.

These results are in accordance with the study of Spott & Stange (2007), which found that denitrification is indeed overestimated when hybrid molecules are formed. Their study only focused on the overestimation of purely denitrified molecules ($\boldsymbol{d_{denitrification}}$, which is called "***B***" in the cited study, see Figure 3 of Spott & Stange, 2007). However, we did not find that this overestimation was dependent on the ^{15}N enrichment of the soil nitrate pool, nor on the fraction of atmospheric N_2 (neither with the model of Arah nor with the model of Mulvaney & Boast). We did find however, as in the study of Spott & Stange (2007), that this overestimation is dependent on the proportion of emitted hybrid molecules.

2.5.2.3) Mitigation

Laughlin & Stevens (2002) have developed a method to calculate the contribution of co-denitrification based on previous work by Clough et al. (2001). This model should be applicable no matter the process (or processes) emitting hybrid molecules in a mix with classical denitrification and atmosphere. However, it is important to remember that this method is largely dependent on the assumption that the soil denitrifying pool is at isotopic equilibrium, which as shown before, is unlikely to be true due to heterogeneous distribution of the ^{15}N label (**Chapter 2.5.1**). Violation of this principle could even lead to the assumption that hybrid molecules are being emitted when actually, only classic denitrification is occurring. The best solution would probably be to confirm the presence of hybrid molecules before trying to calculate their contribution, which is unfortunately not easy. Clough et al. (2001) demonstrated that $\frac{\Delta R29}{\Delta R30} = 272$ when co-denitrification occurs (or other processes emitting hybrid molecules) but it is very important to note that this is only the case when all emitted molecules are hybrid (***H***=100%). In the case of classic denitrification (***H***=0), the

quantity $\frac{\Delta R29}{\Delta R30}$ only depends on the ^{15}N enrichment of the soil denitrifying pool (the natural ^{15}N abundance of the atmosphere being considered constant). This can be seen in equation 17 of the study of Mulvaney & Boast (1986). Thus, if the quantity $\frac{\Delta R29}{\Delta R30}$ is not equal to its hypothetic value using the ^{15}N abundance of the soil denitrifying pool, one might suspect the presence of hybrid molecules as in Laughlin & Stevens (2002). However again, because the soil isotopic equilibrium hypothesis might be violated, this might not be a reliable option. Spott & Stange (2007) have developed a model to quantify the contributions of anammox and denitrification to N_2 emissions in aquatic environments when both processes are occurring simultaneously, based on previous work from Tharmdrup & Dalsgaard (2002). According to Spott & Stange (2007), this model can also be used for terrestrial systems when hybrid molecules are emitted. The case is obviously more delicate here since the atmosphere plays a much bigger part in the mix, reducing greatly the sensitivity. The authors also emphasized the need to know if hybrid molecule sources are actually present before using this model. Spott & Stange (2011**a**) proved the presence of a source of hybrid molecules in soil using a sophisticated system combining a soil suspension in water and a flushing of the headspace by a stream of Helium. Precise equations for the exact determination of the contributions of non-hybrid and hybrid molecules were derived as well as the factor R_{binom}, which enables quick assessment of the presence of multiple sub-pools (see **Chapter 2.5.1.1**) or hybrid molecules. Unfortunately, this precise model can only be used in the absence of atmospheric N_2 (using a Helium atmosphere in the example of the cited study), which complicates its use. These new equations were later used by Lewicka-Szczebak et al. (2017) under artificial atmosphere which might explain why they found a more reasonable percentage of co-denitrification (5 and 18% in two different experiments) than Laughlin & Stevens (2002) or Selbie et al. (2015), who both

used the method of Laughlin & Stevens (2002) and found contributions of 92 and 97% respectively of co-denitrification. **Figure 11** shows that if these two contributions were true, applying the ^{15}NGF without taking them in account would result in high overestimations (> 260 and 780% respectively for d_{total}, and > 4 400 and 29 000% respectively for $d_{denitrification}$). The contributions of 5 and 18% found by Lewicka-Szczebak et al. (2017) would result in overestimations of 0.07 and 0.99% respectively for d_{total}, and 5.3 and 23.16% respectively for $d_{denitrification}$.

2.5.3) Quantitative recovery of denitrification products in the flux chamber

Similarly to other incubation techniques, the ^{15}NGF is subject to error due to diffusive losses when used *in situ*. As Myrold (1990) mentioned, the fluxes of gas emissions from soil are a function of not only the production rate but also transport processes. Although convective movements can occur, diffusion is considered the predominant process of gas transport in soil (Clough et al., 2005). Diffusion in one dimension can be modelled by Fick's first law, which states that the diffusion of molecules is proportional to the gradient of their concentration:

$$J_i = -D_i \frac{dC_i}{dz} \qquad [15a]$$

Where J_i is the flux of molecules of the species ***i*** (in mol.m^{-2}.s^{-1}), C_i is the concentration of the species ***i*** (in mol.m^{-3}), D_i is the binary gas coefficient of the species ***i*** (in m².s^{-1}), and ***z*** is the distance from the production zone in this case.

In a first approximation for short-term experiments and for unlabelled gases (N_2O in this case), Hutchinson & Mosier (1981) suggested the following model to predict the evolution of concentration of unlabelled N_2O inside a chamber based on Fick's first law:

$$\frac{dC_t}{dt} = \frac{A}{V}\frac{D_p}{d}(\varphi - C_t) \qquad [15b]$$

Equation [9b] was rewritten with the nomenclature of Pedersen (2000), where $\boldsymbol{\varphi}$ is the hypothetical constant concentration in the production zone at the depth $\boldsymbol{d}$, $\boldsymbol{C_t}$ is the headspace concentration (mol.m^{-3}) at time $\boldsymbol{t}$, $\boldsymbol{V}$ is the volume of the headspace in the chamber (m^3), $\boldsymbol{A}$ is the area of soil incubated (m^2) and $\boldsymbol{D_p}$ is the binary molecular diffusion coefficient of the studied gas in the air at ambient temperature and pressure (in m².s^{-1}).

It is possible to theoretically resolve the model of Hutchinson & Mosier (1980) to determine the concentration profile of unlabelled N_2O in the headspace of the chamber as a function of time (Pedersen et al., 2010):

$$C(t) = \varphi + (C_0 - \varphi)e^{(-\kappa t)} \qquad [15c]$$

With $\kappa = \frac{D_p.A}{V.d}$.

Plotting this evolution as in Pedersen et al. (2001) can give a good idea of how underestimation of a non-labelled gas flux can happen, as illustrated in **Figure 12**.

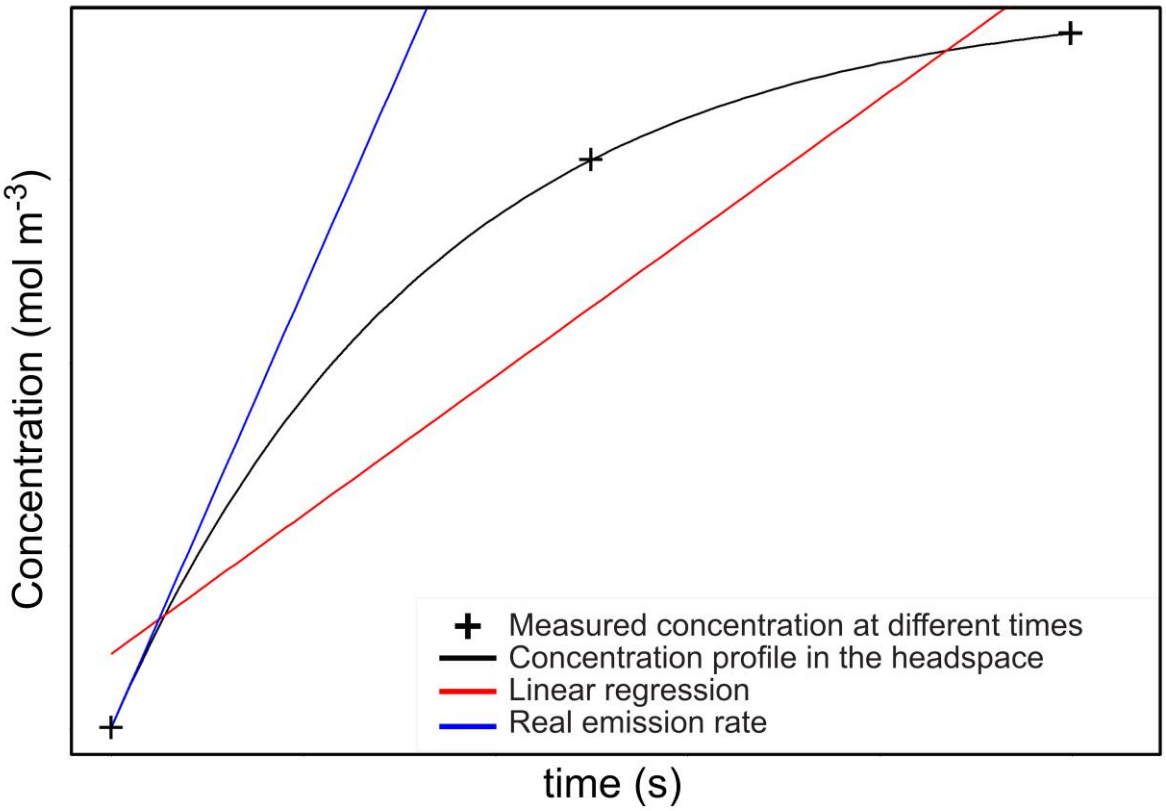

***Figure 12**: Theoretical evolution of unlabelled N_2O concentration inside an accumulation chamber with time (light blue)*

The red line represents a linear regression made using the three hypothetic measurements made at different time steps (light blue crosses). The black line represents the real emission rate of N_2O, as would be measured without the diffusion issues caused by the accumulation of emitted N_2O inside the headspace of the chamber.

The concentration initially increases in an almost linear trend but as accumulation occurs in the headspace of the chamber, this trend slowly declines to reach a plateau. Measuring the initial flux $f_0 = \frac{V}{A}\frac{dC}{dt}_{t=0}$ is thus the best estimate of the magnitude of gas emissions since the effects of diffusion are negligible at that time. If diffusion is ignored and a linear model is applied, then the emission rate is largely underestimated (slope of the red line compared to

the slope of the black line). Several models of diffusion have been developed for non-labelled gases and are summed up in **Table 3**.

***Table 3**: Main diffusion models applicable for measurement of a non-labelled greenhouse gas using an accumulation chamber.*

Parkin et al. (2012) reviewed most of these models for comparison (at the exception of the stochastic extension of the HM and the NDFE models) and estimated their limits of detection.

Method	Profile	Pros	Cons	Reference
Linear regression	Line	Easy and does not require more than two measurements per plot.	Probably the least accurate estimation.	Forthofer et al. (2007).
Hutchinson & Mosier 1981 ("HM")	Exponential	Needs "only" three measurements per plot, improved accuracy.	Relies on the condition $\frac{(C_1-C_0)}{(C_2-C_1)}>1$ (where C_n is the concentration at the time step **n**), which is not true always true. Needs regular time intervals between measurements.	Hutchinson & Mosier (1981), Anthony et al. (1995).
Stochastic model	Exponential	HM approach but more than 3 points can be used for better sensitivity, time intervals don't have to be equals.	Complicated mathematical expression.	Pedersen et al. (2000 & 2001).
Quadratic model	Quadratic	Easier than other models.	Does not take in account the complex physical and physiological mechanisms of gas emission in soil.	Wagner et al. (1997).
Non-steady-state Diffusive Flux Estimator (NDFE)	Square root (at long times)	Uses the general equation of diffusion (more precise).	Complicated mathematical expression.	Livingston et al. (2006), Hossler and Bouchard (2008).
Extended HM	Exponential	Robust against horizontal gas transport and patterns of non-linearity. Included in the "HMR" R package available on CRAN (http://www.r-project.org).	Qualified handling of data in the concentration range near the detection limit of the experimental system.	Pedersen et al. (2010).

The case is however different with the ^{15}NGF due to the presence of ^{15}N-labelled molecules. Firstly, we can note that the one-dimensional law of Fick mentioned above is normally defined for a binary mix and is somewhat simplistic. The real multicomponent model is described by the equations of Stefan and Maxwell, which are more complex. Jaynes & Rogowski (1986) showed, however, that for a tracer in a multicomponent mix, the tracer will diffuse according to Fick's first law. A new diffusion coefficient $\boldsymbol{D_{Fi}}$ must be calculated as shown by equation 17 of the cited reference. Furthermore, in soil, the flux J_i needs to be multiplied by a coefficient of tortuosity $\boldsymbol{\tau}$ and the air-filled porosity of the soil $\boldsymbol{\varepsilon}$ (m^3 of air per m^3 of soil) to better describe the heterogeneous nature of this medium (Jaynes & Rogowski, 1983; Hutchinson & Livingston, 2002). This leads to the following relation:

$$J_i = -\tau\varepsilon D_{Fi}\frac{dC_i}{dz} \qquad [15d]$$

The complexity of the system leads to the calculation of new (and somewhat challenging) parameters but overall, the diffusion of ^{15}N-labelled molecules is still ruled by a Fickian model. This means that these new parameters can be determined with experimental data.

The main issue with the gas dynamics in the ^{15}NGF however, is that the production of ^{15}N-labelled gases (N_2 and N_2O alike) after labelling causes build-up of their concentration in pore space (referred as "storage flux"). This leads to fluxes according to concentration gradients (Fick's first law) to the atmosphere, but also to the subsoil, sooner or later reaching a steady state concentration profile in case of a constant production. Already at this steady state, before closing the flux chamber, a significant part of the produced gases diffuses to subsoil (up to 40% according to Well et al., 2019**b**). Closing the chamber leads to increasing concentration of ^{15}N-labelled molecules inside the chamber headspace, leading to a decrease in surface flux with accumulation time while subsoil and storage fluxes go up.

The total flux of denitrification is the sum of the surface, storage and subsoil fluxes; but only the surface flux is measured with the ^{15}NGF. Therefore, diffusion dynamics lead to severe underestimation of denitrification if subsoil and storage fluxes are not taken into account, where this bias is higher for extend accumulation times. Well et al. (2019**b**) showed that the ratio between surface flux to the sum of storage and subsoil fluxes at a given accumulation time depends on the geometry of the cylinder confining the ^{15}N-labelled soil, the depth distribution of the ^{15}N label, depth of distribution of denitrification, gas diffusivity and soil moisture. The share of surface flux increases with soil moisture, diffusivity and length of confinement (height of the collar confining the labelled soil). It decreases with depth of labelling and accumulation time.

Well et al. (2019**b**) showed through simulation that ignoring diffusive losses could lead to great underestimation (from 28% to 71%) but a parallel field study using a bottom-closed cylinder showed that their model was not in perfect adequacy with the experiment, predicting twice the observed underestimation. This is largely due to the inability to assess the complexity of the processes occurring in the soil, especially temporal and spatial dynamics of denitrification as well as diffusivity. Nonetheless, the bottom-closed cylinder experiment revealed an underestimation of 37% of the flux of denitrification due to diffusive losses.

It can also be said that increased storage flux can modify the product ratio of denitrification (equation [12b]). Indeed, accumulation of N_2O in pore space tends to favour N_2O reduction into N_2 (Well et al., 2019**b**).

There is no evident solution to mitigate the effects of diffusion on the ^{15}N-labelled molecules for accurate measurement of denitrification with the ^{15}NGF. Using a diffusion model as presented in **Table 3** will only get a more accurate estimation of the surface flux at t=0 and will not account for subsoil and storage fluxes. While a bottom closed cylinder as in Well et al. (2019**b**) is principally suitable, it leads to serious disturbance of the soil and root system and is thus not adequate for continuous experiments with repeated sampling. The main strength of the ^{15}NGF is precisely the possibility to be used *in situ* with little disturbance to the soil. The other solution could be to a use simulation as in Well et al. (2019**b**) and allow sufficient time after labelling the soil (few hours to a day; since it was shown in **Chapter 2.5.1.2** that soil is still labelled for at least several days after application of the tracer) before closing the flux chamber. This would allow equilibration of the tracer solution and build-up of near-steady-state profiles of gas concentrations and diffusive fluxes and thus a better quantification of denitrification.

2.5.4) Stimulation of denitrifying microbes (fertilization effect)

As the ^{15}N tracer is injected in the form of a nitrate solution (the substrate of denitrification), it is possible that microbial activity may be stimulated and thus more denitrification products emitted, leading to an overestimation of this process. Although acknowledged by various authors (Groffman et al., 2006; Sgouridis & Ullah, 2015; Dodds et al., 2017; Warner et al., 2019; Lewicka-Szczebak & Well, 2020**a**) it has not in fact been investigated extensively. As mentioned by Groffman et al. (2006), Yang et al. (2014) and Sgouridis & Ullah (2015), this is mainly an issue in natural environments where low levels of nitrogen are available, typically where the only sources of nitrogen are natural (such as fixation and mineralization) or

eventually from atmospheric deposition. On the other hand, agricultural lands managed under intensive nitrogen fertilization should not be as sensitive to added nitrates.

When studying denitrification in agricultural soil, Loick et al. (2017) “fed” microbes large amounts of nitrate and glucose. This resulted in higher N_2O and N_2 emissions compared to their control treatment (see Figure 2 of the cited reference). Similarly, Clayton et al. (1997) studied the influence of different nitrogen treatments on denitrification from fertilised grasslands over two years. In Figure 1 of the cited reference, it is visible that when treated with calcium nitrate (CN), N_2O fluxes are considerably greater than the control. It is also worth mentioning that the added nitrates particularly stimulated emissions under wet and warm conditions in the same study (by almost two orders of magnitude). Jarvis et al. (1991) also correlated high *in situ* rates of denitrification with fertilizer application, especially again when the soils were wet or after a rainfall event.

It is difficult to compare these studies to the use of the ^{15}NGF given that the amount of applied tracer will vary from one study to another (and will be much lower than a fertilizer application); but they show however that a denitrification stimulation can occur when adding nitrate to soil. Ideally, further studies would be necessary to thoroughly assess the impact of added nitrates on the denitrification process under the use of the ^{15}NGF, but some fertilization effect has to be accepted (especially for the natural environment), and thus observed rates may have to be interpreted with care. In agricultural systems, the tracer is often injected to mimic a realistic fertilization input from farming practices as in Buchen et al. (2016). In such a case, we can expect a stimulation as observed in the studies mentioned in the previous paragraph; however this stimulation would be the realistic consequence of fertilizer application anyway. For natural ecosystems, tracer is usually added to target a small

^{15}N enrichment α_p of the soil nitrate pool, like 5% in the case of Kulkarni et al. (2014). As will be shown in **Chapter 2.6.2** of this study, the use of a ^{15}N tracer does not always guarantee a perfect sensitivity and measurements are often below the limit of detection of the IRMS. It is thus desirable to inject as much tracer as possible without stimulating denitrification.

2.6) Recommendations for addressing technical challenges

2.6.1) Tracer application methods

Different methods of tracer application have been used in the past, such as injection through a syringe, application using a watering can or via a sprayer, as reviewed by Berendt et al. (2020). As shown in the same study, none of these three methods achieves perfect homogenisation of the tracer in the soil and losses are inevitable. The authors indeed found a theoretical ^{15}N enrichment of 57-59 % in the upper 2.5 cm and 26-57 % in 5-10 cm when targeting a 60% enrichment using a Bromide (Br^-) tracer. This is particularly relevant as in the ^{15}NGF, the tracer is also an anion (NO_3^-) and can therefore move more freely in the soil solution than a cation, which would rather remain in the upper layers. In the same study, distribution of the tracer is also shown to be more homogenised in dry soils. Application using a syringe can be challenging if they get clogged, however, this problem can be solved by using a metal wire inside the needle (obturator) as in Davidson et al. (1991).

Lewicka-Sczcebak & Well (2020**a**) studied in detail the injection approach through three different methods; injection into an intact core (I+I), injection into a homogenised core (H+I) or mixed into a homogenised core (H+M). Obviously, the advantage of using the ^{15}NGF is to perform measurements directly *in situ*, which means that only the I+I approach is usable in the field. It was found that the determined N_2 fluxes and the denitrification product ratios did not differ significantly between intact and homogenised cores. Similarly, although soil

properties are more homogeneous in mixed cores, it appears that the ^{15}N label is actually more evenly distributed in the I+I treatment. Notably, within the I+I treatment, the measured values of α_p from the gas emissions are closer to the determined ^{15}N abundance of the soil nitrate α_{NO3}.

When choosing the injection method, the best way to homogenize the distribution of the tracer is to define a grid on the surface of the incubated soil and to use several injections of equal volume at different depths (Davidson et al., 1991; Tauchnitz et al., 2015; Sgouridis et al., 2016; Lewicka-Sczcebak & Well 2020**a**). Wu et al. (2011) determined in their experiments that the best compromise was 38 injections at 4 different depths. Buchen et al. (2016) used a more sophisticated system using a peristaltic pump and steel capillaries for better distribution of the tracer.

Finally, it is important to remember that since the tracer is diluted in water, injections will increase the soil moisture, which in turn will stimulate denitrification (Jarvis et al., 1991; Hwang & Hanaki, 2000). Usually, a soil moisture increase inferior to 3-5% is considered reasonable (Buchen et al., 2016; Sgouridis et al., 2016).

2.6.2) Sensitivity of the ^{15}NGF and use of a N_2-depleted atmosphere:

The N_2 emitted from denitrification is challenging to measure and even the use of a ^{15}N tracer does not always guarantee a good signal on the IRMS. In cause is the sensitivity needed to detect the small amounts of produced N_2 against the high atmospheric N_2 background. Baily et al. (2012) reported the same limits of detection as Stevens & Laughlin (2001) on their IRMS, which were 8.0×10^{-6} for R29 and 3.2×10^{-7} for R30. Sgouridis et al. (2016) reported 7.7×10^{-7} for R29 and 6.1×10^{-7} for R30 while Friedl et al. (2017) reported 9.1×10^{-7} for R29 and 9.8×10^{-7} for R30. A simulation using Excel (Microsoft, Redmond, WA) has been used to determine

how these limits of detection translate in terms of coefficient ***d*** that can be measured for a conventional use of the ^{15}NGF. Considering a 4 L incubation chamber, the ideal gas law and atmospheric pressure, different realistic values of $\boldsymbol{\alpha_p}$ (ranging from 5% to 50%) and ***d*** (ranging from 1.10^{-8} to 5.10^{-4}) were used to calculate the associated ΔR29 and ΔR30, assuming isotopic equilibrium of the atmospheric and soil denitrifying pools. The values of ***d*** were translated into theoretical gas fluxes for informal reference, considering a 0.05 m² basal area of the incubation chamber and a time of incubation of 1-hour. The results are reported in **Table 4**. The values of ΔR29 and ΔR30 that were beneath the smallest cited limit of detection appear in red, while the values greater than the highest cited limit of detection appear in green. The values in between are in yellow. This means that the values in red probably cannot be detected with the current routinely available technology whereas the values in yellow can only be detected if the IRMS has a good sensitivity. As expected, ΔR29 and ΔR30 tend to be more detectable when increasing both $\boldsymbol{\alpha_p}$ and ***d.*** Unfortunately, they are not detectable in most cases. Typically, ***d*** is rarely superior to 1.10^{-6}, which is not detectable even at a high ^{15}N abundance (50%) of the soil denitrifying pool. In addition, values in green in the simulation are only just above the detection limit in most cases, which is not ideal for accurate measurements. It is not rare to have gaps in a dataset of N_2 measurements because of this poor sensitivity (Mulvaney & Kurtz, 1984; Kulkarni et al., 2014; Buchen et al., 2016 amongst others; acknowledged by Friedl et al., 2020 as one of the main challenges of the ^{15}NGF).

***Table 4**: Simulation of the sensitivity of the ^{15}NGF.*

Simulation of the sensitivity of the ^{15}NGF through a 1-hour incubation using a 4L chamber (0.05 m² basal area) with different values of a_p and d, considering isotopic equilibrium of atmospheric and soil denitrifying pools, atmospheric pressure and the ideal gas law. Values in red cannot be detected with routinely available IRMS where values in yellow could be with higher sensitivity instruments. Values in green can be detected.

ΔR29: Red < 9.1×10^{-7} < Yellow < 8.0×10^{-6} < Green

ΔR30: Red < 3.2×10^{-7} < Yellow < 9.8×10^{-7} < Green

a_p	d	Flux (gN/ha/d)	ΔR29	ΔR30
5%	1E-08	0.19	8.90E-10	2.51E-11
	5E-08	0.94	4.45E-09	1.25E-10
	1E-07	1.88	8.90E-09	2.51E-10
	5E-07	9.36	4.45E-08	1.25E-09
	1E-06	18.74	8.90E-08	2.51E-09
	5E-06	93.6	4.45E-07	1.25E-08
	1E-05	187.4	8.90E-07	2.51E-08
	5E-05	936	4.45E-06	1.25E-07
	1E-04	1874	8.90E-06	2.51E-07
	5E-04	9366	4.45E-05	1.25E-06
10%	1E-08	0.19	1.75E-09	1.01E-10
	5E-08	0.94	8.77E-09	5.03E-10
	1E-07	1.88	1.75E-08	1.01E-09
	5E-07	9.36	8.77E-08	5.03E-09
	1E-06	18.74	1.75E-07	1.01E-08
	5E-06	93.6	8.77E-07	5.03E-08
	1E-05	187.4	1.75E-06	1.01E-07
	5E-05	936	8.77E-06	5.03E-07
	1E-04	1874	1.75E-05	1.01E-06
	5E-04	9366	8.76E-05	5.03E-06
20%	1E-08	0.19	3.18E-09	4.03E-10
	5E-08	0.94	1.59E-08	2.01E-09
	1E-07	1.88	3.18E-08	4.03E-09
	5E-07	9.36	1.59E-07	2.01E-08
	1E-06	18.74	3.18E-07	4.03E-08
	5E-06	93.6	1.59E-06	2.01E-07
	1E-05	187.4	3.18E-06	4.03E-07
	5E-05	936	1.59E-05	2.01E-06
	1E-04	1874	3.18E-05	4.03E-06
	5E-04	9366	1.59E-04	2.01E-05

a_p	d	Flux (gN/ha/d)	ΔR29	ΔR30
30%	1E-08	0.19	4.19E-09	9.07E-10
	5E-08	0.94	2.10E-08	4.53E-09
	1E-07	1.88	4.19E-08	9.07E-09
	5E-07	9.36	2.10E-07	4.53E-08
	1E-06	18.74	4.19E-07	9.07E-08
	5E-06	93.6	2.10E-06	4.53E-07
	1E-05	187.4	4.19E-06	9.07E-07
	5E-05	936	2.10E-05	4.53E-06
	1E-04	1874	4.19E-05	9.07E-06
	5E-04	9366	2.10E-04	4.53E-05
40%	1E-08	0.19	4.81E-09	1.61E-09
	5E-08	0.94	2.40E-08	8.06E-09
	1E-07	1.88	4.81E-08	1.61E-08
	5E-07	9.36	2.40E-07	8.06E-08
	1E-06	18.74	4.81E-07	1.61E-07
	5E-06	93.6	2.40E-06	8.06E-07
	1E-05	187.4	4.81E-06	1.61E-06
	5E-05	936	2.40E-05	8.06E-06
	1E-04	1874	4.81E-05	1.61E-05
	5E-04	9366	2.40E-04	8.06E-05
50%	1E-08	0.19	5.02E-09	2.52E-09
	5E-08	0.94	2.51E-08	1.26E-08
	1E-07	1.88	5.02E-08	2.52E-08
	5E-07	9.36	2.51E-07	1.26E-07
	1E-06	18.74	5.02E-07	2.52E-07
	5E-06	93.6	2.51E-06	1.26E-06
	1E-05	187.4	5.02E-06	2.52E-06
	5E-05	936	2.51E-05	1.26E-05
	1E-04	1874	5.02E-05	2.52E-05
	5E-04	9366	2.51E-04	1.26E-04

One way to improve this sensitivity is to only use the R29 data in combination with the ^{15}N abundance α_p calculated through the N_2O data, as explained in **Chapter 2.4.2.3**. Using this method, Baily et al. (2012) reported a sensitivity 16 times greater than when calculating α_p from the N_2 data. In order to optimize the R29 ratio, a 50% ^{15}N enrichment of the soil denitrifying pool represents an ideal target. Indeed, for a pool of N_2 at isotopic equilibrium, this is the enrichment for which the proportion of $^{29}N_2$ is the highest (equations [8a] to [8c]) as shown on **Figure 13**.

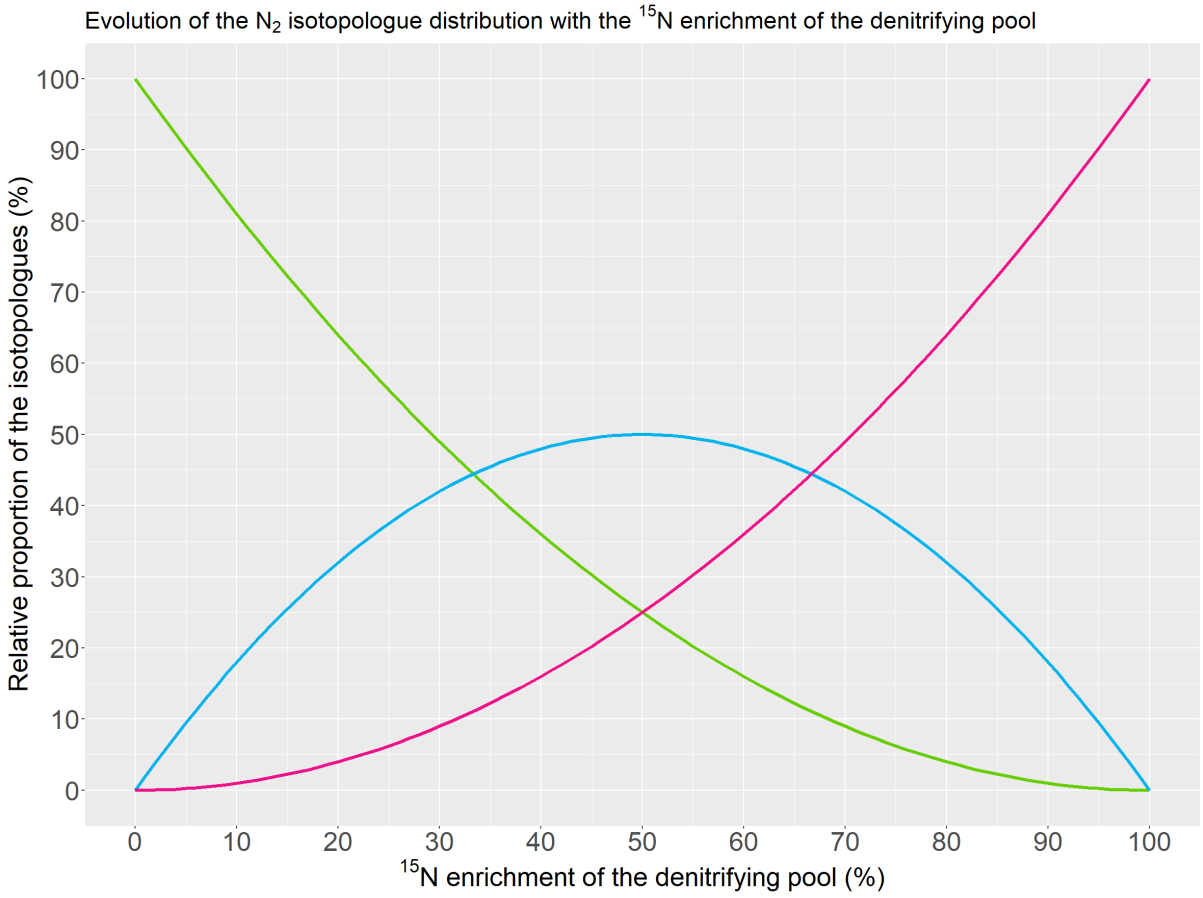

Figure 13: *Evolution of the three N_2 isotopologue proportions for different values of the soil denitrifying pool ^{15}N abundance (considering isotopic equilibrium).*

The proportion of $^{29}N_2$ is maximal for a ^{15}N enrichment of 50%.

If no denitrification stimulation occurs, targeting a 50% ^{15}N enrichment of the soil denitrifying pool is a good way to increase sensitivity.

Another way to increase sensitivity is to use a hybrid method as mentioned before. More precisely, it means using an N_2-depleted atmosphere in addition to ^{15}N tracer. This new atmosphere should still contain a small amount of N_2 since the calculations of the ^{15}NGF require an [N_2] background. Similarly to **Table 4**, we can calculate the new ΔR29 and ΔR30 if the atmospheric background contains less N_2. We took the same cases as before ($\boldsymbol{\alpha_p}$ ranging from 5% to 50% and $\boldsymbol{d}$ ranging from 1.10^{-8} to 5.10^{-4}) but now with a variable [N_2] background that contains either 78% (atmospheric), 20%, 10%, 5% or 1% of N_2 (see **Table 9** from the **Supporting Information** ,**Chapter 2.8.2**). The results for the case where $\boldsymbol{\alpha_p}$ equals 20% can be seen in **Table 5a** (ΔR29 only, for clarity) and show as expected that ΔR29 tends to be more easily detected as the N_2 background drops. For identical values of $\boldsymbol{\alpha_p}$ and $\boldsymbol{d}$, we can express the ratio G_{29} defined as:

$$G_{29} = \frac{\Delta R29 \text{ (low } N_2 \text{ background)}}{\Delta R29 \text{ (atmospheric } N_2 \text{ background)}} \text{ (and } G_{30} \text{ similarly for } \Delta R30) \qquad [16a]$$

If this ratio equals 4 (as it is approximately the case when $\boldsymbol{d} = 5.10^{-8}$, $\boldsymbol{\alpha_p}$ = 20%, and [N_2] = 20%), then the limit of detection is increased 4 times. These ratios are compiled in **Table 5b** for the case $\boldsymbol{\alpha_p}$=20%.

***Table 5**: Effect of N_2 background reduction on sensitivity*

a) Comparison of ΔR29 with different N_2 backgrounds (cases where α_p = 20%) as calculated by simulation of a 4L chamber, assuming atmospheric pressure, the ideal gas law and isotopic equilibrium of the atmospheric and soil denitrifying pools. The ΔR29 ratios tend to be more detectable with lower N_2 background. Values in red cannot be detected with routinely available IRMS whereas values in yellow can be detected with higher resolution instruments. Values in green can be detected.

ΔR29: Red < 9.1×10^{-7} < Yellow < 8.0×10^{-6} < Green

d	Flux (gN/ha/d)	[N_2] Atmospheric Background	[N_2] = 20%	[N_2] = 10%	[N_2] = 5%	[N_2] = 1%
		ΔR29	ΔR29	ΔR29	ΔR29	ΔR29
1E-08	0.19	3.18E-09	2.48E-09	2.48E-08	4.95E-08	2.48E-07
5E-08	0.94	1.59E-08	6.19E-08	1.24E-07	2.48E-07	1.24E-06
1E-07	1.88	3.18E-08	1.24E-07	2.48E-07	4.95E-07	2.48E-06
5E-07	9.36	1.59E-07	6.19E-07	1.24E-06	2.48E-06	1.24E-05
1E-06	18.74	3.18E-07	1.24E-06	2.48E-06	4.95E-06	2.48E-05
5E-06	93.6	1.59E-06	6.19E-06	1.24E-05	2.48E-05	1.24E-04
1E-05	187.4	3.18E-06	1.24E-05	2.48E-05	4.95E-05	2.48E-04
5E-05	936	1.59E-05	6.19E-05	1.24E-04	2.48E-04	1.24E-03
1E-04	1874	3.18E-05	1.24E-04	2.48E-04	4.95E-04	2.47E-03
5E-04	9366	1.59E-04	6.19E-04	1.24E-03	2.47E-03	1.21E-02

ΔR30: Red < 3.2×10^{-7} < Yellow < 9.8×10^{-7} < Green

Values of ***d*** are defined against atmospheric background. Fluxes values are given as informal example considering a 1-hour incubation and a chamber basal area of 0.05 m^2.

b) Evolution and comparison of G29 and G30 ratios (see equation [10a] in **chapter 2.6.2**) with different N_2 backgrounds for the cases where $\boldsymbol{\alpha_p}$ = 20 %. We can see that G29 and G30 are identical for every similar situation (identical parameters $\boldsymbol{\alpha_p}$, ***d*** and $[N_2]$ background). Furthermore, these ratios are almost invariant with ***d*** (nor with $\boldsymbol{\alpha_p}$ as shown in **Annex 2**, **chapter 2.9.2**).

d	$[N_2]$ = 20%		$[N_2]$ = 10%		$[N_2]$ = 5%		$[N_2]$ = 1%	
	G29	**G30**	**G29**	**G30**	**G29**	**G30**	**G29**	**G30**
1E-8	3.90	3.90	7.80	7.80	15.60	15.60	78.00	78.00
5E-8	3.90	3.90	7.80	7.80	15.60	15.60	78.00	78.00
1E-7	3.90	3.90	7.80	7.80	15.60	15.60	78.00	78.00
5E-7	3.90	3.90	7.80	7.80	15.60	15.60	78.00	78.00
1E-6	3.90	3.90	7.80	7.80	15.60	15.60	78.00	78.00
5E-6	3.90	3.90	7.80	7.80	15.60	15.60	77.98	77.98
1E-5	3.90	3.90	7.80	7.80	15.60	15.60	77.96	77.96
5E-5	3.90	3.90	7.80	7.80	15.59	15.59	77.81	77.81
1E-4	3.90	3.90	7.80	7.80	15.59	15.59	77.61	77.61
5E-4	3.90	3.90	7.78	7.78	15.53	15.53	76.11	76.11

Upon inspection of this table, it appears that G_{29} and G_{30} are equal for every identical situation (same parameters ***d***, $\boldsymbol{\alpha_p}$ and $[N_2]$ background). Furthermore, the values of G_{29} and G_{30} do not seem to depend on the values of ***d*** and $\boldsymbol{\alpha_p}$. This is demonstrated in the **Supporting Information** (**Chapter 2.8.2**) and therefore; much like **Figure 11**, we can extrapolate a specific case (here we used ***d*** = 5.10^{-7} and $\boldsymbol{\alpha_p}$= 50%) to plot the evolution of the ratio G29 (equal to G30) as a function of the $[N_2]$ background for every scenario. **Figure 14** represents this evolution:

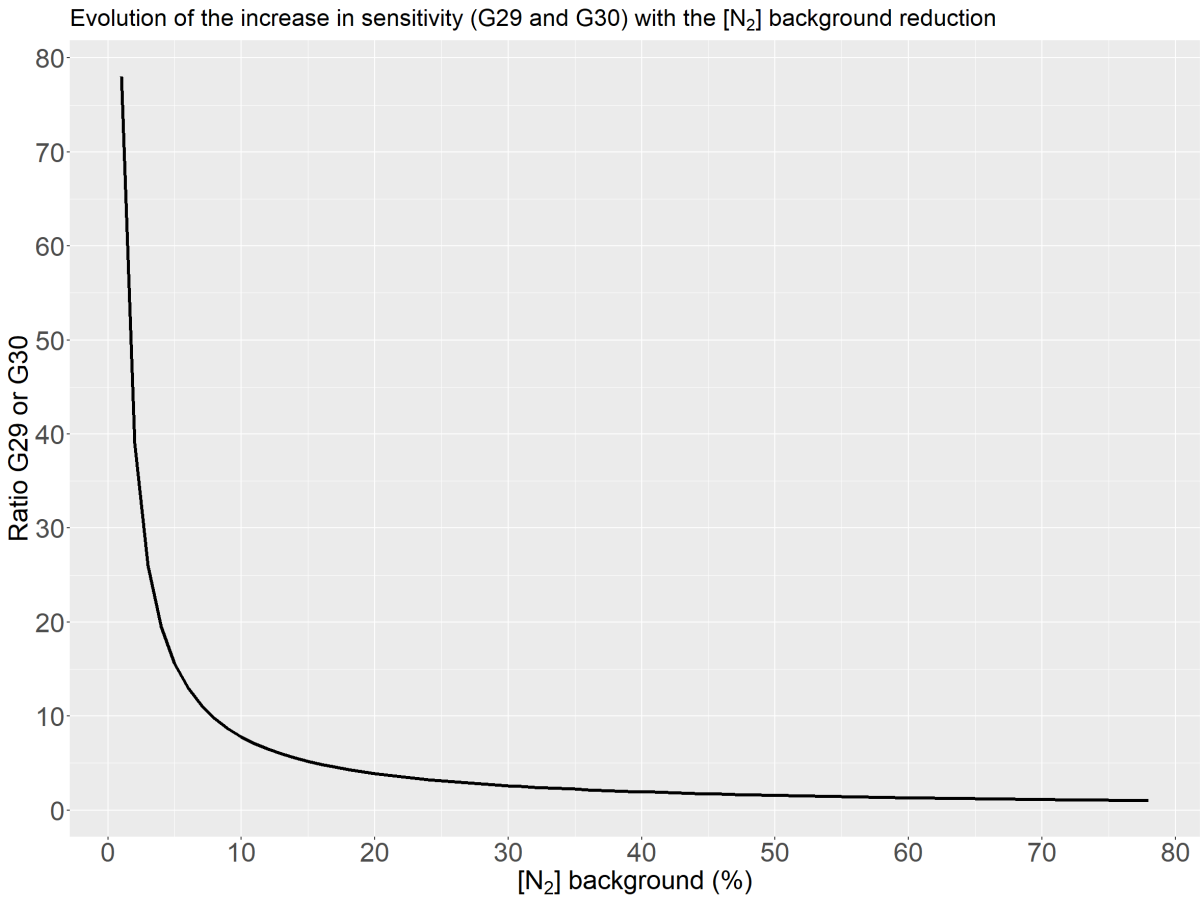

***Figure 14**: Evolution of G_{29} (or G_{30}) with a background of [N_2] ranging from 78% to 1% with an increment of 1%, as calculated through simulation.*

Maximum is G_{29} = 78 when [N_2] = 1%. Minimum is G_{29} = 1 when [N_2] = 78%.

We can see from **Figure 14** that no matter the quantity of tracer applied or the number of molecules emitted, the sensitivity dramatically increases when the background in [N_2] < 10%. It is approximately enhanced 10 times when [N_2] = 8%. If the background drops below 1%, even better sensitivity can be obtained; for example, G_{29} is equal to 156 and 780 when the [N_2] background reaches 0.5% and 0.1%, respectively. It can be very challenging to maintain these low levels of N_2 however, even in the laboratory as can be seen in Well et al. (2019**a**). As mentioned previously, this method has not been used extensively because of its complexity (laboratory studies: Meyer et al., 2010; Scheer et al., 2016; Lewicka-Szczebak et

al., 2017; Lewicka-Szczebak & Well, 2020; Kemmann et al., 2021; *in situ* studies: Well et al., 2019**a**; Buchen-Tschiskale et al., 2023).

Finally, it is important to remember that R29 and R30 after incubation are necessarily greater than their initial values, as shown in the **Supporting Information** (**Chapter 2.8.3**). Therefore, any value of R29 or R30 after incubation lower than its initial value can only be noise from the IRMS and cannot give any realistic value.

Similarly, it is also worth noting that $(R29)_0$ and $(R30)_0$ are supposedly constant and equal to 7.35×10^{-3} and 1.35×10^{-5}, respectively. These values are easily found using a binomial distribution with a ^{15}N enrichment equal to natural abundance $\boldsymbol{\alpha_a}$ (~0.37%):

$$R29_{(0)} = \frac{2\times0.003663\times(1-0.003663)}{(1-0.003663)^2} = 7.35 \times 10^{-3} \qquad [16b]$$

$$R30_{(0)} = \frac{0.003663^2}{(1-0.003663)^2} = 1.35 \times 10^{-5} \qquad [16c]$$

Thus, a good way to calibrate the IRMS is to perform tests on atmospheric samples and try to find these values as in Lewicka-Szczebak et al. (2013). Care must be taken for m/z=30 as shown next.

2.6.3) Interferences at m/z=30 and gas-purification preparation unit

If trace amounts of oxygen are present in the ion source of the IRMS, various species with m/z= 30 can be formed; such as $(^{13}C^{17}O)^+$, $(^{12}C^{18}O)^+$ or $(^{14}N^{16}O)^+$ (Russow et al., 1996). It has been suggested that the removal of hindering gaseous species such as H_2O, CO_2, CO and N_2O (the last one only when studying N_2) would allow for a better sensitivity (Lewicka-Szczebak et al., 2013). Siegel et al. (1982) were the first ones to develop a gas-purification preparation

unit for the use of the ^{15}NGF. More recently, such systems were also developed and used by Lewicka-Szczebak et al. (2013), Yang et al. (2014) and Sgouridis et al. (2016).

However, this usually does not solve entirely the problem as shown by the results in Table 2 from Lewicka-Szczebak et al. (2013); where R30 from the atmosphere is approximately 10 times greater than the expected value. As explained in the same study, the magnitude of NO^+ formed in the ion source of the IRMS depends on the quantity of injected N_2. Thus, the authors applied a drift correction as a linear function of $^{28}N_2$. Russow et al. (1996) solved this problem more directly by using standards and a linear drift correction as:

$$R30_{true} = a \times R30_{measured} + b \qquad [17a]$$

Excellent correlation was obtained (R^2=1) and the coefficient ***a*** in their case was close to 1. This means that calculations based on ΔR30 such as the ones from Mulvaney & Boast (1986) would still give a good result without correction. However, the equations based on the approach of Arah (1992) would lead to error given that R30 in the following equations would not have been corrected:

$$a_m = \frac{R_{29}+2R_{30}}{2(1+R_{29}+R_{30})} \qquad [17b]$$

$$\alpha_m = \frac{R_{30}}{1+R_{29}+R_{30}} \qquad [17c]$$

Modern ultrahigh resolution mass spectrometers can separate $^{14}N^{16}O$ from $^{30}N_2$ (Yeung et al., 2017; Yeung et al., 2019) but these instruments are not routinely available and current sample throughput is limited due to an analysis time of a few hours per sample.

Finally, it is worth mentioning that in the past, some authors have avoided the issue at m/z=30 by isotopically equilibrating the mix of emitted and atmospheric N_2 through high voltage arc, electrodeless discharge or microwave equilibration (Well et al., 1998). These techniques have

been of little use lately because it required two runs per sample and modern IRMS have a better sensitivity towards $^{30}N_2$.

2.7) Conclusion and future research

The ^{15}NGF method remains today, the most suitable technique for studying denitrification *in situ* in soil. However, its results can be biased by different factors as shown here, especially the non-homogeneous distribution of the label in the soil, the formation of hybrid molecules, the diffusion issues and the addition of substrate labelled tracer. The non-homogeneous distribution of the label and the diffusion issues tend to result in an underestimation of the true potential of denitrification. On the other hand, the potential stimulation of denitrification due to substrate addition and the eventual formation of hybrid molecules would tend to overestimate it. We demonstrate herein that a better precision in the measurement of denitrification can be obtained by:

1) Ensuring the most homogeneous label application so that the soil denitrifying pool is as close as possible to isotopic equilibrium as originally presumed in the ^{15}NGF method.
2) Accounting for diffusion by allowing time after label application in order to reach near-steady-state profiles of gas concentration and diffusive fluxes; and using a simulation to calculate storage and subsoil fluxes. Alternatively, the use of a bottom-closed cylinder in the field can also be a viable option although it leads to soil and root system disturbances.
3) Define a level of tracer addition that reduces and/or eliminate denitrification stimulation.
4) Check if hybrid processes are occurring in the type of soil system studied.

A preparation unit for gas purification is also very valuable but does not entirely solve the problems that occur at m/z=30. A drift correction might still be needed.

Furthermore, because the atmospheric N_2 background is so high and denitrification can emit very small amounts of N_2, sensitivity might still not be sufficient to quantify denitrification beyond peak events. The only experimental parameters one can modify to increase sensitivity are the time of incubation, the size of the headspace inside the incubation vessel, the amount of ^{15}N label used (optimizing the ^{15}N enrichment of the nitrate pool) and the level of N_2 concentration in the atmospheric background. Increasing the time of incubation and decreasing the size of the headspace can both increase sensitivity but they will also cause further diffusion issues when using the ^{15}NGF *in situ*. Labelling 50% of the soil denitrifying pool represents an ideal target to increase sensitivity towards R29. If no denitrification stimulation occurs at this level, this is a good way to increase sensitivity. The reduction of the N_2 atmospheric background *in situ* can be challenging, given that it requires a tightly sealed incubation chamber system and that air can still circulate through soil pores. Nonetheless, this was achieved recently by Well et al. (2019**a**) using a sophisticated incubation and soil flushing system. However, this method is difficult to use at a wider scale and is not appropriated for intensive sampling campaigns. It is not necessary to get rid of all the native atmospheric N_2, reducing it to a lower and known concentration (~<10%) can already increase sensitivity significantly. To help users in the successful application of the ^{15}NGF, we have summarized our conclusions into a decision tree (see **Figure 15**).

It will need further work and innovation to further increase the sensitivity of the ^{15}NGF and allow robust and reproducible measurements of field denitrification in the future.

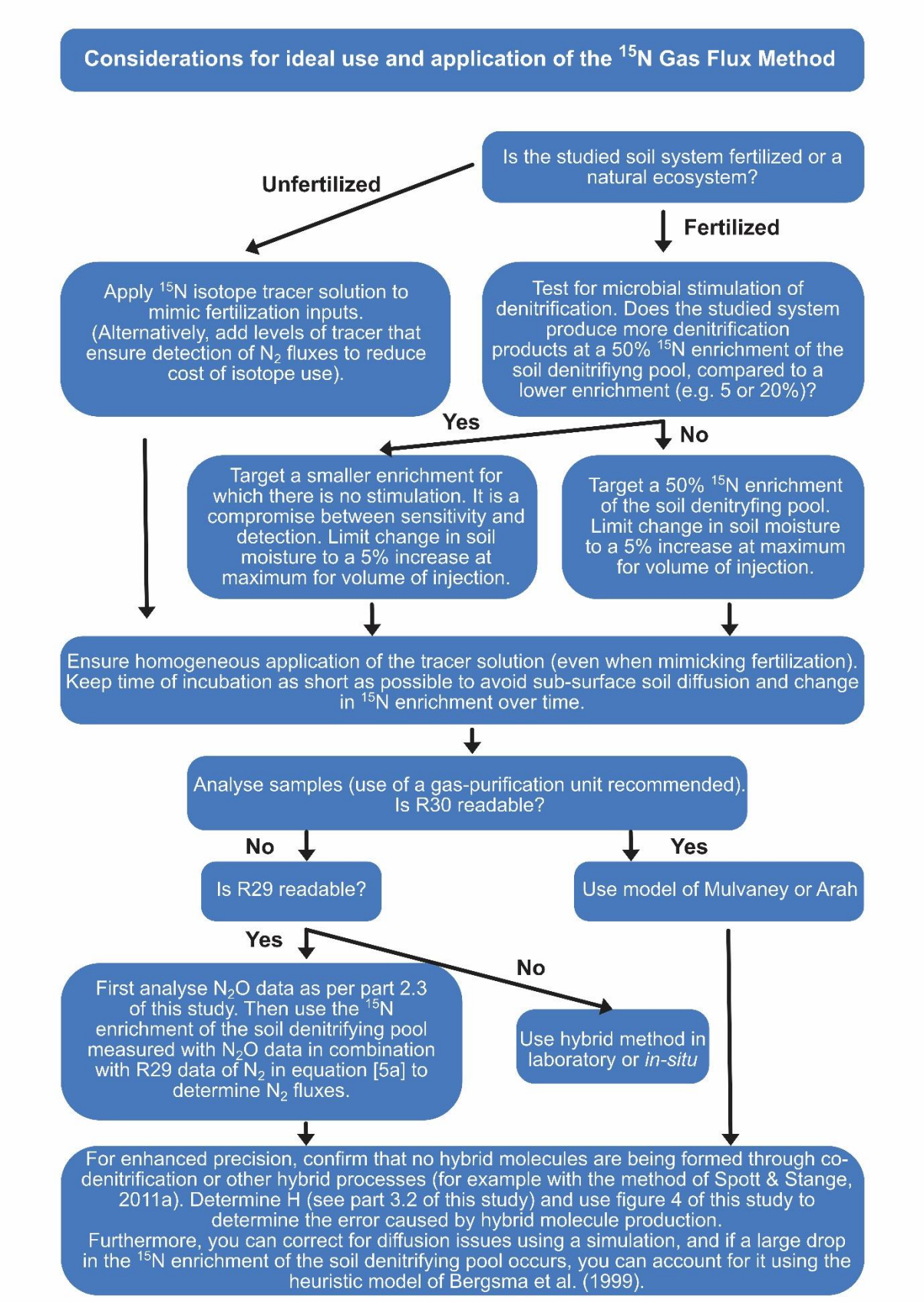

***Figure 15**: Decision tree of the considerations for an ideal use and application of the ^{15}NGF*

2.8) Supporting Information

2.8.1) Annex 1:

***Table 6**: Table of parameters used in the simulation of Chapter 2.5.2.1.*

Parameters			
H	a_p	***d*(N_2)**	***d*(N_2O)**
0,01%	5%	1,00E-08	0,10%
0,10%	10%	5,00E-08	0,50%
1%	20%	1,00E-07	1%
5%	30%	5,00E-07	5%
10%	40%	1,00E-06	10%
20%	50%	5,00E-06	30%
50%		1,00E-05	50%
80%		5,00E-05	60%
100%		1,00E-04	70%
		5,00E-04	80%
		1,00E-03	99%

Number of molecules		
Total (in vessel)	**N_2 background**	**N_2O background**
1.08E+23	8.39E+22	3.23E+16

***Table 7**: Maximum errors (%) on $a_{p\ total}$, $a_{p\ denitrification}$, d_{total} and $d_{denitrification}$ for the cases **H** = 0.01 or 0.1%.*

These errors at low hybrid source contributions are negligible (maximum 4.97×10^{-2}%).

	Max error (%)			
H	$a_{p\ total}$	$a_{p\ denitrification}$	d_{total}	$d_{denitrification}$
0,01%	-3.37E-07	-4.96E-03	4.50E-07	1.00E-02
0,10%	-2.48E-05	-4.97E-02	2.52E-05	1.00E-01

***Table 8**: Table of correlation of the errors made on $a_{p\ total}$, $a_{p\ denitrification}$, d_{total} and $d_{denitrification}$ with the parameters **d**, a_p and **H**.*

Table of correlation					
	$a_{p\ total}$	$a_{p\ denitrification}$	d_{total}	$d_{denitrification}$	n
d	all errors similar.	**Kendal**: 7 coefficients significant at the 0.01 level and 3 where all errors are similar (out of 36 cases). **Pearson**: 7 coefficients significant at the 0.01 level and 3 where all errors are similar (out of 36 cases). **However**, maximum absolute CV in a sub-dataset: -6.41×10^{-6} %. Max relative difference to the mean: 3.52×10^{-5}%.	all errors similar.	all errors similar.	36 sub-datasets of 11 values each.
a_p	all Kendal and Spearman coefficients are equal to (-1).	all Kendal and Spearman coefficients are equal to (-1).	**Kendal**: 2 coefficients significant at the 0.01 level, 1 at the 0.05 level and 35 where all errors are similar (out of 66 cases). **Pearson**: 3 coefficients significant at the 0.01 level, 2 at the 0.05 level, and 35 where all errors are similar (out of 66 cases). **However**, max absolute CV in a sub-dataset: 4.62×10^{-3} %. Max relative difference to the mean: 1.30×10^{-2} %.	**Kendal**: 2 coefficients significant at the 0.01 level, 1 at the 0.05 level and 35 where all errors are similar (out of 66 cases). **Pearson**: 3 coefficients significant at the 0.01 level, 2 at the 0.05 level, and 35 where all errors are similar (out of 66 cases). **However**, max absolute CV in a sub-dataset : 1.16×10^{-5} %. Max relative difference to the mean 3.26×10^{-5} %.	66 sub-datasets of 6 values each.
H	all Kendal and Spearman coefficients are equal to (-1).	all Kendal and Spearman coefficients are equal to (-1).	all Kendal and Spearman coefficients are equal to 1.	all Kendal and Spearman coefficients are equal to 1.	66 sub-datasets of 6 values for $a_{p\ total}$ and $a_{p\ denitrification}$. 6 sub-datasets of 66 values for d_{total} and $d_{denitrification}$.

Statistical tests realised on sub-datasets where 2 parameters are constant while the studied one varies. The number of values included in each sub-dataset and the number of sub-datasets studied for each case can be known in column "n" at the end of the table. Different sub-dataset sizes and numbers are used for the correlations with H, since $\alpha_{p\ total}$ and $\alpha_{p\ denitrification}$ were correlated with α_p while d_{total} and $d_{dentrification}$ were not. However, since both $\alpha_{p\ total}$ and $\alpha_{p\ denitrification}$ were independent with d, we used the means of data with same parameters α_p and H but different parameter d for the $\alpha_{p\ total}$ and $\alpha_{p\ denitrification}$ correlations.

The colour green indicates a correlation whereas the colour red indicates an absence of correlation. Correlation was determined if all coefficients of Kendal and Spearman were equal to 1 or (-1) for the sub-datasets of the considered case. The absence of correlation was determined when all the errors caused on either $\alpha_{p\ total}$, $\alpha_{p\ denitrification}$, d_{total} or $d_{denitrification}$ (depending on the studied case) were identical. For three cases (correlation of d_{total} or $d_{dentrification}$ with α_p and correlation of $\alpha_{p\ denitrification}$ with d), these errors were not all identical and some Kendal and Spearman coefficients were significant, indicating potential correlations. We found out however that the magnitude of evolution of error was negligible in these cases. This was determined by the maximum coefficient of variation (CV) of the sub-datasets and the highest relative difference between a value of a sub-dataset and the mean of this sub-dataset, for the studied case. This highest relative difference was calculated as:

$$max \left| \frac{X_i - X_{average}}{X_{average}} \right| \qquad [18]$$

where X_i is a value in a sub-dataset and $X_{average}$ is the average of this sub-dataset. Since for all these cases, the highest observed CV was 4.62×10^{-3} % and the highest relative difference was 0.013%, we ruled out correlation despite some Kendal and Spearman coefficients being significant.

***Table 9**: Errors made on the quantification of (a) d_{total} and (b) $d_{denitrification}$ with H when using the ^{15}NGF and ignoring the hybrid sources of denitrification, as determined by simulation.*

These errors are the mean of the different combinations of selected a_p and d parameters for the same values of H, since d_{total} and $d_{denitrification}$ are not correlated with the parameters a_p and d.

(a)

H	error d_{total} (%)	Std deviation	CV	n
1%	2.53E-03	5.10E-08	2.02E-05	66
5%	6.58E-02	2.29E-08	3.48E-07	66
10%	0.28	1.81E-08	6.53E-08	66
20%	1.25	3.70E-08	2.96E-08	66
50%	12.50	4.38E-08	3.50E-09	66
80%	80.00	7.01E-08	8.76E-10	66

(b)

H	error $d_{denitrification}$ (%)	Std deviation	CV	n
1%	1.01	5.15E-08	5.09E-08	66
5%	5.33	2.41E-08	4.51E-09	66
10%	11.42	2.01E-08	1.76E-09	66
20%	26.56	4.62E-08	1.74E-09	66
50%	125	8.76E-08	7.01E-10	66
80%	800	3.51E-07	4.38E-10	66

***Table 10**: Highest relative differences of the errors made on $a_{p\ total}$, $a_{p\ denitrification}$, d_{total} and $d_{denitrification}$ between the models for N_2 and N_2O.*

The N_2 and N_2O models are similar at the exception of the one for N_2O using higher coefficients ***d*** and a smaller number of molecules in the background (see **Table 6**). For sub-datasets of constant $\boldsymbol{a_p}$ and ***H*** parameters (n=11), we expressed the average error on either $\boldsymbol{a_{p\ total}}$, $\boldsymbol{a_{p\ denitrification}}$, $\boldsymbol{d_{total}}$ or $\boldsymbol{d_{denitrification}}$ for both N_2 and N_2O and compared them as per equation [14e]. Since the highest relative mean of error difference was for $\boldsymbol{d_{total}}$ and was 1.5×10^{-3} %, and the highest coefficient of variation (CV) of a sub-dataset of constant ***H*** and $\boldsymbol{a_p}$ values was 1.18×10^{-8} %; we can consider that the model for N_2O is similar to the model of N_2 and thus, similar conclusions can be drawn.

	$\boldsymbol{d_{total}}$ **(%)**	$\boldsymbol{d_{denitrification}}$ **(%)**	$\boldsymbol{a_{p\ total}}$ **(%)**	$\boldsymbol{a_{p\ denitrification}}$**(%)**
Max relative difference of mean	1.50E-03	3.77E-06	7.17E-04	3.58E-06
Max CV of a sub-dataset of constant *H* and $\boldsymbol{a_p}$ values	1.18E-08	2.95E-11	5.78E-09	2.89E-11

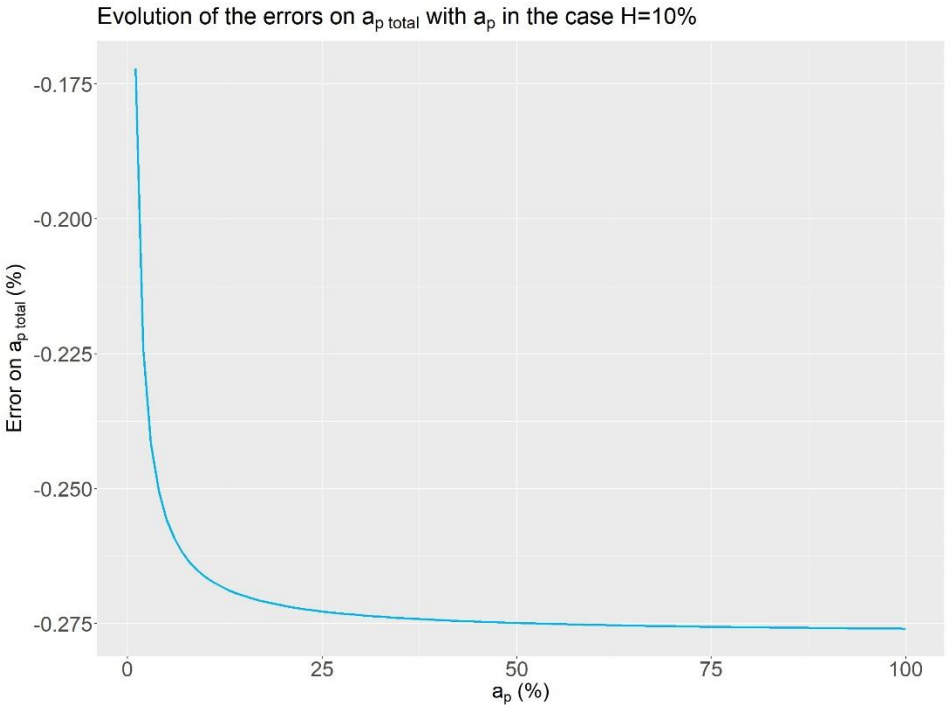
Evolution of the errors on $a_{p\ total}$ with a_p in the case H=10%
-0.175
-0.200
-0.225
-0.250
-0.275
Error on $a_{p\ total}$ (%)
0
25
50
75
100
a_p (%)

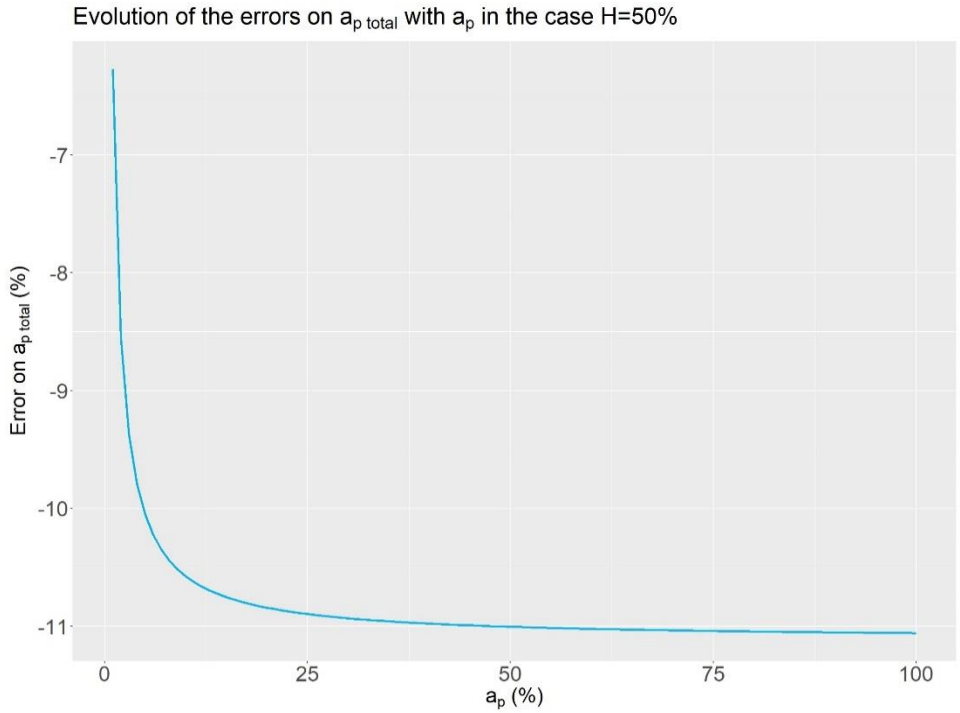
Evolution of the errors on $a_{p\ total}$ with a_p in the case H=50%
-7
-8
-9
-10
-11
Error on $a_{p\ total}$ (%)
0
25
50
75
100
a_p (%)

(b)

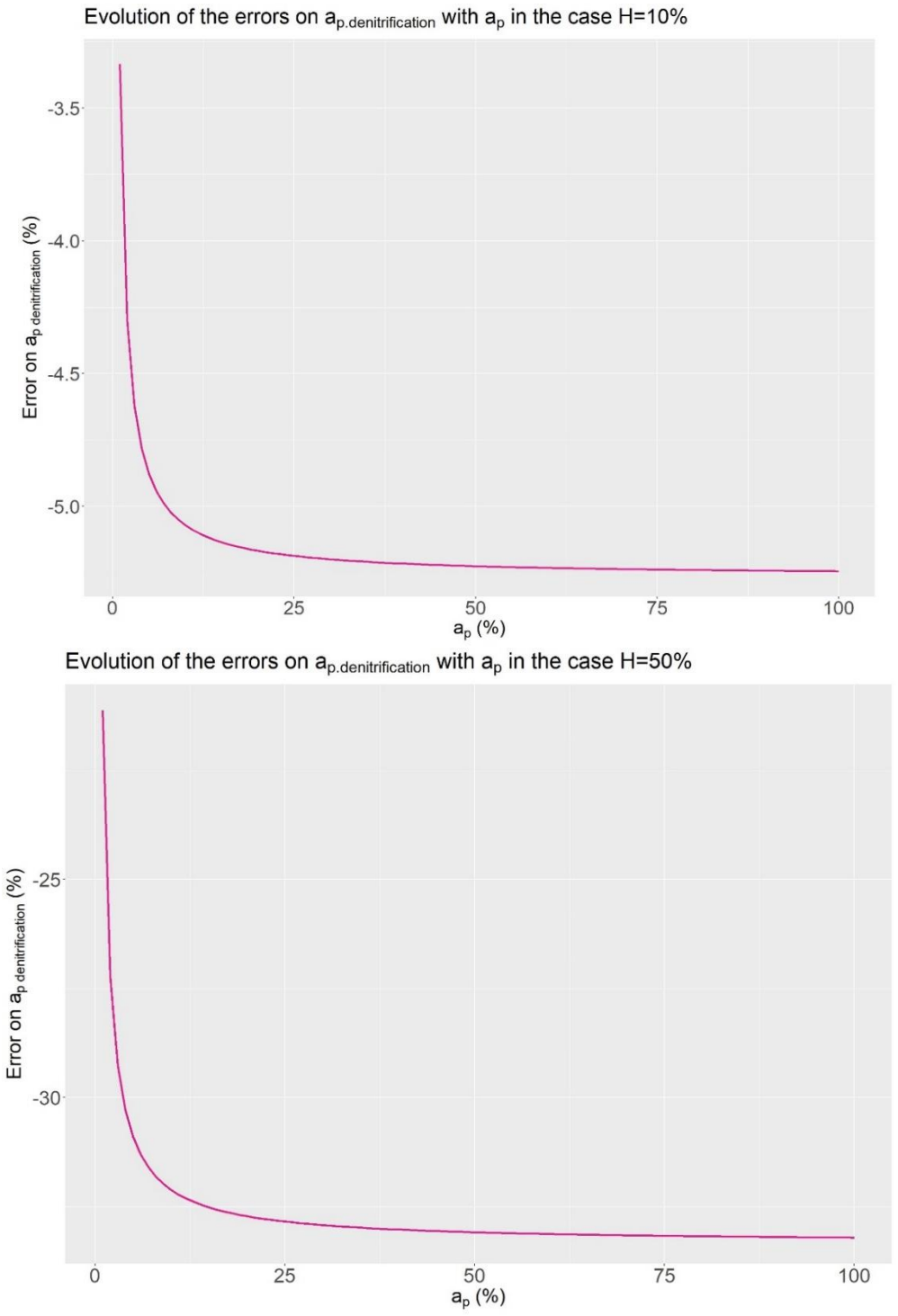

***Figure 16**: Evolution of the errors made on the measurement of the soil denitrifying pool enrichment*

Total apparent enrichment $\boldsymbol{a_{p\ total}}$ in blue for Figure (a); only the labelled pool enrichment $\boldsymbol{a_{p\ denitrification}}$ in pink for Figure (b) with the parameter $\boldsymbol{a_p}$ when using the ^{15}NGF and ignoring hybrid

molecule contribution (cases ***H*** = 10 or 50%).These errors are high at low enrichments of the soil denitrifying pool but reaching a plateau at higher values (for both $a_{p\ denitrification}$ and $a_{p\ total}$).

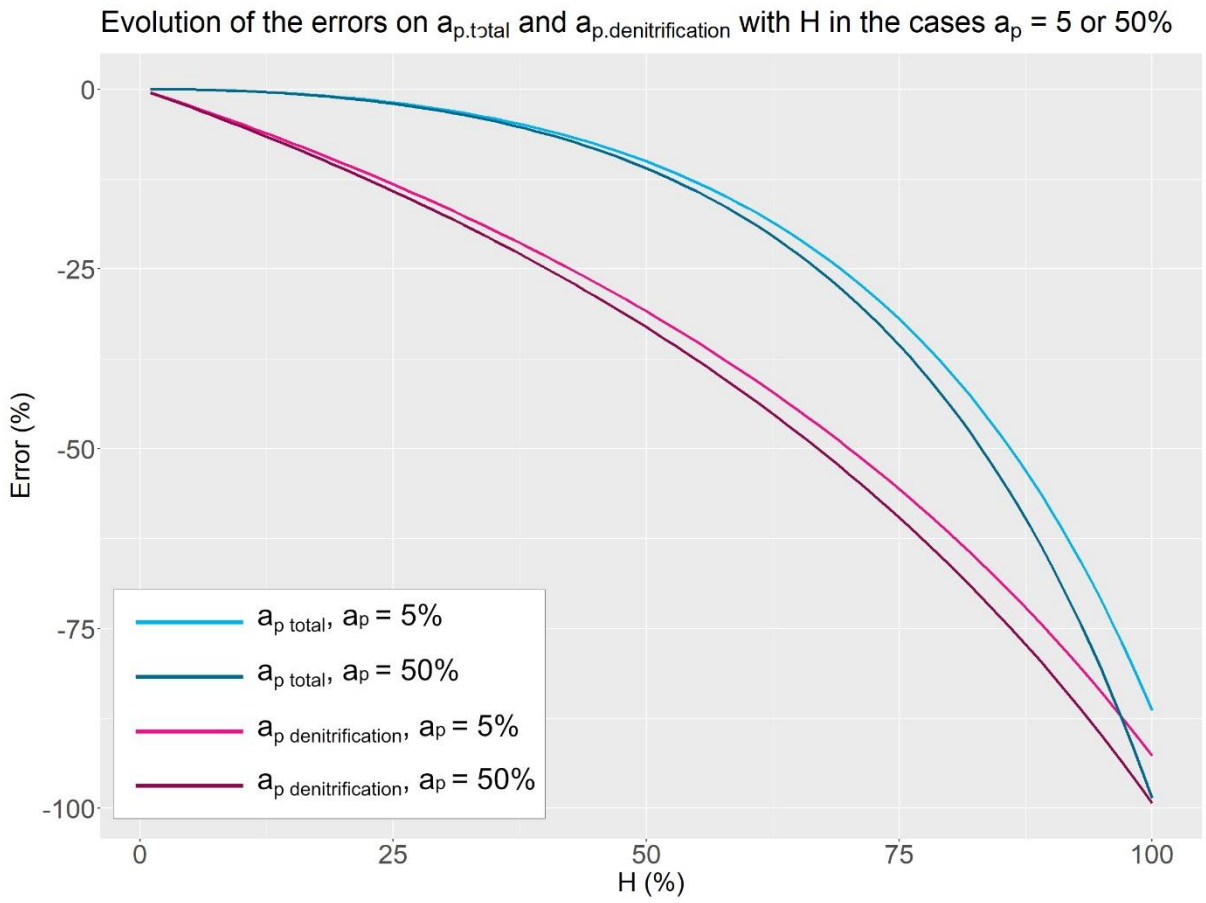

Figure 17*: Evolution of the errors made on the measurement of the soil denitrifying pool enrichment with the parameter* ***H***

Total apparent enrichment $\boldsymbol{a_{p\ total}}$ in blue; only the labelled pool enrichment $\boldsymbol{a_{p\ denitrification}}$ in pink. Cases where $\boldsymbol{a_p}$ = 5% or 50%.

The errors on both $\boldsymbol{a_{p\ total}}$ and $\boldsymbol{a_{p\ denitrification}}$ increase when increasing the parameter $\boldsymbol{a_p}$. For the same value of $\boldsymbol{a_p}$, the error on $\boldsymbol{a_{p\ denitrification}}$ is always higher (in absolute value) than the one on $\boldsymbol{a_{p\ total}}$.

2.8.2) Annex 2:

We simulated ΔR29 and ΔR30 values for 300 cases, with the parameters shown in **Table 11**.

***Table 11**: Parameters used for the simulation of R29 and R30 with reduction of the [N_2] atmospheric background*

d	***a_p*(%)**	**N_2 background (%)**
1E-08	5	78
5E-08	10	20
1E-07	20	10
5E-07	30	5
1E-06	40	1
5E-06	50	
1E-05		
5E-05		
1E-04		
5E-04		

Then we expressed G29 and G30 as in equation [16a] for all treatments except in the cases where [N_2] = 78% since it is the reference for all ratios G29 and G30.

For each case of similar ***d***, ***a_p*** and [N_2] background parameters, the ratios $\frac{G29}{G30}$ equal approximately 1. To have an idea of how close to 1 these ratios are, we looked for the highest difference defined as:

$$\max\left(\left|1-\frac{G29}{G30}\right|\right) \qquad [19]$$

and found a maximum of 3.69×10^{-10}. Given this very small deviation from 1, we will consider that G29 = G30 for all cases, meaning that lowering the N_2 background affects G29 and G30 similarly. From this point we will thus only focus on G29, knowing that exact same conclusions can be drawn for G30.

To show that G29 and G30 are independent with ***d*** and $\boldsymbol{\alpha_p}$, we cannot use correlation tests like we did for the presence of hybrid molecules (**Table 8, Chapter 2.8.1**). Indeed, as can be seen in **Table 5**, G29 and G30 appear to be correlated with ***d*** (and $\boldsymbol{\alpha_p}$, not shown); however, the magnitude of evolution with these parameters is very small through the large range of realistic parameters used for the simulation. For example, for the case where $\boldsymbol{\alpha_p}$ = 50% and $[N_2]$ = 20%, G29 goes from 3.90000 to 3.89858 when ***d*** goes from 1.10^{-8} to 5.10^{-4}.

When studying series with similar $\boldsymbol{\alpha_p}$ and $[N_2]$ background parameters while ***d*** varies, the highest coefficient of variation found is 2.61%. For each series, we also expressed the maximum difference of any value to the mean of that series with equation [20]:

$$\frac{\max\left(|X_i - \bar{X}|\right)}{\bar{X}} \qquad [20]$$

where X_i is a value in the series and $\bar{X}$ is the mean of that series. The maximum of these series maximums was 2.94%.

Similarly, if studying series with similar ***d*** and $[N_2]$ background parameters while $\boldsymbol{\alpha_p}$ varies, the highest coefficient of variation found is 0.88%. The maximum of series maximum differences of any value to the mean was 1.24%.

We verified that all these results and trends were still valid at very high ^{15}N enrichment of the soil denitrifying pool and found similar results even at the extreme limit $\boldsymbol{\alpha_p}$ = 100% (although G29 = 0 in this particular case, since an enrichment $\boldsymbol{\alpha_p}$ = 100% leads to the formation of $^{30}N_2$ molecules only). Given the small observed variations (<3%) through the large range of realistic parameters used, we will consider G29 (and thus G30) to be independent of both ***d*** and $\boldsymbol{\alpha_p}$.

2.8.3) Annex 3:

Let us prove that the ratios R29 and R30 are necessarily greater after incubation than their initial values when using the ^{15}NGF.

We first need to prove that R29 and R30 are strictly increasing with $\boldsymbol{a_p}$ for a pool of N_2 at isotopic equilibrium. These ratios are defined for $\boldsymbol{a_p} \in [0;1[$ as:

$$R29 = \frac{2a_p(1-a_p)}{(1-a_p)^2} \qquad [21]$$

$$R29 = \frac{2a_p}{(1-a_p)} \qquad [22]$$

$$\frac{d(R29)}{d(a_p)} = \frac{2}{(1-a_p)^2} > 0 \qquad [23]$$

Since the first derivative of R29 with $\boldsymbol{a_p}$ is strictly positive, R29 is strictly increasing with $\boldsymbol{a_p}$.

$$R30 = \frac{{a_p}^2}{(1-a_p)^2} \qquad [24]$$

The numerator of R30 is strictly increasing with $\boldsymbol{a_p}$. The denominator is strictly decreasing for $\boldsymbol{a_p} \in [0;1[$, thus the ratio R30 is strictly increasing with $\boldsymbol{a_p}$.

The rest of the study will focus on R29 but similar conclusions can be drawn for R30.

Since the soil denitrifying pool has necessarily a higher ^{15}N enrichment than the atmosphere after tracer injection and consequently to the fact that R29 and R30 are strictly increasing with $\boldsymbol{a_p}$, we can conclude that:

$$\frac{(^{29}N_2)_{denitrified}}{(^{28}N_2)_{denitrified}} > \frac{(^{29}N_2)_{atmosphere}}{(^{28}N_2)_{atmosphere}} \qquad [25]$$

We can then prove that:

$$R29_{(t)} > R29_{(0)} \qquad [26]$$

$$\frac{(^{29}N_2)_{atmosphere} + (^{29}N_2)_{denitrified}}{(^{28}N_2)_{atmosphere} + (^{28}N_2)_{denitrified}} > \frac{(^{29}N_2)_{atmosphere}}{(^{28}N_2)_{atmosphere}} \qquad [27]$$

when inequation [25] is verified.

Let us call $(^{29}N_2)_{atmosphere}$ and $(^{28}N_2)_{atmosphere}$ ***a*** and ***b*** respectively and $(^{29}N_2)_{denitrified}$ and $(^{28}N_2)_{denitrified}$ ***x*** and ***y*** respectively.

Then, inequation [27] can be written as:

$$\frac{a+x}{b+y} > \frac{a}{b} \qquad [28]$$

$$\frac{a+x}{b+y} - \frac{a(1+\frac{y}{b})}{b+y} > 0 \qquad [29]$$

$$\frac{x-\frac{ay}{b}}{b+y} > 0 \qquad [30]$$

In our model, ***b*** and ***y*** are necessarily positive, thus, inequation [30] is verified if its numerator is positive. This numerator is necessarily positive when inequation [25] is verified. Thus, the ratios R29 and R30 are necessarily greater after incubation than their initial values when using the ^{15}NGF.

2.9) References

Almaraz, M., Wong, M. Y., & Yang, W. H. (2020). Looking back to look ahead: a vision for soil denitrification research. Ecology, 101(1). https://doi.org/10.1002/ecy.2917

Anthony, W. H., Hutchinson, G. L., & Livingston, G. P. (1995). Chamber Measurement of Soil-Atmosphere Gas Exchange : Linear vs. Diffusion-Based Flux Models. Soil Science Society of America Journal, 59(5), 1308-1310. https://doi.org/10.2136/sssaj1995.03615995005900050015x

Arah, J. R. M. (1992). New formulae for mass spectrometric analysis of nitrous oxide and dinitrogen emissions. Soil Science Society of America Journal 56(3), 795-800. https://doi.org/10.2136/sssaj1992.03615995005600030020x.

Arah, J. R. M., Crichton, I. J., & Smith, K. A. (1993). Denitrification measured directly using a single-inlet mass spectrometer and by acetylene inhibition. Soil Biology and Biochemistry (Vol. 25, Issue 2) 233-38. https://doi.org/10.1016/0038-0717(93)90032-7.

Arah, J. R. M. (1997). Apportioning nitrous oxide fluxes between nitrification and denitrification using gas-phase mass spectrometry. Soil Biology and Biochemistry (Vol. 29, Issue 8), 1295-99. https://doi.org/10.1016/S0038-0717(97)00027-8.

Baily, A., Watson, C. J., Laughlin, R., Matthews, D., McGeough, K., & Jordan, P. (2012). Use of the ^{15}N gas flux method to measure the source and level of N_2O and N_2 emissions from grazed grassland. Nutrient Cycling in Agroecosystems, 94(2–3), 287–298. https://doi.org/10.1007/s10705-012-9541-x

Berendt, J., Tenspolde, A., Rex, D., Clough, T. J., & Wrage-Mönnig, N. (2020). Application methods of tracers for N_2O source determination lead to inhomogeneous distribution in field plots. Analytical Science Advances, 1(4), 221–232. https://doi.org/10.1002/ansa.202000100

Bergsma, T. T., Bergsma, Q. C., Ostrom, N. E., & Robertson, G. P. (1999). A heuristic model for the calculation of dinitogen and nitrous oxide flux from nitrogen-15-labeled soil. Soil Science Society of America Journal 63(6), 1709-16. https://doi.org/10.2136/sssaj1999.6361709x.

Bergsma, T. T., Ostrom, N. E., Emmons, M., & Robertson, G. P. (2001). Measuring simultaneous fluxes from soil of N_2O and N_2 in the field using the ^{15}N-gas “nonequilibrium” technique. Environmental Science and Technology, 35(21), 4307–4312. https://doi.org/10.1021/es010885u

Boast, C. W., Mulvaney, R. L., & Baveye, P. (1988). Evaluation of Nitrogen-15 Tracer Techniques for Direct Measurement of Denitrification in Soil: I. Theory. Soil Science Society of America Journal 52(5), 1317–1322. https://doi.org/10.2136/sssaj1988.03615995005200050020x

Bollmann, A., & Conrad, R. (1997). Acetylene blockage technique leads to underestimation of denitrification rates in oxic soils due to scavenging of intermediate nitric oxide. Soil Biology and Biochemistry (Vol. 29, Issue 7), 1067-77. https://doi.org/10.1016/S0038-0717(97)00007-2

Bremner, J. M. (1997). Sources of nitrous oxide in soils. Nutrient Cycling in Agroecosystems (Vol. 49). Kluwer Academic Publishers. https://doi.org/10.1023/A:1009798022569

Buchen, C., Lewicka-Szczebak, D., Fuß, R., Helfrich, M., Flessa, H., & Well, R. (2016). Fluxes of N_2 and N_2O and contributing processes in summer after grassland renewal and grassland conversion to maize cropping on a Plaggic Anthrosol and a Histic Gleysol. Soil Biology and Biochemistry (Vol. 101), 6–19. https://doi.org/10.1016/j.soilbio.2016.06.028

Buchen-Tschiskale, C., Well, R., & Flessa, H. (2023). Tracing nitrogen transformations during spring development of winter wheat induced by ^{15}N labeled cattle slurry applied with different techniques. Science of the Total Environment, 871(February), 162061. https://doi.org/10.1016/j.scitotenv.2023.162061

Butterbach-Bahl, K., Willibald, G., & Papen, H. (2002). Soil core method for direct simultaneous determination of N_2 and N_2O emissions from forest soils. Plant and Soil (Vol. 240), No. 1, pp. 105-116. https://doi.org/10.1023/A:1015870518723

Cárdenas, L. M., Hawkins, J. M. B., Chadwick, D., & Scholefield, D. (2003). Biogenic gas emissions from soils measured using a new automated laboratory incubation system. Soil Biology and Biochemistry (Vol. 35, Issue 6), 867–870. https://doi.org/10.1016/S0038-0717(03)00092-0

Cho, C. M., & Sakdinan, L. (1978). Mass spectrometric investigation on denitrification. Canadian Journal of Soil Science 58, nº 3: 443-57. https://doi.org/10.4141/cjss78-051

Clayton, H., Mctaggart, I. P., Parker, J., Swan, L., Smith, K. A., & Smith, K. A. (1997). Nitrous oxide emissions from fertilised grassland: A 2-year study of the effects of N fertiliser form and environmental conditions. Biology and Fertility of Soils (Vol. 25), nº 3: 252-60. https://doi.org/10.1007/s003740050311.

Clough, T. J., Stevens, R. J., Laughlin, R. J., Sherlock, R. R., & Cameron, K. C. (2001). Transformations of inorganic-N in soil leachate under differing storage conditions. Soil Biology and Biochemistry (Vol. 33, Issue 11): 1473-80. https://doi.org/10.1016/S0038-0717(01)00056-6.

Clough, T. J., Sherlock, R. R., & Rolston, D. E. (2005). A review of the movement and fate of N_2O in the subsoil. Nutrient Cycling in Agroecosystems, 72(1), 3–11. https://doi.org/10.1007/s10705-004-7349-z

Clough, T. J., Lanigan, G. J., de Klein, C. A. M., Samad, M. S., Morales, S. E., Rex, D., Bakken, L. R., Johns, C., Condron, L. M., Grant, J., & Richards, K. G. (2017). Influence of soil moisture on codenitrification fluxes from a urea-affected pasture soil. Scientific Reports, 7(1). https://doi.org/10.1038/s41598-017-02278-y

Cuhel, J., Simek, M., Laughlin, R. J., Bru, D., Chèneby, D., Watson, C. J., & Philippot, L. (2010). Insights into the effect of soil pH on N_2O and N_2 emissions and denitrifier community size and activity. Applied and Environmental Microbiology, 76(6), 1870–1878. https://doi.org/10.1128/AEM.02484-09

Davidson, E.A., Hart, S.C., Shanks, C.A. and Firestone, M.K. (1991), Measuring gross nitrogen mineralization, and nitrification by ^{15}N isotopic pool dilution in intact soil cores. Journal of Soil Science, 42: 335-349. https://doi:10.1111/j.1365-2389.1991.tb00413.x

Deppe, M., Well, R., Giesemann, A., Spott, O., & Flessa, H. (2017). Soil N_2O fluxes and related processes in laboratory incubations simulating ammonium fertilizer depots. Soil Biology and Biochemistry (Vol. 104), 68–80. https://doi.org/10.1016/j.soilbio.2016.10.005

Dodds, W. K., Burgin, A. J., Marcarelli, A. M., & Strauss, E. A. (2017). Nitrogen transformations. Methods in Stream Ecology: Third Edition (Vol. 2, pp. 173–196). Elsevier. https://doi.org/10.1016/B978-0-12-813047-6.00010-3

Focht, D.D. & Stolzy, L.H. (1978). Long-term denitrification studies in soils fertilized with $(^{15}NH_4)_2SO_4$. Soil Science Society of America Journal 42: 894-898. https://doi.org/10.2136/sssaj1978.03615995004200060012x.

Focht, D.D., Stolzy, L.H. & Meek, B.D. (1979). Sequential reduction of nitrate and nitrous oxide under field conditions as brought about by organic amendments and irrigation management, Soil Biology and Biochemistry (Vol. 11, Issue 1), 37-46. https://doi.org/10.1016/0038-0717(79)90116-0.

Focht, D. D., Valoras, N., & Letey, J. (1980). Use of interfaced gas chromatography-mass spectrometry for detection of concurrent mineralization and denitrification in soil. Journal of Environmental Quality 9, n° 2, 218-23. https://doi.org/10.2134/jeq1980.00472425000900020011x.

Forthofer, R. N., Lee, E. S., & Hernandez, M. (2007). Linear Regression. In Biostatistics (p. 349-386). Elsevier. https://doi.org/10.1016/B978-0-12-369492-8.50018-2

Friedl, J., Scheer, C., Rowlings, D. W., Mumford, M. T., & Grace, P. R. (2017). The nitrification inhibitor DMPP (3,4-dimethylpyrazole phosphate) reduces N_2 emissions from intensively managed pastures in subtropical Australia. Soil Biology and Biochemistry (Vol. 108), 55–64. https://doi.org/10.1016/j.soilbio.2017.01.016

Friedl, J., Cardenas, L. M., Clough, T. J., Dannenmann, M., Hu, C., & Scheer, C. (2020). Measuring denitrification and the N_2O:(N_2O + N_2) emission ratio from terrestrial soils. Current Opinion in Environmental Sustainability (Vol. 47, pp. 61–71). Elsevier B.V. https://doi.org/10.1016/j.cosust.2020.08.006

Groffman, P. M., & Tiedje, J. M. (1989). Denitrification in north temperate forest soils: Spatial and temporal patterns at the landscape and seasonal scales. Soil Biology and Biochemistry (Vol. 21, Issue 5), 613-620. https://doi.org/10.1016/0038-0717(89)90053-9.

Groffman, P.M., Altabet, M.A., Böhlke, J.K., Butterbach-Bahl, K., David, M.B., Firestone, M.K., Giblin, A.E., Kana, T.M., Nielsen, L.P. and Voytek, M.A. (2006) Methods for measuring denitrification: diverse approaches to a difficult problem. Ecological Applications (Vol. 16, Issue 6). https://doi.org/10.1890/1051-0761(2006)016[2091:MFMDDA]2.0.CO;2.

Guiraud, G., & Berlier, Y (1970). Quantitative and isotopic determination by mass spectrometry of gaseous compounds produced during denitrification. Chim. Anal. (Paris), 52, 53-56.

Hauck, R. D., & Melsted, S. W. (1956) Some aspects of the problem of evaluating denitrification in soils. Soil Science Society of America Journal 20(3), 361-64. https://doi.org/10.2136/sssaj1956.03615995002000030017x.

Hauck, R. D., Melsted, S. W., & Yankwich, P. E. (1958). Use of N-isotope distribution in nitrogen gas in the study of denitrification. Soil Science, 86, 287. https://doi.org/10.1097/00010694-195811000-00011

Hauck, R., & Bouldin, D. (1961). Distribution of isotopic nitrogen in nitrogen gas during denitrification. Nature 191, 871–872. https://doi.org/10.1038/191871a0

Hayes, J. M. In organic geochemistry of contemporaneous and ancient sediments; Meinschein, W. G., Ed.; Society of Economic Paleontologists and Minerologists: Bloomington, 1993; p 5-1.

Hossler, K., & Bouchard, V. (2008). The joint estimation of soil trace gas fluxes. Soil Science Society of America Journal 72(5), 1382–1393. https://doi.org/10.2136/sssaj2007.0232

Humbert, S., Tarnawski, S., Fromin, N., Mallet, M. P., Aragno, M., & Zopfi, J. (2010). Molecular detection of anammox bacteria in terrestrial ecosystems: Distribution and diversity. ISME Journal, 4(3), 450–454. https://doi.org/10.1038/ismej.2009.125

Hutchinson, G. L., & Mosier, A. R. (1981). Improved soil cover method for field measurement of nitrous oxide fluxes. Soil Science Society of America Journal 45(2), 311-16. https://doi.org/10.2136/sssaj1981.03615995004500020017x.

Hutchinson, G.L. & Livingston, G.P. (2002). 4.5 Soil–atmosphere gas exchange. In Methods of Soil Analysis (eds J.H. Dane and G. Clarke Topp). https://doi.org/10.2136/sssabookser5.4.c47

Hwang, S., & Hanaki, K. (2000). Effects of oxygen concentration and moisture content of refuse on nitrification, denitrification and nitrous oxide production. Bioresource Technology, Volume 71, Issue 2, Pages 159-165 - https://doi.org/10.1016/S0960-8524(99)90068-8.

IPCC (2013). Climate change 2013: The physical science basis. Contribution of Working Group I to the Fifth Assessment Report of the Intergovernmental Panel on Climate Change (Rep., 1535 pp.). Cambridge, UK and New York.

Jarvis, S. C., Barraclough, D., Williams, J., & Rook, A. J. (1991). Patterns of denitrification loss from grazed grassland: Effects of N fertilizer inputs at different sites. Plant and Soil (Vol. 131). https://doi.org/10.1007/BF00010422

Jaynes, D. B., & Rogowski, A. S. (1983). Applicability of Fick's law to gas diffusion. Soil Science Society of America Journal 47: 425-430. https://doi.org/10.2136/sssaj1983.03615995004700030007x

Kemmann, B., Wöhl, L., Fuß, R., Schrader, S., Well, R., & Ruf, T. (2021). N_2 and N_2O mitigation potential of replacing maize with the perennial biomass crop Silphium perfoliatum—An incubation study. GCB Bioenergy, 13(10), 1649–1665. https://doi.org/10.1111/gcbb.12879

Krause, H. M., Thonar, C., Eschenbach, W., Well, R., Mäder, P., Behrens, S., Kappler, A., & Gattinger, A. (2017). Long term farming systems affect soils potential for N_2O production and reduction processes under denitrifying conditions. Soil Biology and Biochemistry (Vol. 114), 31–41. https://doi.org/10.1016/j.soilbio.2017.06.025

Kulkarni, M. V., Burgin, A. J., Groffman, P. M., & Yavitt, J. B. (2014). Direct flux and ^{15}N tracer methods for measuring denitrification in forest soils. Biogeochemistry, 117(2–3), 359–373. https://doi.org/10.1007/s10533-013-9876-7

Lassaletta, L., Billen, G., Grizzetti, B., Anglade, J., & Garnier, J. (2014). 50 year trends in nitrogen use efficiency of world cropping systems: The relationship between yield and nitrogen input to cropland. Environmental Research Letters, 9(10). https://doi.org/10.1088/1748-9326/9/10/105011

Laughlin, R. J., & Stevens, R. J. (2002). Evidence for fungal dominance of denitrification and codenitrification in a Grassland Soil. Soil Science Society of America Journal 66(5), 1540-48. https://doi.org/10.2136/sssaj2002.1540.

Laughlin, R. J., & Stevens, R. J. (2003). Changes in composition of nitrogen-15-labeled gases during storage in septum-capped vials. Soil Science Society of America Journal 67, 540-543. https://doi.org/10.2136/sssaj2003.5400

Lewicka-Szczebak, D., Well, R., Giesemann, A., Rohe, L., & Wolf, U. (2013). An enhanced technique for automated determination of ^{15}N signatures of N_2, (N_2+N_2O) and N_2O in gas samples. Rapid Communications in Mass Spectrometry, 27(13), 1548–1558. https://doi.org/10.1002/rcm.6605

Lewicka-Szczebak, D., Augustin, J., Giesemann, A., & Well, R. (2017). Quantifying N_2O reduction to N_2 based on N_2O isotopocules - validation with independent methods (helium incubation and ^{15}N gas flux method). Biogeosciences, 14(3), 711–732. https://doi.org/10.5194/bg-14-711-2017

Lewicka-Szczebak, D., & Well, R. (2020**a**). The ^{15}N gas-flux method to determine N_2 flux: A comparison of different tracer addition approaches. SOIL, 6(1), 145–152. https://doi.org/10.5194/soil-6-145-2020

Lewicka-Szczebak, D., Piotr Lewicki, M., & Well, R. (2020**b**). N_2O isotope approaches for source partitioning of N_2O production and estimation of N_2O reduction-validation with the ^{15}N gas-flux method in laboratory and field studies. Biogeosciences, 17(22), 5513–5537. https://doi.org/10.5194/bg-17-5513-2020

Liu, Y., Wang, R., Pan, Z. L., Zheng, X. H., Wei, H. H., Zhang, H. R., Mei, B. L., Quan, Z., Fang, Y. T., & Ju, X. T. (2022). Quantifying in situ N_2 fluxes from an intensively managed calcareous soil using the ^{15}N gas-flux method. Journal of Integrative Agriculture, 21(9), 2750–2766. https://doi.org/10.1016/j.jia.2022.07.016

Livingston, G. P., Hutchinson, G. L., & Spartalian, K. (2006). Trace gas emission in chambers. Soil Science Society of America Journal 70(5), 1459–1469. https://doi.org/10.2136/sssaj2005.0322

Loick, N., Dixon, E. R., Abalos, D., Vallejo, A., Matthews, G. P., McGeough, K. L., Well, R., Watson, C. J., Laughlin, R. J., & Cardenas, L. M. (2016). Denitrification as a source of nitric oxide emissions from incubated soil cores from a UK grassland soil. Soil Biology and Biochemistry (Vol. 95), 1–7. https://doi.org/10.1016/j.soilbio.2015.12.009

Loick, N., Dixon, E., Abalos, D., Vallejo, A., Matthews, P., McGeough, K., Watson, C., Baggs, E. M., & Cardenas, L. M. (2017). “Hot spots” of N and C impact nitric oxide, nitrous oxide and nitrogen gas emissions from a UK grassland soil. Geoderma, 305, 336–345. https://doi.org/10.1016/j.geoderma.2017.06.007

Long, A., Heitman, J., Tobias, C., Philips, R., & Song, B. (2013). Co-occurring anammox, denitrification, and codenitrification in agricultural soils. Applied and Environmental Microbiology, 79(1), 168–176. https://doi.org/10.1128/AEM.02520-12

McGeough, K. L., Laughlin, R. J., Watson, C. J., Müller, C., Ernfors, M., Cahalan, E., & Richards, K. G. (2012). The effect of cattle slurry in combination with nitrate and the nitrification inhibitor dicyandiamide on in situ nitrous oxide and dinitrogen emissions. Biogeosciences, 9(12), 4909–4919. https://doi.org/10.5194/bg-9-4909-2012

Meyer, M.L., Bloom, P.R. & Grava, J. (1989). Transformation and losses of applied nitrogen-15 labeled ammonium in a flooded organic soil. Soil Science Society of America Journal 53, 79-85. https://doi.org/10.2136/sssaj1989.03615995005300010015x

Meyer, A., Bergmann, J., Butterbach-Bahl, K., & Brüggemann, N. (2010). A new ^{15}N tracer method to determine N turnover and denitrification of Pseudomonas stutzeri. Isotopes in Environmental and Health Studies, 46(4), 409–421. https://doi.org/10.1080/10256016.2010.528840

Morse, J. L., & Bernhardt, E. S. (2013). Using ^{15}N tracers to estimate N_2O and N_2 emissions from nitrification and denitrification in coastal plain wetlands under contrasting land-uses. Soil Biology and Biochemistry (Vol. 57), 635–643. https://doi.org/10.1016/j.soilbio.2012.07.025

Müller, C., Laughlin, R. J., Spott, O., & Rütting, T. (2014). Quantification of N_2O emission pathways via a ^{15}N tracing model. Soil Biology and Biochemistry (Vol. 72), 44–54. https://doi.org/10.1016/j.soilbio.2014.01.013

Mulvaney, R. L., & Kurtz, L. T. (1982). A new method for determination of ^{15}N-labeled nitrous oxide. Soil Science Society of America Journal 46, n° 6, 1178-84. https://doi.org/10.2136/sssaj1982.03615995004600060012x

Mulvaney, R. L. (1984). Determination of ^{15}N-labeled dinitrogen and nitrous oxide with triple-collector mass spectrometers. Soil Science Society of America Journal 48, 690–692. https://doi.org/10.2136/sssaj1984.03615995004800030045x

Mulvaney, R. L., & L. T. Kurtz (1984). Evolution of dinitrogen and nitrous oxide from nitrogen-15 fertilized soil cores subjected to wetting and drying cycles. Soil Science Society of America Journal 48(3), 596-602. https://doi.org/10.2136/sssaj1984.03615995004800030026x

Mulvaney, R. L., & Boast, C. W. (1986). Equations for determination of nitrogen-15 labeled dinitrogen and nitrous oxide by mass spectrometry. Soil Science Society of America Journal, 50(2), 360-363. https://doi.org/10.2136/sssaj1986.03615995005000020021x

Mulvaney, R. L. (1988). Evaluation of nitrogen-15 tracer techniques for direct measurement of denitrification in soil: III. laboratory studies. Soil Science Society of America Journal 52(5), 1327-32. https://doi.org/10.2136/sssaj1988.03615995005200050022x

Mulvaney, R. L., & Vanden Heuvel, R. M. (1988). Evaluation of nitrogen-15 tracer techniques for direct measurement of denitrification in soil: IV. field studies. Soil Science Society of America Journal 52(5), 1332-37. https://doi.org/10.2136/sssaj1988.03615995005200050023x

Myrold, D.D. (1990). Measuring denitrification in soils using 15N techniques. In: Revsbech, N.P., Sørensen, J. (eds) Denitrification in Soil and Sediment. Federation of European Microbiological

Societies Symposium Series, vol 56. Springer, Boston, MA. https://doi.org/10.1007/978-1-4757-9969-9_11

Nadeem, S., Dörsch, P., & Bakken, L. R. (2013). Autoxidation and acetylene-accelerated oxidation of NO in a 2-phase system: Implications for the expression of denitrification in ex situ experiments. Soil Biology and Biochemistry (Vol. 57), 606–614. https://doi.org/10.1016/j.soilbio.2012.10.007

Parkin, T. B., Venterea, R. T., & Hargreaves, S. K. (2012). Calculating the detection limits of chamber-based soil greenhouse gas flux measurements. Journal of Environmental Quality, 41(3), 705–715. https://doi.org/10.2134/jeq2011.0394

Pedersen, A. R. (2000). Estimating the nitrous oxide emission rate from the soil surface by means of a diffusion model. Scandinavian Journal of Statistics 27, 385-403. https://doi.org/10.1111/1467-9469.00196.

Pedersen, A. R., Petersen, S. O., & Vinther, F. P. (2001). Stochastic diffusion model for estimating trace gas emissions with static chambers. Soil Science Society of America Journal 65(1), 49-58. https://doi.org/10.2136/sssaj2001.65149x.

Pedersen, A. R., Petersen, S. O., & Schelde, K. (2010). A comprehensive approach to soil-atmosphere trace-gas flux estimation with static chambers. European Journal of Soil Science, 61(6), 888–902. https://doi.org/10.1111/j.1365-2389.2010.01291.x

Phillips, R. L., Song, B., McMillan, A. M. S., Grelet, G., Weir, B. S., Palmada, T., & Tobias, C. (2016). Chemical formation of hybrid di-nitrogen calls fungal codenitrification into question. Scientific Reports, 6. https://doi.org/10.1038/srep39077

Ravishankara, A. R., Daniel, J. S., & Portmann, R. W. (2009). Nitrous oxide (N_2O): The dominant ozone-depleting substance emitted in the 21st century. Science, 326(5949), 123–125. https://doi.org/10.1126/science.1176985

Rohe, L., Anderson, T.H., Flessa, H., Goeske, A., Lewicka-Szczebak, D., Wrage-Mönnig, N., & Well, R. (2021). Comparing modified substrate-induced respiration with selective inhibition (SIRIN) and N_2O isotope approaches to estimate fungal contribution to denitrification in three arable soils under anoxic conditions. Biogeosciences, 18(15), 4629 4650. https://doi.org/10.5194/bg-18-4629-2021

Rolston, D. E., Hoffman, D. L., & Toy, D. W. (1978). Field measurement of denitrification: I. Flux of N_2 and N_2O. Soil Science Society of America Journal, 42: 863-869. https://doi.org/10.2136/sssaj1978.03615995004200060004x

Rolston, D. E., Sharpley, A. N., Toy, D. W., & Broadbent, F. E. (1982). Field measurement of denitrification: III. Rates during irrigation cycles. Soil Science Society of America Journal, 46: 289-296. https://doi.org/10.2136/sssaj1982.03615995004600020015x

Rummel, P. S., Well, R., Pfeiffer, B., Dittert, K., Floßmann, S., & Pausch, J. (2021). Nitrate uptake and carbon exudation – do plant roots stimulate or inhibit denitrification? Plant and Soil, 459(1–2), 217–233. https://doi.org/10.1007/s11104-020-04750-7

Ruser, R., Flessa, H., Russow, R., Schmidt, G., Buegger, F., & Munch, J. C. (2006). Emission of N_2O, N_2 and CO_2 from soil fertilized with nitrate: Effect of compaction, soil moisture and rewetting. Soil

Biology and Biochemistry (Vol. 38, Issue 2), 263–274. https://doi.org/10.1016/j.soilbio.2005.05.005

Russow, R., Stevens, R. J., & Laughlin, R. J. (1996). Accuracy and precision for measurements of the mass ratio 30/28 in dinitrogen from air samples and its application to the investigation of N losses from soil by denitrification. Isotopes in Environmental and Health Studies, 32(2–3), 289–297. https://doi.org/10.1080/10256019608036322

Saggar, S., Jha, N., Deslippe, J., Bolan, N. S., Luo, J., Giltrap, D. L., Kim, D. G., Zaman, M., & Tillman, R. W. (2013). Denitrification and N_2O: N_2 production in temperate grasslands: Processes, measurements, modelling and mitigating negative impacts. In Science of the Total Environment (Vol. 465, pp. 173–195). https://doi.org/10.1016/j.scitotenv.2012.11.050

Scheer, C., Meier, R., Brüggemann, N., Grace, P. R., & Dannenmann, M. (2016). An improved ^{15}N tracer approach to study denitrification and nitrogen turnover in soil incubations. Rapid Communications in Mass Spectrometry : RCM, 30(18), 2017–2026. https://doi.org/10.1002/rcm.7689

Seitzinger, S. P., Nielsen, L. P., Caffrey, J., & Christensen, P. B. (1993). Denitrification measurements in aquatic sediments: A Comparison of Three Methods. Biogeochemistry 23(3), 147–67. http://www.jstor.org/stable/1469044

Seitzinger, S., Harrison, J. A., Böhlke, J. K., Bouwman, A. F., Lowrance, R., Peterson, B., Tobias, C., & Drecht, G. V. (2006). Denitrification across landscapes and waterscapes : a synthesis. Ecological Applications, 16(6), 2064-2090. https://doi.org/10.1890/1051-0761(2006)016[2064:DALAWA]2.0.CO;2

Selbie, D. R., Lanigan, G. J., Laughlin, R. J., Di, H. J., Moir, J. L., Cameron, K. C., Clough, T. J., Watson, C. J., Grant, J., Somers, C., & Richards, K. G. (2015). Confirmation of co-denitrification in grazed grassland. Scientific Reports, 5. https://doi.org/10.1038/srep17361

Sgouridis, F., & Ullah, S. (2015). Relative magnitude and controls of in Situ N_2 and N_2O fluxes due to denitrification in natural and seminatural terrestrial ecosystems using ^{15}N tracers. Environmental Science and Technology, 49(24), 14110–14119. https://doi.org/10.1021/acs.est.5b03513

Sgouridis, F., Stott, A., & Ullah, S. (2016). Application of the ^{15}N gas-flux method for measuring in situ N_2 and N_2O fluxes due to denitrification in natural and semi-natural terrestrial ecosystems and comparison with the acetylene inhibition technique. Biogeosciences, 13(6), 1821–1835. https://doi.org/10.5194/bg-13-1821-2016

Shoun, H., Kim, D.-H., Uchiyama, H., & Sugiyama, J. (1992). Denitrification by fungi. FEMS Microbiology Letters, 94(3), 277-281. https://doi.org/10.1111/j.1574-6968.1992.tb05331.x

Siegel, R. S., Hauck, R. D., & Kurtz, L. T. (1982). Determination of $^{30}N_2$ and application to measurement of N_2 evolution during denitrification. Soil Science Society of America Journal, 46: 68-74. https://doi.org/10.2136/sssaj1982.03615995004600010013x

Simarmata, T., Benckiser, G., & Ottow, J. C. G. (1993). Effect of an increasing carbon: nitrate-N ratio on the reliability of acetylene in blocking the N_2O-reductase activity of denitrifying bacteria in soil. Biology and Fertility of Soils (Vol. 15), 107–112 https://doi.org/10.1007/BF00336427

Spott, O., Russow, R., Apelt, B., & Stange, C. F. (2006). A ^{15}N-aided artificial atmosphere gas flow technique for online determination of soil N_2 release using the zeolite Köstrolith SX6®. Rapid Communications in Mass Spectrometry, 20(22), 3267–3274. https://doi.org/10.1002/rcm.2722

Spott, O., & Stange, C. F. (2007). A new mathematical approach for calculating the contribution of anammox, denitrification and atmosphere to an N_2 mixture based on a ^{15}N tracer technique. Rapid Communications in Mass Spectrometry, 21(14), 2398–2406. https://doi.org/10.1002/rcm.3098

Spott, O., & Florian Stange, C. (2011**a**). Formation of hybrid N_2O in a suspended soil due to co-denitrification of NH_2OH. Journal of Plant Nutrition and Soil Science, 174(4), 554–567. https://doi.org/10.1002/jpln.201000200

Spott, O., Russow, R., & Stange, C. F. (2011**b**). Formation of hybrid N_2O and hybrid N_2 due to codenitrification: First review of a barely considered process of microbially mediated N-nitrosation. In Soil Biology and Biochemistry (Vol. 43, Issue 10), 1995–2011. https://doi.org/10.1016/j.soilbio.2011.06.014

Stevens, R. J., Laughlin, R. J., Atkins, G. J., & Prosser, S. J. (1993). Automated determination of nitrogen-15-labeled dinitrogen and nitrous oxide by mass spectrometry. Soil Science Society of America Journal 57(4), 981-988. https://doi.org/10.2136/sssaj1993.03615995005700040017x

Stevens, R. J., Laughlin, R. J., Burns, L. C., Arah, J. R. M., & Hood, R. C. (1997). Measuring the contributions of nitrification and denitrification to the flux of nitrous oxide from soil. Soil Biology and Biochemistry (Vol. 29, Issue 2), 139-151. https://doi.org/10.1016/S0038-0717(96)00303-3

Stevens, R. J., & Laughlin, R. J. (2001). Lowering the detection limit for dinitrogen using the enrichment of nitrous oxide. Soil Biology and Biochemistry (Vol. 33, Issue 9), 1287-1289. https://doi.org/10.1016/S0038-0717(01)00036-0

Stevens, R. J., & Laughlin, R. J. (2002). Cattle slurry applied before fertilizer nitrate lowers nitrous oxide and dinitrogen emissions. Soil Science Society of America Journal 66(6), 647-652. https://doi.org/10.2136/sssaj2002.6470

Tanimoto, T., Hatano, K.-I., Kim, D.H., Uchiyarna, H., & Shoun, H. (1992). Co-denitrification by the denitrifying system of the fungus Fusarium oxysporum. FEMS Microbiology Letters (Vol. 93), 177-80. https://doi.org/10.1111/j.1574-6968.1992.tb05086.x.

Tauchnitz, N., Spott, O., Russow, R., Bernsdorf, S., Glaser, B., & Meissner, R. (2015). Release of nitrous oxide and dinitrogen from a transition bog under drained and rewetted conditions due to denitrification: results from a [^{15}N]nitrate–bromide double-tracer study. Isotopes in Environmental and Health Studies, 51(2), 300–321. https://doi.org/10.1080/10256016.2015.1011634

Thamdrup, B., & Dalsgaard, T. (2002). Production of N_2 through anaerobic ammonium oxidation coupled to nitrate reduction in marine sediments. Applied and Environmental Microbiology, 68(3), 1312–1318. https://doi.org/10.1128/AEM.68.3.1312-1318.2002

Vanden Heuvel, R. M., Mulvaney, R. L., & Hoeft, R. G. (1988). Evaluation of nitrogen-15 tracer techniques for direct measurement of denitrification in soil: II. Simulation studies. Soil Science Society of America Journal 52(5), 1322-26. https://doi.org/10.2136/sssaj1988.03615995005200050021x.

Wagner, S. W., Reicosky, D. C., & Alessi, R. S. (1997). Regression models for calculating gas fluxes measured with a closed chamber. Agronomy Journal, 89(2), 279-284. https://doi.org/10.2134/agronj1997.00021962008900020021x

Wang, R., Feng, Q., Liao, T., Zheng, X., Butterbach-Bahl, K., Zhang, W., & Jin, C. (2013). Effects of nitrate concentration on the denitrification potential of a calcic cambisol and its fractions of N_2, N_2O and NO. Plant and Soil, 363(1–2), 175–189. https://doi.org/10.1007/s11104-012-1264-x

Warner, D. I., Scheer, C., Friedl, J., Rowlings, D. W., Brunk, C., & Grace, P. R. (2019). Mobile continuous-flow isotope-ratio mass spectrometer system for automated measurements of N_2 and N_2O fluxes in fertilized cropping systems. Scientific Reports, 9(1), 11097. https://doi.org/10.1038/s41598-019-47451-7

Well, R., Becker, K.-W., Meyer, B., Langel, R., & Reineking, A. (1998). Continuous flow equilibration for mass spectrometric analysis of dinitrogen emissions. Soil Science Society of America Journal, 62(4), 906-910. https://doi.org/10.2136/sssaj1998.03615995006200040008x

Well, R., & Butterbach-Bahl, K. (2013). Comments on "A test of a field-based ^{15}N-nitrous oxide pool dilution technique to measure gross N_2O production in soil" by Yang et al. (2011), Global Change Biology, 17, 3577-3588. In Global Change Biology (Vol. 19, Issue 1, pp. 133–135). https://doi.org/10.1111/gcb.12005

Well, R., Burkart, S., Giesemann, A., Grosz, B., Köster, J. R., & Lewicka-Szczebak, D. (2019**a**). Improvement of the ^{15}N gas flux method for in situ measurement of soil denitrification and its product stoichiometry. Rapid Communications in Mass Spectrometry, 33(5), 437–448. https://doi.org/10.1002/rcm.8363

Well, R., Maier, M., Lewicka-Szczebak, D., Köster, J. R., & Ruoss, N. (2019**b**). Underestimation of denitrification rates from field application of the ^{15}N gas flux method and its correction by gas diffusion modelling. Biogeosciences, 16(10), 2233–2246. https://doi.org/10.5194/bg-16-2233-2019

Wijler, J., & Delwiche, C.C. (1954). Investigations on the denitrifying process in soil. Plant and Soil 5(2), 155–169. https://doi.org/10.1007/BF01343848

Wrage, N., Velthof, G. L., van Beusichem, M. L., & Oenema, O. (2001). Role of nitrifier denitrification in the production of nitrous oxide. Soil Biology and Biochemistry (Vol. 33, Issue 12-13), 1723-1732. https://doi.org/10.1016/S0038-0717(01)00096-7

Wu, H., Dannenmann, M., Fanselow, N., Wolf, B., Yao, Z., Wu, X., Brüggemann, N., Zheng, X., Han, X., Dittert, K., & Butterbach-Bahl, K. (2011). Feedback of grazing on gross rates of N mineralization and inorganic N partitioning in steppe soils of Inner Mongolia. Plant and Soil, 340(1), 127–139. https://doi.org/10.1007/s11104-010-0575-z

Xi, D., Fang, Y., & Zhu, W. (2022). Spatial Variations of Soil N_2 and N_2O Emissions from a Temperate Forest: Quantified by the In Situ ^{15}N Labeling Method. Forests, 13(9). https://doi.org/10.3390/f13091347

Yang, W. H., Teh, Y. A., & Silver, W. L. (2011). A test of a field-based ^{15}N-nitrous oxide pool dilution technique to measure gross N_2O production in soil. Global Change Biology, 17(12), 3577–3588. https://doi.org/10.1111/j.1365-2486.2011.02481.x

Yang, W. H., McDowell, A. C., Brooks, P. D., & Silver, W. L. (2014). New high precision approach for measuring ^{15}N-N_2 gas fluxes from terrestrial ecosystems. Soil Biology and Biochemistry (Vol. 69), 234–241. https://doi.org/10.1016/j.soilbio.2013.11.009

Yeung, L. Y., Li, S., Kohl, I. E., Haslun, J. A., Ostrom, N. E., Hu, H., Fischer, T. P., Schauble, E. A., & Young, E. D. (2017). Extreme enrichment in atmospheric $^{15}N^{15}N$. Science Advances, 3(11), eaao6741. https://doi.org/10.1126/sciadv.aao6741

Yeung, L. Y., Haslun, J. A., Ostrom, N. E., Sun, T., Young, E. D., van Kessel, M. A. H. J., Lücker, S., & Jetten, M. S. M. (2019). In situ quantification of biological N_2 production using naturally occurring $^{15}N^{15}N$. Environmental Science and Technology, 53(9), 5168–5175. https://doi.org/10.1021/acs.est.9b00812

Yoshida, N., & Toyoda, S. (2000). Constraining the atmospheric N_2O budget from intramolecular site preference in N_2O isotopomers. Nature, 405(6784), 330-334. https://doi.org/10.1038/35012558

Yu, K., Seo, D. C., & Delaune, R. D. (2010). Incomplete acetylene inhibition of nitrous oxide reduction in potential denitrification assay as revealed by using ^{15}N-Nitrate tracer. Communications in Soil Science and Plant Analysis, 41(18), 2201–2210. https://doi.org/10.1080/00103624.2010.504800

Yu, L., Harris, E., Lewicka-Szczebak, D., Barthel, M., Blomberg, M. R. A., Harris, S. J., Johnson, M. S., Lehmann, M. F., Liisberg, J., Müller, C., Ostrom, N. E., Six, J., Toyoda, S., Yoshida, N., & Mohn, J. (2020). What can we learn from N_2O isotope data? – Analytics, processes and modelling. Rapid Communications in Mass Spectrometry, 34(20). https://doi.org/10.1002/rcm.8858

Zaman, M., Heng, L., & Müller, C. (eds). (2021). Measuring emission of agricultural greenhouse gases and developing mitigation options using nuclear and related techniques : applications of nuclear techniques for GHGs. Springer International Publishing. https://doi.org/10.1007/978-3-030-55396-8

Zhu-Barker, X., Cavazos, A. R., Ostrom, N. E., Horwath, W. R., & Glass, J. B. (2015). The importance of abiotic reactions for nitrous oxide production. Biogeochemistry, 126(3), 251–267. https://doi.org/10.1007/s10533-015-0166-4

Zou, Y., Hirono, Y., Yanai, Y., Hattori, S., Toyoda, S., & Yoshida, N. (2014). Isotopomer analysis of nitrous oxide accumulated in soil cultivated with tea (Camellia sinensis) in Shizuoka, central Japan. Soil Biology and Biochemistry (Vol. 77), 276-291. https://doi.org/10.1016/j.soilbio.2014.06.016

Chapter 3: Developing a new method for the measurement of *in situ* denitrification

In this chapter, we will combine the ^{15}N Gas flux method to an artificial atmosphere depleted in N_2 to derive a new methodology of denitrification measurement. Our aim is to get *in situ* data, since the magnitude of difference between field and laboratory is usually very high. To that end, we developed two approaches, either using modified static chambers or small liners for the incubation of soil cores (**Figure 18**).

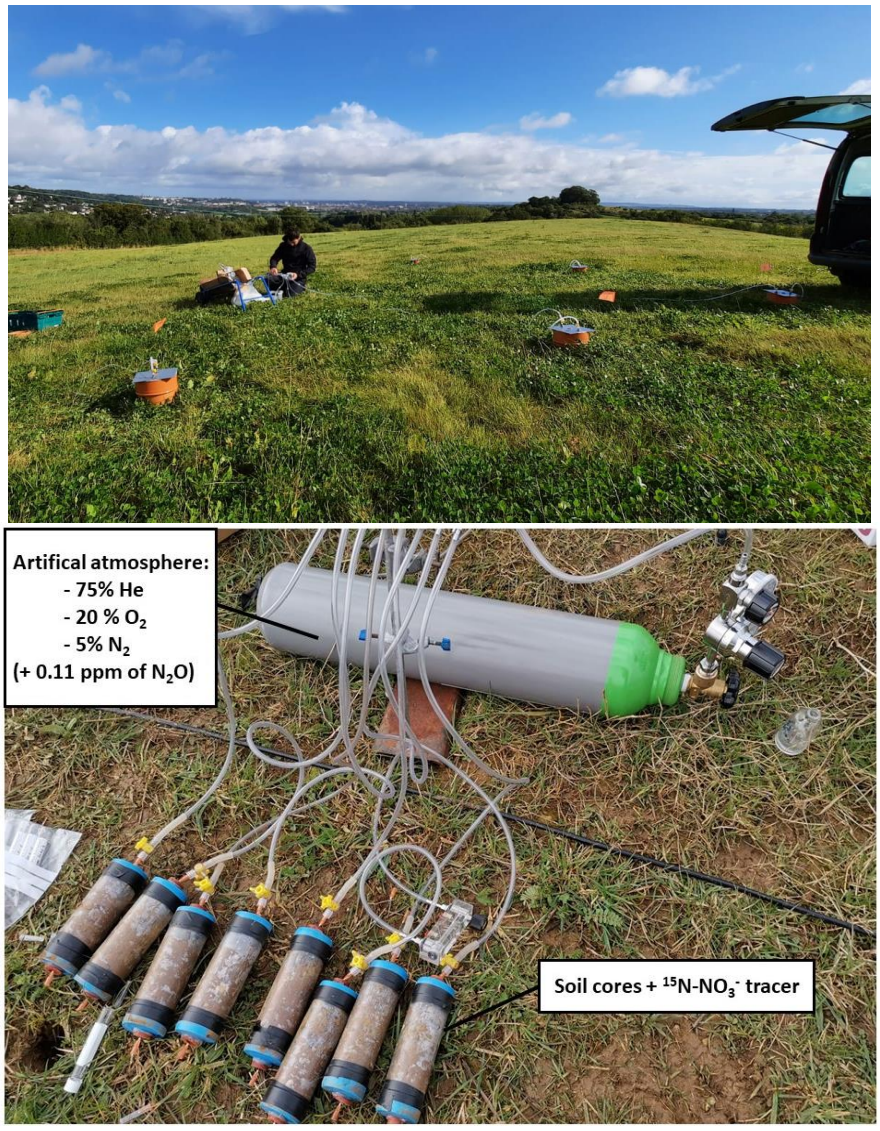

***Figure 18**: The chamber and liner approaches for the new method of denitrification measurement.*

This chapter is currently under review at the Soil Biology and Biochemistry Journal (Ms. Ref. No.: SBB22457) for publication as peer-reviewed article.

Under the supervision of Sami Ullah and Fotis Sgouridis, Gianni Micucci formulated the research questions, designed the experimental layout, ran the experiments, analysed the data and wrote the manuscript. Gianni Micucci further analysed the samples for gas chromatography in experiments 1 and 2. On the other hand, Fotis Sgouridis ran all isotopic analyses and the gas chromatography samples of experiments 3 and 4. Glória Pereira ran some IRMS samples to confirm the precision of the instrument of Fotis Sgouridis (see **Figure 19**). All the cited co-authors reviewed and corrected the manuscript.

Towards enhanced sensitivity of the ^{15}N Gas Flux Method for quantifying denitrification in soil

Gianni Micucci[1,*], Fotis Sgouridis[2], Niall P. McNamara[3], Stefan Krause[1], Iseult Lynch[1], Felicity Roos[4], M. Glória Pereira[3] and Sami Ullah[1,5]

- 1. School of Geography, Earth and Environmental Sciences, University of Birmingham, Edgbaston, B15 2TT Birmingham, United Kingdom.
- 2. School of Geographical Sciences, University of Bristol, BS8 1SS Bristol, United Kingdom.
- 3. UK Centre for Ecology & Hydrology, Lancaster Environment Centre, LA1 4AP Lancaster, United Kingdom.
- 4. UK National Trust, SN2 2NA Swindon, United Kingdom.
- 5. Birmingham Institute of Forest Research, University of Birmingham, Birmingham, UK.

Keywords: Denitrification, ^{15}N Gas Flux Method, Artificial Atmosphere, Nitrous Oxide Emission, Stable Isotope Tracing.

3.1) Abstract

Denitrification is the least studied process of the global N cycle mainly due to the sensitivity required to discriminate small fluxes of soil emitted N_2 against the high atmospheric N_2 background. We aimed to enhance the sensitivity of the ^{15}N Gas Flux method to measure *in situ* denitrification rates by optimising the quantity of ^{15}N-NO_3 tracer applied and by using an artificial atmosphere (containing 5 % N_2, 20 % O_2, 75 % He and 0.11 ppm of N_2O) during field incubation. We first conducted a dose-response laboratory study to assess the stimulation effect of nitrate tracer addition. Subsequently, we developed two novel approaches to measure *in situ* denitrification rates, using either modified static chambers or intact soil cores inside plastic liners; where in both cases the entire headspace was replaced by the artificial atmosphere prior to incubation. Furthermore, we compared the two models of calculations of the ^{15}N Gas Flux method (i.e. the "Mulvaney & Boast" and "Arah" models) as well as the calculated ^{15}N enrichment of the soil denitrifying pool based on either N_2 or N_2O isotopologue distribution data. The results show that doubling the amount of ambient nitrate does not lead to a significant stimulation of denitrification activity. However, excessive amendment of nitrate (e.g. 20 times the ambient levels) increased the denitrification product ratio by stimulating nitrous oxide emission. Our two novel field techniques were successful in measuring *in situ* denitrification rates. On average, the N_2 background concentration inside the static chambers increased to 29 % and 43 % after one and two hours of incubation; which resulted in 2.7 and 1.8 times greater sensitivities respectively compared to regular static chambers. On the other hand, the N_2 background concentration inside the liners increased to only 18 % after two hours on average. Combined with a smaller headspace (83 mL compared to 5.3 L), this approach enabled a more reliable detection of *in situ* N_2 emission rates. The smallest

denitrified N_2 concentration detected in the field was 0.77 ppm which is around 8-fold better than the classic ^{15}N Gas Flux method. Although this about 10 times higher than values reported using sophisticated flow through chamber combined with an artificial atmosphere, our method enabled the simultaneous incubation of 16 cores from different fields at the same time, enabling much wider spatial resolution. The Mulvaney & Boast model performed better than the Arah one and consistently yielded higher fluxes (17 % at maximum), especially for low ^{15}N enrichments of the soil denitrifying pool and short times of incubation. The ^{15}N enrichments calculated with either N_2 or N_2O data differed statistically, but the magnitude of difference was small (4.6 % at maximum). Measuring *in situ* denitrification is imperative to quantify realistic fluxes and the two methods presented here are inexpensive, reproducible and high resolution candidates. For increased sensitivity, we recommend using the method of Mulvaney & Boast for N_2O emissions and the resulting ^{15}N enrichment in combination with $^{29}N_2$ data (only) to determine N_2 emissions.

3.2) Introduction

Denitrification in soil is the sequential reduction of soil nitrate (NO_3^-) to gaseous dinitrogen (N_2) through microbial respiration under suboxic conditions. This sequential process includes nitrite (NO_2^-), nitric oxide (NO) and nitrous oxide (N_2O) as obligatory intermediates of reaction. Denitrification is considered the major pathway of reactive nitrogen (N) removal in terrestrial systems, which is of particular relevance for agricultural land uses (arable and grasslands) receiving large inputs of synthetic and organic N fertilizer (Lassaletta. et al, 2014). The last intermediate of this sequential process is nitrous oxide (N_2O), a greenhouse gas with 298 times greater radiative forcing than CO_2 (IPCC, 2013) which is also involved in the depletion of the ozone layer (Ravishankara et al., 2009). Denitrification has the ambiguous role of being both the only natural sink for

respiratory reduction of N_2O into N_2 but also a source of N_2O through incomplete denitrification. To guide future N_2O emission reduction strategies and close the nitrogen budget of ecosystems, it is of primary importance to fully characterize this process and particularly the reduction of N_2O to N_2.

Measuring small amounts of soil evolved N_2 against the high atmospheric N_2 background (78 % v/v) is very challenging (Groffman et al., 2006) and historically, denitrification has mainly been measured using three different techniques (Well et al. 2019**a**): the He/O_2 Gas Flow Soil Core method (He/O_2 GFSC), the Acetylene Inhibition Technique (AIT) and the ^{15}N Gas Flux method (^{15}NGF). Briefly, the He/O_2 GFSC is a laboratory-based incubation method where ambient atmosphere is replaced by a N_2-gas free mix of Helium (He) and dioxygen (O_2) in a tightly sealed vessel (Butterbach-Bahl et al., 2002; Cárdenas et al., 2003; Wang et al., 2013; Kulkarni et al., 2014; Loick et al., 2016; Wang et al., 2020). The AIT uses acetylene to block N_2O reduction to N_2 so that denitrification can be measured as total N_2O production. This technique has been very popular since its original application in the mid 1970's due to its simplicity and low cost but is today considered unsuitable due to several limitations (Seitzinger et al., 1993; Simarmata et al. 1993; Yu et al., 2010; Saggar et al., 2013; Sgouridis et al., 2016). Finally, the ^{15}NGF uses ^{15}N-labelled nitrate tracer applied to soil incubated in gas tight vessels under laboratory conditions or within static chambers in field applications to measure the abundance of ^{15}N atoms in both denitrified N_2 and N_2O molecules (Stevens & Laughlin 2002; Ruser et al., 2006; Baily et al., 2012; Sgouridis & Ullah, 2015; Deppe et al., 2017; Rummel et al., 2021; Liu et al., 2022**a**). The ^{15}NGF can be used with two main models of calculation, the "Mulvaney & Boast" model (based on Mulvaney & Boast, 1986) or the "Arah" model (based on Arah, 1992), as recently reviewed in Micucci et al. (2023). They both use the distribution of the ^{15}N atoms in the N_2 and N_2O isotopologues (molecules with same atomic identity but different isotopic composition) to derive the fluxes of denitrification, but they differ in their approach. The Mulvaney

& Boast model is based on the differences in isotopic ratios before and after incubation while the Arah approach is a mixing model of different ^{15}N pools. They both rely on the hypothesis that the soil denitrifying pool forms a sole pool at isotopic equilibrium after label injection. Since this assumption is most likely violated due to the non-homogenous distribution of the added tracer (but still valid to some extent, Mulvaney & Vanden Heuvel, 1988; Stevens et al., 1997), it is difficult to predict which model is the most adapted.

The main advantage of the ^{15}NGF method is its applicability under *in situ* conditions, which provides more robust estimations of the real dynamics of denitrification compared to laboratory experiments (as in the He/O_2 GFSC). Additionally, coupled with Gas Chromatography (GC) measurements or laser spectroscopy methods for the quantification of total N_2O emission, the ^{15}NGF enables the partitioning of the sources of N_2O between denitrification and other potential sources (Stevens et al., 1997). Since both denitrified N_2 and N_2O emissions are measured with the same technique, the denitrification product ratio $PR = N_2O/(N_2 + N_2O)$ is also more accurately determined (Bergsma et al., 2001). Nevertheless, the ^{15}NGF also has limitations and in particular, its sensitivity through Isotope Ratio Mass Spectrometry (IRMS) might not be high enough to discriminate small fluxes of N_2 emissions from soil because of the presence of naturally abundant ^{15}N isotopes in the atmosphere (~0.37 %).

One way to increase the sensitivity of the ^{15}NGF is to combine it with the use of an artificial atmosphere depleted in N_2. As shown in Micucci et al. (2023; Figure 7), reducing the atmospheric N_2 concentration below 10 % highly increases the sensitivity of the ^{15}NGF. Maintaining this low level in the field might be challenging however, due to the diffusion of atmospheric N_2 inside the incubation vessel. This was achieved by Well et al. (2019**a**) using a sophisticated gas chamber system

that kept a low N_2 background by continuously flushing both the chamber's headspace and the incubated soil with the artificial atmosphere gas mixture. This very same method has recently been used by Buchen-Tschiskale et al. (2023) to follow N transformations following cattle slurry application. It is however an expensive and complex technique to use, which may preclude its use at wider spatial scales.

Another way to enhance the sensitivity of the ^{15}NGF is to optimize the quantity of ^{15}N tracer applied to reach a 50 % ^{15}N enrichment of the soil denitrifying pool, which leads to a higher abundance of the $^{15}N^{14}N$ isotopologue and thus a higher detection probability via IRMS (Stevens & Laughlin, 2001). We further demonstrate in **Supporting Information** (**Chapter 3.7.1**) why this particular enrichment is ideal for ^{15}NGF; however, it requires to double the quantity of available nitrate (**Figure 27**, **Supporting Information, Chapter 3.7.1**). It has been reported that denitrification emissions as well as the product ratio increase with external nitrate inputs (Jarvis et al., 1991; Clayton et al., 1997; Blackmer & Bremner, 1978; Firestone & Tiedje, 1979; Loick et al., 2017; Warner et al., 2019). We thus need to assess if a fertilization effect leading to higher denitrification rates occurs at a 50 % ^{15}N enrichment before using this enrichment for enhanced sensitivity of the ^{15}NGF.

Finally, it is also possible to increase the limit of detection of the ^{15}NGF by combining the N_2 and N_2O isotopologue distribution data, assuming that both gases originate from the same and sole denitrifying pool (Bergsma et al., 2001) and that no hybrid molecules are emitted (Philips et al., 2016; Micucci et al., 2023). More detail can be found in Micucci et al. (2023) and in this study but briefly, by discarding the measurement of the $^{30}N_2$ molecules (for which the IRMS sensitivity is very limited) and by focusing only on the $^{29}N_2$ molecules; while the ^{15}N enrichment of the soil denitrifying pool is determined with the N_2O data, a better sensitivity can be achieved (Stevens & Laughlin, 2001;

Spott et al., 2006; Sánchez-García et al., 2014; Friedl et al., 2020). Using this method enabled Baily et al. (2012) to report a sensitivity 16 times greater than when using $^{29}N_2$ and $^{30}N_2$ data.

In order to address the important methodological gap of accurate quantification of denitrification, we aimed to create a robust, easy to apply at wider spatial scales and inexpensive method for *in situ* measurement of denitrification. Our approach was to optimize the quantity of applied tracer to reach a 50 % ^{15}N enrichment of the soil nitrate pool and to use an artificial atmosphere depleted in N_2 (containing 5 % N_2, 20 % O_2, 75 % He and 0.11 ppm of N_2O) under field conditions. To that end, we developed modified static chambers that could be connected to a gas cylinder containing the artificial atmosphere gas mixture for an initial flush and replacement of the ambient atmospheric headspace prior to incubation. The obvious diffusion issues due to the open-bottom nature of the developed static chambers were not incompatible with this approach. Indeed, keeping a constant N_2 background during the length of the incubation is not necessary if this background can be quantified at each sampling time. Thus, if the N_2 concentration background rises slowly enough, detection could occur for short incubations. As an alternative to the challenges of open-bottom static chambers, we also developed an incubation approach using intact soil cores sampled directly into plastic liners where the bottom and top lids were modified to enable incubation of small soil cores with a similar initial flush of the ambient atmosphere. Our research objectives were thus to:

(i) Assess whether the addition of nitrate tracer stimulates the denitrification process through a dose-response laboratory study (**Experiments 1 and 2**).

(ii) Characterize how fast the N_2 background rises in the developed static chamber and core liner systems, and validate if these two systems enable reliable measurement of denitrification under field conditions (**Experiments 3 and 4**).

(iii) Compare the "Mulvaney & Boast" and "Arah" models for the calculation of the ^{15}NGF to determine if one of them is more adapted than the other (**Experiment 1**).

(iv) Compare the ^{15}N enrichments of the soil denitrifying pool determined with either the N_2 or the N_2O isotopic gas data, confirming that these two gases originate from the same mineral pool (**Experiment 3**).

3.3) Material and methods

3.3.1) Laboratory study, impact of the nitrate tracer addition on denitrification fluxes

For the laboratory study, soil was sampled at the Allerton Project in Loddington, Leicestershire UK (52.617659,-0.833060), which displays three different agricultural land uses as shown in **Supporting Information** (**Chapter 3.7.2**).

These agricultural land uses were, a conventional arable field (**A1**), an intensively managed grass-clover ley (**GC1**) and an herbal rich ley (**H1**) where a mix of 20 grasses, forbs and herbs were planted as an alternative to grass-clover leys. The exact species mix can be found in **Supporting Information** (**Chapter 3.7.2**).

3.3.1.1) Experiment 1: Focus study on the herbal ley and comparison of the two calculation methods

We incubated 6 replicates of 50 g of sieved soil from the herbal ley (**H1**, sampled 30th of April 2021) in 450 mL sealed gas-tight jars with modified lids containing septa. The gas-tightness of the jars was tested by introducing 800 ppm of CO_2 in 6 closed jars and by measuring the CO_2 concentration after 6 hours. On average, the CO_2 concentration only dropped by 0.4 %. ^{15}N-labelled nitrate (as KNO_3, 98 at % ^{15}N, Merck) was added to 5 different treatments targeting a 0, 20, 30, 40 or 50 % ^{15}N enrichment of the total nitrate pool (after tracer application). The quantity of tracer to add in order to reach these enrichments was determined as:

$$n_{add} = \frac{[NO_3^-] \times m_{soil} \times a_p}{0.98 - a_p} \qquad [31]$$

Where n_{add} is the quantity of $^{15}NO_3$ tracer to add (mol), $[NO_3^-]$ the soil nitrate concentration (mol g^{-1}), m_{soil} the mass of incubated soil (g) and a_p the targeted ^{15}N enrichment of the soil denitrifying pool.

The control treatment (0 %) consisted of addition of deionised water only (at the same volume as the tracer) and thus can only be used to compare total emissions of N_2O. The 20 % enrichment is representative of a standard target in the context of the ^{15}NGF (Mulvaney, 1984) and was used as our minimum enrichment treatment. Gravimetric moisture was also increased to 45 % in order to increase the probability of detection of N_2O and N_2. Indeed, a preliminary incubation showed no detectable amounts of denitrification products when using a 5 % increase in soil moisture as per the use of the ^{15}NGF. However we did not increase soil moisture further and reach the optimal conditions for denitrification (60 - 70 %, Wang et al., 2023) in order to stay as close as possible to field conditions. The $^{15}N\text{-}NO_3$ tracer was diluted in deionised water, bubbled with gaseous N_2 to remove dissolved oxygen; and 9.5 mL of this solution were applied to each jar using 30 syringe injections while gently rotating the jars to ensure homogenous application. Sampling took place at times 0, 3, 6 and 24 hours, where 15 mL of gas were sampled from the jars headspace into 12 mL pre-evacuated Exetainer vials (Labco Limited, UK) and 15 mL of He were added to equilibrate for the loss of pressure. Replacing the sampled volume with pure He creates slightly anoxic conditions but given the small observed increases in N_2O concentration after incubation, we did not want to contaminate the jars headspace with ambient N_2O. Emissions of N_2O were calculated with measurements at times 0, 3 and 6 hours only; while times 24 h were only sampled to increase the

probability of N_2 flux detection. After two samplings, 30 mL of the headspace have been replaced with He, leaving about 19 % of O_2 in the jars, which was considered reasonable.

Under this experimental setup, we directly compared the ^{15}N enrichments of the incubated soils calculated with either the Mulvaney & Boast or Arah models to the targeted enrichments. The denitrification fluxes derived from both methods were also compared.

3.3.1.2) Experiment 2: Dose-response study of all three fields of the Allerton project site

The protocol of **Experiment 1** was adapted to enable replacement of the jars headspace with a custom-made artificial atmosphere containing 5 % of N_2, 20 % of O_2, 75 % of He and 0.11 ppm N_2O (CK Isotopes Limited, UK). Using a 6-port gas manifold connected to the artificial atmosphere gas cylinder, the headspaces of six jars were replaced simultaneously 10 times with a gas flow of 400 mL min^{-1} for 10 minutes before incubation. The same artificial atmosphere was used for headspace pressure equilibration after sampling.

Soil sampling in the **H1**, **GC1** and **A1** land uses occurred on the 9th of July 2021. For each of them, we added tracer to target a 0, 20 or 50 % ^{15}N enrichment of the soil denitrifying pool.

3.3.2) Field Study: development of a new method for *in situ* denitrification measurement

To measure denitrification *in situ*, we developed modified static chambers and plastic liners (for incubation of 10 cm long soil cores) that would be compatible with an initial flush of artificial atmosphere prior to incubation. The designs of these modified chambers and liners can be found in **Supporting Information** (**Chapter 3.7.3**).

3.3.2.1) Experiment 3: Chamber and liner tests, comparison of the ^{15}N enrichment calculated through N_2 or N_2O isotopic data

Experiment 3 took place in different grassland sites in England. The test of the chambers took place in a 5 year old grass/clover ley at the Fenswood Farm near Bristol UK (51.421083,-2.662733) while the test of the liners took place in a grass/clover ley nearby the Allerton Project site.

Static chamber test

The chamber test took place on the 27th of September 2021. One week prior to incubation, five chamber collars were inserted 10 cm deep into the soil and soil samples were collected and brought back to the laboratory for determination of the nitrate content. Isotopic solutions targeting a ^{15}N enrichment of 50 % of the soil denitrifying pool and inducing a 5 % moisture increase were prepared.

On the day of the incubation, isotopic solutions (~ 200 mL) were applied to soil within the chamber collars using syringes (40 injections; at 0, 2.5, 5 and 10 cm depth). The top chambers were mounted and connected to the artificial atmosphere gas cylinder for a flushing of 15 minutes at a rate of 2.8 L min^{-1} (ambient atmosphere replaced 5 times). Gas sampling (15 mL) occurred at times 0, 1, 2, 3, 4, 5, 6 and 24 h and we did not replace the sampled volume by an equal volume of artificial atmosphere. The samplings after 4 hours of incubation were only used for N_2 background characterization and not flux measurements.

Liner test

The liner test took place on the 15th of October 2021. Soil sampling, nitrate content determination and isotopic solution preparation occurred in the same way as for the chamber test. The day before incubation, we sampled five intact cores (10 cm height) inside plastic liners that were left to pre-incubate overnight under environmental conditions in freshly dug holes.

On the day of the incubation, we injected the tracer (~ 10 mL) inside the soil cores using a syringe (24 injections; at 0, 2.5, 5 and 10 cm depth). The liners were then capped and flushed with the artificial atmosphere at a rate of 200 mL min^{-1} for 5 minutes (headspace replaced 10 times). We directed the gas flow from the top to the bottom of the liners (using a vent needle inserted in the bottom lid septum) to flush the soil pores and avoid the diffusion of soil pore N_2 towards the headspace of the liners. Sampling occurred at times 0, 2, 4, 7, 9 and 24 hours, at which times 15 mL of the headspace were sampled and 15 mL of artificial atmosphere were added for pressure equilibration. The samplings after 4 hours of incubation were only used for N_2 background characterization and not flux measurements. This setup enabled us to compare the ^{15}N enrichment of the soil denitrifying pool based on the N_2 or N_2O data.

3.3.2.2) Experiment 4: Application of the liner method for the measurement of denitrification

Experiment 4 took place at the FarmED site, near Shipton-under Wychwood UK (51.869981,-1.581136). The experimental layout at the FarmED site consisted of strips of the same soil under herbal leys of different ages compared to an arable control. We studied the 4-year-old herbal ley (**H2**) and arable (**A2**) strips (more information can be found in **Annex II**, **SI**). The **A2** land use had been fertilized just before our experiment there, 50 kgN ha^{-1} had been applied a month prior and 70 kgN ha^{-1} ten days prior, using a mix of nitrate (23%), ammonium (30%) and urea (47%) both times.

Experiment 4 took place on the 19th of May 2022 and replicated the liner test of **Experiment 3** in the **H2** and **A2** land uses with 8 replicates for each. Our goal was to confirm the liner approach as a method of *in situ* denitrification measurement.

3.3.3) Equivalent fertilizer rate of applied ^{15}N tracer

For an easier assessment of a hypothetical fertilizer effect, we calculated an equivalency between tracer application and fertilizer rate for each experiment (**Table 1**). For the laboratory experiments (where sieved soil was used) we worked out how the amendment of nitrate tracer could be translated as a fertilizer application by assuming that fertilizer was applied to the top 15 cm of soil and that 26 % of a soil volume sampled in the field would be sievable soil (< 2 mm) that can be used for laboratory incubation (after subtraction of rocks, roots, etc.; based on results from the present study).

***Table 12**: Equivalency between added tracer amounts and fertilizer rate for each experiment.*

Experiment	Treatment – Enrichment	Added N-NO_3 (kgN ha^{-1})
Exp1	H1 - 20%	0.75
Exp1	H1- 30%	1.28
Exp1	H1- 40%	1.99
Exp1	H1 - 50%	2.99
Exp2	H1 - 20%	0.60
Exp2	H1 - 50%	2.42
Exp2	GC1 - 20%	1.40
Exp2	GC1 - 50%	5.62
Exp2	A1 - 20%	1.03
Exp2	A1 - 50%	4.11
Exp3	Chambers	2.04
Exp3	Liners	12.46
Exp4	H2	1.38
Exp4	A2	23.96

3.3.4) Soil characterization

Upon sampling, soil was sieved (< 2 mm) and placed in the fridge to be stored at 6°C. For mineral nitrogen characterization, 5 g of soil were extracted in a solution of 0.5 M Potassium Sulphate (K_2SO_4) at a ratio 1:8, shaken for 2 hours at 200 rpm and centrifuged at a speed of 3 000 rpm for 5 minutes. The supernatant was then filtered through a 0.45 µm syringe filter and analysed over San++ continuous flow analyser (Skalar, Breda, Netherlands). NO_3^- was determined via cadmium reduction and NH_4^+ via the modified Berthelot reaction. The limit of detection was 0.02 mgN L^{-1} for NO_3^- and 0.05 mg N L^{-1} for NH_4^+, the samples were blank corrected. For pH, 10 mL of deionised water were added to 5 g of soil, shaken for one hour and left to rest for another hour before measurement. Moisture was determined gravimetrically on loss of mass after 24 hours at 105°C and is reported on a per dry mass basis.

For the soil particle size, we added 5 mL of hydrogen peroxide solution (H_2O_2 30 % v/v in water) to oven dried samples (24 hours at 105°C, 3 replicates per land use) at room temperature for one hour, and then again at 60°C. These operations were repeated the next day and deionised water was added (20 mL) before the samples were centrifuged (4 000 rpm for 5 minutes). The supernatant was discarded and soil particles were then dispersed into 30 mL of a sodium hexametaphosphate solution (50 g L^{-1}) and analysed over a Mastersizer 2 000 (Malvern, Malvern, UK).

3.3.5) Gas characterization

3.3.5.1) Gas Sampling

For each experiment, 15 mL of gas were sampled into a 12 mL pre-evacuated Exetainer. From the same vial, 1 mL was used for GC analysis and the rest was dedicated to IRMS analysis.

3.3.5.2) Gas Chromatography

The Gas Chromatography (GC) analyses were performed as described by Comer-Warner et al. (2022). We employed an Agilent 7890A Gas Chromatograph with a PAL3 autosampler (Agilent Technologies Ltd, USA) and a splitless 1-ml sample loop for the measurement of N_2O, CH_4, and CO_2 concentrations in all of our samples. The GC was equipped with a flame ionisation detector (FID) for CH_4 analysis and a micro-electron capture detector (µECD) for N_2O analysis.

Since FID detectors cannot measure CO_2 directly, it was converted into CH_4 before analysis. The GC oven operated at 60 °C, the FID at 250 °C, and the µECD at 350 °C. The FID used an N_2 make-up flow of 2 ml min^{-1} with 48 ml min^{-1} of hydrogen and 500 ml min^{-1} of air, while the µECD had a make-up flow of argon and methane at 2 ml min^{-1}. Each run took nine minutes, with CH_4, CO_2, and N_2O eluting at 3.6, 5.0, and 7.0 minutes, respectively. For precision, we conducted repeated analyses of 8 lab air samples at atmospheric concentrations. The relative standard deviation was consistently below 5% for all gases. The minimum detectable concentration difference was 9 ppb for N_2O, 72 ppb for CH_4, and 31 ppm for CO_2. Calibration was performed using handmade dilution of a gas standard (6 ppm of N_2O, 1 000 ppm of CO_2 and 10 ppm of CH_4) and a linear regression, achieving a minimum R^2 of 0.95.

3.3.5.3) IRMS

The IRMS analyses were performed as described by Sgouridis et al. (2023). The ^{15}N content of N_2 and N_2O was assessed using a continuous flow Isotope Ratio Mass Spectrometer (IRMS) system (Elementar Isoprime PrecisION; Elementar Analysensysteme GmbH, Hanau, Germany) coupled with a trace-gas pre-concentrator inlet and an autosampler (isoFLOW GHG; Elementar Analysensysteme GmbH, Hanau, Germany). The gas content from the Exetainers vials was purged into a helium (He)

stream through the autosampler. After CO_2 and H_2O removal, the gases were directed into a liquid nitrogen trap designed to isolate and cryofocus N_2O. A subsample of N_2 was taken through a 7 µL sub-sampling loop and was directed to the IRMS after O_2 reduction through a copper furnace at 600 °C. The three different N_2 isotopologues ($^{28}N_2$, $^{29}N_2$, and $^{30}N_2$) were measured with a trap current of 100 µA. The remaining gas samples underwent further concentration in another liquid nitrogen trap, and the remaining CO_2 was removed through a Poraplot Q gas chromatography column. Subsequently, the N_2O isotopologues ($^{44}N_2O$, $^{45}N_2O$, and $^{46}N_2O$) were measured with a trap current of 600 µA. Performance checks were carried out before each analysis with a series of 10 reference pulses of pure N_2 and N_2O (BOC special gases) until a standard deviation of $\delta^{15}N$ better than 0.05‰ was achieved.

Ratios R29 ($^{29}N_2/^{28}N_2$) and R30 ($^{30}N_2/^{28}N_2$) for N_2 as well as ratios R45 ($^{45}N_2O/^{44}N_2O$) and R46 ($^{46}N_2O/^{44}N_2O$) for N_2O were acquired with this protocol. The instrument precision for these four ratios at atmospheric ^{15}N enrichment was determined from repeated analyses of 6 laboratory air samples and the relative standard deviation was < 5% for all of them. The minimum detectable ratio difference was (4.36×10^{-6}) for R29, (2.55×10^{-5}) for R30, (9.40×10^{-5}) for R45 and (2.22×10^{-5}) for R46.

3.3.6) N_2O and N_2 gas flux calculations

3.3.6.1) N_2O isotopic calculations

Denitrified N_2O emissions were determined by first correcting the R46 and R45 ratios to account for oxygen isotopes in accordance with Bergesma et al. (2001):

$$R29 = R45 - R17 \quad [32]$$

$$R30 = R46 - (R29)(R17) - R18 \quad [33]$$

Where R17 is the $^{17}O/^{16}O$ ratio and R18 is the $^{18}O/^{16}O$ ratio. We used the values of 0.000373 and 0.0020052 respectively, based on Bergsma et al. (2001).

Then, we calculated $\boldsymbol{a_p}$ the ^{15}N enrichment of the soil nitrate pool undergoing denitrification and the coefficient ***d'*** which represents the proportion of total N_2O that derives from denitrification with the method of Mulvaney & Boast (1986). These quantities can also be determined with the method of Arah (1992) and both methods have been used and compared during **Experiment 1**. It should be noted that since the tracer is applied before flushing the headspace with the artificial atmosphere, by the time the first measurement is made (t = 0), soil has been labelled for 15 minutes and denitrification of the tracer has already started. Although most of the labelled denitrification products are probably flushed with the gas flow, we realised that the isotopic ratios of N_2O at time 0 were usually already high. Indeed, after flushing, the average ambient ^{15}N enrichment of the liners headspace was 2.78 %, instead of the atmospheric value of 0.37 %. Therefore, we recommend using a laboratory or field air reference for the R46 and R45 ratios at time 0.

The concentration of denitrification-derived N_2O is obtained as:

$$[N_2O]_{denitrified} = d' \times [N_2O]_{background} \quad [34]$$

Where $\boldsymbol{[N_2O]_{background}}$ is the total N_2O concentration measured through GC (in ppm).

We then calculated the N_2O source partitioning coefficient as:

$$SPC = \frac{f_{N2O\ denitrified}}{f_{N2O\ total}} \quad [35]$$

Where ***f*** is the flux of N-N_2O (in µgN kg^{-1} h^{-1} for the jar measurements and in µgN m^{-2} h^{-1} for the chamber and liner measurements).

3.3.6.2) N_2 isotopic calculations

Since the ratios R30 were under the limit of detection of the IRMS most of the time, denitrified N_2 emissions were determined by using the ^{15}N enrichment of the soil nitrate pool undergoing denitrification (***α_p***) calculated with the N_2O data (with the assumption that N_2 and N_2O derive from the same nitrate pool), and by calculating the coefficient ***d*** as in Spott et al. (2006):

$$d = \frac{1}{1-\frac{R29(1-ap)^2-2ap(1-ap)}{R29(1-aa)^2-2ap(1-aa)}} \qquad [36]$$

Where ***α_a*** is the ^{15}N enrichment of the atmosphere (~0.37 %) that we recalculated as:

$$a_a = \frac{R_{29}}{2+R_{29}} \qquad [37]$$

Similarly to N_2O emissions, the concentration of denitrified N_2 is given by:

$$[N_2]_{denitrified} = d \times [N_2]_{background} \qquad [38]$$

Where ***$[N_2]_{background}$*** is the total N_2 concentration measured through IRMS (in ppm).

Usually, the atmospheric $[N_2]$ background (~780 000 ppm) is used for equation [8], but under the artificial atmosphere conditions, this was not possible. It thus had to be quantified at each time step as shown in the next section.

Finally, we calculated the denitrification product ratio as:

$$PR = \frac{f_{N2O\ denitrified}}{f_{N2O\ denitrified}+f_{N2\ denitrified}} = 1 - NOSE \qquad [39]$$

Where ***f*** is a flux of nitrogen (either as $N\text{-}N_2O$ or $N\text{-}N_2$; in µgN kg^{-1} h^{-1} for the jar measurements and µgN m^{-2} h^{-1} for the chamber and liner measurements) and NOSE is the nitrous oxide sink efficiency,

thus a product ratio of 5% means that 95% of the denitrified N_2O emissions were successfully converted into N_2.

3.3.6.3) Background of N_2:

The N_2 concentration background was also measured through IRMS, using the peak height of the $^{28}N_2$ isotopologue. Calibration was made by diluting pure N_2 in He for the high end of the calibration and our custom artificial atmosphere (5 % N_2) for the low end ($R^2 > 0.95$). The robustness of our N_2 background quantification using IRMS was evaluated by direct comparison of identical manual N_2 dilution samples between our IRMS and an Agilent 7890A (Agilent, Böblingen, Germany) equipped with a thermal conductivity detector (TCD). Results are shown in **Figure 19**.

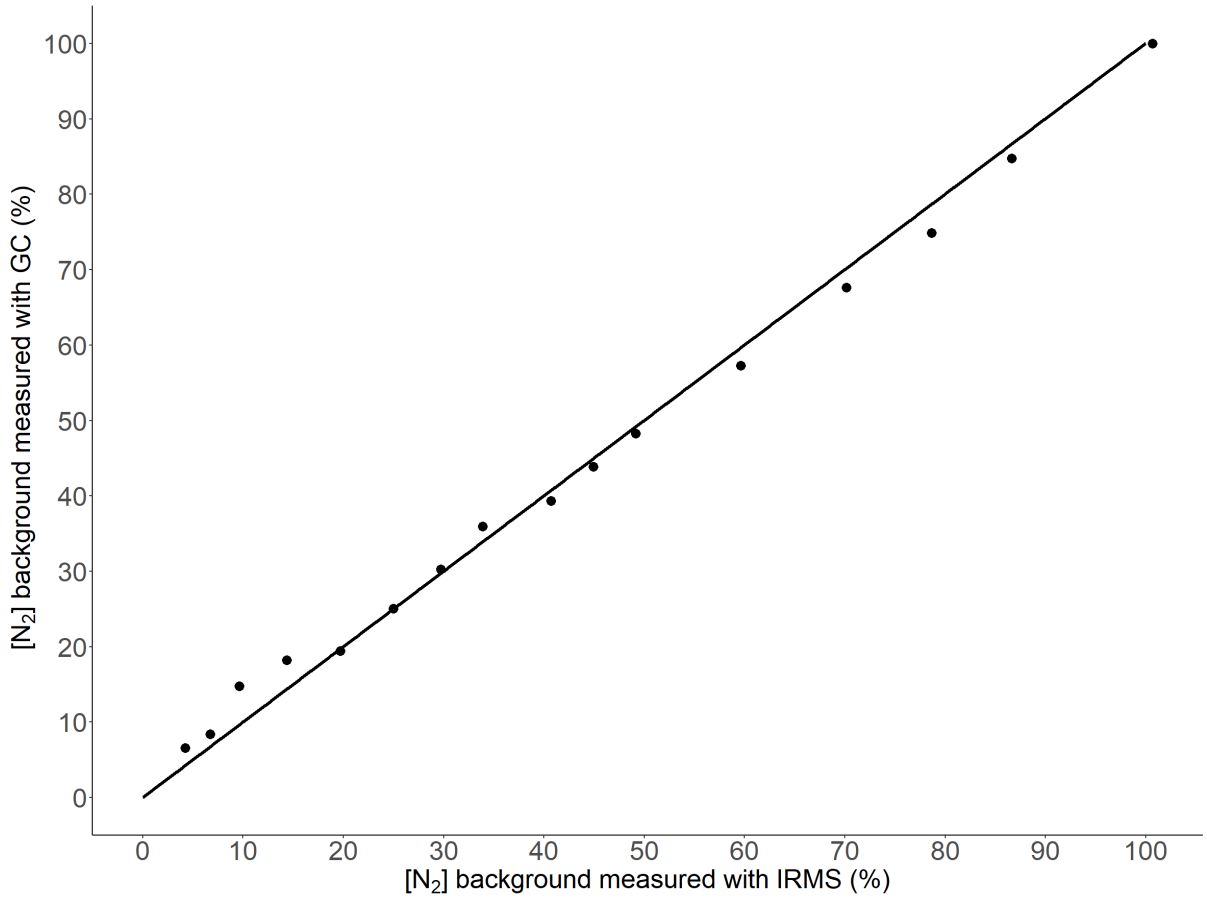

***Figure 19**: Direct comparison of the N_2 concentration background measured in identical handmade dilution samples via either IRMS or GC. The 1:1 line is represented in black (R^2= 0.9933).*

3.3.6.4) Liner and jar flux calculations:

When using small incubation vessels, sampling can be rather disruptive. On average, a 15 mL sampling represented about 5 % of the jars headspace and 18 % of the liners headspace. Therefore, 15 mL of artificial atmosphere (or He in the case of **Experiment 1**) had to be replaced to compensate for the change in pressure. We corrected for the sampling error as:

$$C_n = C'_n + \frac{V_{sample}}{V_{headspace}}\left[\left(\sum_{i=o}^{i=n-1} C'_i\right) - nC_{gas\ mix}\right] \quad [40]$$

With $C_0=C'_0$.

Where, $\boldsymbol{C_n}$ is the corrected concentration at the n^{th} measurement (ppm), $\boldsymbol{C'_n}$ is the uncorrected concentration at the n^{th} measurement (ppm) and $\boldsymbol{V}$ is the volume (mL).

A model was derived to account for the leaking of the liners and used to correct the concentrations of the studied gases (**Supporting information**, **Chapter 3.7.4**). We found that on average, neglecting these leaks only resulted in an 8.7 % underestimation of the denitrified N_2O fluxes. In closed systems (jars and liners), the issues of gas diffusion from soil to headspace are much smaller than when using static chambers. Therefore, linear regressions were applied to the data corrected for sampling and leaks, with a criterion $R^2 > 0.90$.

It can also be challenging to consistently sample 10 cm high soil cores when using the liners. A liner has a surface of 16.62 cm^2, but we calculated a corrected surface as:

$$S^* = \frac{m}{h \times BD} \quad [41]$$

Where $\boldsymbol{S^*}$ is the corrected surface (cm^2) to account for the differences in heights of soil cores, $\boldsymbol{m}$ is the mass of the soil core (g), $\boldsymbol{h}$ its height (cm) and $\boldsymbol{BD}$ the Bulk Density of the studied soil (g cm^{-3}).

Finally, fluxes were calculated on a per mass basis for the jars and on a per surface basis for the liners.

3.3.6.5) Static chamber flux calculations:

The chambers did not need equilibrium of the pressure after sampling. However, prolonged incubation times can lead to diffusive issues. To mitigate these diffusive errors, we applied the HMR model (Pedersen et al. 2010), using the associated R script (R Core Team 2023) from CRAN (Comprehensive R Archive Network). This model is based on a revised version of the model of Hutchinson & Mosier (1981). It should be noted that emissions of ^{15}N-labelled molecules induce further diffusive issues that cannot be totally corrected through this model (Well et al., 2019**b**; Micucci et al., 2023). Fluxes from the chambers were measured on a per surface basis.

3.3.7) Statistics and modelling

Before statistical analysis, data were tested for normality and homoscedasticity. Normality was tested by visual inspection of a QQ plot combined with a Shapiro-Wilk test (p-value > 0.05). If the data were found to be non-normally distributed, they were log-transformed and normality as well as homoscedasticity tests were run again. If the data still did not meet the requirements, non-parametric statistical tests were used (Wilcoxon or Kruskal-Wallis tests). Homoscedasticity was checked with Levene test (p value > 0.05). If data met all the requirements, one-way ANOVA or student-t tests were used to compare means. If an ANOVA showed significant effect of the studied parameter, TuckeyHSD post hoc test was applied to determine which treatments were significantly different. All statistical analyses were performed using statistical packages of R.

All results in this study are given ± standard error.

The non-linear regressions for the modelling of the N_2 background concentration inside the static chambers and liners were done using SPSS (IBM Corp. Released 2021. IBM SPSS Statistics for Windows, Version 28.0. Armonk, NY: IBM Corp).

3.4) Results

3.4.1) Soil properties

The different land uses at the Allerton Project site (**H1**, **GC1**, **A1**) were all silt loams, with the two leys having very similar texture and the arable having a higher proportion of clay (**Table 13**). On the other hand, the two land uses of the FarmED site (**H2**, **A2**) were clay soils. In July 2021 (**Experiment 2**), the **GC1** ley had higher content of mineral N due to a higher proportion of N-fixing plants, compared to the **H1** ley. At the same time period, the arable **A1** at the Allerton Project site was significantly drier than the leys (**H1** and **GC1**). During **Experiment 3**, the grass-clover ley of the liner test also exhibited high levels of nitrate and ammonium while in **Experiment 4**, two successive applications of fertilizer in the **A2** land use resulted in high levels of nitrate but not of ammonium.

***Table 13**: Properties of the studied soils.*

NT = no tested.

	NO_3^- (mg/kg)	NH_4^+ (mg/kg)	Gravimetric moisture (%)	pH	Clay (%)	Silt (%)	Sand (%)
Experiment 1 H1	6.17 ± 0.03	1.93 ± 0.14	21.53	6.45	12	75	13
Experiment 2 H1	5.32 ± 0.15	1.93 ± 0.17	29.60	6.89	12	75	13
Experiment 2 GC1	12.28 ± 0.23	2.74 ± 0.46	28.74	6.45	12	72	16
Experiment 2 A1	8.16 ± 0.10	2.24 ± 0.27	16.78	6.72	22	64	14
Experiment 3 Chamber	5.39 ± 0.80	3.73 ± 0.55	26.36	NT	NT	NT	NT
Experiment 3 Liner test	25.61 ± 5.41	12.62 ± 3.26	33.16	NT	NT	NT	NT
Experiment 4 H2	3.00 ± 0.29	1.99 ± 0.13	19.23	7.94	81	10	9
Experiment 4 A2	53.44 ± 10.22	1.67 ± 0.10	15.82	7.97	82	13	5

3.4.2) Laboratory study, impact of the nitrate tracer addition on denitrification fluxes

3.4.2.1) Experiment 1: Focus study on the herbal ley and comparison of the two calculation methods

The total N_2O emissions were correlated with the addition of nitrate (ANOVA; F= 3.23, $p < 0.05$), but only the control and 30 % treatments were significantly different (TuckeyHSD; $p < 0.05$). The average

total N_2O emissions did not increase with the addition of nitrate as the maximum of emissions was for the control treatment, with (13.66 ± 2.36) × 10^{-2} µgN kg^{-1} h^{-1} (**Figure 20**). The minmum of emission was for the 30 % treatment with (6.18 ± 0.52) × 10^{-2} µgN kg^{-1} h^{-1}.

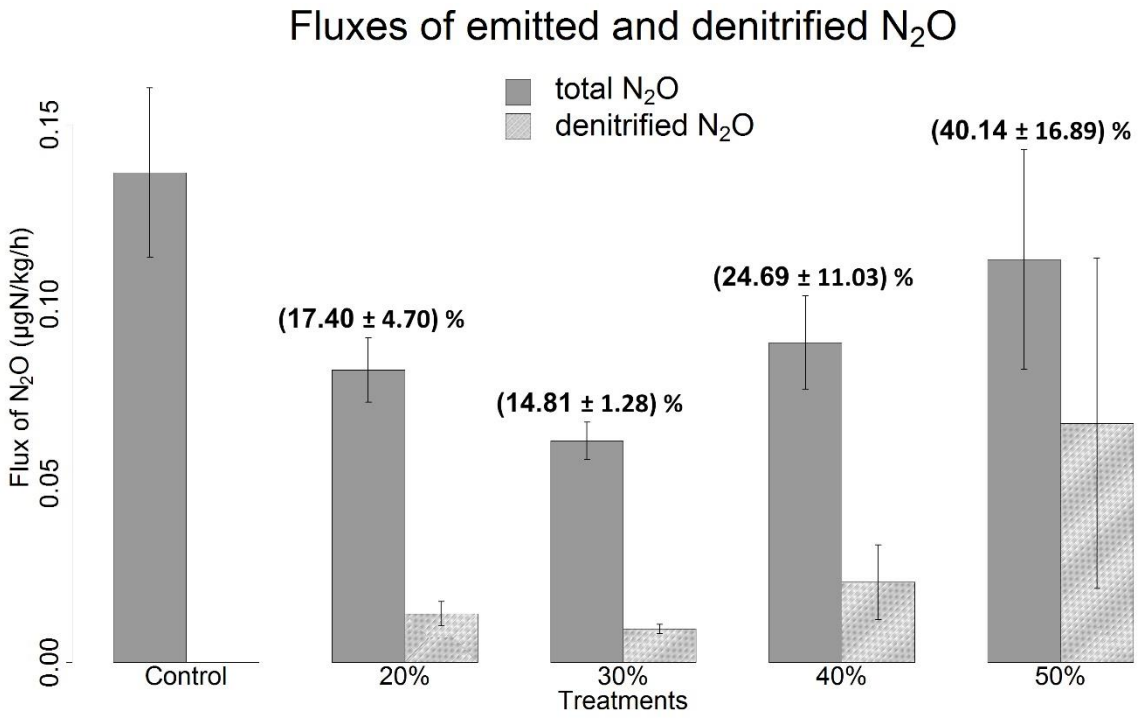

***Figure 20**: Mean fluxes of total and denitrified N_2O during laboratory incubation for different ^{15}N-labelled nitrate addition treatments (0, 20, 30, 40 or 50 % ^{15}N enrichment of the soil denitrifying pool).*

The percentages on top of each bar are the averages of the N_2O source partitioning coefficients, i.e. how much denitrification contributed to the total N_2O emissions. The error bars represent the standard errors of the means.

The denitrified N_2O emisisions were not statistically correlated with the amendement of nitrate (Kruskal–Wallis; χ^2=2.09, p > 0.05); although the 50 % treatment emitted more than any other

treatment, with an average of $(6.67 \pm 4.61) \times 10^{-2}$ µgN kg^{-1} h^{-1}. However, one of the six replicates of this treatment drove the average and variability much higher with emission of 29.34×10^{-2} µgN kg^{-1} h^{-1}. We did not consider this replicate to be an outlier since both GC and IRMS data agreed and were unexpectedly high. Without this replicate however, the 50 % treatment emitted $(2.13 \pm 0.97) \times 10^{-2}$ µgN kg^{-1} h^{-1}, which is comparable to the other treatments emitting between $(0.93 \pm 0.13) \times 10^{-2}$ and $(2.24 \pm 1.04) \times 10^{-2}$ µgN kg^{-1} h^{-1}. The source partitioning coefficients were also non-significantly correlated with the addition of nitrate (Kruskal–Wallis; $\chi^2=1.56$, $p > 0.05$) although their averages are increasing from the 30 to the 50 % treatments. No amount of evolved N_2 could be detected in this experiment.

The addition of ^{15}N-labelled nitrate for each treatment resulted in measured ^{15}N enrichments close to the targeted ones (**Figure 31**, **Supporting Information**, **Chapter 3.7.5**). These enrichments decreased with time in each case. The calculation of these enrichments using either the "Mulvaney & Boast" or "Arah" methods differed significantly (paired student t-tests for each enrichment and each sampling time, $p < 0.05$). For each replicate, the ^{15}N enrichment calculated with the model of Arah was strictly superior to the one calculated with the model of Mulvaney & Boast. The difference between the two models decreased with time, the Arah model being on average 14.35, 8.79 and 2.22 % higher after 3, 6 and 24 hours respectively (**Figure 32, Supporting Information**, **Chapter 3.7.5**). The mean calculated enrichments determined with both methods are reported in **Table 14**. The resulting fluxes also differed significantly between the two models (paired Wilcoxon tests for each ^{15}N enrichment treatment, $p < 0.05$), with the magnitude of difference decreasing when the ^{15}N enrichment increased. In each case, the model of Mulvaney & Boast yielded a higher flux than the model of Arah. On average, the flux calculated with the Arah model was 17.18, 7.82, 5.22 and 3.24 % lower for the 20, 30, 40 and 50 % ^{15}N enrichment treatments respectively.

***Table 14**: Mean calculated ^{15}N enrichments during **Experiment 1** using either the model of Arah or the model of Mulvaney & Boast.*

The reported means are the averages of all replicates at all times of sampling.

^{15}N enrichment target	Method of Arah	Method of Mulvaney & Boast
20 %	(25.92 ± 2.49) %	(21.43 ± 1.63) %
30 %	(31.56 ± 2.30) %	(28.98 ± 1.84) %
40 %	(42.18 ± 2.17) %	(40.08 ± 1.80) %
50 %	(45.37 ± 1.40) %	(43.95 ± 1.29) %

3.4.2.2) Experiment 2: Dose-response study of all three treatments of the Allerton project site

Once again, the addition of ^{15}N-labelled nitrate for each treatment resulted in measured ^{15}N enrichments close to the targeted ones (**Figure 33**, **Supporting Information**, **Chapter 3.7.5**).

In this experiment, the N_2O emissions of the **A1** land use increased slowly and similarly to the other land uses during the first six hours of incubation; however, every replicate of the three enrichment levels showed very high N_2O concentrations after 24 hours (**Figure 21**). The N_2O source partitioning coefficients after 24 hours were (105.5 ± 2.3) % and (103.1 ± 1.1) % for the 20 and 50 % treatments respectively and show that these large N_2O emissions originated strictly from denitrification.

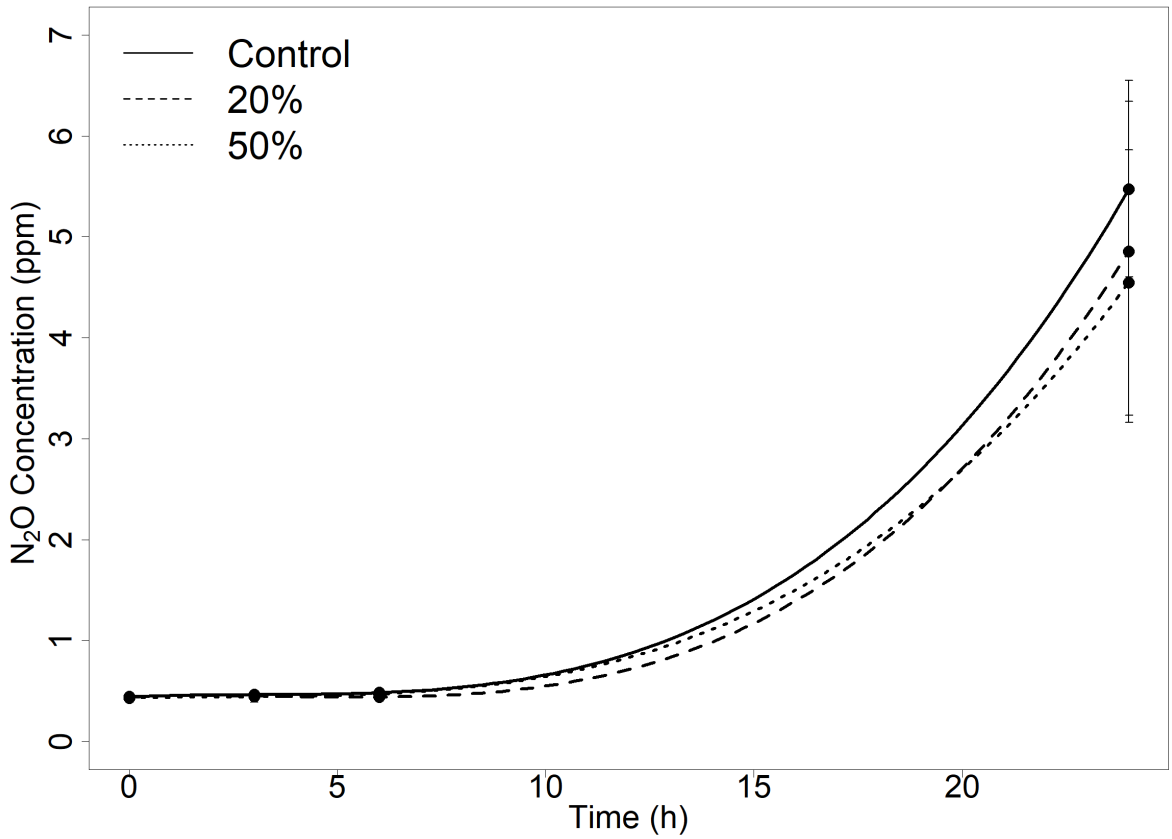

***Figure 21**: Mean measured N_2O concentrations of the **A1** land use for the three ^{15}N enrichment treatments (6 replicates) during **Experiment 2**.*

An exponential model was fitted for better visual assessment. The error bars represent the standard errors of the means.

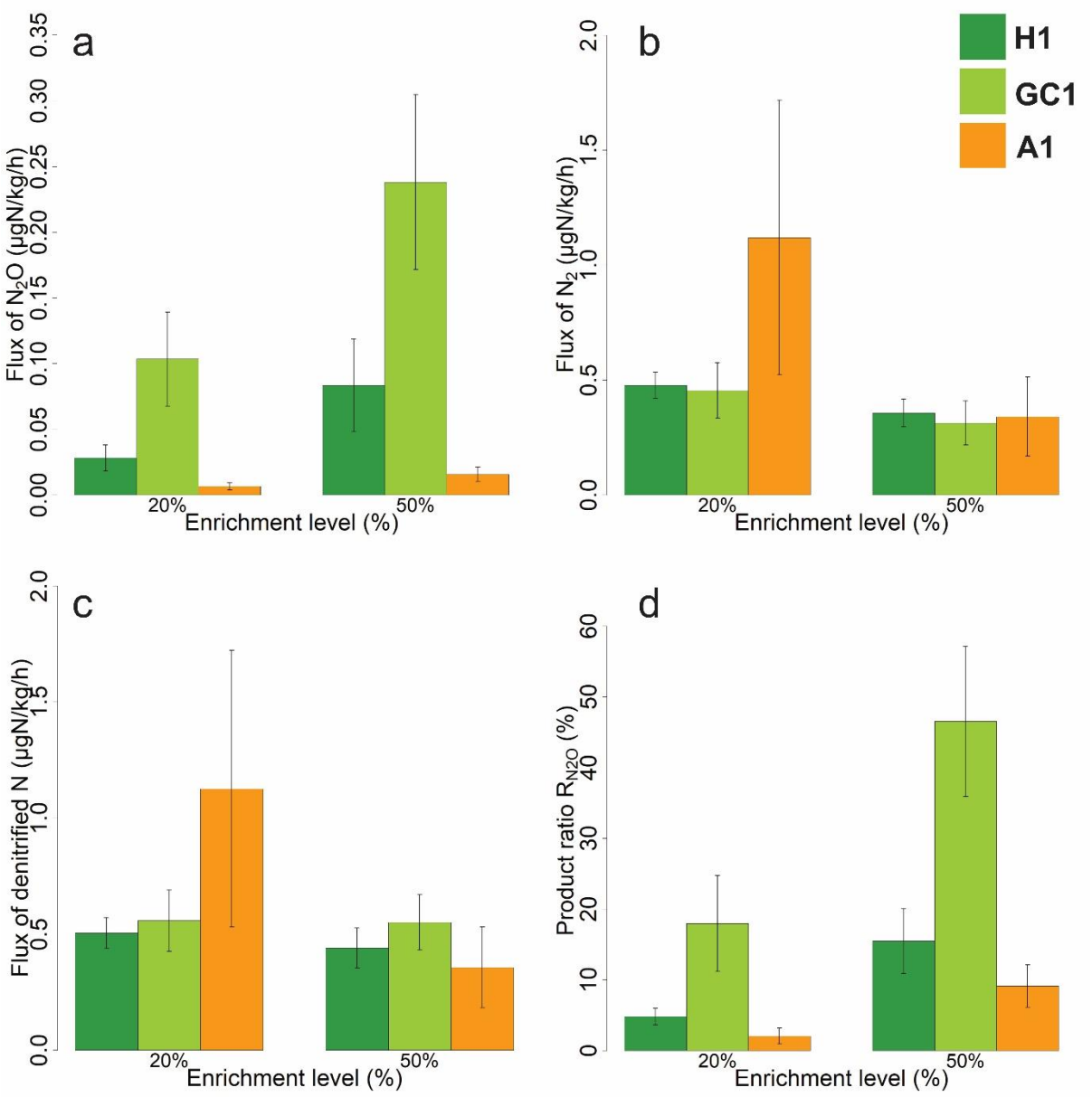

***Figure 22**: Main results from **Experiment 2**.*

a) Fluxes of denitrified N_2O, b) fluxes of denitrified N_2, c) fluxes of total denitrification (N_2O + N_2) and d) denitrification product ratios for all treatments. All fluxes are expressed in µgN kg^{-1} h^{-1} while the denitrification product ratios are expressed in %. The error bars represent standard errors of the means.

In **Experiment 2**, the fluxes of denitrified N_2O increased for all land uses when targetting a 50% ^{15}N enrichment of the soil denitrifying pool; especially for the **GC1** land use where the average of emissions more than doubled. These increases were however non-statistically significant (ANOVA, F_H=2.19, F_{GC}=2.50, F_A=2.89, $p > 0.05$) due to the high variability between replicates. The use of the artifical atmosphere gas mix enabled the successful detection of the the emissions of N_2 for all replicates. These emissions were relatively steady and did not increase significantly when increasing the amounts of available nitrate (ANOVA, F_H=2.25, F_{GC}=1.65, F_A=3.04, $p > 0.05$). The **A1** land use exhibited higher N_2 emissions under the 20 % treatment, however two replicates at this enrichment level showed abnormally high N_2 emissions. If ignoring these two replicates, this treatment emitted only (0.32 ± 0.06) µgN kg^{-1} h^{-1}, which is comparable to the 50 % treatment emitting (0.34 ± 0.17) µgN kg^{-1} h^{-1}. The N_2 fluxes dominated the denitrification emissions and thus, the fluxes of total denitrification (N_2O + N_2) were very comparable to these N_2 fluxes and were also non-statistically different between treatments (ANOVA, F_H=0.62, F_{GC}=0.08, F_A=2.81, $p > 0.05$). The denitrification product ratios were inferior to 20 % except for the **GC1** land use at a 50 % ^{15}N enrichment, which reached almost 50 %. These product ratios were statistically different between the 20 and 50 % ^{15}N enrichment treatments for all three land uses (ANOVA, F_H=8.34, F_{GC}=5.40, F_A=6.00, $p < 0.05$).

3.4.3) Field Study: development of a new method for denitrification measurement

3.4.3.1) Experiment 3: Chamber and liner tests, comparison of the ^{15}N enrichment calculated through N_2 or N_2O isotopic data

As expected, the diffusion of atmospheric N_2 inside the chambers occurred at a faster rate than inside the liners (**Figure 23**). The N_2 concentration profiles inside these two systems followed a

Fickian model and data in **Figure 23** were fitted with the following model equation, in accordance with Pedersen et al. (2010):

$$C(t) = \varphi + (C_0 - \varphi)e^{(-\kappa t)} \quad [42]$$

Where ***C*** is the concentration of N_2 inside the chamber (in %), ***φ*** is the N_2 concentration outside the chamber (assumed constant at 78 %) and ***κ*** is an experimental constant (which depends on the coefficient of diffusion of N_2 as well as the chamber dimensions). This parameter was determined via a non-linear regression using equation [12].

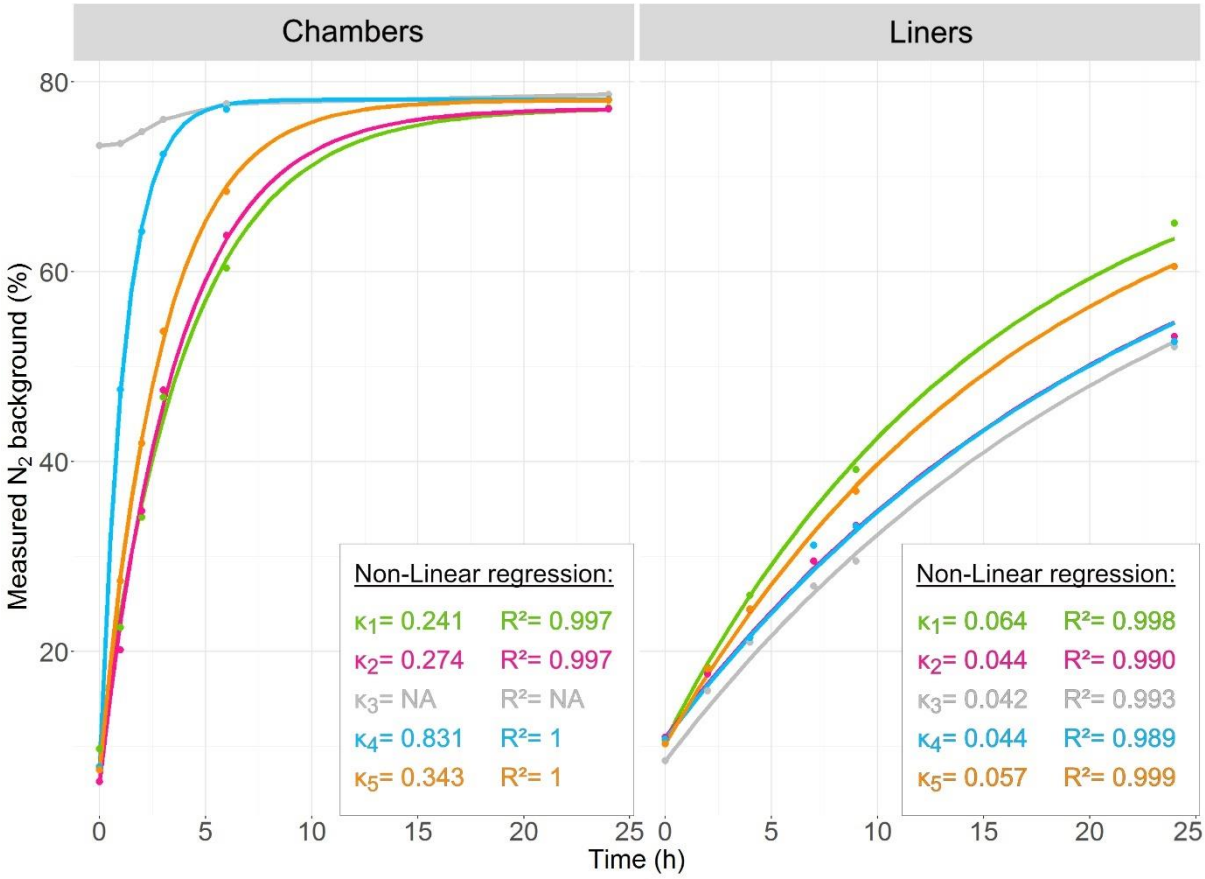

***Figure 23**: Evolution of the N_2 background concentration inside the modified static chambers and inside the liners.*

Following flushing of the headspace with the artificial atmosphere gas mix.

Each profile represents a replicate (5 for both chambers and liners). The data were fitted with a Fickian model (see equation [12]) for which the parameter κ has been calculated using a non-linear regression. This parameter is given for each replicate along with the coefficient of determination (R^2) in the figure legends.

It can be seen in **Figure 23** that the flushing of chamber 3 (grey in the left panel) failed. The average N_2 concentration background for the chambers after flushing was about (8 ± 0.7) % which is close to the 5 % contained in the artificial atmosphere mixture. However, this background evolved rapidly and rose to an average of (29 ± 6) % after an hour and (43 ± 7) % after two hours. In comparison, the liners started with an average background of (10 ± 0.5) % in N_2 but only rose to (18 ± 0.6) % after two hours. They reached an average of (34 ± 2) % after nine hours which is still less than the chambers after two hours.

The chamber and liner incubations took place in different locations and at different times. Although we can compare the evolution of the N_2 backgrounds, we cannot compare denitrification activities. Through chambers, denitrification emitted an average of (20.02 ± 7.96) µgN m^{-2} h^{-1} of N_2O as well as (2 768 ± 775) µgN m^{-2} h^{-1} of N_2, with an average source partitioning coefficient of (21.59 ± 4.09) % and a product ratio of (1.23 ± 0.55) %.

Through liners, denitrification emitted an average of (1 100 ± 343) µgN m^{-2} h^{-1} of N_2O as well as (257 ± 55) µgN m^{-2} h^{-1} of N_2, with an average source partitioning coefficient of (94.27 ± 1.92) % and a product ratio of (76.81 ± 4.45) %. The N_2O emissions clearly dominated the denitrification fluxes in this case.

During this first test of the liners, heterogeneity of soil was not taken into account in the calculation of the tracer solution concentrations. Indeed, a subsequent test revealed that only 26 % of a core contained inside a liner was sievable soil (< 2 mm, after subtraction of rocks, roots, etc.). This resulted in large excesses of tracer application. Nonetheless, the resulting high enrichments of the soil denitrifying pools coupled with high sensitivity (due to the low N_2 background) allowed us to obtain both reliable R29 and R30 data. This enabled us to compare the calculated α_p based on either the N_2O or N_2 data via the method of Mulvaney & Boast as shown in **Figure 24**.

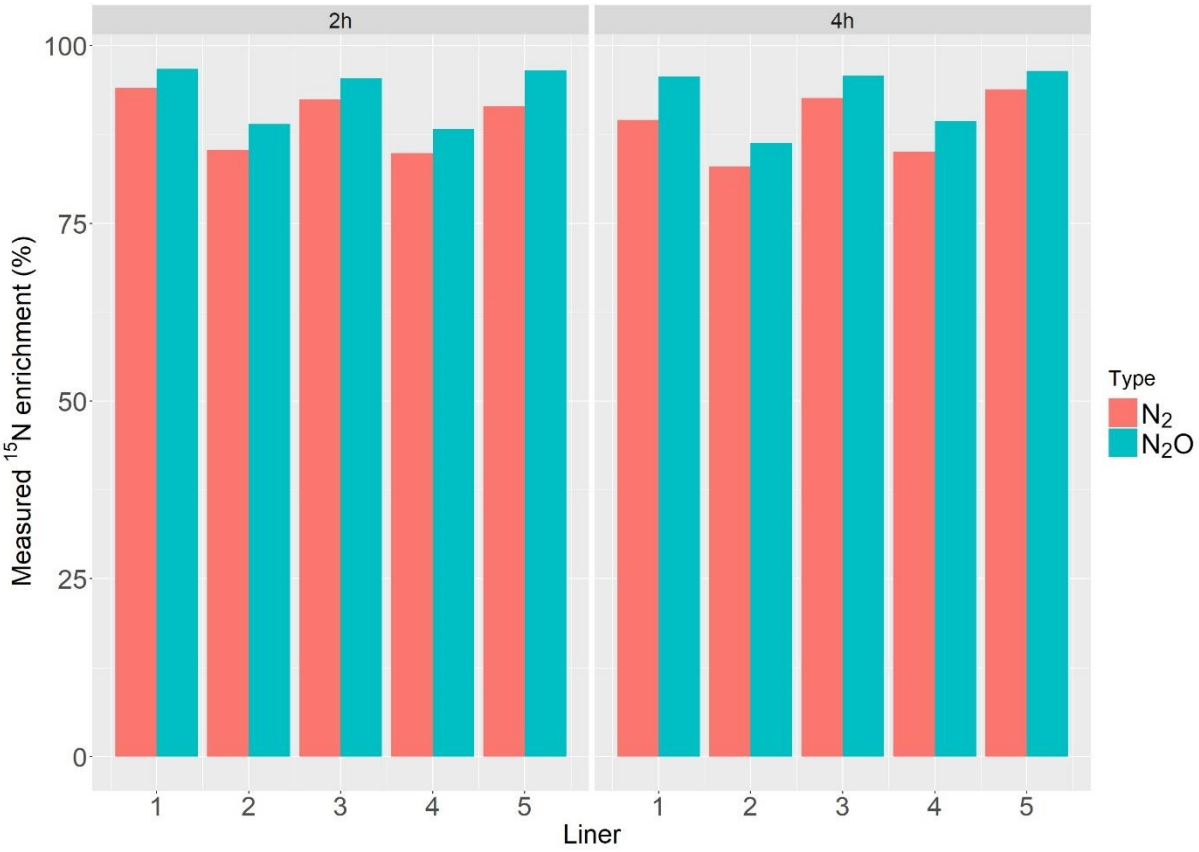

***Figure 24**: Comparison of the ^{15}N enrichment of the soil denitrifying pool (α_p) measured with either the N_2 or N_2O data during an in situ incubation.*

These enrichments are given individually for each replicate and for the two times of sampling.

The ^{15}N enrichment of the soil denitrifying pool calculated with either the N_2 or N_2O data were significantly different (paired student t-tests for both times of sampling; $p < 0.05$). For each replicate, the ^{15}N enrichment of the soil denitrifying pool derived from the N_2O data was strictly superior to the one derived from the N_2 data. The N_2O data predicted an average α_p of (93.48 ± 1.72) % after two hours and (93.09 ± 1.91) % after four hours. In comparison, the N_2 data predicted respectively (89.64 ± 1.90) % and (88.83 ± 2.10) %. As shown by **Figure 7** (**Supporting Information**, **Chapter 3.7.1**), in order to reach an α_p of 93 %, one needs to add approximately 20 times the quantity of originally present nitrate, compared to only 1 time for an α_p of 50%.

3.4.3.2) Experiment 4: Application of the liner method for the measurement of denitrification

During this experiment, we took specific care to reach the targeted ^{15}N enrichment (50 % for both **H2** and **A2** treatments) compared to **Experiment 3**. We reached an average enrichment of (58.86 ± 2.36) % for **H2** and (37.54 ± 5.30) % for **A2** (**Figure 34**, **Supporting Information**, **Chapter 3.7.5**). The higher variability in the **A2** treatment can be correlated with the variability in nitrate content resulting from recent application of fertilizer.

Denitrification was successfully measured *in situ* using the liner method (5 replicates out of 8 showed detectable N_2 for both the **H2** and **A2** treatments) and was dominated by N_2 emissions (**Figure 25**) as shown by the average product ratios of (11.05 ± 1.80) % in **H2** and (32.30 ± 9.74) % in **A2**. The N_2O emissions were dominated by denitrification in the case of **H2** but not in the case of **A2**, as shown by the source partitioning coefficients of (56.35 ± 7.77) % and (41.88 ± 6.05) % respectively (**Figure 25**). The smallest denitrified N_2 concentration detected was 0.77 ppm, after two hours of incubation. This is equivalent to a N_2 flux of 36.9 $\mu gN\ h^{-1}\ m^{-2}$.

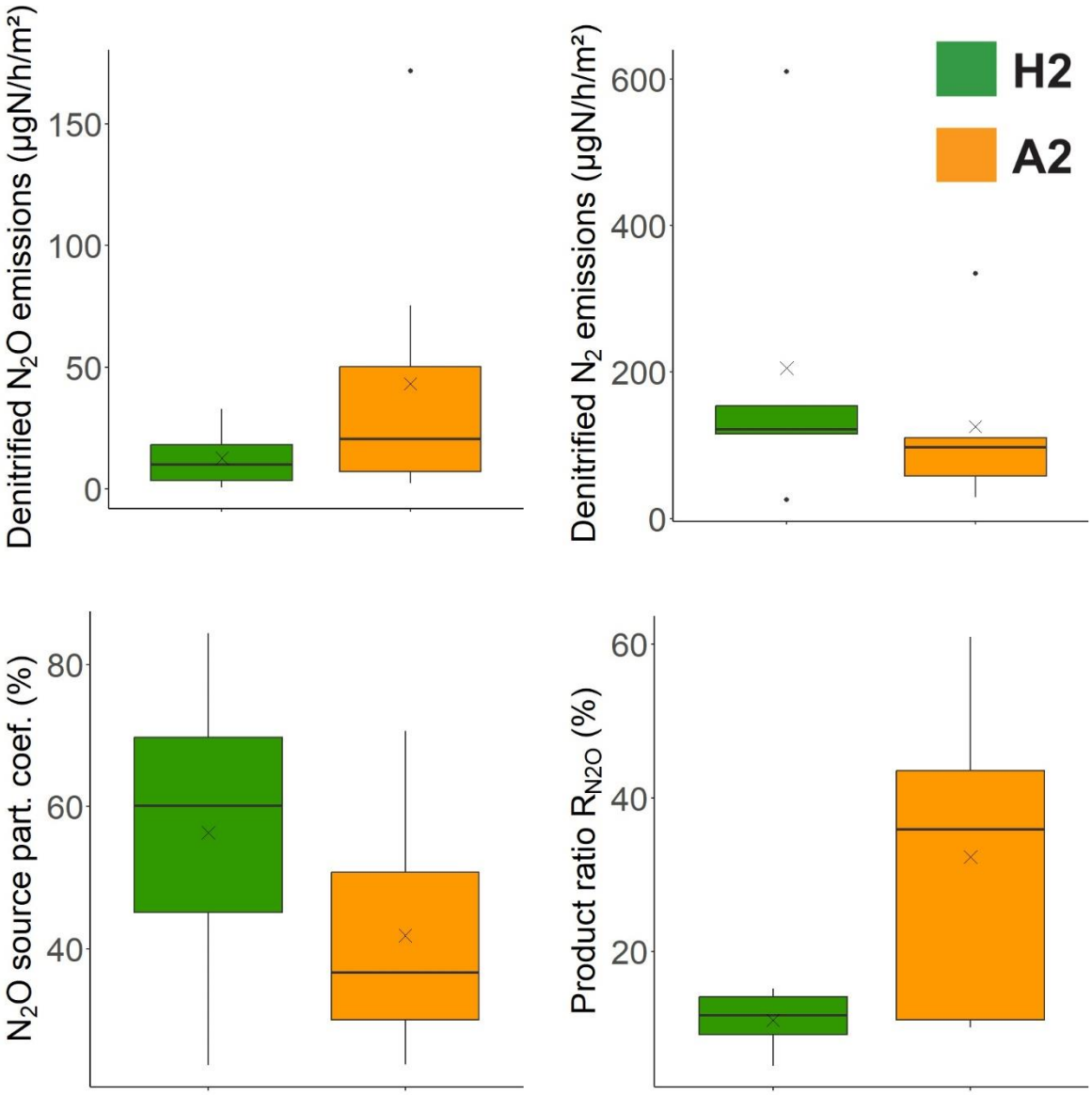

***Figure 25**: Denitrification measurement of **Experiment 4**.*

a) Fluxes of denitrified N_2O, b) fluxes of denitrified N_2, c) N_2O source partitioning coefficients and d) denitrification product ratios. All fluxes are expressed as µgN kg^{-1} h^{-1} while the source partitioning coefficients and denitrification product ratios are expressed in %. The crosses in the middle of the boxes represent the averages.

3.5) Discussion

3.5.1) Fertilization effect

We did not observe higher total denitrifying activity (N_2O + N_2) when increasing the amount of available nitrate under laboratory conditions (**Experiments 1 and 2**), but rather a non-significant increase in N_2O emissions. This could be due to the fact that, as shown in **Table 12**, the amendments of nitrate in our study were too low to stimulate denitrification significantly. Indeed, some studies reported higher denitrifying activity under amendment of nitrate, but after several applications of at least 75 kgN ha^{-1} (e.g. Jarvis et al., 1991; Loick et al., 2017), which do not really compare with the present rates. Or it could be that the peak of emissions after amendment had not been reached yet. Loick et al. (2017) observed peak of denitrification emissions 3 to 5 days after application of nitrate for example. If our experiments followed the same pattern, our approach would not measure an artefact due to tracer application, but still background fluxes labelled with isotopes.

We did however observe significantly different denitrification product ratios in laboratory (**Experiment 2**). This result seems to be confirmed in **Experiment 3** where incorrect application of large amounts of $^{15}N\text{-}NO_3$ tracer (20 times the quantity of ambient nitrates) resulted in large emissions of denitrified N_2O as well as high denitrification product ratios (77 % on average). The denitrification product ratio depends on many parameters but mainly on the nitrate concentration (Clayton et al., 1997; Blackmer & Bremner, 1978; Firestone & Tiedje, 1979; Warner et al., 2019). It seems that under higher nitrate conditions, microbes tend to favour N_2O over N_2 and incomplete denitrification is promoted.

In the context of enhancing the current sensitivity of the ^{15}NGF, increasing the quantity of $^{15}N\text{-}NO_3^-$ tracer applied only makes sense if it does not create significant artefacts due to stimulation. In a

recent meta-analysis, Scheer et al. (2020) reported a mean denitrification product ratio of (12.40 ± 3.1) % for soils under natural vegetation and (10.90 ± 2.0) % for agricultural soils. The denitrification product ratio measured in **Experiment 4** for the herbal ley (**H2**) was 11 % and thus fell in the expected range; while the average α_p reached was 40 %. During the chamber test (**Experiment 3**), the denitrification product ratio was only 1.2 % with an average α_p of 63 % and thus, does not seem to have been stimulated. The **A2** soil in **Experiment 4** showed a high product ratio (32 %) for an agricultural soil but this could rather be explained by recent amendment of fertilizer than tracer application. Indeed, this field received 2 applications of nitrate (11.57 kgN ha^{-1} a month prior as well as 17.36 kgN ha^{-1} ten days prior, along with similar quantities of ammonium and urea). This accumulation of nitrate may have resulted in a saturation that drove this high product ratio. The addition of nitrate tracer (23.96 kgN ha^{-1} equivalent fertilizer rate) resulted in less than doubling the amount of present nitrate. We hypothesize here that the product ratio of 32 % observed in the **A2** soil during **Experiment 4** is representative of a product ratio for an arable soil after fertilization events and that the addition of nitrate tracer did not impact significantly this ratio, as it did when adding 20 times the quantity of ambient nitrates in **Experiment 3** (product ratio of 77 %).

In conclusion, using ^{15}N enrichments up to 50 % does not stimulate denitrification activity significantly in the selected land types and thus, the denitrification product ratios measured with our method are representative of field rates.

3.5.2) A new *in situ* method of denitrification measurement

Denitrification is an extremely challenging process to measure (Groffman et al., 2006), especially under field conditions. As recently mentioned by Scheer et al. (2020), there is a real need to increase the number of observations of *in situ* denitrification rates and product ratios. Here we report the

development of two techniques that have a great potential to address the important methodological gap needed for this task. Using relatively inexpensive technology, they both enable a good spatial coverage and high resolution *in situ* measurements. This is especially relevant for the liner approach, where cores can be sampled from virtually anywhere and be incubated at once in the same place. These liners can also sustain the artificial atmosphere background for longer, which, combined with a smaller headspace (83 mL compared to 5.3 L for the chambers), offers a higher chance of N_2 flux detection. During **Experiment 4**, 62.5 % of our replicates showed detectable N_2 fluxes, but over a one-year campaign (unpublished results), the detection was successful 90 % of the time. Contrarily to the chambers however, the liner approach only isolates the top 10 cm of soil. These 10 cm are however within the tillage zone where most of the denitrification activity is supposedly occurring due to higher organic matter and nitrate contents, root exudates, plant litter, fertilizer application etc. (Well et al. 2019**b**, Groffman et al., 2009). It is at this point unclear how to upscale liner fluxes, this approach would probably work best in combination with regular static chambers on top of undisturbed soil. Then, the denitrification product ratio measured from the cores could be applied to the total N_2O emissions measured from the chambers. This is similar to the approach of Wang et al. (2020) or Bizimana (2022) who applied laboratory derived product ratios to field chamber measurements; although in our case, the product ratio would be determined under *in situ* conditions and thus would be more accurate.

On the other hand, the modified chambers sit on top of the soil and thus capture the net fluxes of denitrification. The rapid increase of the N_2 background inside these chambers headspace after the flush of artificial atmosphere shows however that this technique will most likely work if high denitrification activity is occurring and if using a sensitive IRMS. On average, the N_2 concentration background inside the chambers was 29 and 43 % after one and two hours of incubation respectively

(**Experiment 3**). Using data from Micucci et al. (2023) shows that this theoretically results in 2.7 and 1.8 times greater sensitivities respectively compared to regular static chambers (which can be further enhanced with higher ^{15}N enrichments).

The soil cores inside the liners are much more sensitive to soil heterogeneity than the incubated soil under the chambers. We found that only 26 % of the core contained inside a liner was sievable soil (< 2 mm). This needs to be taken into account when preparing the tracer solutions. In **Experiment 3,** this caused a large excess of $^{15}N\text{-}NO_3^-$ tracer application inside the liners, resulting in an average $\boldsymbol{\alpha_p}$ of (93.29 ± 1.79) % reached. In comparison, although we considered a volume of pure sieved soil as well in the case of the chamber test, we reached an $\boldsymbol{\alpha_p}$ of (63.06 ± 3.79) %. For both cases, the targeted enrichment was 50 %. It can be added that sampling the small headspace of the liners can potentially draw soil pore air. Since the pores and headspace are flushed with the artificial atmosphere, it should not cause much disturbance in theory. One way to mitigate this effect can be to sample times 0 with atmospheric air (outside of the liner) and only sample the final time of incubation inside the liner. Finally, the liners were slightly leaking (as shown by the N_2 background concentration, **Figure 23**); in the case of denitrified N_2O fluxes, this only resulted in an 8.7 % underestimation according to our diffusion model (**Chapter 3.7.4**). Given the complexity of this model and its reliance on flux linearity, a case could be made to ignore diffusive losses for liner incubation.

Compared to the method of Well et al. (2019**a**), our chamber approach is easier to apply in the field, enables a greater spatial resolution and is cheaper. It is however a static approach which is probably less representative of the real denitrification dynamics. Indeed, flow-through chambers are considered as more reliable for flux estimations (Kostyanovsky et al., 2018) and they reduce the

diffusion issues caused by the accumulation of gas inside the chamber (Well et al., 2019**a**). The N_2 concentration background is also higher in our case and thus does not increase sensitivity as much. In our case, the smallest denitrified N_2 concentration detected was 0.77 ppm, after two hours of incubation. In the reported methodology of Well et al. (2019**a**), the smallest detection limit was 0.80 ppm, approximately 10 times lower than our new method. However, our approach was able to incubate 16 soil cores at the same time, originating from two different fields. In **Chapter 4**, 24 cores were incubated at the same time each month, originating from three different fields. On the other hand, the methodology of Well et al. (2019**a**) enables one incubation at a time. Given the large spatial variability of denitrification, increasing the number of replicates can be more valuable than further lowering the limit of detection. Since Well et al. (2019**a**) method was 80 times better than the classic ^{15}NGF, we can consider our method 8 times better than the regular approach. Compared to the He/O_2 GFSC method, the liner approach enables to get *in situ* flux estimations and is less disruptive, since the soil cores are only flushed for 5 minutes rather > 16 hours (as in Scholefield et al., 1997; Butterbach-Bahl et al., 2002; Cárdenas et al., 2003; Wang et al., 2020 for example). This limits the drying effect on soil and probably offers more accurate results.

3.5.3) Comparison of the "Mulvaney & Boast" and "Arah" models

On average, the model of Mulvaney & Boast yielded ^{15}N enrichment values closer to the targets and with less variability (**Table 14**); which tends to demonstrate that this model performs better. The difference between the two models decreased as the ^{15}N enrichment of the soil denitrifying pool and the time of incubation both increased. For the 20% treatment, the Arah model yielded fluxes that were on average 17.18 % inferior to the ones calculated with the model Mulvaney & Boast, which represents a non-negligible error. To our knowledge, this is the first time that these two

models are compared. The Arah model is more often found in the literature (Russow et al., 1996; Spott et al., 2006; Tauchnitz et al., 2015; Buchen et al., 2016; Krause et al., 2017; Rummel et al., 2021) due to its simplicity. It does however perform similarly to the Mulvaney & Boast model for higher ^{15}N enrichments of the soil denitrifying pool (3.24 % difference for the 50 % treatment) and should not make a significant difference at these levels.

3.5.4) Comparison of the ^{15}N enrichment calculated via either N_2 or N_2O isotopic data

The ^{15}N enrichment of the soil denitrifying pool calculated with either the N_2 or N_2O data during the liner test of **Experiment 3** were significantly different. **Figure 24** shows however that the magnitude of difference was almost negligible, the N_2 data yielding an average ^{15}N enrichment only 4.6 % lower at maximum (after four hours of incubation). The ^{15}N enrichments of the soil denitrifying pool derived from the N_2O data were strictly superior to the ones derived from N_2 data in every case. This is contrary to the observations of Warner et al. (2019, SI) who reported ^{15}N enrichments from N_2 being consistently higher than the ones calculated with N_2O. Buchen et al. (2016) observed mixed trends but most of the time, the ^{15}N enrichment based on N_2 was the highest. Nonetheless, we present further evidence that the ^{15}N enrichment calculated via N_2O is a good proxy for the ^{15}N enrichment of a single denitrifying soil nitrate pool, and should be used for enhanced sensitivity of the N_2 flux measurement via the ^{15}NGF (Baily et al., 2012).

3.5.5) Wetting effect due to tracer addition

The high N_2O concentrations observed in **Experiment 2** after 24 hours (**Figure 21**) were most likely the consequence of a wetting effect. Indeed, we targeted a 45% gravimetric moisture for each soil; and while the leys (**H1** and **GC1**) had a comparable moisture content in July 2021 (~ 29 %), the **A1** soil was significantly drier (~17 %). This resulted in a larger application of tracer solution to **A1** in

order to achieve the same gravimetric moisture content for each land use. Denitrification is an anaerobic process and has been shown to be stimulated by sudden wetting of previously aerobic soil pore space (Ruser et al., 2006; Berendt et al., 2023). This quick deprivation of oxygen has driven high denitrification activity as shown by the N_2O source partitioning coefficients for the 20 % and 50 % enrichments after 24 hours (~ 100 %), which indicate that denitrification was the only source of N_2O. N_2O emissions were derived from concentrations at times 0, 3 and 6 hours (before the wetting effect was significant), so this profile of emission should not impact the conclusions made for N_2O. The case is a bit more complex for N_2, for which we had to use the concentration data after 24 hours of incubation because of low sensitivity. Only two replicates (both of them for the 20 % enrichment treatment) showed abnormally high N_2 production, driving the average of emissions (as well as the variability) quite high compared to the other treatments (**Figure 22**). Otherwise, the N_2 emissions were similar to the other treatments. There exist many evidences that the wetting (in particular rewetting) effect causes increase in N_2O emissions (Gao et al., 2020; Liu et al., 2022**b**; Jiao et al., 2023), but fewer observations have been made for N_2. It has been suggested however that, as soil becomes anoxic, the denitrification product ratio shifts towards 0 and N_2 is favoured (Weier et al., 1993; Parton et al., 1996; Grosso et al., 2000; Ruser et al., 2006). The opposite is observed here; with average product ratios of 54.5 and 76.1 % for the 20 % and 50 % ^{15}N enrichment treatments respectively after 24 hours. When the N_2O fluxes are calculated over 6 hours, these ratios are respectively 2.8 and 10.7 % (**Figure 22**). This could either be explained by the fact that the full extent of a wetting effect can span over several days (Ruser et al., 2006) or by a lack of available organic matter (Weier et al., 1993). The first hypothesis is corroborated by the fact that N_2O emissions were still low 6 hours after water addition and that N_2 is the end product of denitrification. Since the N_2 emissions do not seem to have been stimulated by water addition after 24 hours, the fluxes of N_2

were calculated with data at times 0 and 24 hours while the fluxes of N_2O were calculated with data at times 0,3 and 6 hours. Finally, this demonstrates the importance of limiting water addition to a 5 % moisture increase after tracer application.

3.6) Conclusion

Combining the ^{15}NGF method with an N_2-depleted artificial atmosphere is the most promising way to increase its sensitivity, ensuring robust, reproducible and reliable *in situ* denitrification rate measurements. The use of this hybrid method in the field is very delicate but imperative to report representative fluxes. The two approaches presented in this study (static chambers and core liners) are suitable candidates to measure such fluxes. Ideally, high precision IRMS would be needed with the chamber method since on average, it only increases the sensitivity 2.7 and 1.8 times after one and two hours of incubation respectively. On the other hand, the liners combine a smaller headspace and a longer lasting low N_2 background (due to limited leakages), which highly enhance the probability of N_2 flux detection. The smallest denitrified N_2 concentration detected with this method was 0.77 ppm after two hours (36.9 µgN h^{-1} m^{-2}), which is not as low as recently developed sophisticated approaches (0.08 ppm), but which enables a much greater spatial resolution; further constraining the high variability of denitrification. For both the liner and chamber methods, the sensitivity can further be enhanced by targeting a 50 % ^{15}N enrichment of the soil denitrifying pool and by calculating this enrichment through the N_2O isotopic data with the model of Mulvaney and Boast. One of the key benefits of the liner method is the ability to reliably quantify true *in situ* denitrification product ratios. This ratio could be used to derive global denitrification fluxes and help improve N budget quantification. It is however dependent on the concentration of available nitrate and thus, on the quantity of applied tracer. Our *in situ* experiments showed that using a reasonable amount of tracer (i.e. not more than doubling the quantity of ambient soil nitrate) should not impact

the product ratio in a significant way. It might still be worth to report the range of ^{15}N enrichments reached during an *in situ* study along with denitrification measurements when using the ^{15}NGF. Furthermore, we targeted here a 50% ^{15}N enrichment of the soil denitrifying pool to increase probability of N_2 flux detection, but lower levels of enrichment can be used; particularly if the main interest is the partition of N_2O sources. It is a compromise between sensitivity and disturbance. Finally, a better sensitivity for the liner method could probably be achieved by using longer cores, which would enable to fully sample the tillage zone (where most of the denitrification activity occurs) and leave a bigger gas headspace where sampling would be less disruptive.

3.7) Supporting Information

3.7.1) Annex I: Optimizing the levels of ^{15}N tracer application for the use of the ^{15}NGF

It is demonstrated here that a 50 % ^{15}N enrichment of the soil denitrifying pool is an ideal target for the use of the ^{15}NGF. It is indeed the enrichment for which the proportion of emitted $^{29}N_2$ molecules is the highest as shown in **Figure 26**. The required sensitivity for $^{30}N_2$ being very high, calculations used here (and in general) only take in account the $^{29}N_2$ molecules. It is also shown in **Figure 26** that the enrichment of the soil denitrifying pool does not increase linearly from 0 to 100 % with the addition of ^{15}N labelled nitrate (labelled at 98 at %). It is almost linear up to 50 % (at which point the quantity of available nitrate has been doubled) but reaches a plateau towards the high enrichments (> 70 %). At these levels, large amounts of tracer need to be applied to only increase the ^{15}N enrichment of the soil denitrifying pool by a few percents. Thus, a ^{15}N labelling of 50% of the soil nitrate pool represents and ideal compromise for the use of the ^{15}NGF, given that no stimulation of denitrification occurs.

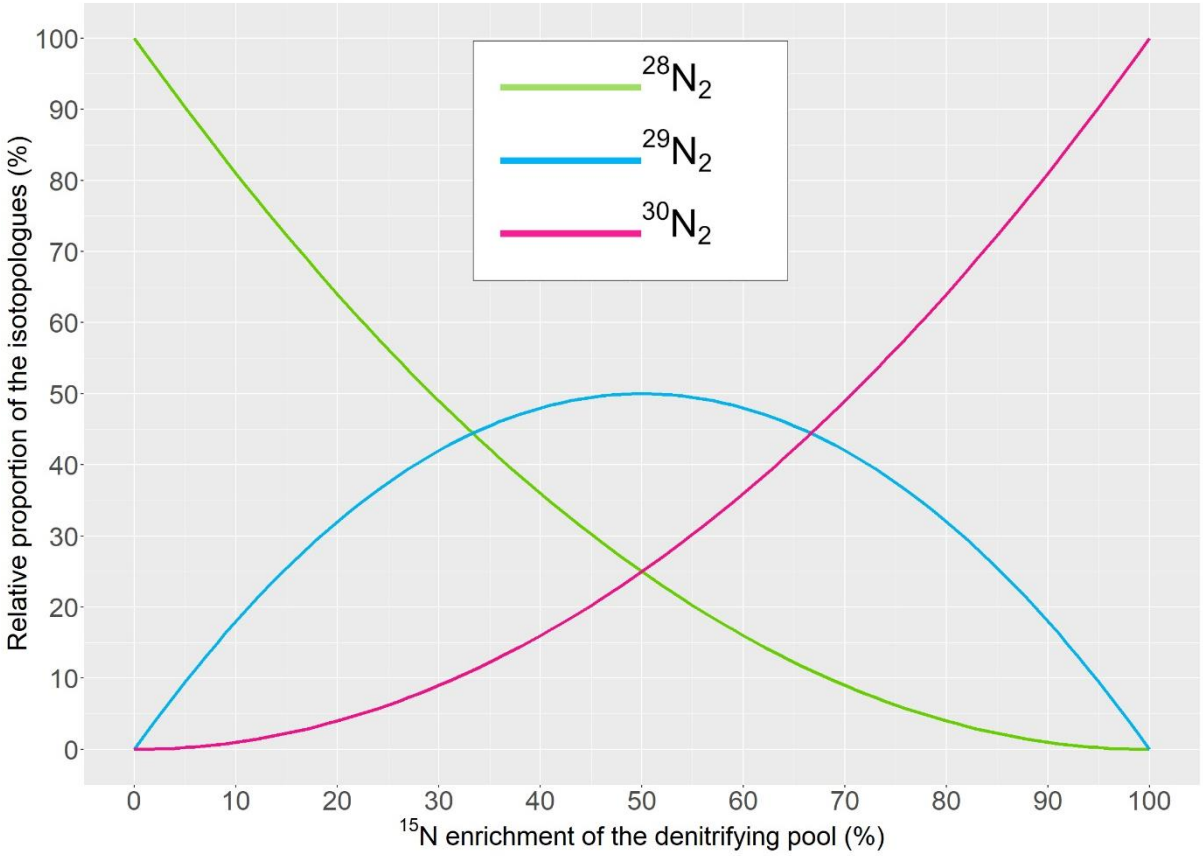

***Figure 26**: Evolution of the three N_2 isotopologue proportions for different values of the soil denitrifying pool ^{15}N abundance (considering isotopic equilibrium).*

The proportion of $^{29}N_2$ is maximal for a ^{15}N enrichment of 50%.

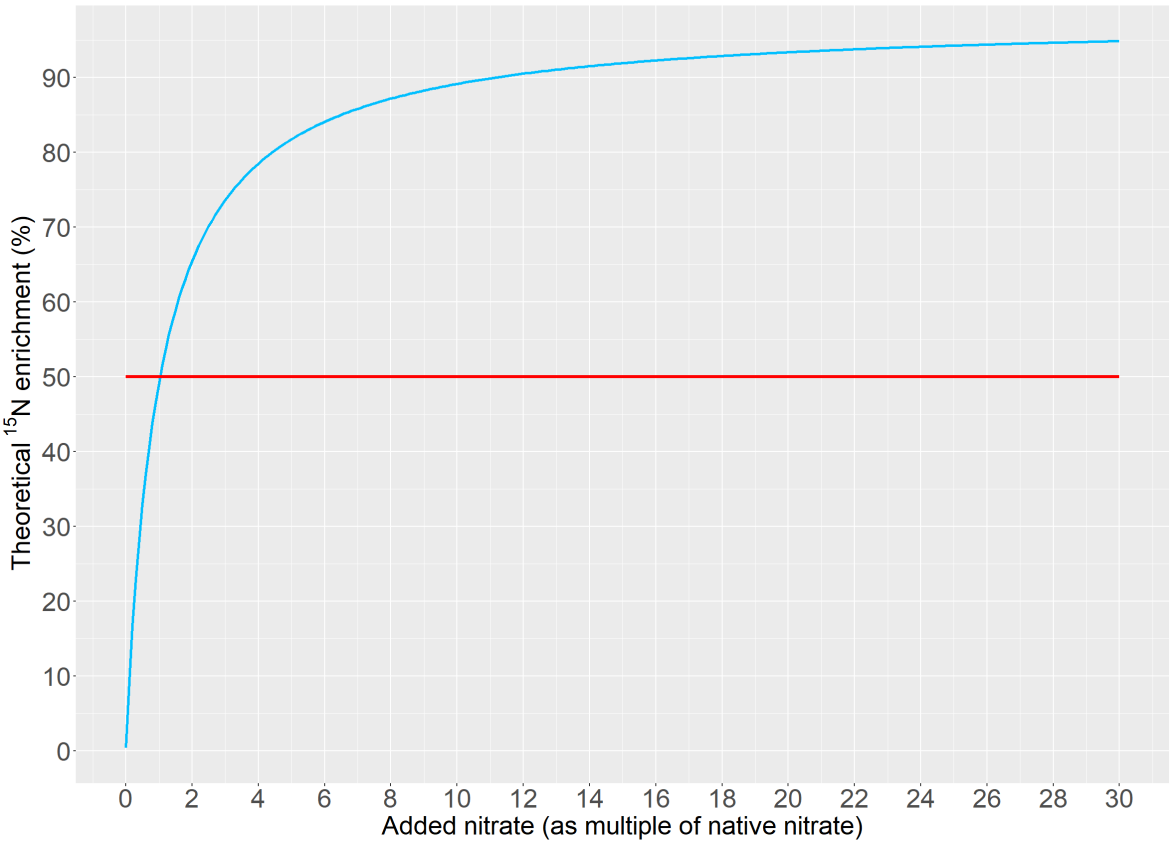

***Figure 27**: Theoretical evolution of the ^{15}N enrichment of the soil denitrifying pool after addition of labelled nitrate (98 at % in our case).*

The quantity of added nitrate is expressed as equivalents of native nitrate. Thus, after application of 1 time the quantity of native nitrate, the amount of available nitrate has doubled and the ^{15}N enrichment of the soil denitrifying pool reaches approximately 50%. This enrichment does not evolve linearly with the quantity of added nitrate and reaches a plateau with larger applications of tracer.

3.7.2) Annex II: Sampling strategy and experimental layout

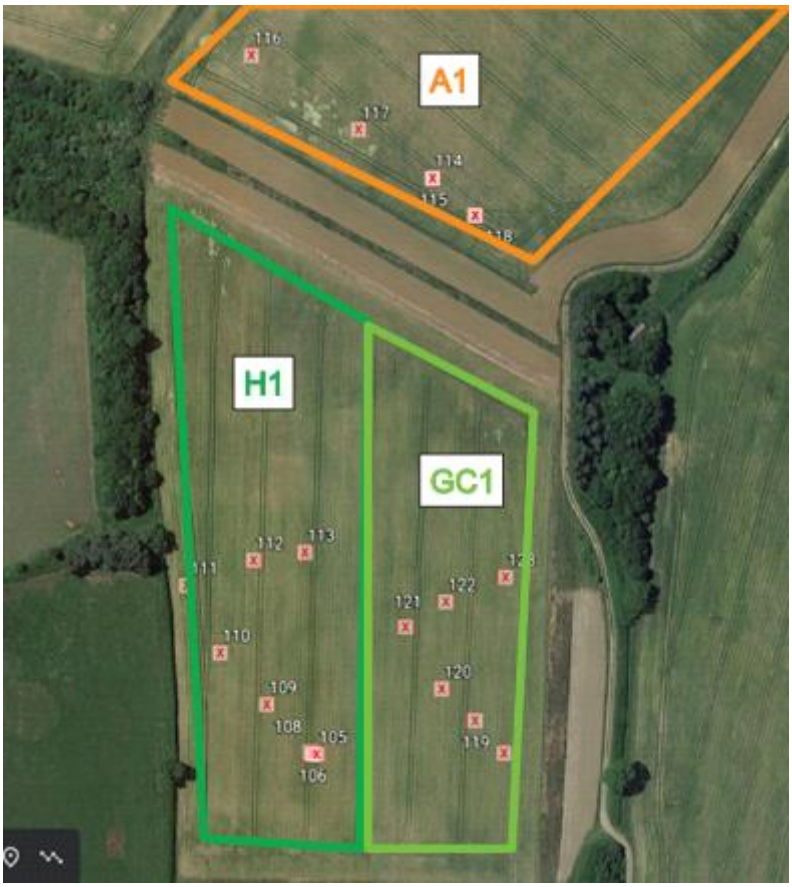

***Figure 28**: Sampling strategy at the Allerton Project site for the laboratory incubations (**Experiment 1** and **Experiment 2**).*

The Allerton Project site presents a slope following a vertical line in the picture. For the **H1** and **GC1** treatments (bottom left and right respectively), sampling stopped approximately in the middle of the fields to avoid slope effects. The **A1** treatment at the top was very difficult to sample due to it hardness and thus, only four locations were sampled. These four locations were as close as possible to the leys, since the slope could affect soil properties.

The **GC1** land use consisted of a mix of ray-grass (*Lolium perenne L.*) and white clover (*Trifolium repens*). In the **H1** land use, a mix of 20 species was planted as found here: https://www.cotswoldseeds.com/products/542/herbal-grazing-ley-four-year-drought-resistant-ley

***Figure 29**: Sampling strategy at the FarmED site for in situ incubations (**Experiment 4**).*

The **H2** (left) and **A2** (right) treatments were subdivided in 4 longitudinal segments and 16 latitudinal segments. Then, following the longitudinal direction, locations were randomly chosen between the 4 available slots (same patterns for both treatments). The blue pins represent the sampling locations for the liners.

The soil at the FarmED site was an inceptisol (oolitic limestone) which has been conventionally managed for wheat or barley production for thirty years.

Species mix in **H2** was the 'HERBAL' Grazing Ley - Four Year Drought Resistant Ley from Cotswold Seeds (https://www.cotswoldseeds.com/products/542/herbal-grazing-ley-four-year-drought-resistant-ley).

3.7.3) Annex III: Designing the chambers and liners for *in situ* measurement of denitrification

3.7.3.1) Chambers design:

Static greenhouse gas chambers were designed in three parts. Firstly, a double socket PVC coupler (20 cm ID) was cut in half to form a connector with a black rubber O ring at the bottom. Secondly, a plain PVC drainage pipe (20 cm OD) was cut in a 7 cm long cylinder and was glued to the top of the connector. As the connector was already 5 cm long, it created a 12-cm long chamber. This was deliberately slightly small in order to enhance the probability of N_2 detection and to reduce the volume of gas needed to flush the chamber's headspace.

A PVC square sheet (21 x 21 x 3 cm) was used as a top lid and was pierced to insert a septum in the middle. On a horizontal line, two other holes were made to insert bulkhead threaded to tube adaptors. Small tubes connected to 3-way stopcocks were plugged in these adaptors to form the inlet and outlet of gas flow.

Collars were made from the same drainage pipe as the top half of the chambers, only cut in 15 cm long cylinders this time. The bottom of a chamber (which is made of a socket PVC coupler) fits perfectly on top of the collar thanks to the rubber O-ring and guarantees a secure seal (we recommend using grease for smooth insertion).

3.7.3.2) Plastic liners:

Plastic liners (2.5 cm OD, 15 cm long) were purchased along with a dedicated hammer corer (AMS Inc., USA). We used this corer to sample 10 cm high intact soil cores inside the liners, leaving 5 cm of headspace for gas sampling. These 10 cm are within the tillage zone where most of the denitrification activity is supposedly going due to high content in organic matter, root exudates, plant litter, fertilizer application etc. (Well et al. 2019**b**, Groffman et al., 2009). The lids of the liners were modified to insert septa (both top and bottom lids) so the liners could be flushed with the gas mix. With a height of 5 cm and an ID of 2.3 cm, the liners have an average headspace of 83 mL. Sampling 15 mL represents 18 % of this headspace which can be quite disruptive. It can potentially draw soil pore air into the headspace to compensate for the loss of pressure, but the pore air of the soil cores is flushed with the gas mix before incubation.

3.7.4) Annex IV: Model of diffusion inside the liners

Issue: The liners are flushed with a gas mixture containing 75 % of He, 20 % of O_2 and 5 % of N_2 to improve sensitivity of the ^{15}NGF. However, we can see the background of N_2 concentration rising through time, which means that the cores are leaky. Thus, we aimed to correct the fluxes of studied gases to account for this leakiness. In this model, we assume constant atmospheric pressure inside the liner and we consider that all the studied gases (N_2, N_2O, CO_2 and CH_4) move at the same speed (same coefficients of diffusion) for simplicity.

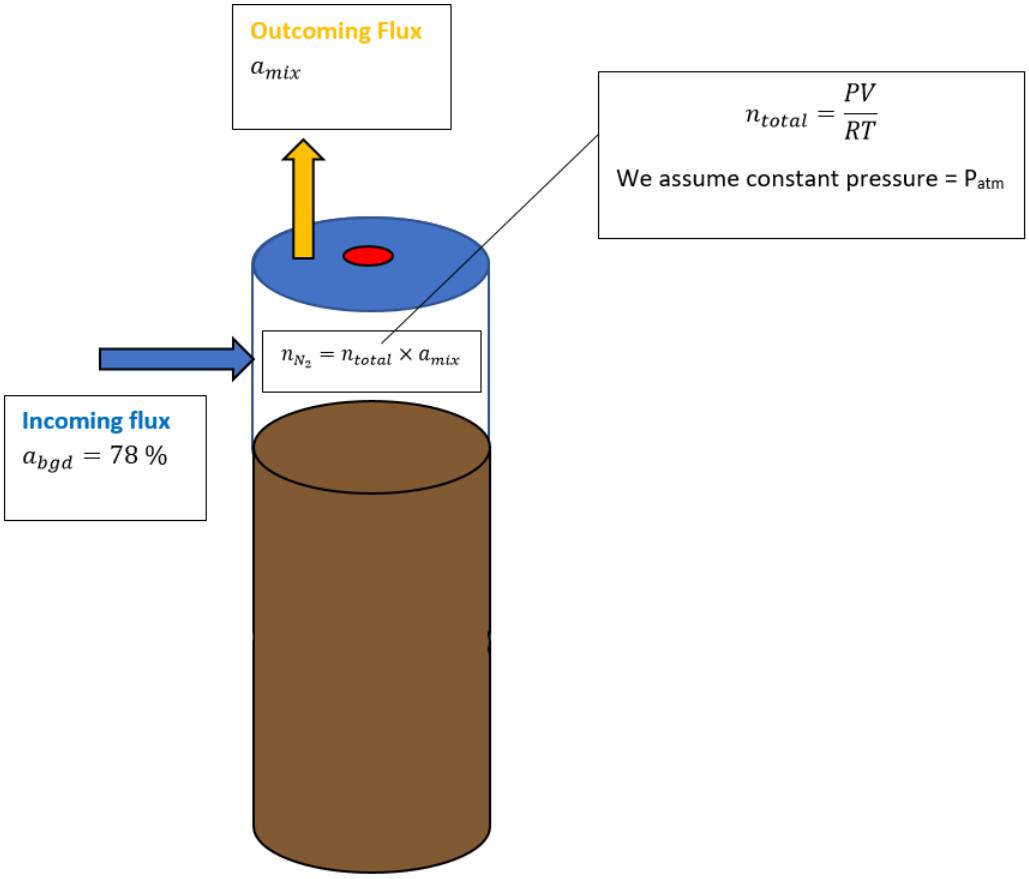

***Figure 30**: Schematic view of our model of diffusion for leakiness correction.*

Considering constant atmospheric pressure inside the liner's headspace (and thus constant total number of molecules), we model the leakiness by a constant flux of gas from atmosphere to the liner's headspace, while an equal flux exits the liner's headspace to the atmosphere. The N_2 concentration background (α_{bgd} = 78 % for the atmosphere; α_0 for the liner initial background after artificial atmosphere flush, usually around 9%; and α_{mix} for the liner background at any time) is a good indicator of the diffusive dynamics going on and is used for the applied corrections.

The first step is to measure the rate of leakiness using the background of N_2 concentration data. **Figure 23** of our main study shows that the N_2 dynamics inside the liners after flushing of the artificial atmosphere follow a Fickian model. Thus, one can apply the HMR model (Pedersen et al. 2010) or

Hutchinson & Mosier (1981) model to derive the rate of leakiness. However, in first approximation for short incubation times, we can consider that the N_2 background inside the liners evolves linearly with time.

Let us call $\boldsymbol{a_i}$ the N_2 concentration (%) of the pool ***i***.

If we ignore the evolved N_2 we can write:

$$a_{mix} = g a_0 + (1 - g) a_{bgd} \quad [43]$$

With $\boldsymbol{a_0}$ being the N_2 concentration just after the artificial atmosphere flush (usually around 9 %) and ***g*** being the proportion of the new atmosphere (after flushing) still present inside the liners at the time of measurement ($0 < \boldsymbol{g} < 1$). The quantity **(1-*g*)** thus represents the proportion of this new atmosphere that has diffused outside of the liner at the time of sampling.

$$g = \frac{a_{mix} - a_{bgd}}{a_0 - a_{bgd}} \quad [44]$$

An example of values of ***g*** can be seen in **Table 15**.

Table 15*: Example of values of* ***g*** *and* ***(1-g)*** *during one of our core incubations (*$\boldsymbol{a_0}$ *= 9.66 % and* $\boldsymbol{a_{bgd}}$ *= 78 %).*

We can see that after two hours, 93.5 % of the atmosphere that was initially present after the flush of artificial atmosphere is still present inside the liner's headspace, while 6.5% has diffused outside of the liner. This approach is somewhat simplistic and doesn't take in account the diffusive nature of the gas exchange between liner and atmosphere, but it is a good approximation for short incubation times. Alternatively, one can use a model of diffusion to calculate the rate of leakiness.

***t* (h)**	**a_{mix} (%N_2)**	***g***	**(1-*g*)**
0	9.70	100%	0
2	14.13	93.5%	6.5%
4	19.89	85%	15%

Since the pressure inside the liner is constant (and equal to atmospheric pressure), the total number of molecules is also constant. Considering atmosphere as a mix of ideal gases, we have:

$$n_{total} = \frac{1}{\bar{V}} \times V_{liner} = 3.45 \times 10^{-3}\ mol \qquad [45]$$

Where $\bar{V}$ is the standard molar volume of an ideal gas (24.06 L mol^{-1} under 20°C and 1 atm) and V_{liner} is the headspace volume of a liner (83.05×10^{-3} L on average).

Thus, in the example of **Table 15** after 2 hours, we can write:

$$n_{exch} = n_{total} \times 6.5\% = 2.24 \times 10^{-4}\ mol \qquad [46]$$

Where n_{exch} is the number of molecules exchanged between the liner's headspace and the atmosphere during the 2 hours of incubation (mol). From there, we can determine the flux of leakiness ***o*** as

$$o = \frac{n_{exch}}{\Delta t} = \frac{2.24 \times 10^{-4}}{2} = 1.12 \times 10^{-4}\ mol/h \qquad [47]$$

In the case of **Table 15** after 2 hours, the rate of leakiness was thus approximately 1.12×10^{-4} mol h^{-1}. In case of multiple measurements occurring in the same core, the rate of leakage is better determined using the initial time step if no model of diffusion is used. Therefore, if the core's headspace is sampled at times 0, 2 and 4 hours, we recommend determining the leakage rate with

the measurements at times 0 and 2 hours and use this rate again for the correction of the flux occurring between times 2 and 4 hours.

Now, let us focus on a study gas, which could be denitrified N_2, denitrified N_2O, total N_2O, CO_2 or CH_4 in our case. For a first part however, we will focus on denitrified N_2 and denitrified N_2O alone, since these gases are only evolved from soil and are not present in the atmosphere. If we follow the quantity of the studied gas ***M(t)*** (mol), it will depend on the rates of emission and leakiness. We will consider both these rates constant in between two measurement points. Although the rate of leakiness is constant, the quantity of the studied gas exiting through this flux is dependent on the ratio $\frac{M(t)}{n_{total}}$. However, the quantity M(t) is not constant through the duration of the incubation.

We can write:

$$M_{t+1} = M_t + cdt - \left(\frac{M_t + cdt}{n_{total}}\right) \times odt \qquad [48]$$

Where $\boldsymbol{M_{t+1}}$ is the quantity of the studied gas (mol) an infinitesimal increment of time (***dt***) after $\boldsymbol{M_t}$ and ***c*** is the rate of emission (or production) of the studied gas. The product ***c*** × ***dt*** inside the parentheses tends to be negligible as ***dt*** tends to 0. Therefore, we can rewrite equation **[48]** as:

$$\frac{dM(t)}{dt} + \left(\frac{o}{n_{total}}\right) M(t) = c \qquad [49]$$

The differential equation **[49]** can be resolved as:

$$M(t) = \frac{n_{total}}{o} c + \left(M_0 - \frac{n_{total}}{o} c\right) e^{\left(\frac{-o}{n_{total}}\right)t} \qquad [50]$$

Where $\boldsymbol{M_0}$ is the quantity ***M(t)*** at t = 0. In order to correct for leakiness, we need to re-express the quantity ***M(t)*** without the contribution of the leakiness flux ***o***, thus as:

$$M_{t+1} = M_t + cdt \qquad [51]$$

Which solves as:

$$M_t = M_0 + ct \qquad [52]$$

Therefore, ***c*** needs to be isolated from equation **[50]**:

$$c = \frac{o}{n_{total}} \times \frac{M(t) - \left(M_0 \times e^{\left(\frac{-o}{n_{total}}\right)t}\right)}{1 - e^{\left(\frac{-o}{n_{total}}\right)t}} \qquad [53]$$

Using the calculated emission rate ***c*** from equation **[53]** into equation **[52]** will yield the corrected concentration. It is worth mentioning that ***M(t)*** is initially expressed as a quantity of matter (mol) but can be also expressed as a concentration (ppm). The calculation of ***c*** through equation **[52]** will work if ***M(t)*** is expressed as a concentration (ppm). The coefficient ***c*** will thus be expressed in (ppm h^{-1}) instead of (mol h^{-1}). Since the liner has a constant volume, this is not an issue and makes calculations easier. Equation **[52]** used to get the corrected concentration of the study gas can also use concentration units. Since we took three measurements per liner (times 0, 2 and 4 hours), we had to correct for samples collected at times 2 and 4 hours. Thus, for the second time period (from hour 2 to 4), we considered the corrected concentration at the time 2 hours as our new M_0 and performed correction as shown above.

Table 16 shows an example of correction of denitrified N_2O emissions during one of our liner measurements. It has been corrected for both diffusion issues and sampling as per equation **[40]** of our main study (see **Chapter 3.3.5.1**). Note that when using equation **[40]** to add the quantity of gas taken out of the liner by the sampling, raw concentrations should be used (i.e. not the concentrations corrected for diffusion).

***Table 16**: Example of denitrified N_2O concentration correction for liner incubations.*

The first correction ("diffusion corrected" column) calculates what would be the measured concentration if none of the denitrified N_2O diffused outside of the liner. The second concentration ("sampling corrected" column) adds the quantity removed by the sampling of gas at the previous time step.

t	Raw concentration (ppm)	Diffusion corrected (ppm)	Sampling corrected (ppm)
0	0	0	0
2	1.15	1.25	1.25
4	3.11	3.27	3.50

This first model of correction was for the case of denitrified N_2 and N_2O only. In the case of the greenhouse gases (CO_2, CH_4 and total N_2O), we need to take in account the fact that these gases are present in the atmosphere. Therefore, during ***dt***, if a flux of diffusion escapes the liner, an equal flux of atmospheric air will enter the liner (as shown in **Figure 30**), containing atmospheric concentrations of CO_2, CH_4 and total N_2O.

The differential equation for a greenhouse gas is therefore:

$$M_{t+1} = M_t + cdt + oAdt - \left(\frac{M_t}{n_{total}}\right) \times odt \qquad [54]$$

Where ***A*** is the atmospheric concentration of the studied gas (ppm). This differential equation solves as:

$$M(t) = \frac{n_{total}}{o}(c + oA) + \left(M_0 - \frac{n_{total}}{o}(c + oA)\right) e^{\left(\frac{-o}{n_{total}}\right)t} \qquad [55]$$

We can isolate the rate of gas emission ***c*** as:

$$c_t = \frac{o}{n_{total}} \times \frac{M(t) - \left(M_0 \times e^{\left(\frac{-o}{n_{total}}\right)t}\right) - nA\left(1 - e^{\left(\frac{-o}{n_{total}}\right)t}\right)}{1 - e^{\left(\frac{-o}{n_{total}}\right)t}} \qquad [56]$$

Once this rate ***c*** is determined, the corrected concentration can be calculated using equation **[52]**. Just as in the previous case, concentration units can be used here. **Table 17** shows an example of correction of total N_2O emissions during one of our liner measurements

Table 17*: example of total N_2O concentration correction for liner incubations.*

The first correction ("diffusion corrected" column) calculates what would be the measured concentration if none of the total N_2O diffused outside of the liner. The second concentration ("sampling corrected" column) adds the quantity removed by the sampling of gas. In this particular example, it can be seen during the first time period (hour 0 to hour 2) that the diffusion-corrected concentration is lower than the uncorrected one. This comes from diffusion of atmospheric N_2O inside the liner's headspace being taken in account for the case of greenhouse gases. This pattern was not observed during the second time period (hour 2 to hour 4) because the rate of emission was greater than during the first time period.

t	Raw concentration (ppm)	Diffusion corrected (ppm)	Sampling corrected (ppm)
0	0.22	0.22	0.22
2	0.68	0.67	0.68
4	1.14	1.20	1.29

Since N_2 data are a bit more difficult to detect, there were cases where only the measurement after 4 hours was readable, and more rarely, cases where only the measurement after 2 hours was readable. We still performed the corrections shown above in these cases by calculating a simulated concentration at the time where data were missing, assuming a linear flux of gas emissions. Furthermore, it is important to remember that this model assumes constant fluxes in between two measurement points. Hence, if a "pulse" of gas emission happens in between two measurements, corrected concentrations could be biased.

Finally, it can be said that the diffusion correction can be challenging to take in account. Fluxes uncorrected for diffusion were underestimated by 8.7% on average (for denitrified N_2O). A case could be made to ignore these corrections for future use of the liner method for denitrification measurements.

3.7.5) Annexe V: Additional data of the main experiments

3.7.5.1) Experiment 1:

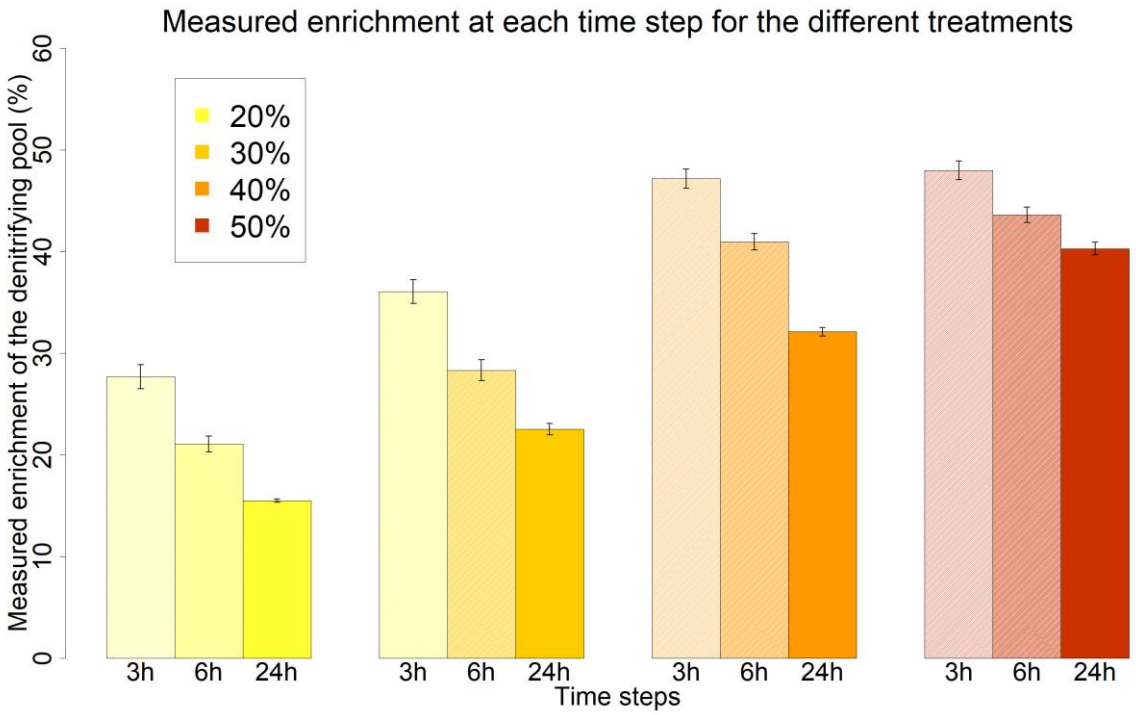

***Figure 31**: Average measured ^{15}N enrichment of the denitrifying pool (α_p) for each treatment and at each sampling time.*

The error bars represent the standard errors of the mean.

The results indicate that the right amounts of tracer were added for each treatment if taking in account the experimental variability. The 50 % treatment had a ^{15}N enrichment of nitrate pool close to the one of the 40 % treatment after 3 hours, with (47.9 ± 2.54) % and (47.1 ± 2.31) % respectively. However this enrichment decreased more slowly in the case of the 50 % treatment.

For all treatments, the measured enrichments decreased with time as would be expected with organic nitrogen mineralization and nitrification happening at the same time (Russow et al. 1996). However, this decrease looks abnormally fast. For example, Stevens et al. (1997) observed an α_p

decrease from 10 % to 5 % over ten days and under three different moisture contents, Ruser et al. (2006) observed very little variations over 70 days, usually less than 10% drop. Bergsma et al. (1999) observed a drop from 82% to 72% after three days and half and Rummel et al. (2021) observed different patterns of dilution of the ^{15}N label for different fertilization/plant treatments over a 10-day period. These results show that the ^{15}N enrichment of the soil nitrate pool should not be so variable in the first 24 hours following tracer application. In our case, it could be that the measured ^{15}N abundance of the soil denitrifying pool seems to be decreasing because the ^{15}N tracer diffuses into soil with time and tends to be more homogenously distributed in the soil. It has been proved that heterogeneous distribution of the tracer within the use of the ^{15}NGF results in an overestimation of the calculated α_p (see Micucci et al., 2023). This hypothesis seems a bit more likely than rapid dilution of the tracer with nitrogen mineralization and nitrification.

This would also explain why the difference between the “Arah” and “Mulvaney & Boast” models tends to be smaller after 24 hours compared to after 3 hours (**Figure 32**). At time 3 and 6 hours, there is however a large difference between the two models, with the Arah model being much more variable. The “Mulvaney & Boast” model is also closer to the targeted enrichment in general. We can note that for each replica and for each time, the Arah model always overestimated the Mulvaney & Boast model for the ^{15}N enrichment, while the opposite trend is observed for the fluxes.

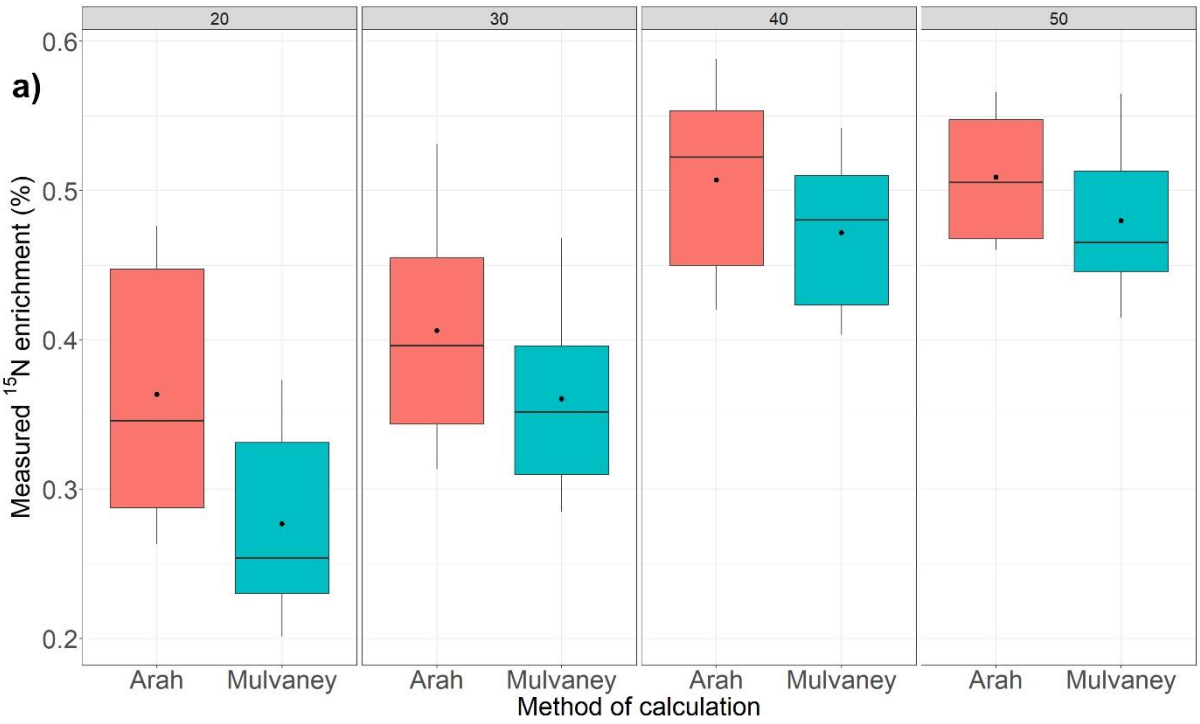
a)
20
30
40
50
0.6
0.5
0.4
0.3
0.2
Measured 15N enrichment (%)
Arah
Mulvaney
Method of calculation

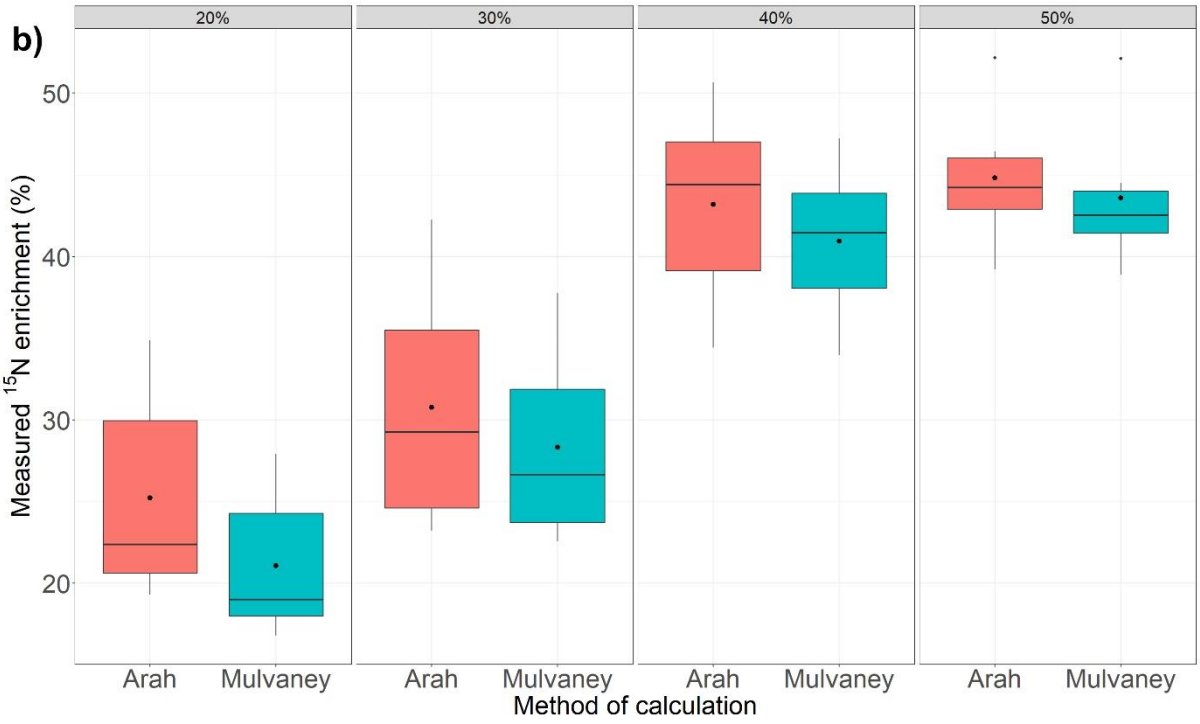
b)
20%
30%
40%
50%
50
40
30
20
Measured 15N enrichment (%)
Arah
Mulvaney
Method of calculation

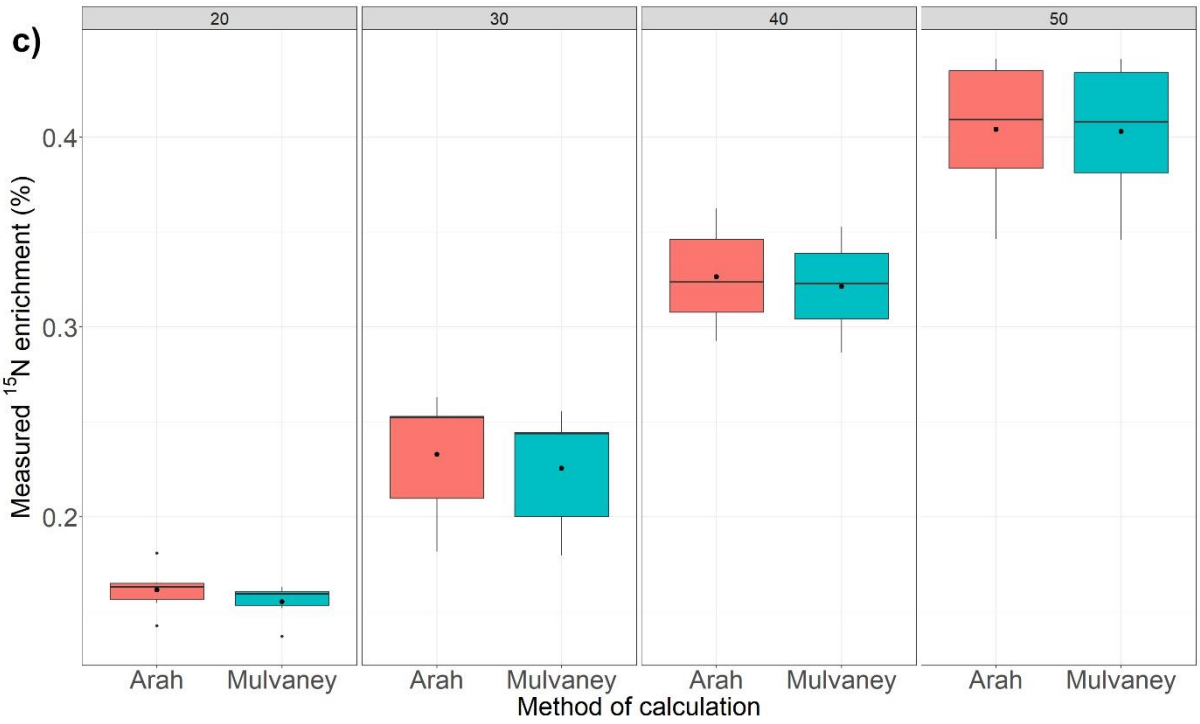

***Figure 32**: Comparison of the "Arah" and "Mulvaney & Boast" models for the calculation of the ^{15}N enrichment of the soil denitrifying pool in Experiment 1 after a) 3 hours, b) 6 hours and c) 24 hours.*

3.7.5.2) Experiment 2:

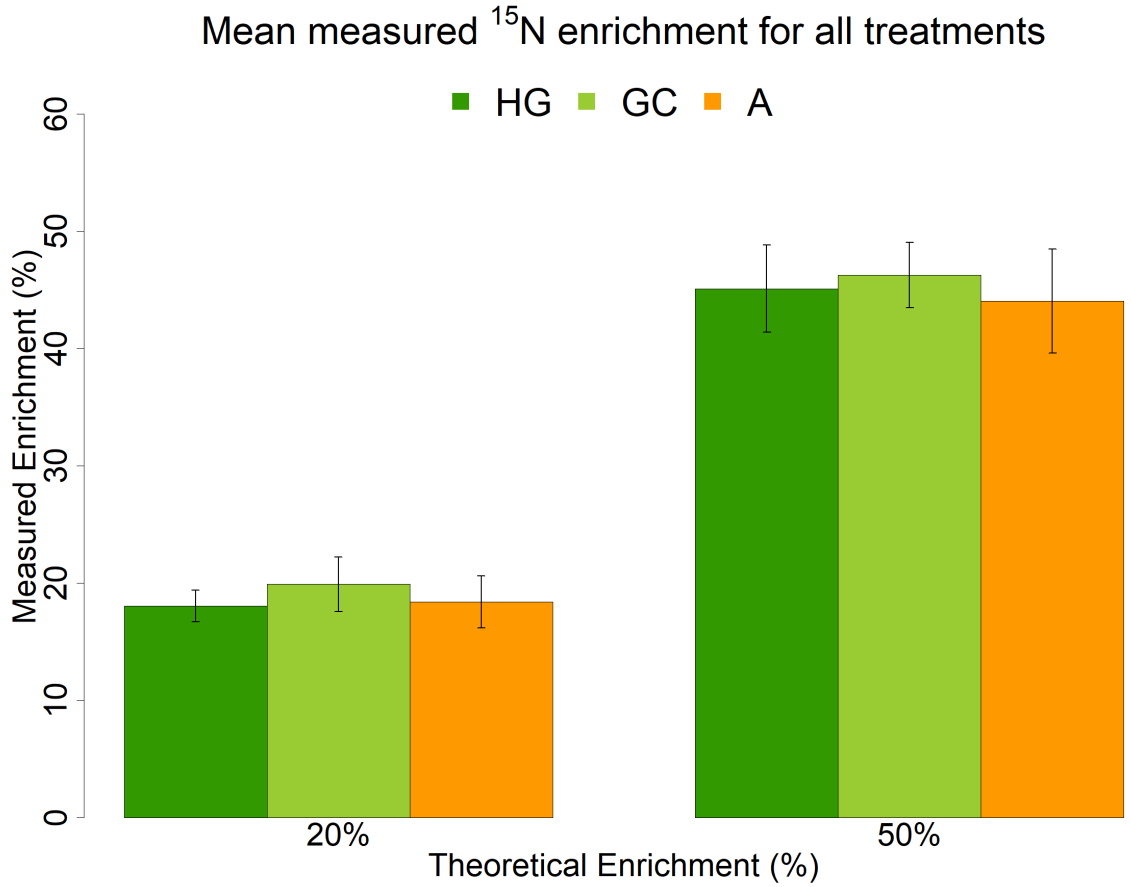

***Figure 33**: Average measured ^{15}N enrichment of the denitrifying pool (α_p) for each treatment.*

The error bars represent the standard errors. This time, the enrichments did not vary as much as **Experiment 1,** thus we took the average of all time steps for each treatment.

3.7.5.3) Experiment 4

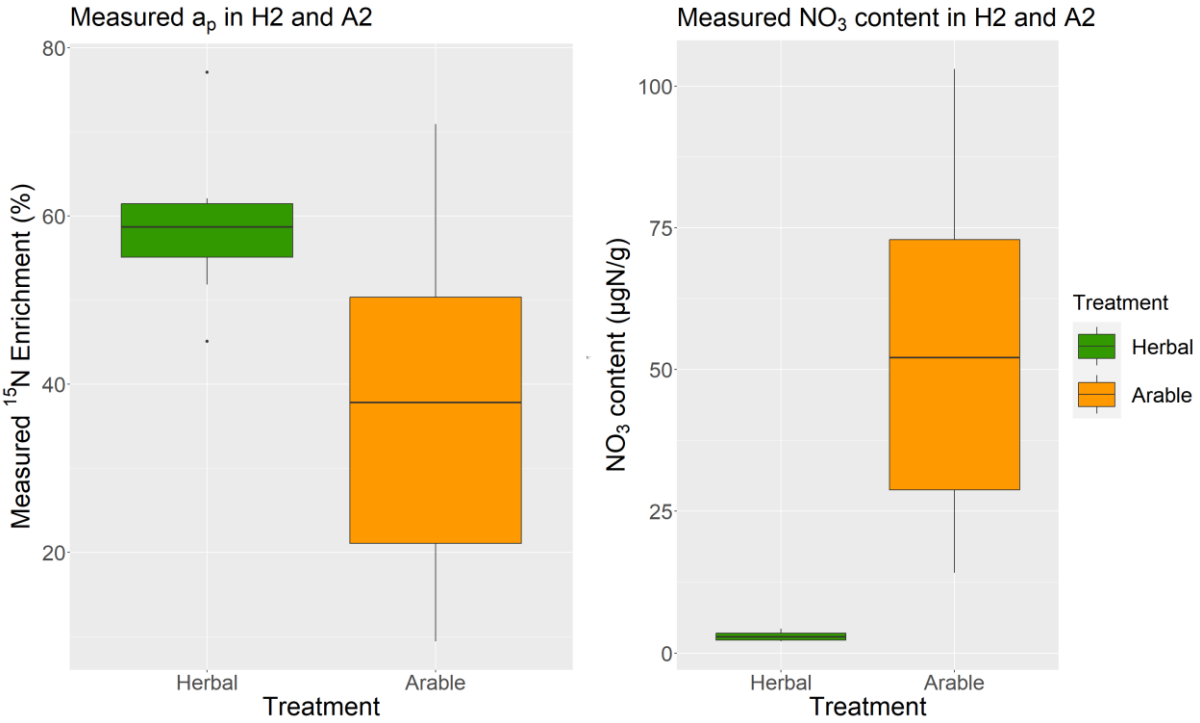

***Figure 34**: Boxplots of the measured ^{15}N enrichment in the different soil cores (right) and the nitrate content (left) in the fields H2 (green) and A2 (orange) during **Experiment 4**.*

3.8) References

Arah, J. R. M. (1992). New Formulae for Mass Spectrometric Analysis of Nitrous Oxide and Dinitrogen Emissions. *Soil Science Society of America Journal*, *56*(3), 795–800. https://doi.org/10.2136/sssaj1992.03615995005600030020x

Baily, A., Watson, C. J., Laughlin, R., Matthews, D., McGeough, K., & Jordan, P. (2012). Use of the 15 N gas flux method to measure the source and level of N2O and N2 emissions from grazed grassland. *Nutrient Cycling in Agroecosystems*, *94*(2–3), 287–298. https://doi.org/10.1007/s10705-012-9541-x

Berendt, J., & Wrage-Mönnig, N. (2023). Denitrification is not Necessarily the Main Source of N2O from Rewetted Fens. *Journal of Soil Science and Plant Nutrition*, *0123456789*. https://doi.org/10.1007/s42729-023-01291-7

Bergsma, T. T., Bergsma, Q. C., Ostrom, N. E., & Robertson, G. P. (1999). A Heuristic Model for the Calculation of Dinitogen and Nitrous Oxide Flux from Nitrogen-15-Labeled Soil. *Soil Science Society of America Journal*, *63*(6), 1709–1716. https://doi.org/10.2136/sssaj1999.6361709x

Bergsma, T. T., Ostrom, N. E., Emmons, M., & Robertson, G. P. (2001). Measuring simultaneous fluxes from soil of N2O and N2 in the field using the 15N-gas "nonequilibrium" technique. *Environmental Science and Technology*, *35*(21), 4307–4312. https://doi.org/10.1021/es010885u

Bizimana, F., Luo, J., Timilsina, A., Dong, W., Gaudel, G., Ding, K., Qin, S., & Hu, C. (2022). Estimating field N2 emissions based on laboratory-quantified N2O/(N2O + N2) ratios and field-quantified N2O emissions. *Journal of Soils and Sediments*, *22*(8), 2196–2208. https://doi.org/10.1007/s11368-022-03212-0

Blackmer, A. M., & Bremner, J. M. (1978). Inhibitory effect of nitrate on reduction of N_2O to N_2 by soil microorganisms. Soil Biology and Biochemistry, 10(3), 187–191. https://doi.org/10.1016/0038-0717(78)90095-0

Buchen-Tschiskale, C., Well, R., & Flessa, H. (2023). Tracing nitrogen transformations during spring development of winter wheat induced by 15N labeled cattle slurry applied with different techniques. *Science of the Total Environment*, *871*(February), 162061. https://doi.org/10.1016/j.scitotenv.2023.162061

Buchen, C., Lewicka-Szczebak, D., Fuß, R., Helfrich, M., Flessa, H., & Well, R. (2016). Fluxes of N2 and N2O and contributing processes in summer after grassland renewal and grassland conversion to maize cropping on a Plaggic Anthrosol and a Histic Gleysol. *Soil Biology and Biochemistry*, *101*, 6–19. https://doi.org/10.1016/j.soilbio.2016.06.028

Butterbach-Bahl, K., Willibald, G., & Papen, H. (2002). Soil core method for direct simultaneous determination of N2 and N2O emissions from forest soils. *Plant and Soil*, *240*(1), 105–116. https://doi.org/10.1023/A:1015870518723

Cárdenas, L. M., Hawkins, J. M. B., Chadwick, D., & Scholefield, D. (2003). Biogenic gas emissions from soils measured using a new automated laboratory incubation system. *Soil Biology and Biochemistry*, *35*(6), 867–870. https://doi.org/10.1016/S0038-0717(03)00092-0

Clayton, H., McTaggart, I. P., Parker, J., Swan, L., & Smith, K. A. (1997). Nitrous oxide emissions from fertilised grassland: A 2-year study of the effects of N fertiliser form and environmental conditions. *Biology and Fertility of Soils*, *25*(3), 252–260. https://doi.org/10.1007/s003740050311

Comer-Warner, S. A., Nguyen, A. T. Q., Nguyen, M. N., Wang, M., Turner, A., Le, H., Sgouridis, F., Krause, S., Kettridge, N., Nguyen, N., Hamilton, R. L., & Ullah, S. (2022). Restoration impacts on rates of denitrification and greenhouse gas fluxes from tropical coastal wetlands. Science of The Total Environment, 803, 149577. https://doi.org/10.1016/j.scitotenv.2021.149577

Deppe, M., Well, R., Giesemann, A., Spott, O., & Flessa, H. (2017). Soil N2O fluxes and related processes in laboratory incubations simulating ammonium fertilizer depots. *Soil Biology and Biochemistry*, *104*, 68–80. https://doi.org/10.1016/j.soilbio.2016.10.005

Firestone, M. K., & Tiedje, J. M. (1979). Temporal change in nitrous oxide and dinitrogen from denitrification following onset of anaerobiosis. Applied and Environmental Microbiology, 38(4), 673–679. https://doi.org/10.1128/aem.38.4.673-679.1979

Friedl, J., Cardenas, L. M., Clough, T. J., Dannenmann, M., Hu, C., & Scheer, C. (2020). Measuring denitrification and the N2O:(N2O + N2) emission ratio from terrestrial soils. *Current Opinion in Environmental Sustainability*, *47*, 61–71. https://doi.org/10.1016/j.cosust.2020.08.006

Gao, D., Bai, E., Li, M., Zhao, C., Yu, K., & Hagedorn, F. (2020). Responses of soil nitrogen and phosphorus cycling to drying and rewetting cycles: A meta-analysis. *Soil Biology and Biochemistry*, *148*(July), 107896. https://doi.org/10.1016/j.soilbio.2020.107896

Groffman, P. M., Altabet, M. A., Böhlke, J. K., Butterbach-Bahl, K., David, M. B., Firestone, M. K., Giblin, A. E., Kana, T. M., Nielsen, L. P., & Voytek, M. A. (2006). Methods for measuring denitrification: Diverse approaches to a difficult problem. In *Ecological Applications* (Vol. 16, Issue 6, pp. 2091–2122). https://doi.org/10.1890/1051-0761(2006)016[2091:MFMDDA]2.0.CO;2

Groffman, P. M., Butterbach-Bahl, K., Fulweiler, R. W., Gold, A. J., Morse, J. L., Stander, E. K., Tague, C., Tonitto, C., & Vidon, P. (2009). Challenges to incorporating spatially and temporally explicit phenomena (hotspots and hot moments) in denitrification models. *Biogeochemistry*, *93*(1–2), 49–77. https://doi.org/10.1007/s10533-008-9277-5

Grosso, S. J. Del, Parton, W., Mosier, A. R., Ojima, D. S., Kulmala, A. E., & Phongpan, S. (2000). General model for N2O and N2 gas emissions from soils. *Global Biogeochemical Cycles*, *14*(4), 1045–1060.

Hutchinson, G. L., & Mosier, A. R. (1981). Improved Soil Cover Method for Field Measurement of Nitrous Oxide Fluxes. *Soil Science Society of America Journal*, *45*(2), 311–316. https://doi.org/10.2136/sssaj1981.03615995004500020017x

IPCC. (2013). Climate change 2013: The physical science basis. Contribution of Working Group I to the Fifth Assessment Report of the Intergovernmental Panel on Climate Change (Rep., 1535 pp.). Cambridge, UK and New York.

Jarvis, S. C., Barraclough, D., Williams, J., & Rook, A. J. (1991). Patterns of denitrification loss from

grazed grassland: Effects of N fertilizer inputs at different sites. *Plant and Soil*, *131*(1), 77–88. https://doi.org/10.1007/BF00010422

Jiao, P., Yang, L., Li, Z., Zheng, P., & Nie, X. (2023). Soil type and wetting intensity control the enhancement extent of N2O efflux in soil with drought and rewetting cycles. *International Soil and Water Conservation Research*, *1*(xxxx). https://doi.org/10.1016/j.iswcr.2023.05.007

Kostyanovsky, K. I., Huggins, D. R., Stockle, C. O., Waldo, S., & Lamb, B. (2018). Developing a flow through chamber system for automated measurements of soil N2O and CO2 emissions. *Measurement: Journal of the International Measurement Confederation*, *113*, 172–180. https://doi.org/10.1016/j.measurement.2017.05.040

Krause, H. M., Thonar, C., Eschenbach, W., Well, R., Mäder, P., Behrens, S., Kappler, A., & Gattinger, A. (2017). Long term farming systems affect soils potential for N2O production and reduction processes under denitrifying conditions. *Soil Biology and Biochemistry*, *114*, 31–41. https://doi.org/10.1016/j.soilbio.2017.06.025

Kulkarni, M. V., Burgin, A. J., Groffman, P. M., & Yavitt, J. B. (2014). Direct flux and 15N tracer methods for measuring denitrification in forest soils. *Biogeochemistry*, *117*(2–3), 359–373. https://doi.org/10.1007/s10533-013-9876-7

Lassaletta, L., Billen, G., Grizzetti, B., Anglade, J., & Garnier, J. (2014). 50 year trends in nitrogen use efficiency of world cropping systems: The relationship between yield and nitrogen input to cropland. *Environmental Research Letters*, *9*(10). https://doi.org/10.1088/1748-9326/9/10/105011

Liu, Y., Wang, R., Pan, Z. L., Zheng, X. H., Wei, H. H., Zhang, H. R., Mei, B. L., Quan, Z., Fang, Y. T., & Ju, X. T. (2022**a**). Quantifying in situ N2 fluxes from an intensively managed calcareous soil using the 15N gas-flux method. *Journal of Integrative Agriculture*, *21*(9), 2750–2766. https://doi.org/10.1016/j.jia.2022.07.016

Liu, Y., Cong, R., Liao, S., Guo, Q., Li, X., Ren, T., Lu, Z., & Lu, J. (2022**b**). Rapid soil rewetting promotes limited N2O emissions and suppresses NH3 volatilization under urea addition. *Environmental Research*, *212*(PC), 113402. https://doi.org/10.1016/j.envres.2022.113402

Loick, N., Dixon, E. R., Abalos, D., Vallejo, A., Matthews, G. P., McGeough, K. L., Well, R., Watson, C. J., Laughlin, R. J., & Cardenas, L. M. (2016). Denitrification as a source of nitric oxide emissions from incubated soil cores from a UK grassland soil. *Soil Biology and Biochemistry*, *95*, 1–7. https://doi.org/10.1016/j.soilbio.2015.12.009

Loick, N., Dixon, E., Abalos, D., Vallejo, A., Matthews, P., McGeough, K., Watson, C., Baggs, E. M., & Cardenas, L. M. (2017). "Hot spots" of N and C impact nitric oxide, nitrous oxide and nitrogen gas emissions from a UK grassland soil. *Geoderma*, *305*, 336–345. https://doi.org/10.1016/j.geoderma.2017.06.007

Mulvaney, R.L. (1984), Determination of 15N-Labeled Dinitrogen and Nitrous Oxide with Triple-Collector Mass Spectrometers. Soil Science Society of America Journal, 48: 690-692. https://doi.org/10.2136/sssaj1984.03615995004800030045x

Mulvaney, R. L., & Boast, C. W. (1986). Equations for determination of nitrogen-15 labeled

dinitrogen and nitrous oxide by mass spectrometry. Soil Science Society of America Journal, 50(2), 360-363. https://doi.org/10.2136/sssaj1986.03615995005000020021x

Mulvaney, R. L., & Vanden Heuvel, R. M. (1988). Evaluation of nitrogen-15 tracer techniques for direct measurement of denitrification in soil: IV. field studies. Soil Science Society of America Journal 52(5), 1332-37. https://doi.org/10.2136/sssaj1988.03615995005200050023x

Micucci, G., Sgouridis, F., Mcnamara, N. P., Krause, S., Lynch, I., Roos, F., Well, R., & Ullah, S. (2023). The 15 N-Gas flux method for quantifying denitrification in soil : Current progress and future directions. *Soil Biology and Biochemistry*, *184*(June), 109108. https://doi.org/10.1016/j.soilbio.2023.109108

Parton, W. J., Mosier, A. R., Ojima, D. S., Valentine, D. W., Schime, D. S., Weier, K., & Kulmala, A. E. (1996). Generalized model for N2 and N2O production from nitrification and denitrification. *Global Biogeochemical Cycles*, *10*(3), 401–412. https://doi.org/10.1029/96GB01455

Pedersen, A. R., Petersen, S. O., & Schelde, K. (2010). A comprehensive approach to soil-atmosphere trace-gas flux estimation with static chambers. *European Journal of Soil Science*, *61*(6), 888–902. https://doi.org/10.1111/j.1365-2389.2010.01291.x

Phillips, R. L., Song, B., McMillan, A. M. S., Grelet, G., Weir, B. S., Palmada, T., & Tobias, C. (2016). Chemical formation of hybrid di-nitrogen calls fungal codenitrification into question. Scientific Reports, 6. https://doi.org/10.1038/srep39077

Ravishankara, A. R., Daniel, J. S., & Portmann, R. W. (2009). Nitrous oxide (N2O): The dominant ozone-depleting substance emitted in the 21st century. *Science*, *326*(5949), 123–125. https://doi.org/10.1126/science.1176985

Rummel, P. S., Well, R., Pfeiffer, B., Dittert, K., Floßmann, S., & Pausch, J. (2021). Nitrate uptake and carbon exudation – do plant roots stimulate or inhibit denitrification? *Plant and Soil*, *459*(1–2), 217–233. https://doi.org/10.1007/s11104-020-04750-7

Ruser, R., Flessa, H., Russow, R., Schmidt, G., Buegger, F., & Munch, J. C. (2006). Emission of N2O, N2 and CO2 from soil fertilized with nitrate: Effect of compaction, soil moisture and rewetting. *Soil Biology and Biochemistry*, *38*(2), 263–274. https://doi.org/10.1016/j.soilbio.2005.05.005

Russow, R., Stevens, R. J., & Laughlin, R. J. (1996). Accuracy and precision for measurements of the mass ratio 30/28 in dinitrogen from air samples and its application to the investigation of n losses from soil by denitrification. *Isotopes in Environmental and Health Studies*, *32*(2–3), 289–297. https://doi.org/10.1080/10256019608036322

Saggar, S., Jha, N., Deslippe, J., Bolan, N. S., Luo, J., Giltrap, D. L., Kim, D. G., Zaman, M., & Tillman, R. W. (2013). Denitrification and N2O: N2 production in temperate grasslands: Processes, measurements, modelling and mitigating negative impacts. In *Science of the Total Environment* (Vol. 465, pp. 173–195). https://doi.org/10.1016/j.scitotenv.2012.11.050

Sánchez-García, M., Roig, A., Sánchez-Monedero, M. A., & Cayuela, M. L. (2014). Biochar increases soil N 2 O emissions produced by nitrification-mediated pathways. *Frontiers in Environmental Science*, *2*(JUL), 1–10. https://doi.org/10.3389/fenvs.2014.00025

Scheer, C., Fuchs, K., Pelster, D. E., & Butterbach-bahl, K. (2020). ScienceDirect Estimating global terrestrial denitrification from measured N 2 O :(N 2 O + N 2) product ratios $. *Current Opinion in Environmental Sustainability*, *47*, 72–80. https://doi.org/10.1016/j.cosust.2020.07.005

Scholefield, D., Hawkins, J. M. B., & Jackson, S. M. (1997). Development of a helium atmosphere soil incubation technique for direct measurement of nitrous oxide and dinitrogen fluxes during denitrification. *Soil Biology and Biochemistry*, *29*(9–10), 1345–1352. https://doi.org/10.1016/S0038-0717(97)00021-7

Seitzinger, S. P., Nielsen, L. P., Caffrey, J., & Christensen, P. B. (1993). Denitrification measurements in aquatic sediments: A comparison of three methods. *Biogeochemistry*, *23*(3), 147–167. https://doi.org/10.1007/BF00023750

Sgouridis, F., & Ullah, S. (2015). Relative Magnitude and Controls of in Situ N2 and N2O Fluxes due to Denitrification in Natural and Seminatural Terrestrial Ecosystems Using 15N Tracers. *Environmental Science and Technology*, *49*(24), 14110–14119. https://doi.org/10.1021/acs.est.5b03513

Sgouridis, F., Stott, A., & Ullah, S. (2016). Application of the 15N gas-flux method for measuring in situ N2 and N2O fluxes due to denitrification in natural and semi-natural terrestrial ecosystems and comparison with the acetylene inhibition technique. *Biogeosciences*, *13*(6), 1821–1835. https://doi.org/10.5194/bg-13-1821-2016

Sgouridis, F., Reay, M., Cotchim, S., Ma, J., Radu, A., & Ullah, S. (2023). Stimulation of soil gross nitrogen transformations and nitrous oxide emission under Free air CO2 enrichment in a mature temperate oak forest at BIFoR-FACE. Soil Biology and Biochemistry, 184, 109072. https://doi.org/10.1016/j.soilbio.2023.109072

Simarmata, T., Benckiser, G., & Ottow, J. C. G. (1993). Effect of an increasing carbon: nitrate-N ratio on the reliability of acetylene in blocking the N2O-reductase activity of denitrifying bacteria in soil. *Biology and Fertility of Soils*, *15*(2), 107–112. https://doi.org/10.1007/BF00336427

Spott, O., Russow, R., Apelt, B., & Stange, C. F. (2006). A 15N-aided artificial atmosphere gas flow technique for online determination of soil N2 release using the zeolite Köstrolith SX6®. *Rapid Communications in Mass Spectrometry*, *20*(22), 3267–3274. https://doi.org/10.1002/rcm.2722

Stevens, R. J., Laughlin, R. J., Burns, L. C., Arah, J. R. M., & Hood, R. C. (1997). Measuring the contributions of nitrification and denitrification to the flux of nitrous oxide from soil. *Soil Biology and Biochemistry*, *29*(2), 139–151. https://doi.org/10.1016/S0038-0717(96)00303-3

Stevens, R. J., & Laughlin, R. J. (2001). Lowering the detection limit for dinitrogen using the enrichment of nitrous oxide. *Soil Biology and Biochemistry*, *33*(9), 1287–1289. https://doi.org/10.1016/S0038-0717(01)00036-0

Stevens, R. J., & Laughlin, R. J. (2002). Cattle Slurry Applied Before Fertilizer Nitrate Lowers Nitrous Oxide and Dinitrogen Emissions. *Soil Science Society of America Journal*, *66*(2), 647–652. https://doi.org/10.2136/sssaj2002.6470

Tauchnitz, N., Spott, O., Russow, R., Bernsdorf, S., Glaser, B., & Meissner, R. (2015). Release of nitrous oxide and dinitrogen from a transition bog under drained and rewetted conditions due to denitrification: results from a [15N]nitrate–bromide double-tracer study. Isotopes in Environmental and Health Studies, 51(2), 300–321. https://doi.org/10.1080/10256016.2015.1011634

Wang, R., Feng, Q., Liao, T., Zheng, X., Butterbach-Bahl, K., Zhang, W., & Jin, C. (2013). Effects of nitrate concentration on the denitrification potential of a calcic cambisol and its fractions of N2, N2O and NO. *Plant and Soil*, *363*(1–2), 175–189. https://doi.org/10.1007/s11104-012-1264-x

Wang, R., Pan, Z., Zheng, X., Ju, X., Yao, Z., Butterbach-Bahl, K., Zhang, C., Wei, H., & Huang, B. (2020). Using field-measured soil N2O fluxes and laboratory scale parameterization of N2O/(N2O+N2) ratios to quantify field-scale soil N2 emissions. *Soil Biology and Biochemistry*, *148*(June), 107904. https://doi.org/10.1016/j.soilbio.2020.107904

Wang, H., Yan, Z., Ju, X., Song, X., Zhang, J., Li, S., & Zhu-Barker, X. (2023). Quantifying nitrous oxide production rates from nitrification and denitrification under various moisture conditions in agricultural soils: Laboratory study and literature synthesis. Frontiers in Microbiology, 13(January), 1–10. https://doi.org/10.3389/fmicb.2022.1110151

Warner, D. I., Scheer, C., Friedl, J., Rowlings, D. W., Brunk, C., & Grace, P. R. (2019). Mobile continuous-flow isotope-ratio mass spectrometer system for automated measurements of N2 and N2O fluxes in fertilized cropping systems. *Scientific Reports*, *9*(1), 11097. https://doi.org/10.1038/s41598-019-47451-7

Weier, K. L., Doran, J. W., Power, J. F., & Walters, D. T. (1993). Denitrification and the Dinitrogen/Nitrous Oxide Ratio as Affected by Soil Water, Available Carbon, and Nitrate. *Soil Science Society of America Journal*, *57*(1), 66–72. https://doi.org/10.2136/sssaj1993.03615995005700010013x

Well, R., Burkart, S., Giesemann, A., Grosz, B., Köster, J. R., & Lewicka-Szczebak, D. (2019**a**). Improvement of the 15 N gas flux method for in situ measurement of soil denitrification and its product stoichiometry. *Rapid Communications in Mass Spectrometry*, *33*(5), 437–448. https://doi.org/10.1002/rcm.8363

Well, R., Maier, M., Lewicka-Szczebak, D., Köster, J. R., & Ruoss, N. (2019**b**). Underestimation of denitrification rates from field application of the 15N gas flux method and its correction by gas diffusion modelling. *Biogeosciences*, *16*(10), 2233–2246. https://doi.org/10.5194/bg-16-2233-2019

Yu, K., Seo, D. C., & Delaune, R. D. (2010). Incomplete acetylene inhibition of nitrous oxide reduction in potential denitrification assay as revealed by using 15N-Nitrate tracer. *Communications in Soil Science and Plant Analysis*, *41*(18), 2201–2210. https://doi.org/10.1080/00103624.2010.504800

Chapter 4: *In situ* measurement of denitrification and greenhouse gas emissions in conventional and regenerative agriculture

This chapter covers the field campaign that started in March 2022 and ended in May 2023. The two main objectives were to confirm our new method of *in situ* denitrification measurement and characterize this process in conventional and regenerative agriculture. Additionally, we aimed to quantify the fluxes of greenhouse gas emissions in these two land uses. Although denitrification was measured for a one-year period, we extended the measurement of greenhouse gases for a few more months in 2023.

This third part of the thesis is written as a research article and will be submitted for publication in the Environmental Science and Technology Journal.

Under the supervision of Sami Ullah and Fotis Sgouridis, Gianni Micucci formulated the research questions, designed the experimental layout, ran all the monthly field experiments, analysed the data and wrote the manuscript. Gianni Micucci was responsible for all soil analyses (mineral nitrogen, DOC and TDN, soil particle sizes, pH, OM, mineralization potential and moisture, see **Chapter 4.3**). On the other hand, Fotis Sgouridis was responsible for all gas analyses. All the cited co-authors reviewed and corrected the manuscript.

In situ measurement of denitrification and greenhouse gas emissions in conventional and regenerative agriculture

Gianni Micucci[1,*], Fotis Sgouridis[2], Jonathan Leake[3], Niall P. McNamara[4], Stefan Krause[1], Iseult Lynch[1], Felicity Roos[5] and Sami Ullah[1,6]

- 1. School of Geography, Earth and Environmental Sciences, University of Birmingham, Edgbaston, B15 2TT Birmingham, United Kingdom.
- 2. School of Geographical Sciences, University of Bristol, BS8 1SS Bristol, United Kingdom.
- 3. Plants, Photosynthesis and Soil, School of Biosciences, University of Sheffield, Sheffield S10 2TN, UK.
- 4. UK Centre for Ecology & Hydrology, Lancaster Environment Centre, LA1 4AP Lancaster, United Kingdom.
- 5. UK National Trust, SN2 2NA Swindon, United Kingdom.
- 6. Birmingham Institute of Forest Research, University of Birmingham, Birmingham, UK.

* Corresponding author.

Email address: [redacted] (G. Micucci).

Colour should be used for figures.

Keywords: Denitrification, ^{15}N Gas Flux Method, Nitrogen cycling, Nitrous Oxide Emission, Regenerative Agriculture.

4.1) Abstract

The purpose of this study was to confirm our new method of *in situ* denitrification measurement through a one-year field campaign, aiming to constrain and characterize the dynamics of denitrification in three different fields: one conventional arable and two types of pasture ("leys"). Our new method combines the application of ^{15}N tracer and artificial atmosphere for the incubation of soil cores under field conditions. Our two methodological objectives were to assess the dependence of added nitrate tracer with a potential process stimulation and determine the best method for upscaling soil core fluxes to field rates. To that end, parallel field incubations were run using conventional static chambers; which also enabled the measurement of greenhouse gas emissions (CO_2, CH_4 and N_2O). Subsequently, we aimed to trace the fate of applied synthetic nitrogen fertilizer via denitrification in conventional agriculture and compare it to background fluxes from pastures under regenerative agriculture practices. Our newly developed method was successful at detecting denitrified N_2 fluxes 90% of the time. The field results show that, although the magnitude of flux derived from the cores appears to be stimulated, two independent denitrification parameters can be assessed and applied to static chamber N_2O emission rates to derive global denitrification fluxes. Using this approach, we estimated that 8% of the applied fertilizer in the arable was lost via denitrification, 9% of this flux being emitted via N_2O rather than N_2. The annual loss of nitrogen through denitrification was 8.5 times higher in the arable than in an unfertilized ley, resulting in the pasture saving around 2 tonnes of $eqCO_2$ of N_2O over a year.

4.2) Introduction

Emerging less than 100 years ago, the Green Revolution has completely transformed the food production system in the world and allows today the production of 9.5 billion tonnes of food annually (FAO, 2022). The combination of high-yield species selection, controlled irrigation, chemical pesticides, mechanization, fossil fuel exploitation and synthetic fertilizer enabled to reach never-seen before yields. While these technical advancements allow to sustain food security (at least in developed countries), it also has many impacts on the environment. Amongst others, it leads to degradation of soils and in particular to a loss of soil organic carbon (Sanderman et al., 2017), pollution and eutrophication of water streams, destruction of fauna natural habitat and emission of greenhouse gases. Indeed, the modern food system is responsible for 19 to 29% of the global emissions of greenhouse gases (Vermeulen et al., 2012). Although its dependence to fuel (cultivation, application of manure, transport of animal, processing and transport of feed) is an important source of carbon dioxide (CO_2), most of the warming potential comes from emissions of methane (CH_4) and nitrous oxide (N_2O). Nitrous oxide in particular has 298 times greater radiative forcing than CO_2 (IPCC, 2013) and is also involved in the depletion of the ozone layer (Ravishankara et al., 2009). Agriculture is responsible for 75% of N_2O emissions globally (Velthof & Rietra, 2018), which mostly result from application of N fertilizer in arable fields. Around 120 million tonnes of N fertilizer are used yearly (FAO, 2017) ; however, it is estimated half of this fertilizer is lost to the environment (Lassaletta et al., 2014), in particular as N_2O.

One of the main sources of nitrous oxide is denitrification, the microbial anaerobic respiration process which converts soil nitrate (NO_3^-) into gaseous dinitrogen (N_2). Incomplete denitrification leads to the emission of nitrous oxide, while the full process sequence is the only natural terrestrial

sink for N_2O emissions (Conthe et al., 2019). However, many uncertainties exist around this process (Almaraz et al., 2020), including its potential magnitude and efficiency as nitrous oxide sink; defined through the quantity of denitrified N_2O relatively to total denitrification flux (product ratio). Denitrification fluxes and dynamics are poorly constrained, especially in intensive agriculture, where large amounts of nitrogen fertilizer are expected to result in increased N emissions (Charles Munch & Velthof, 2007). This comes from the high spatial and temporal variabilities of denitrification as well as the intrinsic difficulties linked to its measurement, i.e. the sensitivity needed to detect small soil N_2 fluxes against the high atmospheric background (78%; Groffman et al., 2006). Therefore, denitrification is often attributed to the unexplained difference between N inputs and outputs in agricultural practices (Soana et al., 2022). We recently developed a new method of in situ denitrification measurement (**Chapter 3**) which combines ^{15}N tracer and artificial atmosphere; however, further validation is needed to estimate its accuracy in quantification of global denitrification rates.

To mitigate the impact of modern agriculture and in particular its contribution to global warming, regenerative agriculture aims to restore degraded lands and prevent the losses of arable lands. It revolves around five principles: minimum mechanical soil disturbance (i.e. no tillage), permanent soil organic cover, species diversification, keeping living roots in the soil and integrating animals (Miller-Klugesherz & Sanderson, 2023). A typical application of regenerative agriculture is the “ley”, introduced during the second agricultural revolution in Europe during the 18^{th} century (Overton, 1996). It consists of converting a farmland into a temporary pasture to restore soil health. The presence of animals through rotational grazing participates to mineral cycling while the presence of legumes associated with nitrogen-fixing bacteria enable the leys to naturally fertilize soil. It has been estimated that biological nitrogen fixation has the ability to fix roughly 200 million tonnes of

nitrogen annually (Biswas & Gresshoff, 2014) and could thus be a reliable alternative to synthetic nitrogen fertilizer. Under the UK target of net zero emissions by 2050 and considering the recent increase in fertilizer price, regenerative agriculture appears a viable solution to sustain food production whilst reducing global warming and restoring degraded soils.

In the study, we aimed to validate our new method of denitrification measurement and use it characterize denitrification in conventional agriculture in comparison to two types of leys, a grass/clover ley and an herbal ley. The traditional grass/clover mix is the most predominant form of ley for rotational grazing in the UK (Kingston-Smith et al., 2013) and its high proportion of white and red clovers (*trifolium repens* and *trifolium pratense* respectively) usually enables higher levels of nitrogen in the soil. Herbal leys have been promoted for over a century in temperate regions (Jordon et al., 2022) and consist in more complex mixes of legumes, perennial forbs and grasses. Our work consisted in field campaigns spanning from March 2022 to May 2023 where denitrification was measured in situ using our newly developed method (**Chapter 3**) and greenhouse gas emissions using static chambers. Soil properties such as ammonium (NH_4^+), nitrate (NO_3^-), dissolved organic carbon (DOC), total dissolved nitrogen (TDN), gravimetric moisture and laboratory-based mineralization potential were also measured. Our research objectives were to:

(1) Validate our newly developed *in situ* denitrification measurement method.
(2) Quantify N losses through denitrification in the different land uses and in particular the nitrous oxide sink efficiency (through the denitrification product ratio).
(3) Quantify the total emissions of greenhouse gases.
(4) Characterize the physical properties and internal nitrogen dynamics of the different land uses.

4.3) Material and method

4.3.1) Study sites and experimental layout:

This study took place at the FarmED site, near Shipton-under Wychwood UK (51.869981,-1.581136, https://www.farm-ed.co.uk/), which is an experimental agricultural station consisting in strips of the same soil under herbal leys of different ages (up to 5 years before being converted back to arable). Prior to this experimental layout, the soil (inceptisol with an oolitic limestone bedrock) had been conventionally managed for wheat or barley production for thirty years. One experimental strip has been conserved for this conventional management and constitutes the "arable control". It includes the production of wheat and barley, tillage and application of fertilizer. The herbal ley strips were all planted with the same mix, which includes white and red clovers, timothy (*Phleum pratense*), chicory (*Cichorium intybus*), lucerne (*Medicago sativa*) or sainfoin (*Onobrychis viciifolia*) amongst others (the full composition can be found in **Chapter 3.7.2**). For the present work, the 4-year-old herbal ley strip (**H**) was studied and compared to the arable control (**A**). Since the experimental strips at FarmED did not include a grass/clover ley, a nearby field (**GC**) under this type of management was selected (**Figure 35**); which makes its comparison with **H** and **A** a bit more complex.

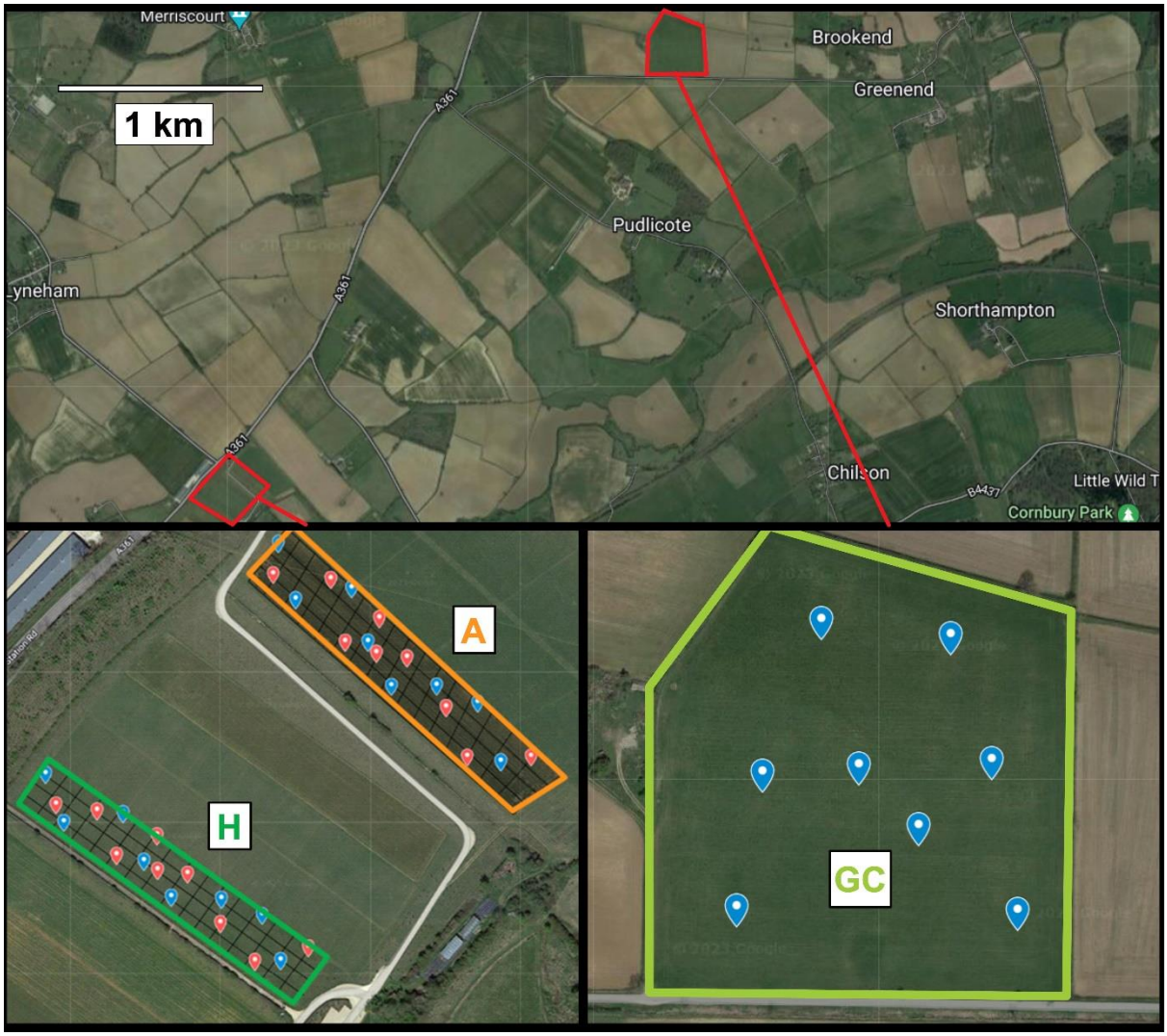

***Figure 35**: Field locations (top) and sampling strategy at the FarmED site (bottom left) and **GC** field (bottom right) for field incubations.*

In FarmED (bottom left), the **H** (left) and **A** (right) fields were subdivided in 4 longitudinal segments and 16 latitudinal segments. Then, following the longitudinal direction, locations were randomly chosen between the 4 available slots (same patterns for both land uses). The red pins represent static greenhouse gas chamber locations while the blue pins represent the sampling locations for the plastic liners. In the **GC** field, we applied a more traditional W-shaped sampling strategy.

During the span of our field campaign, the arable control was cultivated for barley from March to August 2022, winter wheat from September to November 2022 and wheat from March 2023 until the end of the campaign (May 2023). The herbal ley was mob-grazed by cows and sheep in July 2022 and in April 2023. Finally the grass/clover ley was harvested for hay in July 2022.

In 2022, a liquid fertilizer containing 8.1% of nitrate, 10.6% of ammonia and 16.3% of urea was applied three times in the **A** field; 50 kgN/ha in March and 75 kgN/ha in April and May. This fertilizer also contained 7% of sulphite (SO_3^{2-}), which represented 14 kgS ha^{-1}. The same mixture was applied in the **GC** field in April 2022 (50 kgN ha^{-1} and 14 kgS ha^{-1}).

In 2023, a fertilizer solution containing 6.2% of nitrate, 8.1% of ammonium and 12.5% of urea as well as 5.4% of sulphite was again applied three times in the **A** field (60 kgN/ha in February, March and May).

Finally, the denitrification measurements using liners occurred in all three land uses, however, the static chambers were only deployed in the **A** and **H** fields due to the distance between fields (both incubations running at the same time).

4.3.2) Soil characterization

The three land uses were initially tested for organic matter content (OM), total C and total N, soil particle sizes and pH. Additionally, during each campaign, soil samples were collected and brought to the laboratory for DOC, TDN, NH_4^+, NO_3^-, gravimetric moisture and mineralisation potential determinations. The procedures for the determination of soil particle sizes, pH, NH_4^+, NO_3^- and gravimetric moisture are detailed in **Chapter 3.3.4**. Organic matter content was determined by loss

on ignition at 450°C for 5 hours of oven-dried samples (105°C). For the measurement of total C and N contents, oven-dried samples were ground and analysed over a Delta V elemental analyser IRMS (Thermo Fisher). For DOC and TDN quantification, 5 g of soil were extracted in 40 mL of deionised water and shaken at 200 rpm on an orbital shaker for 2 hours and filtrated through n°42 Whatman paper (GE Healthcare). Filtrates were analysed over a TOC-L series (Shimadzu, Japan). In this study, we define the available C:N ratio as the ratio of DOC to TDN, which varied monthly; compared to the total C:N ratio, which is the ratio of total C to total N and which stayed constant over time. Finally, to measure soil mineralization potential, 30 g of soil were transferred in serum bottles directly after NH_4^+ and NO_3^- extraction; the serum bottles were subsequently left at laboratory temperature (20°C) for 28 days before being extracted again. The differences in NH_4^+ and NO_3^- levels before and after incubation were used to derive potential mineralization rates.

4.3.3) In-situ measurement of denitrification

Denitrification was measured *in situ* using our newly developed method (**Chapter 3**). Briefly, 10 cm-high soil cores were sampled inside 15 cm-long plastic liners (2.3 ID) and left to pre-incubate overnight under environmental conditions. The next day, $^{15}N\text{-}NO_3^-$ tracer solutions were applied to reach a 50 % ^{15}N enrichment of the soil denitrifying pool and to induce an increase in soil moisture < 5%. The liners were subsequently flushed with a gas mixture containing 5% N_2, 20% O_2, 75% He and 0.11 ppm of N_2O, and left to incubate in freshly dug hole under environmental conditions. Gas sampling occurred at times 0, 2 and 4 hours where 15 mL of the liners headspace were sampled and replaced with 15 mL of the artificial gas mixture. Samples (~1 mL) were analysed over an Agilent 7890A gas chromatography for the determination of CO_2, CH_4 and N_2O concentrations. The remaining 14 mL were analysed over a continuous flow IRMS (Elementar Isoprime PrecisION;

Elementar Analysensysteme GmbH, Hanau, Germany) for isotopic analysis of N_2O and N_2. The exact protocols and calculations used for these analyses can be found in **Chapter 3.3**.

From the liners measurement, we can calculate two important denitrification parameters, the source partitioning coefficient (SPC) and the product ratio (PR) defined as:

$$SPC = \frac{f_{N2O\ denitrified}}{f_{N2O\ total}} \quad [57]$$

$$PR = \frac{f_{N2O\ denitrified}}{f_{N2O\ denitrified} + f_{N2\ denitrified}} = 1 - NOSE \quad [58]$$

Where ***f*** is a flux of nitrogen (either as N-N_2O or N-N_2; in kgN ha^{-1} $year^{-1}$) and NOSE is the nitrous oxide sink efficiency, thus a product ratio of 5% means that 95% of the denitrified N_2O emissions were successfully converted into N_2.

4.3.4) Static chambers for greenhouse gas measurement

Two weeks before the 2022 April campaign, nine collars (20 cm OD, 15 cm height) have been inserted 10 cm deep into the soil for installation of conventional static chambers (20 cm OD, 20 cm total height) in both **H** and **A** land uses. Concerning the CO_2 emissions, the developed chambers were opaque and thus, can only be used to measure soil respiration and not net emissions (which include CO_2 uptake through photosynthesis). Because of the distance between chambers and the fact that the liner incubation was running at the same time, the sampling of the static chambers headspace had to occur every hour for 2 hours (and more marginally every two hours for 4 hours). These time periods do not respect the criterion of chamber height to deployment time ratio ≥ 40

$cm.h^{-1}$ recommended by Zaman et al. (2021). The diffusion issues caused by these extended times were corrected using the HMR model (Pedersen et al., 2010), with the associated R script (R Core Team 2023) from CRAN (Comprehensive R Archive Network). As a performance indication, during the May campaign, 16 chambers out of 18 required diffusion correction; which resulted in 47 % higher N_2O fluxes on average. This is comparable to the values of 54 % and 52 % reported by Anthony et al. (1995) and Pedersen et al. (2010) respectively. GWP calculated over 100 years were used to express the fluxes of N_2O and CH_4 in $eqCO_2$ (298 and 25 respectively; IPCC, 2013).

4.3.5) Combining liner and chamber measurements to derive global denitrification fluxes

The magnitude of flux emitted by the soil cores is probably not representative of field rates, given the small height of the cores (10 cm). However, since most of the denitrification activity occurs in that zone (more generally in the tillage zone, Groffman et al., 2009; Well et al., 2019), we hypothesized that the dynamics of denitrification and in particular the SPC and PR coefficients measured through these cores were representative of field dynamics. We can thus derive more realistic fluxes as:

$$f_{N2O\ denitrified} = SPC \times f_{N2O\ chamber} \qquad [59]$$

$$f_{N2} = f_{N2O\ denitrified} \times \frac{(1-PR)}{PR} \qquad [60]$$

Where $f_{N2O\ chamber}$ is the flux of nitrogen derived from the static chamber measurements. SPC and PR were replaced with their average monthly values measured during each campaign. We determined the propagation of error on these two fluxes as:

$$SE\left[f_{N2O\ denitrified}\right] = \sqrt{(SPC \times SE[f_{N2O\ chamber}])^2 + (SE[SPC] \times f_{N2O\ chamber})^2} \quad [61]$$

$$SE[f_{N2}] = \sqrt{\left(SE\left[f_{N2O\ denitrified}\right] \times \frac{(1-PR)}{PR}\right)^2 + \left(SE[PR] \times \frac{f_{N2O\ denitrified}}{PR^2}\right)^2} \quad [62]$$

Where SE is the standard error. The fluxes derived from this approach are referred as "LC fluxes" (liner-chamber fluxes).

4.4) Statistics and calculations

For each land use, Pearson Correlation Coefficients (PCC) were calculated between the response variables (denitrification and greenhouse gas emissions) and the predictors (DOC, TDN, NH_4^+, NO_3^-, gravimetric moisture, mineralization potential) to assess their magnitude of dependence. The emissions of CO_2 were also used as predictor of the denitrification measures.

To assess the impact of land use on gas emissions, we had to assume that samples within the same field were independent. Although it is usually recommended to replicate fields rather than increasing the amounts of replicates within the same field, we concluded it would be more beneficial to thoroughly assess the denitrification dynamics of the same fields over time and using a large number of replicates; rather than sampling one time different fields at different times. This is especially relevant given the large spatial and temporal variabilities of denitrification. For the land use comparison, data were firstly log transformed and linear mixed models were used, with the unique combination of "Month" and "Land Use Type" as a random factor. The models were in the form of:

$$response\ variable \sim Field\ +\ (1|unique\ sample) \quad [63]$$

Models were validated by checking the normality and homoscedasticity of the residues. Type III ANOVA was used to compare the land use effect with the Satterthwaite method. All statistical analyses were performed using R (R Core Team 2023).

All results in this study are given ± standard error.

To characterize the temporal patterns of the study variables, we used linear interpolation between monthly means; when calculated, yearly fluxes were derived using the trapezoidal rule.

4.5) Results

4.5.1) Soil Properties

***Table 18**: Soil general properties of the three studied fields.*

Field	pH	Clay	Silt	Sand	OM	Total Carbon (%)	Total Nitrogen (%)	Total C:N ratio
H	7.95 ± 0.03	80.46 ± 0.58	10.41 ± 0.15	9.13 ± 0.43	8.97 ± 0.27	5.58 ± 0.10	0.32 ± 0.01	17.53 ± 0.55
GC	7.74 ± 0.06	78.82 ± 2.31	12.83 ± 1.48	8.35 ± 0.83	10.67 ± 0.43	6.40 ± 0.17	0.43 ± 0.01	14.89 ± 0.38
A	7.97 ± 0.03	81.75 ± 3.81	13.47 ± 2.73	4.78 ± 1.07	8.33 ± 0.08	5.42 ± 0.14	0.31 ± 0.01	17.67 ± 0.54

The OM increase observed in **H** compared to the **A** shows that the herbal ley was efficient at building organic matter (**Table 18**), with a mean increase of 7.7%. Other than that, the **H** and **A** land uses

were similar to each other (at the exception of higher sand content in **H**), which can be explained by the fact that they belong to the same field but only differ in their management. The levels of total C and total N of the three fields were stable over time and were thus averaged as a soil characteristic. All land uses were slightly alkaline and had a high content in clay. The total C:N ratio of the **GC** field was a bit lower than in the other land uses.

A principal component analysis (PCA) of the soil physical properties enabled to identify two principal components (PC1 and PC2) which together explained 70% of the total variance within the dataset (**Figure 36**). Nitrate and DOC levels correlated positively with PC1 while ammonium and available C:N ratio correlated negatively with it. On the other hand, nitrate and ammonium levels both correlated negatively with PC2 while DOC and available C:N ratio correlated positively with it. The different land uses were grouped and are represented by cluster centroids in **Figure 36** (using the average scores and standard errors on PC1 and PC2). From these results, we can see that three fields were relatively different. While **A** was mostly characterized by high nitrate levels, **GC** had higher ammonium levels and **H** more available carbon. The magnitude of total N_2O and denitrified N_2 fluxes (as per measured in the liners, see next section) were significantly correlated with PC1 (Pearson correlation $p < 0.05$), while the PR was significantly correlated with PC2 (Pearson correlation $p < 0.01$). This resulted in higher magnitudes of flux and higher product ratios being more associated with the **GC** and **A** fields.

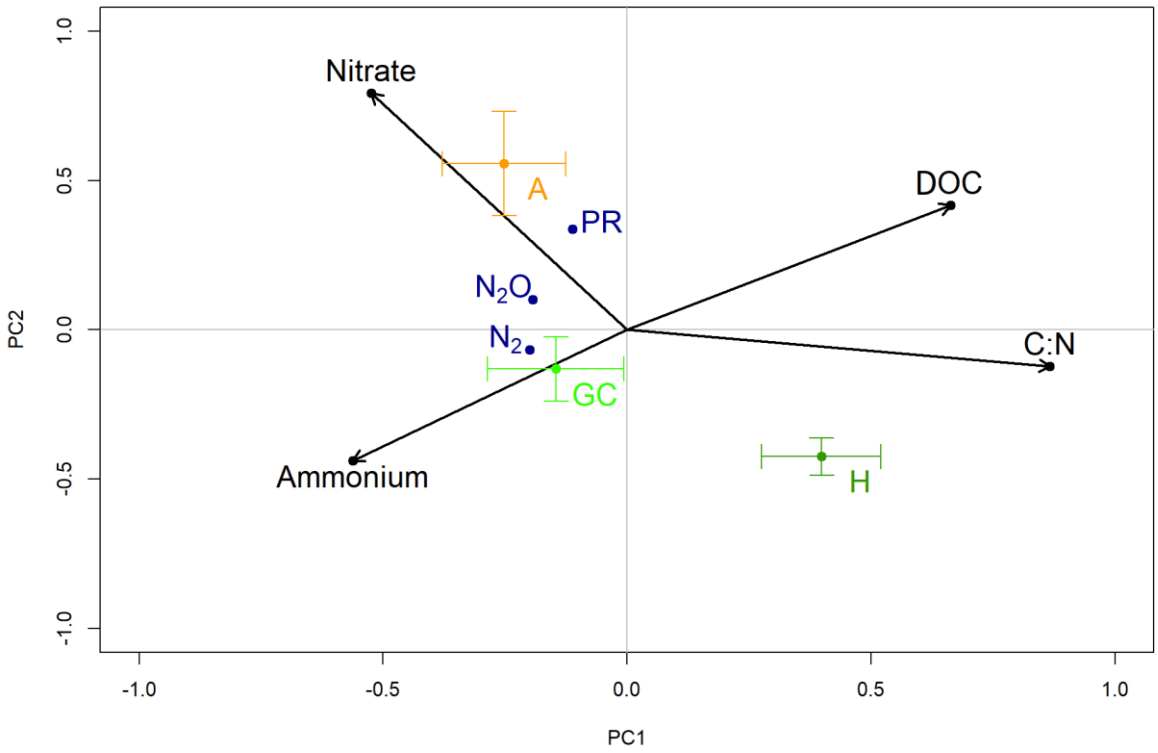

***Figure 36**: Correlation biplot from the PCA scores on soil physical properties.*

The land uses are represented by cluster centroids. Denitrification parameters (measured from the liner method) significantly correlated with PC1 or PC2 are also represented. "N_2O" as represented on the figure refers to total N_2O production and not denitrified N_2O.

4.5.2) *In situ* denitrification measurements from liners

Our newly developed method was successful at measuring denitrified N_2 emissions 90% of the time (208 measurements). In terms of temporal patterns, apart from peak events happening between the months of May and September, denitrified N_2O emissions (as per measured in the liners) were relatively steady and below 2 kgN ha^{-1} $year^{-1}$ (**Figure 37**). Both **GC** and **A** reached their peak of emissions in May, with **GC** emitting the maximum of all land uses and of all campaigns with about 14 kgN ha^{-1} $year^{-1}$ while **A** emitted 4 kgN ha^{-1} $year^{-1}$. The **H** field emitted its maximum in June with

about 5 kgN ha^{-1} $year^{-1}$. The N_2 emissions were characterized by many peak events between the months of April and August whilst being relatively low the rest of the time (< 20 kgN ha^{-1} $year^{-1}$). The **A** land use emitted the maximum of N_2 of all campaign with about 50 kgN ha^{-1} $year^{-1}$ during the month of May 2022. The SPC for all land uses were characterized by an almost Gaussian evolution between the months of March and September, with a little anomaly for **H** having a high coefficient in March (62%). A second peak event was observed for all land uses around the month of October. The denitrification product ratios were mostly under 15% for the **H** and **A** land uses, at the exception of the month of May where **A** had a PR of 32%. The **GC** field had relatively high product ratios every month (between 5 and 18%) with peak events in May and August where the product ratios reached 22 and 27% respectively.

In terms of land use effect, the three fields were found to be not significantly different from each other over time (linear mixed models, type III ANOVA $p > 0.05$) for every denitrification parameter (denitrified N_2O and N_2, SPC, PR). However, in terms of seasonal patterns, fertilization application during the month of May resulted in significantly different denitrified N_2O and N_2 emission rates (ANOVA; $F_{N2O}=3.97$, $F_{N2}=3.48$, $p < 0.05$) and denitrification product ratio (ANOVA; F=6.95, $p \ll 0.05$). The product ratios were also statistically different during the month of August 2022 (ANOVA; F= 7.78, $p \ll 0.05$), although this mostly comes from the **GC** field being very different from **H** and **A**.

In terms of annual fluxes (**Table 20**), the **H** and **A** fields were particularly similar in every parameter and interestingly, the mean annual product ratio was higher in **H.** The **GC** field on the other hand emitted much more N_2O (both total and denitrified) while emitting similar amounts of N_2; which resulted in a higher mean annual product ratio.

In terms of correlation, total and denitrified N_2O emissions were correlated with the nitrate content (PCC of 0.61 and 0.52 respectively) in the **A** field. This resulted in the product ratio being also correlated with the nitrate content (PCC of 0.58). The moisture was negatively correlated with the SPC coefficient (PCC of -0.70). In the **GC** field, total and denitrified N_2O emissions, as well as N_2 emissions were correlated with CO_2 fluxes (PCC of 0.65, 0.65 and 0.52 respectively).

Using data from all land uses together, the SPC and PR coefficients were not correlated with the ^{15}N enrichment of the soil denitrifying pool (PCC of 0.21 and 0.15 respectively, **Figure 38**).

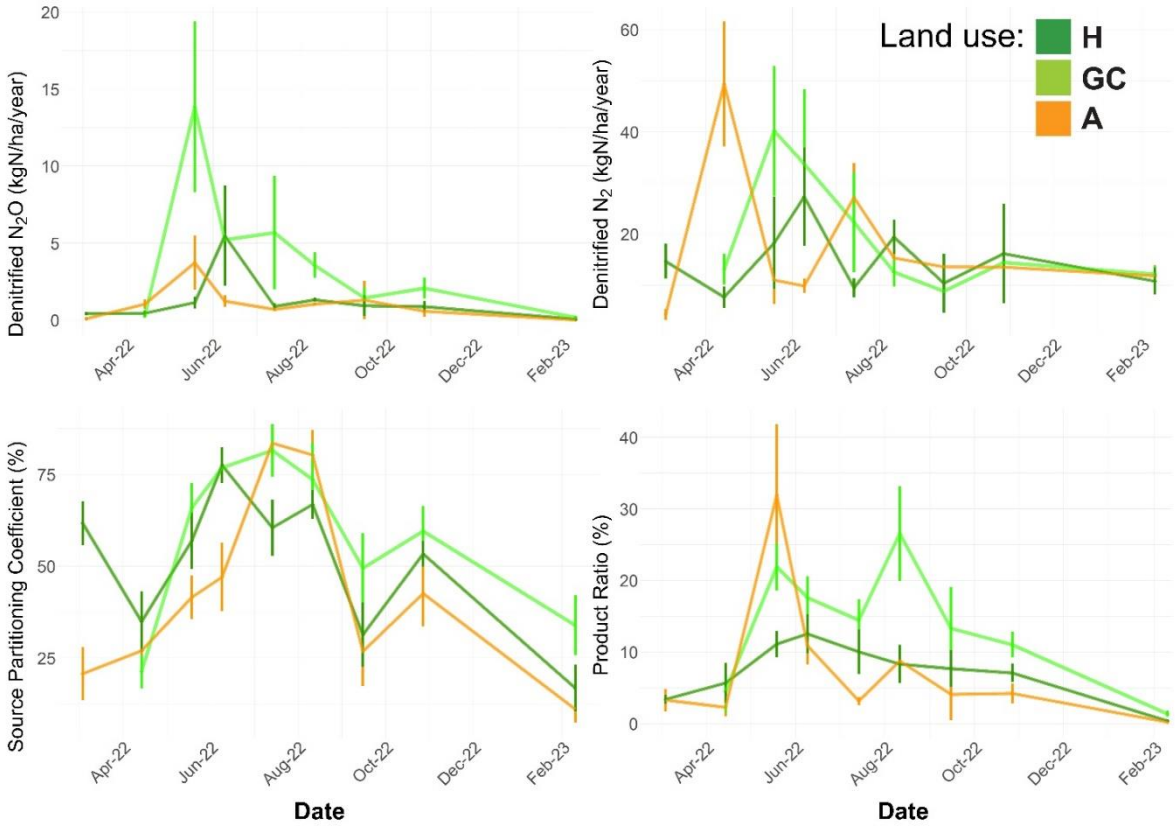

***Figure 37**: Temporal patterns of the denitrification parameters as per measured through the liner method.*

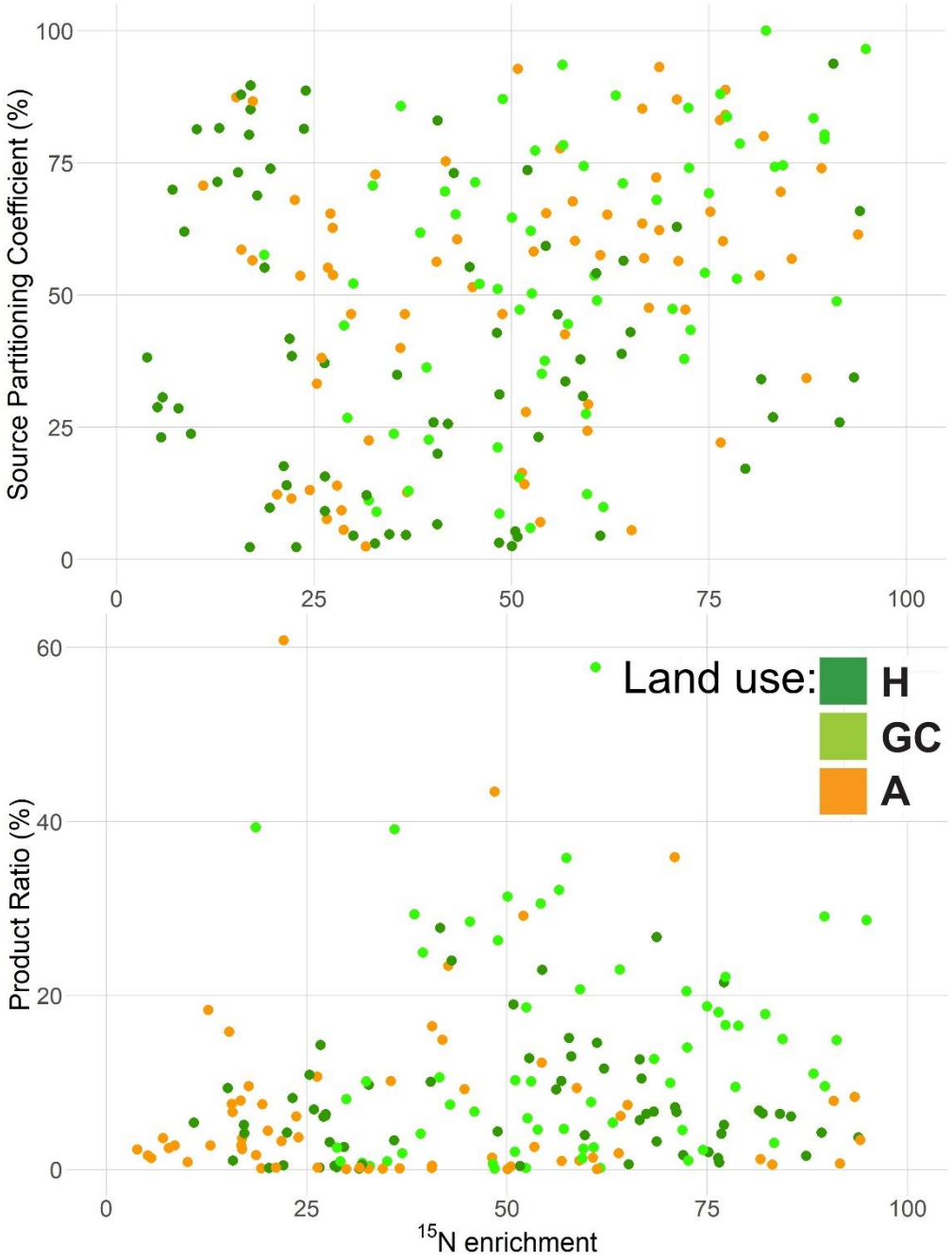

***Figure 38**: Scatter plot of the measured SPC (top) and PR (bottom) coefficients against the measured ^{15}N enrichment of the soil denitrifying pool during the field campaign.*

4.5.3) Greenhouse gases emissions

The emissions of CO_2 of both **H** and **A** decreased steadily from April to August 2022 before reaching a local maximum in September (**Figure 39**). From there, the emissions decreased again until February 2023; before rising again up to May 2023 when the field campaign ended. The **A** land use reached approximately the same levels of CO_2 emissions in May 2023 as it did in May 2022 with around 100 t $eqCO_2$ ha^{-1} $year^{-1}$. On the other hand, **H** had almost half the rate of CO_2 emissions in May 2023 compared to May 2022, with 60 and 120 t $eqCO_2$ ha^{-1} $year^{-1}$ respectively. The **H** land use consistently emitted more soil-respiration CO_2 than **A**, except in May 2023.

Both land uses were minor sinks of CH_4, **A** being slightly more efficient at taking up atmospheric CH_4 with a maximum of 150 kg eqCO2 ha^{-1} $year^{-1}$ in May 2023. The **H** field also had peak events of CH_4 consumption in May 2022 and May 2023 with uptakes of approximately 50 kg eqCO2 ha^{-1} $year^{-1}$.

The total emissions of N_2O measured through static chambers showed clear peak events for the **A** field in April and May 2022 with fluxes slightly above 10 t eqCO2 ha^{-1} $year^{-1}$. During the rest of the campaign, the emissions were pretty low at the exception of three small peak events (< 2 t $eqCO_2$ ha^{-1} $year^{-1}$) in November 2022, March and May 2023. It is worth noting that during the growing season of 2023 (March to May), N_2O fluxes were relatively low despite fertilizer application. In **H**, the emissions were consistently low (< 0.5 t $eqCO_2$ ha^{-1} $year^{-1}$) except in April 2022 where they reached 1.5 t $eqCO_2$ h^{-1} $year^{-1}$.

The fields were not statistically different in terms of emissions of greenhouse gases (mixed models, type III ANOVA $p > 0.05$) although the emissions of N_2O were significantly different during the growing season (April to June) of 2022 (mixed models, type III ANOVA $p < 0.05$).

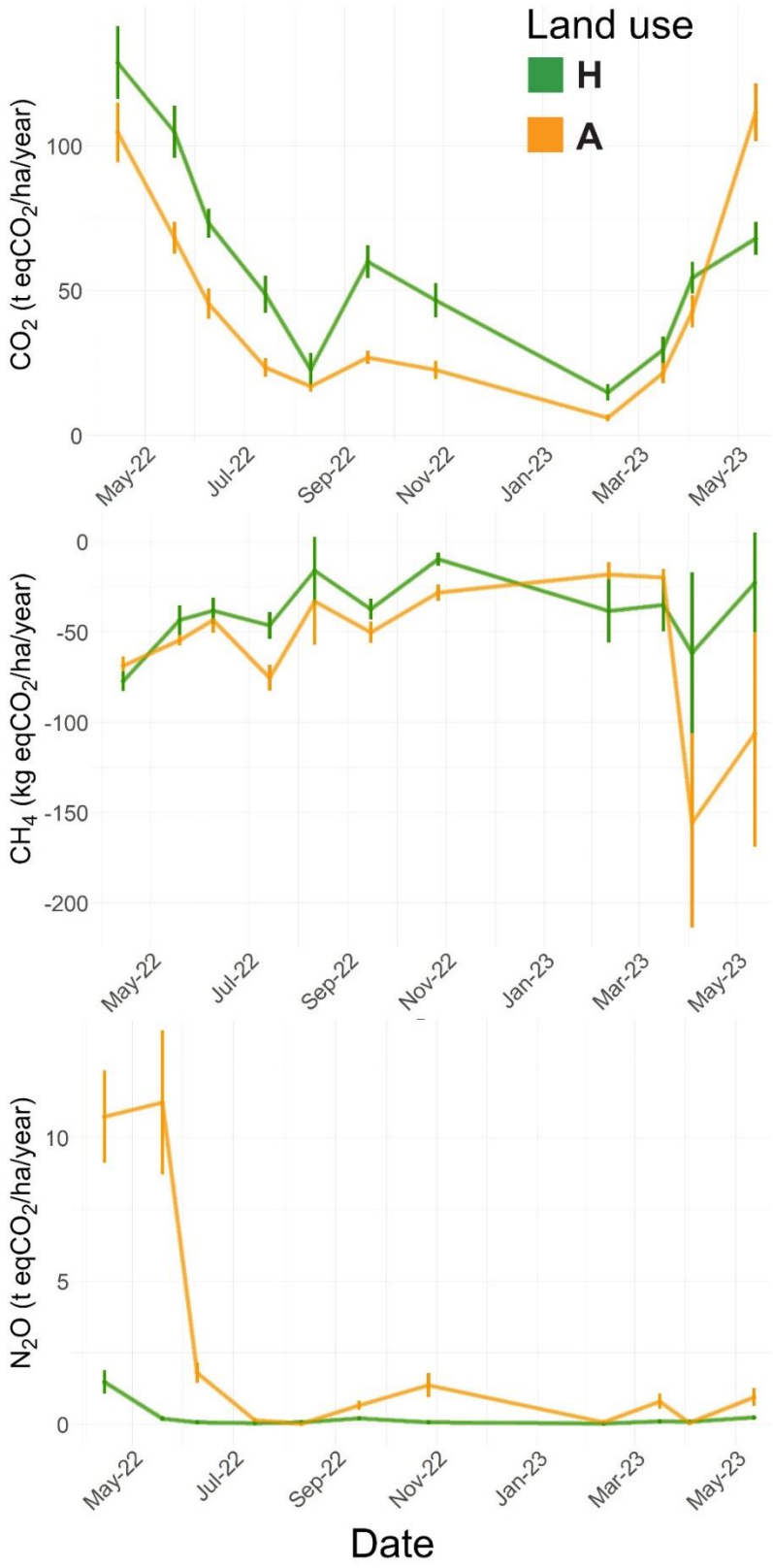

***Figure 39**: Temporal evolution of the greenhouse gas emissions in the H and A fields, as per measured through conventional static chambers.*

In the **A** land use, the flux of total N_2O measured through static chambers was correlated with the nitrate content (PCC of 0.52). In terms of 2022 annual emissions (**Table 19**), the **A** field was responsible for the emissions of almost 2 t $eqCO_2$ h^{-1} $year^{-1}$ compared to **H**, which represents 12.63 times more global warming potential. Around 70% of the N_2O emissions in **A** (~1.4 t $eqCO_2$ h^{-1} $year^{-1}$) occurred from April to May. As mentioned above, the same pattern is not observed in 2023, for which we have unfortunately limited data. Nonetheless, we can estimate that the 2023 GWP of the period from April to May was 22 fold inferior to that of the year 2022.

Finally, the magnitude of methane removal of the two fields were comparable while **H** emitted 68% more respiration-CO_2 than **A**.

***Table 19**: Annual 2022 emissions of greenhouse gases in the H and A fields.*

	CO_2 ($keqCO_2$ ha^{-1} $year^{-1}$)	CH_4 ($kgeqCO_2$ ha^{-1} $year^{-1}$)	N_2O ($kgeqCO2$ ha^{-1} $year^{-1}$)
H	49 384 ± 5661	-34.08 ± 11.41	155.65 ± 51.08
A	29 420 ± 3387	-42.58 ± 9.22	1959.68 ± 440.73

4.5.4) Combining liner and chamber measurements to derive annual denitrification fluxes

The fluxes of CO_2 from liners were on average (7.71 ± 1.14) and (6.00 ± 0.69) times lower than the ones derived from static chambers for the **A** and **H** fields respectively; liners fluxes were thus re-scaled on **Figure 40** using these coefficients to enable pattern comparison. The fluxes of CO_2 measured via either liners or chambers generally followed the same patterns, at the exception of the month of April for both **H** and **A** fields. Although no chamber measurement was performed in March 2022, the liners levels (after upscaling) during that month were similar to the March 2023

chamber levels. The fluxes of total N_2O from liners however did not need re-scaling to be compared with the fluxes derived from chambers. In the **A** land use, fluxes from liners and chambers were similar at the exception of the fertilization period (April to May 2022). In **H** however, the fluxes derived from liners were largely higher than the ones derived from chambers, at the exception of the month of April. A large peak of total N_2O emissions (~5 kgN ha^{-1} $year^{-1}$) during the month of June was notably observed in liners but not in chambers. These results show that a coefficient of proportionality cannot be applied to the liner denitrification measurements to upscale them.

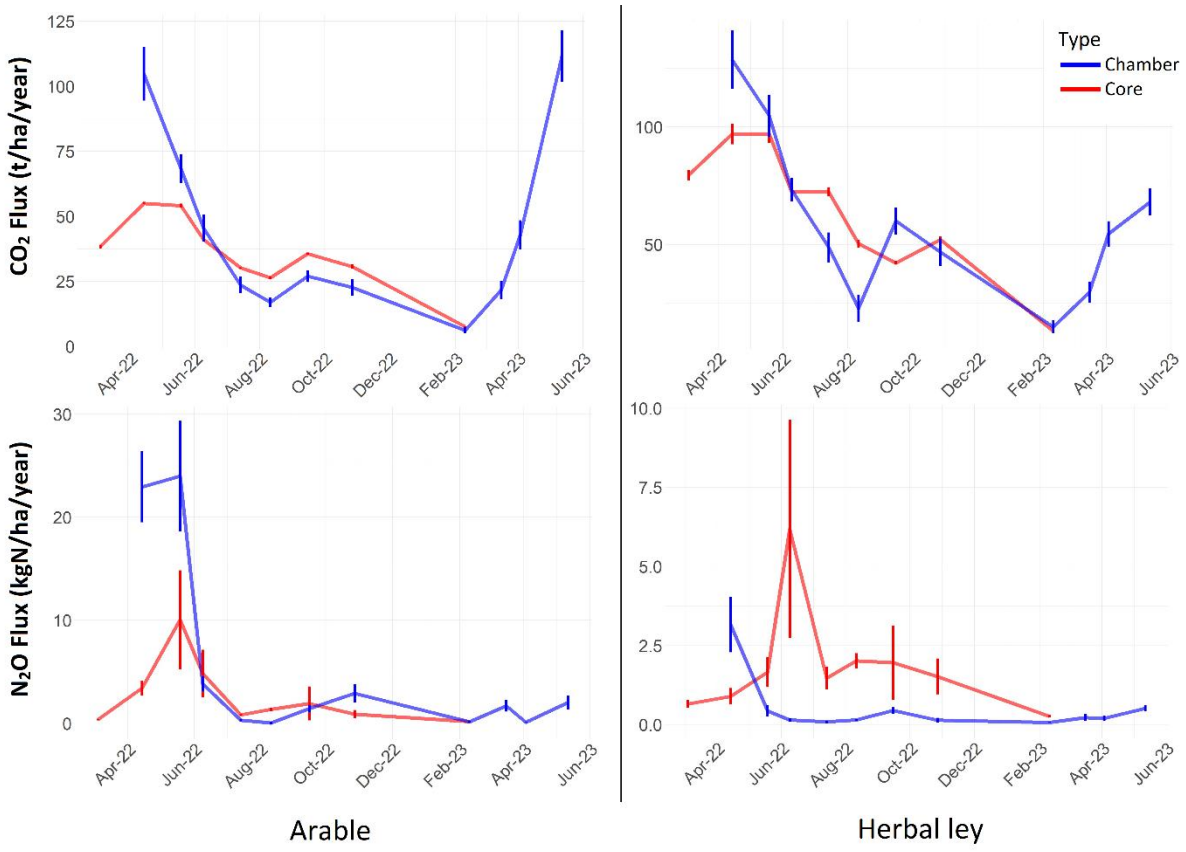

***Figure 40**: Comparison of the CO_2 and total N_2O fluxes between the liner and chamber methods in the A and H fields.*

The fluxes of CO_2 were multiplied by coefficients of proportionality (7.71 and 6.00 for the **A** and **H** fields respectively) to upscale and enable comparison between chambers and liners.

Combining liner and chamber measurements (LC approach) enables us to derive new fluxes of denitrification as per **equations [59]** and **[60]**. To derive these fluxes, we focused on the period from April 2022 to April 2023 (**Figure 41**). The SPC and PR coefficients of March and April 2022 were used with chamber fluxes of March and April 2023 respectively, to derive an annual budget. Comparing the liner and LC fluxes give significantly different results for the **H** field; while these results are moderately different for the **A** field (**Table 20**). For example, in the case of the total loss of nitrogen through denitrification, the liner results were 6 times higher in the case of the **H** field, whilst being only 0.8 times lower for the **A** field. It is worth noting that if the April chamber fluxes of 2023 were as high as in 2022 in the **A** field, it would have led to the emission of another 2.32 kgN ha^{-1}.

***Table 20**: Mean annual denitrification measurements (liner and LC approaches).*

The mean SPC coefficient was calculated by dividing the annual denitrified N_2O emissions by the annual total N_2O emissions. The mean PR was calculated by dividing the annual denitrified N_2O emissions by the annual total denitrification emissions.

Type	Field	Total N_2O (kgN ha^{-1} $year^{-1}$)	Denitrified N_2O (kgN ha^{-1} $year^{-1}$)	Denitrified N_2 (kgN ha^{-1} $year^{-1}$)	Total denitrification (kgN ha^{-1} $year^{-1}$)	Mean source partitioning coefficient (%)	Mean product ratio (%)
Liners	H	1.61 ± 0.63	1.07 ± 0.48	14.35 ± 2.65	15.42 ± 3.13	66.46	6.94
	GC	4.17 ± 1.45	2.91 ± 0.22	17.15 ± 1.01	20.06 ± 1.23	69.78	14.51
	A	2.13 ± 0.90	0.91 ± 0.08	17.06 ± 0.76	17.97 ± 0.84	44.72	5.06
Liners & Chambers	H	0.34 ± 0.12	0.14 ± 0.05	2.27 ± 1.15	2.61 ± 1.20	41.18	5.81
	A	4.21 ± 1.02	1.56 ± 0.43	20.56 ± 11.20	22.12 ± 11.63	37.05	7.05

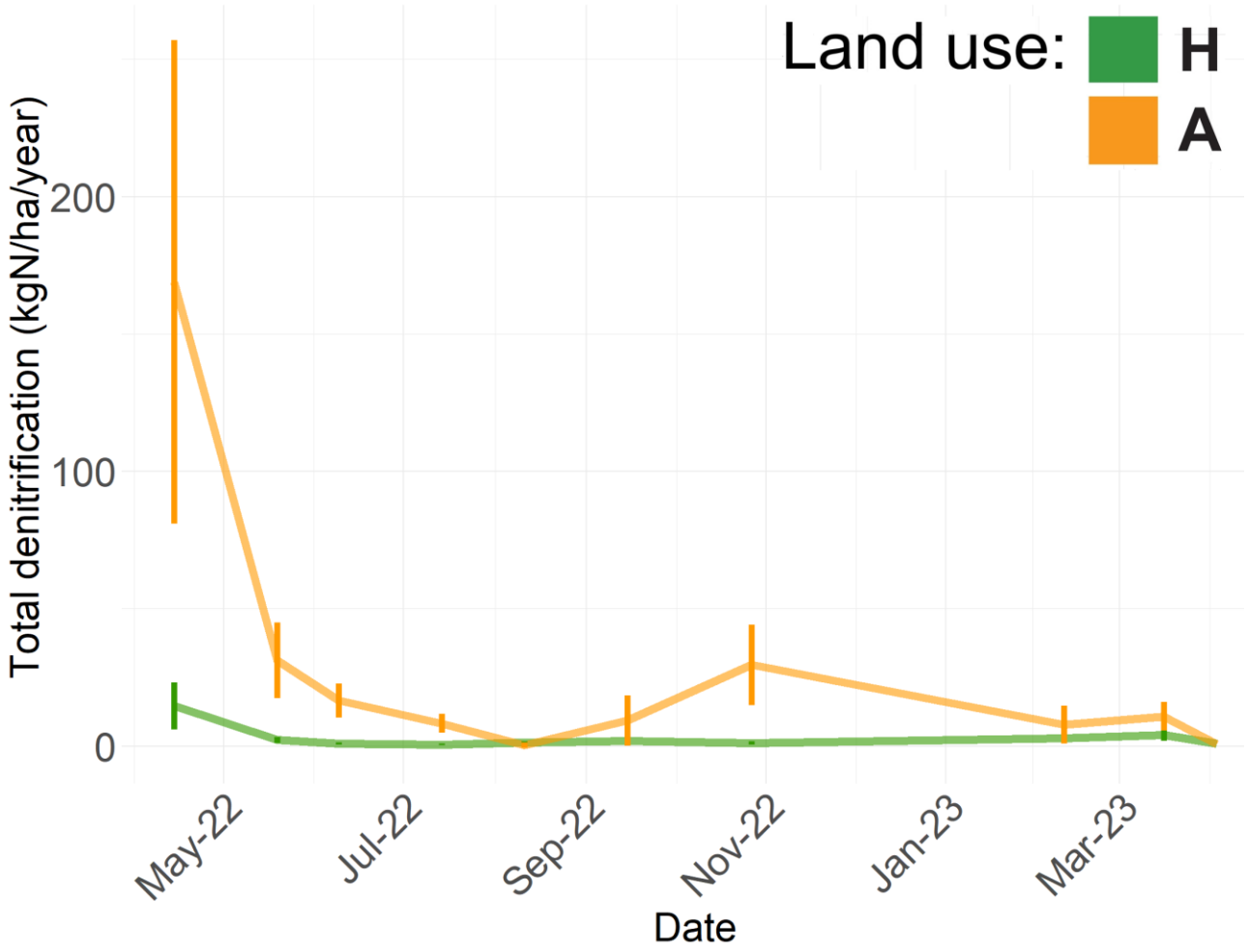

***Figure 41**: Total denitrification activity (N_2O + N_2) in the H and A fields throughout the field campaign as measured using the LC approach.*

4.5.5) Nitrate and ammonium contents

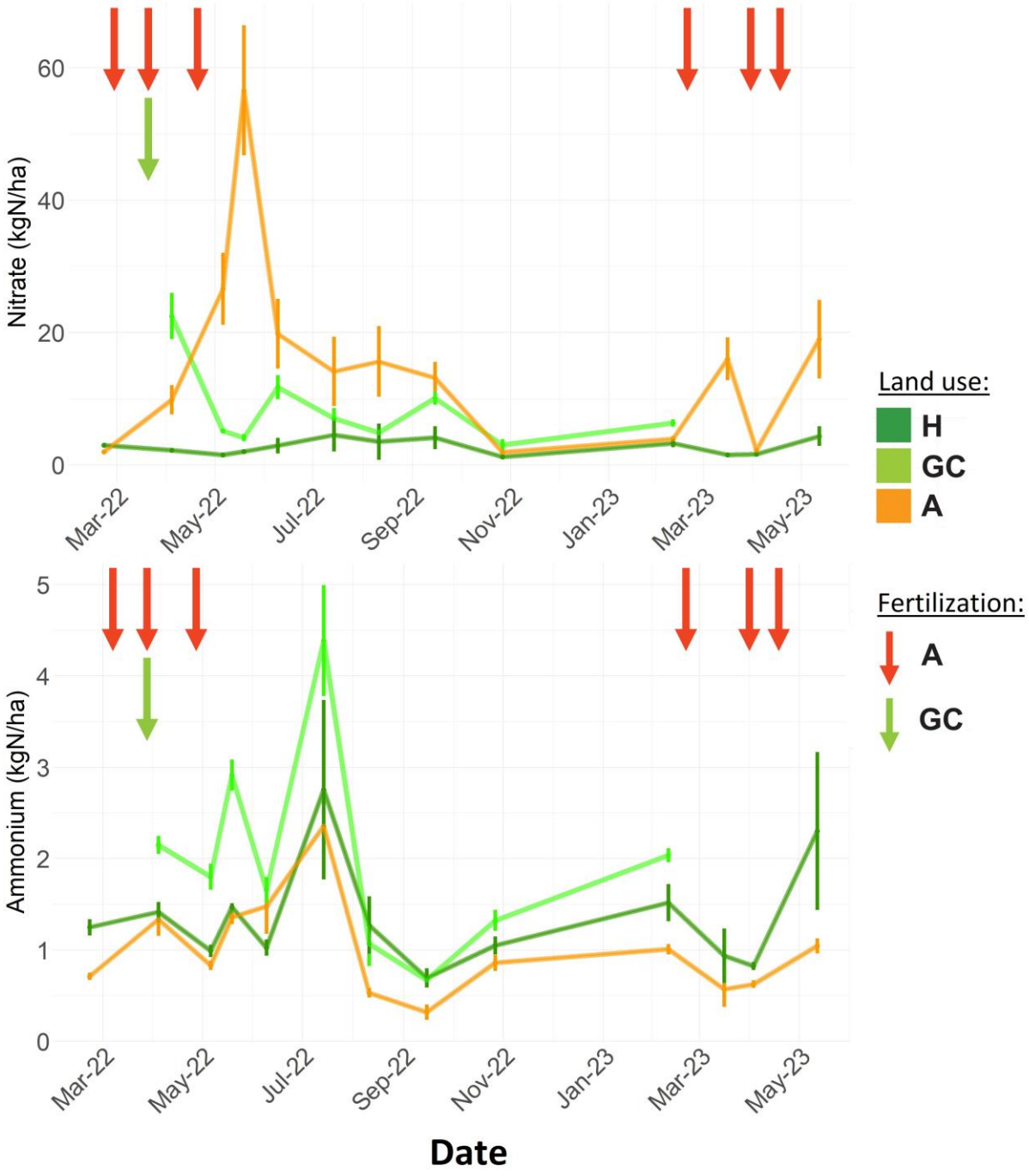

***Figure 42**: Temporal evolution of the nitrate and ammonium levels in the three land uses.*

The ammonium content of the three land uses stayed relatively constant (mainly below 3 kgN ha^{-1}) at the exception of the month of August 2022, where each land use reached its peak of ammonium concentration (**Figure 42**). On average, **GC** had the highest levels ammonium and **A** the lowest ones. Application of fertilizer in these two land uses did not result in an increase of observed soil ammonium concentration.

On the other hand, fertilizer application in 2022 resulted in a clear increase of the observed nitrate concentration, at least in the **A** field. Indeed, the application in **GC** this year happened before our first measurement there and it is thus difficult to conclude that the April 2022 measurement is a peak event. However, the levels of (22.5 ± 3.5) kgN ha^{-1} recorded that month seem to be indeed the result of fertilizer application (~10 kgN ha^{-1} of $N\text{-}NO_3$). In the **A** field, three applications of fertilizer in 2022 (~30 kgN ha^{-1} of $N\text{-}NO_3$ in total) resulted in very high levels of nitrate, with (56.8 ± 9.8) kgN ha^{-1} recorded during the month of May. Nitrate derived from fertilizer persisted until October (**Figure 42**), at which point the nitrate levels reached their pre-fertilization levels (~2 kgN ha^{-1}). Interestingly, the 2023 applications of fertilizer did not result in a build-up of the nitrate pool. The fertilizer applied in March 2023 (nitrate levels of 16.0 ± 3.2 kgN ha^{-1}) was not found in April 2023 (2.2 ± 0.20 kgN ha^{-1}). The last application in May 2023 resulted in increased levels again, with (19.0 ± 3.3) kgN ha^{-1}. The **H** land use had consistently the lowest amounts of available nitrate (< 5 kgN ha^{-1}), despite a moderate increase in July to September 2022 probably due to biological inputs (grazing). Finally, despite low fertilizer input, **GC** maintained relatively high levels of nitrate, with two local maximums during the months of June and September 2022 with levels of (11.7 ± 1.8) kgN ha^{-1} and (10.1 ± 1.0) kgN ha^{-1} respectively.

4.5.6) Moisture

Moisture followed the same pattern for all three land uses, with the highest levels of March 2022 (~30%) consistently dropping down to August 2022 (~10%) at the exception of the campaign of June 2022 which saw a local maximum peak (25 to 30%) due to extremely wet conditions (**Figure 43**). From there, the moisture levels rose again up to the end of October 2022, where the levels stabilized until the end of the campaign in May 2023. Overall, **GC** had the highest levels of moisture (especially in June and October 2022 as well as February 2023) while **A** was consistently the driest field.

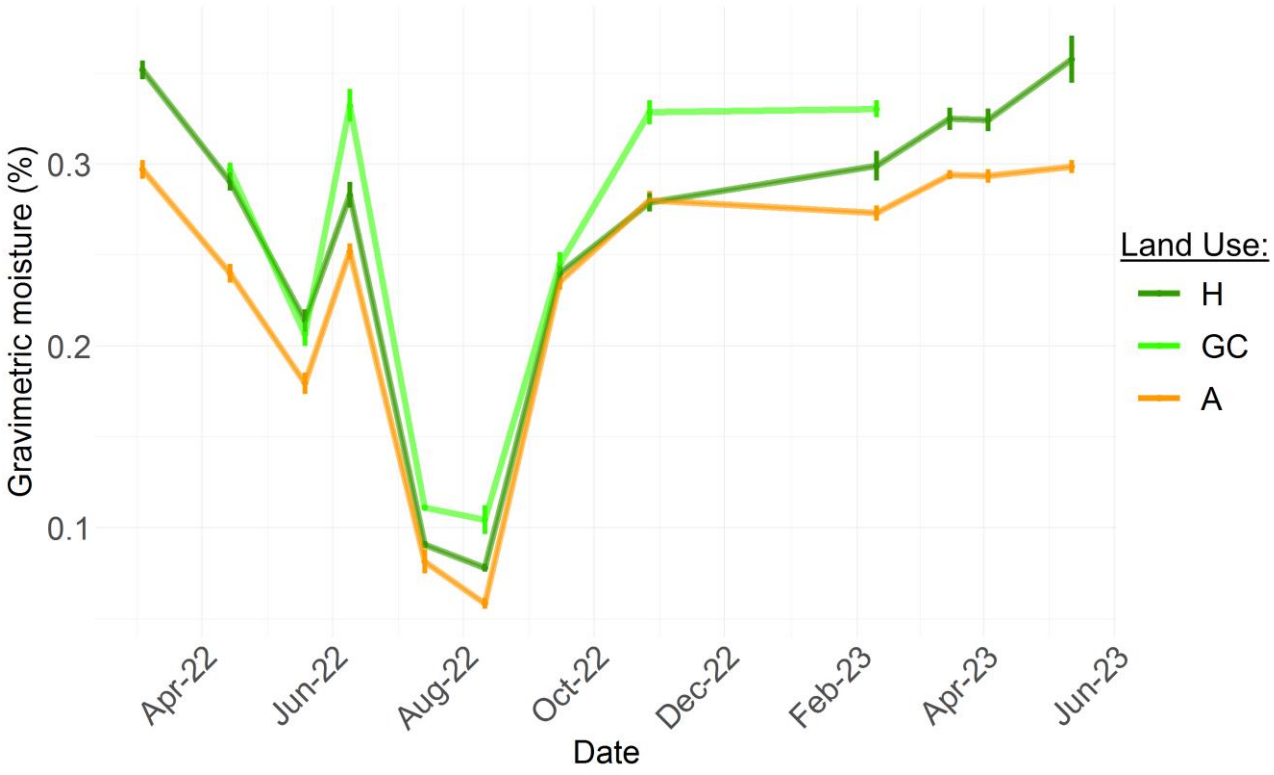

***Figure 43**: Temporal evolution of the moisture levels in the three land uses.*

4.5.7) DOC and TDN:

The levels of TDN followed closely the levels of nitrate, especially for the **A** land use and its distinct pattern after fertilization events (i.e. large peak after application in 2022 and moderate increases in 2023). On average, **H** still had the lowest levels of TDN and **GC** maintained intermediate levels with a peak in April 2022, following fertilizer inputs (**Figure 44**). All three land uses had a small local peak event in August 2022, which can be correlated to the one observed for the ammonium levels at the same period. The TDN levels in the **A** field followed very closely the nitrate levels (PCC of 0.96), highlighting the high proportion of fertilizer in the available nitrogen pool. If we define inorganic nitrogen as the sum of nitrate and ammonium (nitrite levels being usually very low in soil), inorganic N represented only 32% of the **A** TDN pool in March 2022. From April to October that year, this proportion was on average 87%.

The DOC levels were also characterized by a large peak event in August 2022 for all land uses (**Figure 44**). Otherwise, the levels were quite steady (between 25 to 50 kgC ha^{-1}) at the exception of local peak events in March 2022 and April 2023. On average, the two leys had higher levels of DOC than the arable control.

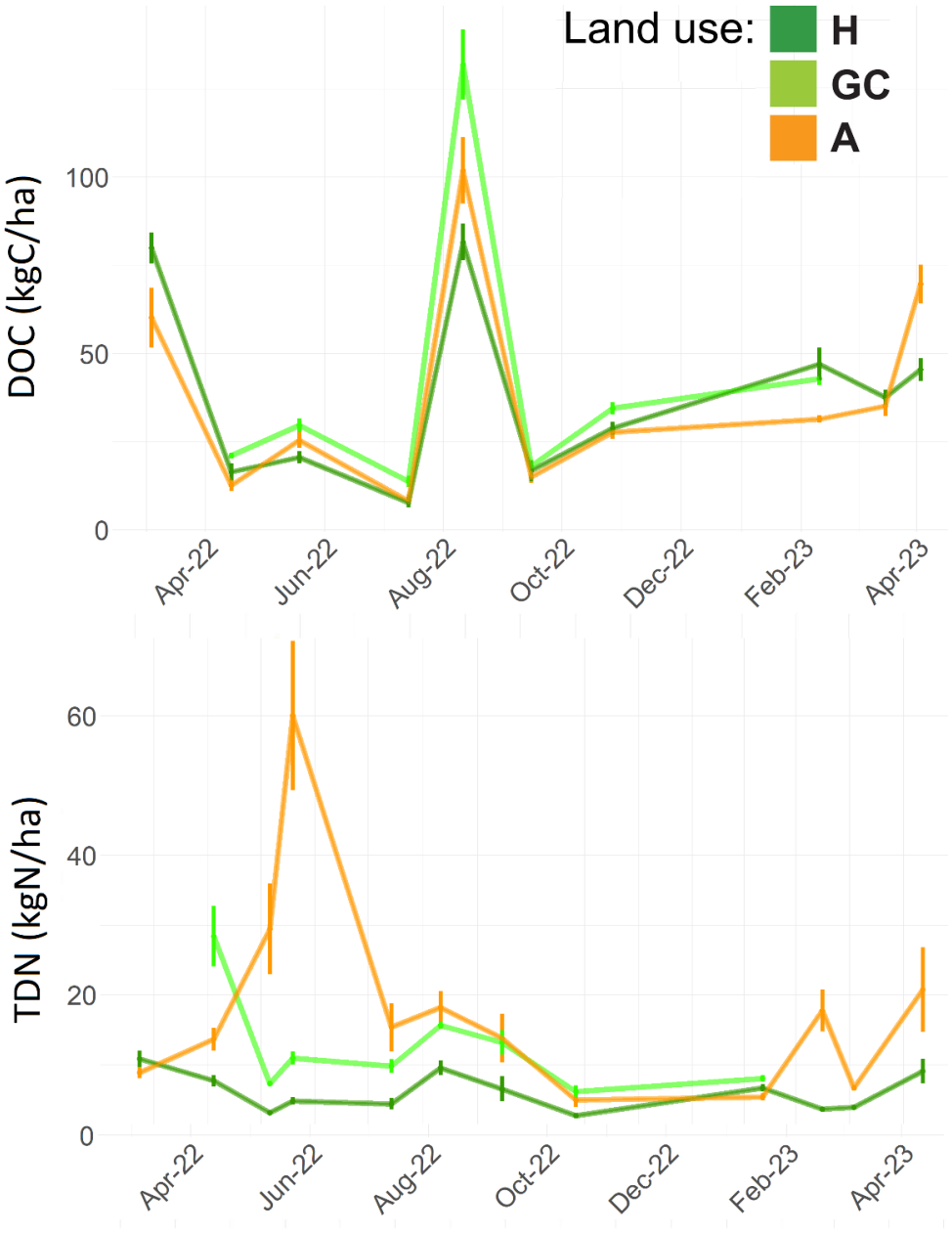

***Figure 44**: Temporal variations of the DOC and TDN levels in the three land uses.*

4.5.8) Mineralization potentials

Ammonification rates exhibited an almost Gaussian evolution for all three land uses between May and August 2022; the peak of activity being reached in early June with values between 30 kgN ha^{-1} $year^{-1}$ for **A** and 63 kgN ha^{-1} $year^{-1}$ for **H** (**Figure 45**). The Gaussian peaks were responsible for the

production of (5.51 ± 3.02) kgN ha^{-1} for **H**, (5.28 ± 1.40) for **GC** and (2.80 ± 0.75) for **A**. This episode represents the majority of the annual production of ammonium (**Table 21**), although these numbers must be considered with care as they were determined under laboratory conditions. In the **GC** field, the relatively large episode of ammonium consumption of April 2022 explains why the annual value is smaller than the production during peak activity. The rest of the time, ammonification was quite steady and close zero, with small episodic events of consumption for all land uses. On average, the two leys had higher ammonification potentials, with **H** having the highest one.

The nitrification potentials of the studied land uses were very variable (**Figure 45**). The two leys were relatively similar and had levels of nitrate production mostly below 50 kgN ha^{-1} $year^{-1}$. The main differences between these two fields were a large production peak in April 2022 (150 kgN ha^{-1} $year^{-1}$) and episodes of consumption in the **GC**; which were not observed in **H**. On the other hand, **A** exhibited very variables patterns, with episodes of consumption and production alike. The growing period in 2022 was characterized by large consumption events (up to 140 kgN ha^{-1} $year^{-1}$) while the one in 2023 was characterized by large production events (up to 161 kgN ha^{-1} $year^{-1}$).

The magnitude of nitrate transformation being much higher than the one of ammonium for all land uses, net mineralization (nitrification + ammonification) was very similar to nitrification (**Figure 45**).

Table 21*: Annual ammonium, nitrate and mineral N (ammonium + nitrate) production via mineralization of organic matter, determined under laboratory conditions.*

	Net Ammonification (kgN ha^{-1})	**Net Nitrification (kgN ha^{-1})**	**Net mineralization (kgN ha^{-1})**
H	6.37 ± 4.66	16.47 ± 13.97	20.47 ± 14.93
GC	4.86 ± 2.10	17.55 ± 7.67	22.71 ± 7.42
A	3.12 ± 1.14	5.62 ± 19.17	8.75 ± 19.50

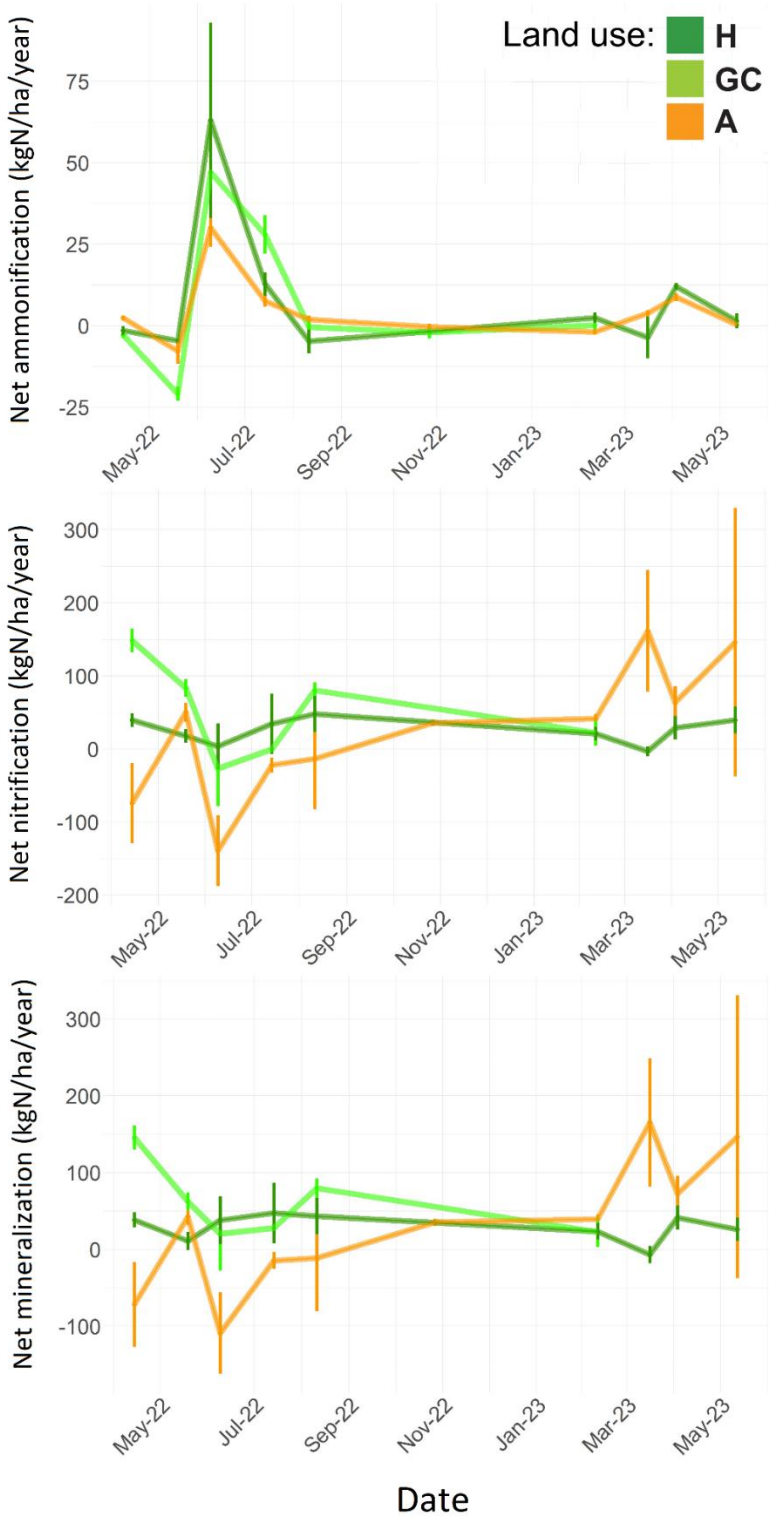

***Figure 45**: Temporal patterns of ammonification (top), nitrification (middle) and total mineralization (bottom) determined under laboratory conditions.*

4.6) Discussion

4.6.1) Validation of the new denitrification measurement method

Our newly developed liner method was characterized by a high success rate of N_2 flux detection (90%). Data gaps in denitrification dataset is very frequent due to the very high sensitivity required to discriminate soil-N_2 fluxes (Buchen et al., 2016; Kulkarni et al., 2014; Mulvaney & Kurtz, 1984). Although no existing number on the proportion of dataset gaps could be found, a 90% success rate is considered very high for denitrification.

The fluxes of CO_2 and total N_2O from soil cores are important tracers that can help upscale the results of our new method of denitrification measurement. In particular, CO_2 emissions are known to be consistent and usually proportional to the amount of soil incubated (Cueva et al., 2019). Here we got consistent coefficients of proportionality from liners to chambers, with 7.71 and 6.00 for the **A** and **H** land uses respectively. Once we account for these coefficients, the emission patterns from the liners are relatively similar to the chamber ones (**Figure 40**). N_2O emissions on the other hand are usually more variable and noisy (Machado et al., 2021; Waldo et al., 2019). Here, multiplying the fluxes of total N_2O from the cores by the inferred coefficients of proportionality would result in a high overestimation since these fluxes are already comparable to chamber fluxes, if not greater (**Figure 40**). There is thus a high chance that the denitrified N_2 and N_2O emissions would be overestimated using this approach. The high magnitude of N_2O emissions from cores (relatively to chamber fluxes) compared to the CO_2 emissions could be explained by a stimulation and disruption effects due to tracer injection (Dodds et al., 2017; Lewicka-Szczebak & Well, 2020; Warner et al., 2019). This is particularly visible in April and May 2022 in the **A** field, where fluxes from liners were significantly lower than chamber measurements. At this period, the nitrate concentration was at its

highest levels following fertilizer application (**Figure 42**) and thus the injection of tracer would only cause moderate impact. One of the key questions raised in **Chapter 3** was the possible influence of nitrate addition on the denitrification dynamics. In particular, a significant correlation between nitrate addition and PR was observed in laboratory but not necessarily in the field. Here, over 208 field measurements spread over a year, neither the product ratio nor the source partitioning coefficient were correlated with the ^{15}N enrichment of the soil nitrate pool; which in turn is directly correlated to the addition of nitrate (**Figure 38**). Furthermore, the SPC coefficients exhibited clear temporal patterns and the calculated PR were within in the expected range (see next section). We can thus consider these two metrics as independent of flux magnitude and use them for the upscaling of denitrification measurements with more confidence than the coefficient of proportionality from liners to chambers. The LC fluxes resulted in much different quantities of annually denitrified nitrogen for the **H** field but not necessarily for the **A** field. This upscaling is however much more plausible, since the resulting difference between the two fields is now around 20 kgN ha^{-1}, which is in the order of magnitude of the applied fertilizer and nitrate levels observed in the **A** field. The estimation of 15.42 kgN ha^{-1} from liner measurements in the **H** field does not really match the observed trends in nitrate levels in that field, while the LC flux estimation of 2.61 kgN ha^{-1} does. The mean annual SPC varied quite a lot between the two methods, especially for the **H** field which went from 66.46% for liner measurements to 42.18% using the LC approach. This can be explained by the fact that monthly SPC are pondered by the magnitude of flux for each month, which again varied significantly between liners and chambers. However, gas fluxes derived from static chambers are much more representative of the real dynamics of gas emissions, since they don't require soil disturbance and they capture the entirety of soil emissions. The mean annual PR

are also pondered by monthly fluxes but this resulted in much lower variations; although with the LC approach, the **H** field has now a lower PR than **A**.

Overall the combination of liners and chamber measurements is a similar method to the recent approaches of Wang et al. (2020) or Bizimana et al. (2022) who applied laboratory derived product ratios to field chamber measurements. In our case however, the product ratio is determined under *in situ* conditions and is thus probably more accurate.

To enhance our current denitrification measurement method, we suggest exploring the following leads:

(i) Applying the ^{15}N tracer at the same time as the sampling of soil cores (i.e. 24 hours before incubation). This will allow for the tracer to diffuse in soil and avoid potential stimulation artefacts. Although we did not see correlation of the PR and the SPC coefficients with the amendment of tracer, the magnitude of flux seemed to have been stimulated under field conditions. In our case, the measurements were made after tracer injection to ensure sensitivity and because samplings at times 0 already shown enrichment in the ^{15}N signature of N_2O, indicating the start of tracer denitrification. However, our high success rate during this one-year field campaign shows that sensitivity is no longer an important issue with our new method.

(ii) Using longer liners which will enable to sample the full soil A horizon and leave a bigger headspace, where gas sampling will be less disruptive.

(iii) Coupling the liner methods with automated chamber and continuous analyser, while analysing diurnal/nocturnal patterns of denitrification for better assessment of global budgets.

4.6.2) Denitrification emissions

4.6.2.1) Patterns of denitrification (liner method)

The denitrification patterns (as per measured in the liners) did not differ significantly between the three studied fields, although a seasonal pattern could be identified in May 2022 due to high product ratios in the **A** and **GC** land uses (32 and 22% respectively) following fertilization. In the **A** land use, the highest product ratio of 32% coincided with the highest levels of nitrate (~55kgN/ha, **Figure 42**), which seems to confirm that high amendments of nitrate stimulate the denitrification product ratio. Outside of the fertilization period, the proximity and similarity of the fields can explain why overall similar patterns are found. Typically, the **H** and **A** land uses belong to the same field but only differ in their management. The **GC** field was a high source of N_2O (total and denitrified) whilst emitting similar amounts of N_2 as the **H** and **A** fields. This resulted in a higher mean annual product ratio (~14.5%) in **GC**, indicating denitrification was a less efficient nitrous oxide sink in this land use.

In a recent meta-analysis, Scheer et al. (2020) reported a mean denitrification product ratio of (12.40 ± 3.1) % for soils under natural vegetation and (10.90 ± 2.0) % for agricultural soils. The annual mean product ratios for the **H** and **A** land uses were slightly under these values (whether derived from liners or LC measurements, **Table 20**). This can probably be explained by temporal patterns that are rarely included in studies, in particular under *in situ* conditions. Indeed, in a meta-analysis compiling 236 studies, it was found that 74% of the reported fluxes were measured instantaneously rather than over a time period (Almaraz et al., 2020). In the present study, the winter period (February 2023) was characterized by very low product ratios (0.39%, 1.37% and 0.22% for the **H**, **GC** and **A** land uses respectively), which resulted in lower annual values. Finally, the **GC** field fell within the upper range of the ratio for soil under natural vegetation, which can be explained by the high density

of clovers and fertilizer application (**GC** is more typical of a semi-improved grassland than a proper soil under natural vegetation).

In terms of source partitioning coefficient, the results revealed the presence of a Gaussian evolution in all three land uses between the months of March and September, which indicate a domination of denitrification in the N_2O emissions in the summer. Although many evidences exist that the highest rates of denitrification generally occur between spring and summer (Smith et al., 2015), this to our knowledge, the first time this Gaussian evolution of the SPC is reported.

4.6.2.2) Annual field budgets of denitrification (liner-chamber method)

As mentioned previously, the magnitude of gas emissions in the liners was not representative of field dynamics and chamber measurements are needed to upscale these fluxes. This means that global rates can only be derived for the **H** and **A** fields.

Using the LC approach reveals that the **A** field was actually a much bigger source of denitrified N_2O and N_2 than the **H** field (**Table 20**). In the first one, denitrification was responsible for the yearly loss of (22.12 ± 11.63) kgN ha^{-1}, with fluxes as high as (169 ± 87) kgN ha^{-1} $year^{-1}$ during the month of April 2022. In the second one, only to (2.61 ± 1.20) kgN ha^{-1} were emitted through denitrification annually, with fluxes as high as (14.56 ± 1.34) kgN ha^{-1} $year^{-1}$ also in April 2022. Considering the consistently higher magnitude of flux and superior product ratios observed in the **GC** field through the liner approach (**Figure 37** and PCA, **Figure 36**), it is highly likely that the global denitrification losses in the **GC** field were greater than those in **H**, possibly including a higher proportion of N_2O.

In the **A** field, the fertilizer applied in 2022 remained in the soil from April to October (as shown by the nitrate levels in **Figure 42**). The cumulative results of total denitrification over this period (**Figure 41**) show that 15.17 kgN ha^{-1} were lost through denitrification, from which 1.34 kgN ha^{-1} (8.83 %)

were emitted as N_2O rather than N_2. These denitrification losses represent 8 % of the applied fertilizer. Another significant loss of N through denitrification occurred during the second growing season (from September to November 2022) although no fertilizer was applied this time. Around 5.40 kgN ha^{-1} were lost during that period, including 0.40 kgN ha^{-1} of N_2O (4.19%; although these measurements could be underestimated due to the lack of measurements between the end of October and early February). These results confirm once again that excessive amounts of nitrate stimulate the product ratio.

In a meta-analysis compiling 336 denitrification measurements (using chambers, cores or N balance techniques), denitrification annual budgets of agricultural soils were mostly found to be in the range of 20 to 30 kgN ha^{-1} $year^{-1}$ (Hofstra & Bouwman, 2005). The results of the **A** field in the present study (22.16 kgN ha^{-1} $year^{-1}$) is thus in good adequacy with this range. More recently, Soana et al. (2022) found a 80 kgN ha^{-1} $year^{-1}$ difference between inputs and outputs of nitrogen in an agricultural study, which was attributed to denitrification. Although it is difficult to compare results from one field to another, the total input of nitrogen in their case was the same as in the **A** field (~200 kg ha^{-1}); and a more modest contribution of denitrification was found in our case. Nonetheless, our value might be underestimated due to low resolution in spring 2022 where a peak of denitrification activity was observed.

Finally, according to (Lassaletta et al., 2014), half of all applied nitrogen fertilizer is lost to the environment. There are several ways nitrogen can escape soil (volatilization of ammonia, surface runoff following rain events or it can leach into the groundwater) and results of this study show that denitrification can represent 16% of the loss of fertilizer.

4.6.3) Greenhouse gases

Budgeting the greenhouse gas emissions in the present case is difficult since only the gross emissions of CO_2 are measured, the contribution of photosynthesis is indeed not taken into account. The **H** ley emitted significantly more respiration-CO_2 than the **A** field (**Table 19**), which might be the result of higher plant density and microbial activity. However, if taking into account photosynthesis, the herbal ley is probably a bigger sink for CO_2 emissions than the arable control. Indeed, conversion of agricultural land to grassland usually comes with a lot of positive effects, including carbon sequestration (Follett, 2001). In a meta-analysis, Conant et al. (2001) estimated that conversion of cultivation to pasture enabled the sequestration of 1.01 Mg C ha^{-1} $year^{-1}$. In terms of N_2O emissions, the results show that fields under herbal ley can save almost 2 t $eqCO_2$ ha^{-1} $year^{-1}$ compared to cultivated arable lands (**Table 19**). If we consider that the difference in total N_2O emissions between the **H** and **A** lands is due to fertilizer application and we integrate the N_2O fluxes between April and October 2022, we can derive an emission factor of 1.86 %. This is within the range of the 2006 IPCC UK default emission factor for N_2O, estimated at 1% (with an uncertainty range from 0.03 to 3%) of the applied N (Buckingham et al., 2014). Interestingly, low N_2O emissions were observed during the growing season of 2023 (around 22 times inferior to the 2022 levels), despite fertilizer application (**Figure 39**). This can be correlated to the nitrate levels observed during the same period (**Figure 42**). Nitrogen plant uptake, a different type of fertilizer or other pathways of N loss have somehow resulted in low nitrate levels that year. As shown previously, high nitrate levels stimulate the denitrification product ratio, leading to high N_2O emissions. Unfortunately, no denitrification measurements were made during these times. We hypothesize however that low PR would have been found. This unexpected pattern emphasizes the importance of constraining denitrification for nitrous oxide mitigation strategies.

Finally, all three fields (even the **GC** one, as revealed by the liners measurements; data not shown) were minor sinks of CH_4, with maximums capture fluxes around -150 kg $eqCO_2$ ha^{-1} $year^{-1}$ but yearly averages around 50 kg $eqCO_2$ ha^{-1} $year^{-1}$. These values are again within the expected ranges although it is unclear why the arable control was a better sink than the herbal ley rather than the opposite, as observed in Castaldi et al. (2007). A possible explanation of this trend could be a predominance of methanotroph organisms in the **A** field due to poorer soil structure and thus more aerobic conditions.

4.6.4) Nitrogen cycle and effect of the leys

As mentioned in the previous section, the application of fertilizer in the arable control resulted in higher amounts of nitrate in 2022 but not in 2023 (**Figure 42**). In 2023, it seems that quantity applied in March has been used by plant or has escaped the environment by April. The static chamber data show that the N_2O fluxes were very low that month (**Figure 39**), and thus we can infer that the applied fertilizer was not lost via gas emissions. It is worth noting that a second type of fertilizer (although very similar) was used this year and might be an explanation of these different dynamics. Furthermore, application of fertilizer did not result in higher amounts of ammonium both years, although it does contain ammonium and urea. One possible explanation for these results could be a plant preference for ammonium (Boudsocq et al., 2012). In the study of Soana et al. (2022), where 200 kgN ha^{-1} were also applied, 120kgN ha^{-1} were taken up plants, which is the order of magnitude of the missing fertilizer. Another explanation could be that a large part of this ammonium has been transformed into nitrate through nitrification. This would explain why around 60 kgN ha^{-1} of nitrate are found in 2022 although only about 30 kgN ha^{-1} have been applied (the rest being ammonium and urea). The applied ammonium may also have volatilized as ammonia. We observe a similar trend

in the **GC** field, where application of fertilizer in April 2022 also resulted in an increase of nitrate but not ammonium. The herbal ley maintained similar levels of available ammonium without application of fertilizer. However, its nitrate levels were generally very low (always <5 kgN ha^{-1}). Its grazing during July 2022 enabled the nitrate levels to rise from an average of 2.18 kgN ha^{-1} pre-grazing to 4.04 kgN ha^{-1} for the next three months, which is a very moderate increase compared to fertilizer application. The ammonium concentration peak observed in all land uses during the month of July 2022 can be correlated to the Gaussian evolution of the ammonification potentials observed in laboratory (**Figure 45**). This seasonal pattern was expected as the growing season and warmer temperatures stimulate bacteria (Contosta et al., 2011). The potential mineralization rates were overall higher in the leys than in the arable control. This can be explained by large episodes of nitrogen consumption in the **A** field. It also indicates a higher microbial mass and potentially higher levels of nitrate and ammonium in the leys than in the arable control in the absence of fertilizer. The peaks of DOC observed during the month of August 2022 can be explained by crops residues left after cultivation in both the **A** and **GC** fields. The grazing of the herbal ley in July also left plant residues in the **H** field. The mineralization of this fresh organic matter has probably driven the observed peaks of DOC in all land uses. In the herbal ley, the presence of cows and sheep may also have contributed to this peak.

Finally, the arable control had a poorer soil structure and would often break when sampling it. This resulted in a low water retention capacity and thus lower moisture of this field in general (**Figure 43**). The herbal ley was efficient at building organic carbon, with an increase of 7.7% compared to the arable control. This is within the expected range for a long term herbal ley rotation in agriculture (Guest et al., 2022). This resulted in the herbal ley having a much better and stronger structure, which in turn, enhanced its water retention capacity and moisture.

4.7) Conclusion

The newly developed liner method enabled the characterization of the *in situ* denitrification dynamics of three different fields over time, at a low cost and without sophisticated equipment. The resulting data highlighted the progressive predominance of denitrification in soil N_2O emissions during the northern temperate summer following a Gaussian curve; which decreased and ended at the start of autumn. It also enabled to reveal the temporal dynamics of the denitrification product ratio, which was stimulated under large amendment of fertilizer during the growing season (reaching an average of 32%) and at its lowest levels during winter (~1%). However, the magnitude of flux derived from the liner method is not representative of field emission rates. This might be due to stimulation and disruption effects during the injection of the tracer. Although this can (and should) be mitigated by applying the tracer at the time of core sampling (i.e. 24 hours before incubation), the combination of this method with conventional flux chambers is probably the best way to derive global denitrification fluxes. This combination enabled us to unravel the mystery of denitrification in the studied lands and revealed that 8% of the applied fertilizer in the arable field during 2022 was removed from soil via denitrification. Around 9% of this nitrogen flux occurred via N_2O rather than N_2. Another high denitrification episode occurred during the second growing season, when no fertilizer was applied. This episode was characterized by a lower rate of nitrogen removal (about a third of the first denitrification event) and a lower contribution of N_2O (4%). In total, the activity of the arable land compared to the herbal ley caused the annual emission of approximately 4 kgN ha^{-1}, which is the equivalent of ca. 2 tonnes of equivalent CO_2 per hectare; with an emission factor of 1.86%. A different pattern of emissions during the year 2023 calls for deeper scientific investigation of the role of denitrification in agriculture. To that end, we recommend

improving our method using longer liners and earlier times of tracer application, while increasing the temporal resolution of measurement (in particular diurnal and nocturnal patterns); to constrain more accurate global nitrogen budgets.

4.8) References

Almaraz, M., Wong, M. Y., & Yang, W. H. (2020). Looking back to look ahead: a vision for soil denitrification research. *Ecology*, *101*(1). https://doi.org/10.1002/ecy.2917

Anthony, W. H., Hutchinson, G. L., & Livingston, G. P. (1995). Chamber Measurement of Soil-Atmosphere Gas Exchange: Linear vs. Diffusion-Based Flux Models. *Soil Science Society of America Journal*, *59*(5), 1308–1310. https://doi.org/10.2136/sssaj1995.03615995005900050015x

Biswas, B., & Gresshoff, P. M. (2014). The role of symbiotic nitrogen fixation in sustainable production of biofuels. *International Journal of Molecular Sciences*, *15*(5), 7380–7397. https://doi.org/10.3390/ijms15057380

Bizimana, F., Luo, J., Timilsina, A., Dong, W., Gaudel, G., Ding, K., Qin, S., & Hu, C. (2022). Estimating field N2 emissions based on laboratory-quantified N2O/(N2O + N2) ratios and field-quantified N2O emissions. *Journal of Soils and Sediments*, *22*(8), 2196–2208. https://doi.org/10.1007/s11368-022-03212-0

Boudsocq, S., Niboyet, A., Lata, J. C., Raynaud, X., Loeuille, N., Mathieu, J., Blouin, M., Abbadie, L., & Barot, S. (2012). Plant Preference for Ammonium versus Nitrate: A Neglected Determinant of Ecosystem Functioning? *The American Naturalist*, *180*(1), 60–69. https://doi.org/10.1086/665997

Buchen, C., Lewicka-Szczebak, D., Fuß, R., Helfrich, M., Flessa, H., & Well, R. (2016). Fluxes of N2 and N2O and contributing processes in summer after grassland renewal and grassland conversion to maize cropping on a Plaggic Anthrosol and a Histic Gleysol. *Soil Biology and Biochemistry*, *101*, 6–19. https://doi.org/10.1016/j.soilbio.2016.06.028

Buckingham, S., Anthony, S., Bellamy, P. H., Cardenas, L. M., Higgins, S., McGeough, K., & Topp, C. F. E. (2014). Review and analysis of global agricultural N2O emissions relevant to the UK. *Science of the Total Environment*, *487*(1), 164–172. https://doi.org/10.1016/j.scitotenv.2014.02.122

Castaldi, S., Costantini, M., Cenciarelli, P., Ciccioli, P., & Valentini, R. (2007). The methane sink associated to soils of natural and agricultural ecosystems in Italy. *Chemosphere*, *66*(4), 723–729. https://doi.org/10.1016/j.chemosphere.2006.07.089

Charles Munch, J., & Velthof, G. L. (2007). Denitrification and Agriculture. In *Biology of the Nitrogen Cycle* (pp. 331–341). Elsevier. https://doi.org/10.1016/B978-044452857-5.50022-9

Conant, R. T., Paustian, K., & Elliott, E. T. (2001). Grassland management and conversion into grassland: Effects on soil carbon. *Ecological Applications*, *11*(2), 343–355. https://doi.org/10.1890/1051-0761(2001)011[0343:GMACIG]2.0.CO;2

Conthe, M., Lycus, P., Arntzen, M. Ø., Ramos da Silva, A., Frostegård, Å., Bakken, L. R., Kleerebezem, R., & van Loosdrecht, M. C. M. (2019). Denitrification as an N2O sink. *Water Research*, *151*, 381–387. https://doi.org/10.1016/j.watres.2018.11.087

Contosta, A. R., Frey, S. D., & Cooper, A. B. (2011). Seasonal dynamics of soil respiration and N mineralization in chronically warmed and fertilized soils. Ecosphere, 2(3), art36. https://doi.org/10.1890/ES10-00133.1

Cueva, A., Volkmann, T. H. M., Haren, J. van, Troch, P. A., & Meredith, L. K. (2019). Reconciling Negative Soil CO2 Fluxes: Insights from a Large-Scale Experimental Hillslope. *Soil Systems*, *3*(1), 10. https://doi.org/10.3390/soilsystems3010010

Dodds, W. K., Burgin, A. J., Marcarelli, A. M., & Strauss, E. A. (2017). Nitrogen Transformations. In *Methods in Stream Ecology: Third Edition* (Vol. 2, pp. 173–196). Elsevier. https://doi.org/10.1016/B978-0-12-813047-6.00010-3

Follett, R. . (2001). Soil management concepts and carbon sequestration in cropland soils. *Soil and Tillage Research*, *61*(1–2), 77–92. https://doi.org/10.1016/S0167-1987(01)00180-5

Groffman, P. M., Altabet, M. A., Böhlke, J. K., Butterbach-Bahl, K., David, M. B., Firestone, M. K., Giblin, A. E., Kana, T. M., Nielsen, L. P., & Voytek, M. A. (2006). Methods for measuring denitrification: Diverse approaches to a difficult problem. In *Ecological Applications* (Vol. 16, Issue 6, pp. 2091–2122). https://doi.org/10.1890/1051-0761(2006)016[2091:MFMDDA]2.0.CO;2

Groffman, P. M., Butterbach-Bahl, K., Fulweiler, R. W., Gold, A. J., Morse, J. L., Stander, E. K., Tague, C., Tonitto, C., & Vidon, P. (2009). Challenges to incorporating spatially and temporally explicit phenomena (hotspots and hot moments) in denitrification models. *Biogeochemistry*, *93*(1–2), 49–77. https://doi.org/10.1007/s10533-008-9277-5

Guest, E. J., Palfreeman, L. J., Holden, J., Chapman, P. J., Firbank, L. G., Lappage, M. G., Helgason, T., & Leake, J. R. (2022). Soil macroaggregation drives sequestration of organic carbon and nitrogen with three-year grass-clover leys in arable rotations. *Science of The Total Environment*, *852*, 158358. https://doi.org/10.1016/j.scitotenv.2022.158358

Hofstra, N., & Bouwman, A. F. (2005). Denitrification in agricultural soils: Summarizing published data and estimating global annual rates. *Nutrient Cycling in Agroecosystems*, *72*(3), 267–278. https://doi.org/10.1007/s10705-005-3109-y

Jordon, M. W., Willis, K. J., Bürkner, P.-C., & Petrokofsky, G. (2022). Rotational grazing and multispecies herbal leys increase productivity in temperate pastoral systems – A meta-analysis. *Agriculture, Ecosystems & Environment*, *337*, 108075. https://doi.org/10.1016/j.agee.2022.108075

Kingston-Smith, A. H., Marshall, A. H., & Moorby, J. M. (2013). Breeding for genetic improvement of forage plants in relation to increasing animal production with reduced environmental

footprint. *Animal*, *7*(SUPPL.1), 79–88. https://doi.org/10.1017/S1751731112000961

Kulkarni, M. V., Burgin, A. J., Groffman, P. M., & Yavitt, J. B. (2014). Direct flux and 15N tracer methods for measuring denitrification in forest soils. *Biogeochemistry*, *117*(2–3), 359–373. https://doi.org/10.1007/s10533-013-9876-7

Lassaletta, L., Billen, G., Grizzetti, B., Anglade, J., & Garnier, J. (2014). 50 year trends in nitrogen use efficiency of world cropping systems: The relationship between yield and nitrogen input to cropland. *Environmental Research Letters*, *9*(10). https://doi.org/10.1088/1748-9326/9/10/105011

Lewicka-Szczebak, D., & Well, R. (2020). The 15N gas-flux method to determine N2 flux: A comparison of different tracer addition approaches. *SOIL*, *6*(1), 145–152. https://doi.org/10.5194/soil-6-145-2020

Machado, P. V. F., Farrell, R. E., & Wagner-Riddle, C. (2021). Spatial variation of nitrous oxide fluxes during growing and non-growing seasons at a location subjected to seasonally frozen soils. *Canadian Journal of Soil Science*, *101*(3), 555–564. https://doi.org/10.1139/cjss-2021-0003

Miller-Klugesherz, J. A., & Sanderson, M. R. (2023). Good for the soil, but good for the farmer? Addiction and recovery in transitions to regenerative agriculture. *Journal of Rural Studies*, *103*, 103123. https://doi.org/10.1016/j.jrurstud.2023.103123

Mulvaney, R. L., & Kurtz, L. T. (1984). Evolution of Dinitrogen and Nitrous Oxide from Nitrogen-15 Fertilized Soil Cores Subjected to Wetting and Drying Cycles. *Soil Science Society of America Journal*, *48*(3), 596–602. https://doi.org/10.2136/sssaj1984.03615995004800030026x

Overton, M. (1996). Re-establishing the english agricultural revolution. *Agricultural History Review*, *44*(1), 1–20.

Pedersen, A. R., Petersen, S. O., & Schelde, K. (2010). A comprehensive approach to soil-atmosphere trace-gas flux estimation with static chambers. *European Journal of Soil Science*, *61*(6), 888–902. https://doi.org/10.1111/j.1365-2389.2010.01291.x

Ravishankara, A. R., Daniel, J. S., & Portmann, R. W. (2009). Nitrous oxide (N2O): The dominant ozone-depleting substance emitted in the 21st century. *Science*, *326*(5949), 123–125. https://doi.org/10.1126/science.1176985

Sanderman, J., Hengl, T., & Fiske, G. J. (2017). Soil carbon debt of 12,000 years of human land use. *Proceedings of the National Academy of Sciences of the United States of America*, *114*(36), 9575–9580. https://doi.org/10.1073/pnas.1706103114

Scheer, C., Fuchs, K., Pelster, D. E., & Butterbach-bahl, K. (2020). ScienceDirect Estimating global terrestrial denitrification from measured N 2 O :(N 2 O + N 2) product ratios $. *Current Opinion in Environmental Sustainability*, *47*, 72–80. https://doi.org/10.1016/j.cosust.2020.07.005

Smith, C. J., Dong, L. F., Wilson, J., Stott, A., Osborn, A. M., & Nedwell, D. B. (2015). Seasonal variation in denitrification and dissimilatory nitrate reduction to ammonia process rates and corresponding key functional genes along an estuarine nitrate gradient. *Frontiers in*

Microbiology, *6*. https://doi.org/10.3389/fmicb.2015.00542

Soana, E., Vincenzi, F., Colombani, N., Mastrocicco, M., Fano, E. A., & Castaldelli, G. (2022). Soil Denitrification, the Missing Piece in the Puzzle of Nitrogen Budget in Lowland Agricultural Basins. *Ecosystems*, *25*(3), 633–647. https://doi.org/10.1007/s10021-021-00676-y

Velthof, G. L., & Rietra, R. P. J. J. (2018). *Nitrous oxide emission from agricultural soils*. https://doi.org/10.18174/466362

Vermeulen, S. J., Campbell, B. M., & Ingram, J. S. I. (2012). Climate change and food systems. *Annual Review of Environment and Resources*, *37*, 195–222. https://doi.org/10.1146/annurev-environ-020411-130608

Waldo, S., Russell, E. S., Kostyanovsky, K., Pressley, S. N., O'Keeffe, P. T., Huggins, D. R., Stöckle, C. O., Pan, W. L., & Lamb, B. K. (2019). N 2 O Emissions From Two Agroecosystems: High Spatial Variability and Long Pulses Observed Using Static Chambers and the Flux-Gradient Technique. *Journal of Geophysical Research: Biogeosciences*, *124*(7), 1887–1904. https://doi.org/10.1029/2019JG005032

Wang, R., Pan, Z., Zheng, X., Ju, X., Yao, Z., Butterbach-Bahl, K., Zhang, C., Wei, H., & Huang, B. (2020). Using field-measured soil N2O fluxes and laboratory scale parameterization of N2O/(N2O+N2) ratios to quantify field-scale soil N2 emissions. *Soil Biology and Biochemistry*, *148*(June), 107904. https://doi.org/10.1016/j.soilbio.2020.107904

Warner, D. I., Scheer, C., Friedl, J., Rowlings, D. W., Brunk, C., & Grace, P. R. (2019). Mobile continuous-flow isotope-ratio mass spectrometer system for automated measurements of N2 and N2O fluxes in fertilized cropping systems. *Scientific Reports*, *9*(1), 11097. https://doi.org/10.1038/s41598-019-47451-7

Well, R., Maier, M., Lewicka-Szczebak, D., Köster, J. R., & Ruoss, N. (2019). Underestimation of denitrification rates from field application of the 15N gas flux method and its correction by gas diffusion modelling. *Biogeosciences*, *16*(10), 2233–2246. https://doi.org/10.5194/bg-16-2233-2019

Zaman, M., Heng, L., & Müller, C. (2021). Measuring emission of agricultural greenhouse gases and developing mitigation options using nuclear and related techniques: Applications of nuclear techniques for GHGs. In *Measuring Emission of Agricultural Greenhouse Gases and Developing Mitigation Options using Nuclear and Related Techniques: Applications of Nuclear Techniques for GHGs*. https://doi.org/10.1007/978-3-030-55396-8

Chapter 5: Partitioning the sources of N_2O combining naturally abundant isotopes and ^{15}N tracer

In this final research chapter, the ^{15}N Gas flux method is combined with naturally abundant isotopes within the N_2O molecule to precisely partition the different sources of nitrous oxide; finalizing the complete characterization of denitrification. The use of naturally abundant isotopes for N_2O source partitioning is at the cutting edge of technology and is currently undergoing dynamic development. Rather than comparing the two methods (which has been done few times in the past), we decided to combine the information provided by both techniques to constrain as accurately as possible the different sources of N_2O. For this laboratory study, we used the arable field plot from **Chapter 4**, which we expected to be dominated by bacteria rather than fungi. The results of this chapter were in accordance with this hypothesis.

This chapter is written as a short communication and will be submitted for publication in the Rapid Communications in Mass Spectrometry Journal.

Under the supervision of Sami Ullah and Fotis Sgouridis, Gianni Micucci formulated the research questions, designed the experimental layout, ran the experiments, analysed the data and wrote the manuscript. Fotis Sgouridis was responsible for the gas analyses of the ^{15}N tracer experiment. The samples under natural abundance were shipped to Germany and analysed by Caroline Buchen-Tschiskale and Reinhard Well. As a leading world expert on naturally abundant ^{15}N isotopes, Dominika Lewicka-Szczebak helped with the calculations although the new model was developed by Gianni Micucci. All the cited co-authors reviewed and corrected the manuscript.

Combining the ^{15}N Gas flux method and isotopocule data for the complete determination of soil N_2O sources

Gianni Micucci[1,*], Fotis Sgouridis[2], Dominika Lewicka-Szczebak[3], Reinhard Well[4], Caroline Buchen-Tschiskale[4], Niall P. McNamara[5], Stefan Krause[1], Iseult Lynch[1], Felicity Roos[6] and Sami Ullah[1,7]

- 1. School of Geography, Earth and Environmental Sciences, University of Birmingham, Edgbaston, B15 2TT Birmingham, United Kingdom.
- 2. School of Geographical Sciences, University of Bristol, BS8 1SS Bristol, United Kingdom.
- 3. Institute of Geological Sciences, University of Wrocław, Wrocław, Poland.
- 4. Thünen Institute of Climate-Smart Agriculture, Bundesallee 65, 38116, Braunschweig, Germany.
- 5. UK Centre for Ecology & Hydrology, Lancaster Environment Centre, LA1 4AP Lancaster, United Kingdom.
- 6. UK National Trust, SN2 2NA Swindon, United Kingdom.
- 7. Birmingham Institute of Forest Research, University of Birmingham, Birmingham, UK.

* Corresponding author.

Email address: [redacted] (G. Micucci).

5.1) Abstract

The analysis of naturally abundant isotopes in biogenic N_2O molecules can give precious information such as the nature of their precursor. However, many uncertainties exist and further validations are needed to confirm this method as a reliable tracer of biogeochemical cycles. In this study, we aimed to determine the full composition of N_2O sources from an agricultural soil by combining naturally abundant isotopes and the use of a ^{15}N tracer (^{15}N Gas Flux method). To that aim, we conducted parallel laboratory incubations in which we enhanced the conditions of denitrification through increase of the gravimetric moisture content (>70 %) and amendment of nitrate; where this nitrate was either unlabelled or labelled with ^{15}N atoms. A new linear system combined with Monte Carlo simulation enabled us to determine the following partition: bacterial denitrification (88.0%), fungal denitrification (8.9%), nitrification (1.5%) and nitrifier denitrification (1.6%). If confirmed by further research, this new approach could constitute a routine test for complete N_2O source partitioning.

5.2) Introduction

The asymmetry of the N_2O molecule enables us to identify N^{α}, the nitrogen atom directly adjacent to the O atom; and N^{β}, the peripheral nitrogen atom of the molecule (Toyoda & Yoshida, 1999). The presence of naturally abundant (NA) isotopes for these three atoms can help to partition the sources of soil-emitted N_2O. Apart from $^{14}N^{14}N^{16}O$, the three most abundant isotopocules (molecules with the same atomic identity but which differ in their isotopic composition or intramolecular position of isotopes) are $^{14}N^{14}N^{18}O$, $^{14}N^{15}N^{16}O$ and $^{15}N^{14}N^{16}O$. We can define their relative abundances as (Yu et al., 2020):

$$\delta X = \frac{R_{sample} - R_{standard}}{R_{standard}} \qquad [64]$$

Where R is the ratio of the studied isotopocule (e.g. $^{14}N^{15}N^{16}O$ in the case X = N^{α}) to the most abundant one ($^{14}N^{14}N^{16}O$). The standard ratios are defined by the international scale, with air N_2 for $^{15}N/^{14}N$ and the Vienna Standard Mean Ocean Water (VSMOW) for $^{18}O/^{16}O$. We can also define:

$$\delta N^{bulk} = \frac{\delta N^{\alpha} + \delta N^{\beta}}{2} \quad [65]$$

$$\delta N^{SP} = \delta N^{\alpha} - \delta N^{\beta} \quad [66]$$

Where "bulk" refers to the average of the two most abundant ^{15}N isotopocules and "SP" to the site preference (Toyoda et al., 2005). The site preference is a parameter of intramolecular distribution of the ^{15}N atoms which remains constant over the course of reactions and does not depend on the isotopic composition of the substrates (Ostrom et al., 2007). The $\delta^{18}O$ value is also a powerful tool since the different soil N_2O sources present a relatively narrow range of $\delta^{18}O$ signatures compared to $\delta^{15}N^{bulk}$ (Ibraim et al., 2019). Furthermore, only the determination of the $\delta^{18}O$ of soil water is needed to interpret $\delta^{18}O$ values, compared to all source substrates for $\delta^{15}N^{bulk}$ (Lewicka-Szczebak et al., 2020). If we consider heterotrophic nitrification, abiotic N_2O formation and ammonia-oxidizing archaea contributions as negligible, four processes are left (Zou et al., 2014): bacterial denitrification (bD), fungi denitrification (fD), nitrification (Ni) and nitrifier denitrification (nD). Each of these four processes emits N_2O with specific ranges of $\delta^{15}N^{SP}$ and $\delta^{18}O$ signatures available in the literature (**Table 22**).

***Table 22**: Isotopic signatures of the different processes (based on Yu et al., 2020) and net isotopic reduction isotope effects (based on Well & Flessa, 2009).*

The standard deviations were calculated by assuming the ranges reported by Yu et al. (2020) represented (mean + 2 standard deviations). The $\delta^{18}O_{N2O/H2O}$ data are given for $\delta^{18}O_{H2O} = 0$.

$\delta^{15}N^{SP}$ **bD** (‰)	$\delta^{18}O_{N2O/H2O}$ **bD** (‰)	$\delta^{15}N^{SP}$ **fD** (‰)	$\delta^{18}O_{N2O/H2O}$ **fD** (‰)	$\delta^{15}N^{SP}$ **Ni** (‰)	$\delta^{18}O_{N2O/H2O}$ **Ni** (‰)	$\delta^{15}N^{SP}$ **nD** (‰)	$\delta^{18}O_{N2O/H2O}$ **nD** (‰)	$\varepsilon_{N\text{-}SP}$ (‰)	ε_O (‰)
-1.90 ± 2.8	19.20 ± 1.65	33.50 ± 3.18	47.20 ± 3.28	35.00 ± 1.68	23.50 ± 3	-5.9 ± 3.88	16.8 ± 1.25	-7 ± 2.8	-17.5 ± 4

When all processes are present, the resulting $\delta^{15}N^{SP}$ and $\delta^{18}O$ signatures of the emitted N_2O will depend on the relative proportions of these four processes ($f_{bD} + f_{fD} + f_{Ni} + f_{nD} = 1$). The reduction of N_2O to N_2 is also associated with a shift in the isotopic signatures of $\delta^{15}N^{bulk}$, $\delta^{15}N^{SP}$ and $\delta^{18}O$ of the residual N_2O (Well & Flessa, 2009). Classically, two scenarios are differentiated (Lewicka-Szczebak et al., 2017). In the first one (Reduction/Mixing, "RM"), N_2O derived from bacterial denitrification is firstly reduced into N_2 by bacteria and then mixes with the other sources of N_2O. In the second scenario (Mixing/Reduction "MR"), N_2O emitted from bacterial denitrification mixes with the other sources of N_2O (including atmospheric N_2O) and the mix is then reduced by bacteria. A combination of both could also theoretically occur. The RM scenario is however considered more realistic as denitrification typically occurs in anaerobic microsites and N_2O is likely to be reduced under these conditions (Ibraim et al., 2019; Verhoeven et al., 2019; Yu et al., 2020). It will be the only scenario considered in this study.

Under the closed-system assumption (which considers unilateral reaction and does not take in account further production of new N_2O; Decock & Six, 2013), the isotopic reduction shift can be approximated by (Mariotti et al., 1981):

$$\delta_r - \delta_0 \approx \varepsilon_{red} \times \ln(r_{N2O}) \quad [67]$$

Where δ_0 (‰) is the isotopic signature (either $\delta^{15}N^{bulk}$, $\delta^{15}N^{SP}$ or $\delta^{18}O$) of the produced N_2O before reduction, δ_r (‰) the isotopic signature of the residual unreduced N_2O, ε_{red} (‰) the net reduction isotopic effect and r_{N2O} the microscopic product ratio, which in case of the RM scenario is defined as:

$$r_{N2O} = \frac{[N_2O]_{bD}}{[N_2O]_{bD}+[N_2]_{bD}} \quad [68]$$

A direct method for the quantification of denitrification products is the ^{15}N Gas Flux method (^{15}NGF), which consists of applying a $^{15}NO_3^-$ tracer to an incubated soil and measuring the abundance of ^{15}N atoms in both denitrified N_2 and N_2O molecules (Micucci et al., 2023). It enables to quantify the source partitioning coefficient (SPC) and the macroscopic product ratio (PR) defined as:

$$SPC = \frac{(N_2O)_{bD}+(N_2O)_{fD}}{(N_2O)_{emitted}} = f_{bD} + f_{fD} \quad [69]$$

$$PR = \frac{(N_2O)_{bD}+(N_2O)_{fD}}{(N_2O)_{bD}+(N_2O)_{fD}+(N_2)_{bD}} \quad [70]$$

Although more disruptive than the study of isotopocules, the ^{15}NGF is generally considered more reliable to quantify denitrification (Stevens et al., 1997).

By combining the ^{15}NGF and the isotopocule approach, we get the following system (S):

$$\left(\begin{array}{cccc|c} f_{bD}[\delta^{18}O_{bD} + \varepsilon_O \times \ln(r_{N2O})] & f_{fD} \times \delta^{18}O_{fD} & f_{Ni} \times \delta^{18}O_{Ni} & f_{nD} \times \delta^{18}O_{nD} & \delta^{18}O_{sample} \\ f_{bd}[\delta^{15}N^{SP}{}_{bD} + \varepsilon_{N^{SP}} \times \ln(r_{N2O})] & f_{fD} \times \delta^{15}N^{SP}{}_{fD} & f_{Ni} \times \delta^{15}N^{SP}{}_{Ni} & f_{nD} \times \delta^{15}N^{SP}{}_{nD} & \delta^{15}N^{SP}{}_{sample} \\ f_{bd} & f_{fD} & 0 & 0 & SPC \\ f_{bd} & f_{fD} & f_{Ni} & f_{nD} & 1 \end{array}\right)$$

Which has 4 equations and 4 unknown parameters; and thus can be solved for f_{bD}, f_{fD}, f_{Ni} and f_{nD}. In this study, we aimed to partition the N_2O sources of an agricultural soil by solving the (S) system using laboratory incubations; where denitrification conditions would be enhanced for reference and for a stronger signal of the ^{15}NGF.

5.3) Material and Methods

***Table 23**: Soil properties of the studied soil (mean ± standard deviation).*

NO_3^- (mgN/kg)	NH_4^+ (mgN/kg)	Gravimetric moisture (%)	pH	Clay (%)	Silt (%)	Sand (%)	DOC (mgC/kg)	TDN (mgN/kg)
11.77 ± 0.44	1.33 ± 0.10	20.34 ± 0.18	7.97	82	13	5	63.78 ± 2.56	14.98 ± 0.52

On the 15th of September 2022, arable soil was sampled at the FarmED site, near Shipton-under Wychwood UK (51.869981,-1.581136). Upon return to the laboratory, soil was sieved, mixed and stored at 4°C. Moisture, nitrate, ammonium, dissolved organic carbon (DOC) and total dissolved Nitrogen (TDN) contents were determined with the protocols described in **Chapter 3** and can be found in **Table 23**. We then incubated 8 replicates of 150 g of soil inside 450 mL sealed jars with modified lids containing septa. Soil gravimetric moisture was adjusted to 70 % using a de-ionised water solution (~60 mL) which resulted in soil being flooded, with about 0.2 cm of water standing on top. The applied de-ionised water contained potassium nitrate (KNO_3, 0.31 g L^{-1}) for 4 replicates and K-$^{15}NO_3$ (98 at %, Merck) for the other 4 replicates. The quantity of added nitrate was the same for both treatments and was optimized to target a 50% ^{15}N enrichment of the soil denitrifying pool in the case of the ^{15}NGF experiment. Gas sampling took place at times 0, 3, 6 and 24 hours where 15 mL of gas were sampled from the jars headspace into 12 mL pre-evacuated Exetainer vials (Labco Limited, UK) and 15 mL of laboratory air were added for pressure equilibration.

All gas samples were analysed for N_2O concentration using an Agilent 7890A Gas Chromatograph (GC). In the case of the ^{15}NGF experiment, isotopic ratios of N_2 and N_2O were acquired using a continuous flow Isotope Ratio Mass Spectrometer (IRMS, Elementar Isoprime PrecisION; Elementar Analysensysteme GmbH, Hanau, Germany). The full procedure of these two analyses is described in **Chapter 3**. For the ^{15}NGF, denitrified N_2O and N_2 emissions were calculated using the equations of Mulvaney & Boast (1986) and Spott et al. (2006) respectively (see Micucci et al., 2023 and **Chapter 3**). The NA isotopic signatures of N_2O were obtained using IRMS (Delta V, Thermo Fisher Scientific, Bremen, Germany) as in Lewicka-Szczebak et al., 2017. This enabled the measurement of the N_2O isotopic signatures ($\delta^{15}N^{bulk}$, $\delta^{15}N^{SP}$ and $\delta^{18}O$). The signatures of the emitted N_2O were extracted from the background using a mixing model as:

$$\delta X_{emitted} = \frac{[N_2O]_{mix}\delta X_{mix} - [N_2O]_{air}\delta X_{air}}{[N_2O]_{emitted}} \qquad [71]$$

Where $[N_2O]$ is the N_2O concentration (ppm). The δX_{air} were determined as the average of measurements at times 0 (prior to incubation). The $\delta^{18}O_{N2O}$ values were corrected by subtracting the $\delta^{18}O$ value of soil water. Since no measurement of $\delta^{18}O_{H2O}$ was made, we used local precipitation isotopic values from a nearby monitoring station (Wallingford, UK) for the month of sampling ($\delta^{18}O_{H2O}$ = - 4.66 ‰; IAEA/WMO, 2023). The 2022 mean annual $\delta^{18}O_{H2O}$ values at this station was (-5.62 ± 2.57 SD) ‰.

5.4) Results and discussion

After 3 and 6 hours of incubation, soil emissions were very low and the resulting data were under the limits of detection for both methods. However, a large activity was observed at time 24 hours (N_2O concentration > 20 ppm) and was very consistent amongst all replicates and between the two experiments. This profile of emission is typical of a wetting effect (**Chapter 3.5.5**). The ^{15}NGF results indicated a predominance of denitrification in the N_2O emissions with a SPC coefficient of 97 % (**Table 24**).

***Table 24**: Results for the ^{15}NGF (first row) and NA (second row) experiments. Results are given as (mean + standard deviation).*

Where a_p is the 15N enrichment of the soil denitrifying pool after $^{15}NO_3$ tracer application in the case of the 15NGF (either based on Mulvaney & Boast, 1986 "MB"; or Arah, 1992).

$a_{p\ (N2O)}$ (%) (MB)	$a_{p\ (N2O)}$ (%) (Arah)	$a_{p\ (N2)}$ (%)	Total N_2O (µgN kg^{-1} h^{-1})	SP (%)	N_2 emissions (µgN kg^{-1} h^{-1})	R_{N2O} (%)
51.14 ± 1.46	51.15 ± 1.46	47.08 ± 2.73	3.08 ± 0.08	97.09 ± 0.67	3.26 ± 0.8	41.57 ± 4.94
$\delta^{15}N^{SP}$ (‰)	$\delta^{18}O_{N2O/H2O}$ (‰)	$\delta^{15}N^{bulk}$ (‰)	Total N_2O (µgN kg^{-1} h^{-1})			
4.01 ± 1.70	32.80 ± 0.21	-43.53 ± 0.53	3.04 ± 0.11			

We hypothesised that $f_{bD} \gg f_{fD}$ and thus $R_{N2O} \simeq r_{N2O}$, which should be verified since agricultural soils are usually bacteria-dominated (MA et al., 2019). This enables (S) to become a linear system that can be more easily solved[1]. Our first attempt at partitioning the four sources yielded some negative source contributions. This highlighted the sensitivity of the model to the numerous parameters. We thus ran a Monte Carlo simulation and generated 100 000 values of all the model parameters (source and emitted N_2O isotopic signatures, isotopic reduction effects, SP and R_{N2O} coefficients) normally distributed around their mean and standard deviation (**Table 22** and **Table 24**); and solve the linear system (S) with the condition that all source coefficients must be positive and smaller than 1.

The algorithm returned 1 500 solutions, which enabled us to constrain the source partition of N_2O (**Table 25**). Using this partition, we can approximate r_{N2O} to 38.41%, which is close to R_{N2O} (41.57%) and which confirms our hypothesis. If $r_{N2O} \not\approx R_{N2O}$, (S) is no longer a linear system and r_{N2O} needs to be replaced with its expression (**equation [68]**).

***Table 25**: Determined composition of the emitted N_2O (mean + standard deviation).*

Bacterial denitrification (%)	Fungal Denitrification (%)	Nitrification (%)	Nitrifier Denitrification (%)
88.00 ± 5.97	8.92 ± 5.95	1.48 ± 0.95	1.60 ± 0.97

It is worth noting that for the ^{15}NGF the ^{15}N enrichment of the denitrifying pool (a_p) calculated with the method of Mulvaney & Boast (1986) or Arah (1992) were almost identical (**Table 24**) and seem to indicate that the soil is at isotopic equilibrium thanks to homogeneous tracer application in the

[1] The system (S) is not a linear system, since r_{N2O} in the logarithm part of the two first rows depends on f_{bD}. However, replacing r_{N2O} with the determined R_{N2O} (which is considered constant in the current experimental conditions) will transform S1 into a linear system.

flooded soil (see Micucci et al., 2023 for model and hypothesis explanations). When calculated with the N_2 data, the a_p values were also in close agreement thanks to a high denitrification activity.

In conclusion, the presented parallel experiments showed very high consistency and their combination enabled the precise determination of all N_2O sources. To our knowledge, this approach has not been attempted in the past. The present experimental conditions strongly favoured denitrification and resulted in a high resolution. The low success rate of the Monte Carlo simulation (~1.5%) can be attributed to the numerous parameters and their associated uncertainty range. It could also indicate a non-negligible contribution of the sources we ignored (heterotrophic nitrification, abiotic N_2O formation and ammonia-oxidizing archaea). Our calculated N_2O source partition was nonetheless within the expected range with a domination of bacterial denitrification and shows that our approach was a good approximation. Such protocol could potentially enable to discriminate bacterial and fungi contributions to denitrification routinely. Further work will be needed to assess to true potential of this approach.

5.5) References

Arah, J. R. M. (1992). New Formulae for Mass Spectrometric Analysis of Nitrous Oxide and Dinitrogen Emissions. *Soil Science Society of America Journal*, *56*(3), 795–800. https://doi.org/10.2136/sssaj1992.03615995005600030020x

Decock, C., & Six, J. (2013). How reliable is the intramolecular distribution of 15N in N2O to source partition N2O emitted from soil? *Soil Biology and Biochemistry*, *65*(2), 114–127. https://doi.org/10.1016/j.soilbio.2013.05.012

IAEA/WMO. (2023). *Global Network of Isotopes in Precipitation. The GNIP Database*.

Ibraim, E., Wolf, B., Harris, E., Gasche, R., Wei, J., Yu, L., Kiese, R., Eggleston, S., Butterbach-Bahl, K., Zeeman, M., Tuzson, B., Emmenegger, L., Six, J., Henne, S., & Mohn, J. (2019). Attribution of N2O sources in a grassland soil with laser spectroscopy based isotopocule analysis. *Biogeosciences*, *16*(16), 3247–3266. https://doi.org/10.5194/bg-16-3247-2019

Lewicka-Szczebak, D., Augustin, J., Giesemann, A., & Well, R. (2017). Quantifying N2O reduction to N2 based on N2O isotopocules-validation with independent methods (helium incubation and 15N gas flux method). *Biogeosciences*, *14*(3), 711–732. https://doi.org/10.5194/bg-14-711-2017

Lewicka-Szczebak, D., Piotr Lewicki, M., & Well, R. (2020). N2O isotope approaches for source partitioning of N2O production and estimation of N2O reduction-validation with the 15N gas-flux method in laboratory and field studies. *Biogeosciences*, *17*(22), 5513–5537. https://doi.org/10.5194/bg-17-5513-2020

MA, S., WANG, J., & YAN, X. (2019). Is Nitrous Oxide Reduction Primarily Regulated by the Fungi-to-Bacteria Abundance Ratio in Fertilized Soils? *Pedosphere*, *29*(5), 569–576. https://doi.org/10.1016/S1002-0160(19)60830-1

Mariotti, A., Germon, J. C., Hubert, P., Kaiser, P., Letolle, R., Tardieux, A., & Tardieux, P. (1981). Experimental determination of nitrogen kinetic isotope fractionation: Some principles; illustration for the denitrification and nitrification processes. *Plant and Soil*, *62*(3), 413–430. https://doi.org/10.1007/BF02374138

Micucci, G., Sgouridis, F., Mcnamara, N. P., Krause, S., Lynch, I., Roos, F., Well, R., & Ullah, S. (2023). The 15 N-Gas flux method for quantifying denitrification in soil : Current progress and future directions. *Soil Biology and Biochemistry*, *184*(June), 109108. https://doi.org/10.1016/j.soilbio.2023.109108

Mulvaney, R. L., & Boast, C. W. (1986). Equations for Determination of Nitrogen-15 Labeled Dinitrogen and Nitrous Oxide by Mass Spectrometry. *Soil Science Society of America Journal*, *50*(2), 360–363. https://doi.org/10.2136/sssaj1986.03615995005000020021x

Ostrom, N. E., Piit, A., Sutka, R., Ostrom, P. H., Grandy, A. S., Huizinga, K. M., & Robertson, G. P.

(2007). Isotopologue effects during N2O reduction in soils and in pure cultures of denitrifiers. *Journal of Geophysical Research: Biogeosciences*, *112*(2), 1–12. https://doi.org/10.1029/2006JG000287

Spott, O., Russow, R., Apelt, B., & Stange, C. F. (2006). A 15N-aided artificial atmosphere gas flow technique for online determination of soil N2 release using the zeolite Köstrolith SX6®. *Rapid Communications in Mass Spectrometry*, *20*(22), 3267–3274. https://doi.org/10.1002/rcm.2722

Stevens, R. J., Laughlin, R. J., Burns, L. C., Arah, J. R. M., & Hood, R. C. (1997). Measuring the contributions of nitrification and denitrification to the flux of nitrous oxide from soil. *Soil Biology and Biochemistry*, *29*(2), 139–151. https://doi.org/10.1016/S0038-0717(96)00303-3

Toyoda, S., Mutobe, H., Yamagishi, H., Yoshida, N., & Tanji, Y. (2005). Fractionation of N2O isotopomers during production by denitrifier. *Soil Biology and Biochemistry*, *37*(8), 1535–1545. https://doi.org/10.1016/j.soilbio.2005.01.009

Toyoda, S., & Yoshida, N. (1999). Determination of Nitrogen Isotopomers of Nitrous. *Anal. Chem.*, *71*(20), 4711–4718.

Verhoeven, E., Barthel, M., Yu, L., Celi, L., Said-Pullicino, D., Sleutel, S., Lewicka-Szczebak, D., Six, J., & Decock, C. (2019). Early season N 2 O emissions under variable water management in rice systems: Source-partitioning emissions using isotope ratios along a depth profile. *Biogeosciences*, *16*(2), 383–408. https://doi.org/10.5194/bg-16-383-2019

Well, R., & Flessa, H. (2009). Isotopologue enrichment factors of N 2 O reduction in soils. *Rapid Communications in Mass Spectrometry*, *23*(18), 2996–3002. https://doi.org/10.1002/rcm.4216

Yu, L., Harris, E., Lewicka-Szczebak, D., Barthel, M., Blomberg, M. R. A., Harris, S. J., Johnson, M. S., Lehmann, M. F., Liisberg, J., Müller, C., Ostrom, N. E., Six, J., Toyoda, S., Yoshida, N., & Mohn, J. (2020). What can we learn from N2O isotope data? – Analytics, processes and modelling. *Rapid Communications in Mass Spectrometry*, *34*(20). https://doi.org/10.1002/rcm.8858

Zou, Y., Hirono, Y., Yanai, Y., Hattori, S., Toyoda, S., & Yoshida, N. (2014). *Isotopomer analysis of nitrous oxide accumulated in soil cultivated with tea (Camellia sinensis) in Shizuoka, central Japan*. https://doi.org/10.3334/CDIAC/atg.032

Chapter 6: Conclusions and future outlook

In the present work, we successfully developed a new methodology for the measurement of *in situ* denitrification and characterized this soil process in conventional and regenerative agriculture. The defined research questions in **Chapter 1.6** were:

- How much can we increase the limit of detection of the ^{15}N Gas Flux method by combining it with an artificial atmosphere?
- Is the denitrification process stimulated by the addition of a ^{15}N-NO3 tracer? And by the addition of large quantities of nitrogen fertilizer?
- How much fertilizer is lost to the environment via denitrification after application?
- How do leys compare to conventional agriculture in terms of denitrification during and outside of the cultivation period? Is there a significant difference between unfertilized and fertilized ley?
- Is denitrification constant over time or does it follow temporal patterns?
- How much global warming potential can be saved with regenerative agriculture?
- Can we combine the ^{15}N Gas Flux method and naturally abundant isotopes to completely partition the sources of N_2O?

We also hypothesized that denitrification would be a less efficient sink for nitrous oxide emissions (higher product ratio) in conventional agriculture than in regenerative agriculture and that the application of fertilizer would result in large quantities of nitrogen lost via denitrification. Furthermore, we hypothesized that denitrification would exhibit large temporal variations that have

not been properly characterized so far due to the technical difficulties involved. Finally, we hypothesized that denitrified N_2O emissions in conventional agriculture would be dominated by bacteria rather than fungi.

The results of the present study enables us to answer these questions and verify these hypotheses as follows:

How much can we increase the limit of detection of the ^{15}N Gas Flux method by combining it with an artificial atmosphere?

We have shown through simulation that the N_2 background reduction affects the sensitivity of the ^{15}N Gas Flux method in a non-linear way (**Figure 14**). In particular, we demonstrated the existence of a 10% N_2 threshold below which the sensitivity increases exponentially. For instance, an atmospheric N_2 background of 1% results in 80 times greater sensitivity. Although recent studies managed to work at these low levels under field conditions and reported an 80-fold increase in sensitivity, our approach using plastic liners for the incubation of small soil cores resulted in an 8-fold greater sensitivity. However, where the former method only enabled one incubation at a time, we were able to simultaneously incubate 24 soil cores (originating from 3 different fields), resulting in a much higher spatial resolution. Given the large spatial variability of denitrification, this can be considered a more effective method to constrain this process. Furthermore, over 208 field measurements, we had a 90% success rate in N_2 flux detection. Nonetheless, the magnitude of flux derived from the liner approach could not be used directly to quantify global denitrification budgets. Rather, this method enables the quantification of independent metrics that can be applied to chamber fluxes.

Is the denitrification process stimulated by the addition of a 15N-NO3 tracer? And by the addition of large quantities of nitrogen fertilizer?

Our method relied on a higher rate of ^{15}N tracer application to achieve the highest possible sensitivity, targeting a 50% ^{15}N enrichment of the soil nitrate pool. This increase could potentially stimulate denitrification and result in the measurement of artefacts. Although we did observe a significant increase in the denitrification product ratio under laboratory conditions; the 208 measurements of the one-year field campaign did not show a significant correlation between tracer application and product ratio. On the other hand, the application of fertilizer in the arable control resulted in the highest observed denitrification product ratio (32%). Similarly, the N_2O losses in this field were correlated with nitrate levels. Therefore, we can assume that very high amendments of nitrate stimulate the denitrification product ratio (and thus the nitrous oxide sink efficiency); but as shown in **Chapter 3.3.3**, the levels of tracer applied with our method do not really compare with fertilizer amendment. If excluding the fertilization periods, the amounts of tracer applied would generally be the equivalent of 1 to 2 kgN ha^{-1}, and are much smaller than the lowest application of fertilizer in the arable control (~50kgN ha^{-1}).

How much fertilizer is lost to the environment via denitrification after application?

We reported in this study that, from the 200 kgN ha^{-1} of applied fertilizer, 15 kgN ha^{-1} were lost via denitrification (8%) in the arable control. Around 9% of this denitrification loss (1.34 kgN ha^{-1}) occurred via N_2O rather than N_2.

How do leys compare to conventional agriculture in terms of denitrification during and outside of the cultivation period? Is there a significant difference between unfertilized and fertilized ley?

Annually, 22 kgN ha^{-1} were lost in the arable field via denitrification, compared to 2.6 kgN ha^{-1} in the unfertilized ley. While this confirms our original hypothesis that denitrification losses would be high under amendment of fertilizer and result in large N_2O emissions, the difference in nitrous oxide sink efficiency is a bit more difficult to assess. While the mean annual product ratio of the arable control is higher than that of the herbal ley, confirming our hypothesis that conventional agriculture is a less efficient sink of nitrous oxide, the difference between the two land uses was not really significant (5.81 for the ley and 7.05 for the arable). However, the fertilization period was associated with high monthly mean product ratios (up to 32%). If during the month of May 2022 the nitrous oxide sink efficiency of denitrification was as high as the annual levels, 0.3 kg-N_2O ha^{-1} or the equivalent of 130 kg of $eqCO_2$ ha^{-1} would have been saved (around 7% of the annual budget). A better temporal resolution during this period would probably reveal that this number is underestimated. Outside of the growing season (thus mostly in winter) denitrification activity was similar and low for the two land uses, although the magnitude of flux in the arable was still double that of the herbal ley. Although we could not derive an annual budget for the fertilized grass/clover ley (due to the lack of chamber measurements there), the *in situ* dynamics of denitrification showed that this field was probably a large emitter of nitrogen. Characterized by the highest product ratio of all studied land uses (14.5% compared to 6-7%) this field was actually the least efficient sink for nitrous oxide. Although the magnitude of N_2O was probably lower than in the arable (due to inferior fertilization rates), it was surely higher than in the herbal ley.

Is denitrification constant over time or does it follow temporal patterns?

As we hypothesized, large variations were observed in the magnitudes of emissions, but most importantly in the source partitioning coefficients and product ratios. Our data indicated a Gaussian evolution of the source partitioning coefficient from March to September and a similar but smaller evolution around October. This is to our knowledge, the first time that this very specific pattern is reported and it indicates a predominance of denitrification in the N_2O emissions during summer; although the magnitude of total N_2O emissions is rather low during these times. This magnitude is however a bit higher around October which contributes to a peak of nitrous oxide emission during the second growing season. This peak is not observed in the herbal ley and is probably due to land use (winter wheat crop, but no fertilizer). We demonstrated that the product ratio was influenced by fertilizer application and therefore, the temporal patterns of this ratio need to be determined through the unfertilized ley. It started at very low levels in March (~3%) and increased until June where it reached its maximum (~13%) before continuously decreasing and reaching its lowest levels in early February (~0.3%). These variations might explain why our mean annual product ratio is smaller than values reported in global meta-analyses (~6% compared to 12%). These temporal patterns are rarely accounted for and are a missing piece of the denitrification puzzle.

How much global warming potential can be saved with regenerative agriculture?

In 2022, we estimated that an unfertilized ley could save around 2 tonnes of equivalent CO_2 per hectare compared to a field under conventional agricultural practices. However, the emissions of N_2O in 2023 followed a completely different pattern and were very low, despite fertilizer

application. This is most likely explained by the low levels of nitrate monitored during that period, which probably made denitrification a better sink for nitrous oxide emissions in addition to reducing the magnitude of flux. It is at this point unclear why fertilizer application did not result in a build-up of nitrate levels, as it did in 2023. It might result from higher fertilizer efficiency or nitrogen plant uptake, or this fertilizer could have been lost in different ways (ammonia volatilization, leaching or surface runoff). This calls for further scientific investigation and shows that better fertilization strategies can be found.

Can we combine the ^{15}N Gas Flux method and naturally abundant isotopes to completely partition the sources of N_2O?

We successfully constrained the contributions of bacteria and fungi to denitrified N_2O emissions by combining the ^{15}N Gas Flux method and naturally abundant isotopes. Although this method does not encompass all the soil microbial and abiotic processes and is still undermined by uncertainties, it confirmed our hypothesis that N_2O denitrification activity in the studied arable field was dominated by bacteria (90%) rather than fungi (10%). This could constitute a routine test for evaluating the contributions of these two microbial populations to denitrified N_2O emissions.

Outlook:

The search for the ideal technique of denitrification measurement continues. While our reported method is a suitable candidate, it also has several limitations, such as potential stimulation effect and non-representative fluxes. To better characterize denitrification, we recommend enhancing our current method by applying the tracer at the time of core sampling and by using longer liners. The former will allow the tracer to diffuse within the soil matrix and avoid the measurement of artefacts. The latter will enable incubation of longer cores, which will be more representative of the denitrification dynamics (mostly occurring within the soil A horizon) and leave a bigger headspace where gas sampling would be less disruptive. Furthermore, we believe that diurnal and nocturnal patterns of denitrification need to be further constrained as there is currently a knowledge gap. Combining the liner approach with automated chambers will also increase the accuracy of the N budgets. Indeed, our low resolution (especially during the fertilization and second growing periods) resulted in uncertainties in our global estimations.

Finally, the application of fertilizer in conventional and regenerative agriculture needs careful consideration and further characterization. Its use is intrinsically linked to the efficiency of denitrification as a sink of nitrous oxide and to the magnitude of N_2O emissions. While it was responsible for ca. 2 tonnes of equivalent CO_2 per hectare in 2022, this pattern was not found in 2023, where emissions during the growing season were 22 times lower than in 2022. This was directly correlated to the soil nitrate levels, which were surprisingly low after fertilizer application. It remains unclear whether this resulted from higher nitrogen plant uptake, fertilizer type or loss of nitrogen via ammonia emissions or leaching. It proves however that better fertilization management strategies can be implemented for greenhouse gas emission reduction. Furthermore,

denitrification was shown to be the least efficient as a sink of nitrous oxide in the fertilized grass/clover ley. Unfortunately, no budget could be derived in this field due to the lack of chamber measurements. A better characterization of the global nitrogen cycle in conventional and regenerative agriculture is needed, which will only be complete with the quantification of denitrification.